

Molecular characterization of virus-host interactions

Wang, Li

2007

Wang, L. (2007). Molecular characterization of virus-host interactions. Doctoral thesis, Nanyang Technological University, Singapore.

<https://hdl.handle.net/10356/35763>

<https://doi.org/10.32657/10356/35763>

Molecular Characterization of Virus-Host Interactions

Wang Li

School of Biological Sciences

A thesis submitted to the Nanyang Technological University
in fulfillment of the requirements for the degree of
Doctor of Philosophy

2007



Abstract

In this thesis, virus-host interactions were studied from different aspects by using Epstein-Barr virus (EBV) and avian coronavirus infectious bronchitis virus (IBV) as two model systems.

In the first part of study, EBV BARF1, a secretory protein with transforming and mitogenic activities was focused. The post-translational modification, folding, maturation and secretion of BARF1 are systematically studied. The protein was shown to be post-translationally modified by N-linked glycosylation on the asparagine 95 residue. This modification was confirmed to be essential for the maturation and secretion of the protein. Cysteine 146 and 201 were also demonstrated to be essential for proper folding and secretion of the protein. To search for human proteins involved in the maturation process of BARF1, a yeast two-hybrid screening was carried out, leading to the identification of hTid1 as a potential interacting protein. This interaction was subsequently confirmed by coimmunoprecipitation and dual immunofluorescent labeling of cells coexpressing BARF1 and hTid1. Interestingly, coexpression of BARF1 with hTid1 demonstrated that hTid1 could promote secretion of BARF1, suggesting that hTid1 may act as a chaperone to facilitate the folding, processing and maturation of BARF1.

In the second part of this thesis, the cell tropism and pathogenesis of IBV were studied in order to understand the relationship between host cell response and their susceptibility to IBV infection. A total of fifteen cell lines were demonstrated to be susceptible to the Vero cell-adapted IBV and five among the fifteen support continuous propagation of IBV. Sequencing of IBV S gene over adaptation of the virus from Vero cells to Huh-7 cells suggested that genetic changes of S gene are not essential in this adaptation. Study of the expression profiles of IFN- β demonstrated

efficient induction of IFN- β by IBV infection in cell lines that support efficient IBV replication, indicating that IBV may exploit certain mechanisms to counteract the IFN- β action. *ISG15*, an IFN- β stimulated gene, was shown to be suppressed at the translational level in IBV infected Vero and HCT116 cells.

Acknowledgements

I would like to express special gratitude to my supervisor Prof. Liu Ding Xiang for his direction, encouragement and help during the process of the project. His forthrightness and serious attitude about science gave me deep impression and had a huge effect on me.

My appreciation is extended to Prof Tam Peter James, my co-supervisor, who gave me important directions as well as many valuable suggestions during my thesis work.

Thanks also go to Dr. Wen Zi Long and Dr. Huang Mei in Institute of Molecular and Cell Biology, Singapore. They gave me a lot help in the yeast two hybrid screening in this study.

I also extend my thanks to my colleagues who provided assistance, convenience and a friendly atmosphere. Without them, my project couldn't be finished so smoothly. Many thanks go to Chen Bo, Li Qi Sheng, Liao Ying, Wang Ji Bin, and Yuan Quan. They also gave me comments and suggestions on the writing of the thesis.

I am grateful for the financial support of scholarship from Nanyang Technological University during my study.

Finally, I will give sincere thanks to my parents and my friends forever. They gave me selfless care and encouragement to finish my Ph.D. study.

Contents

Abstract

Acknowledgements

Contents

Abbreviations

Chapter One: Literature review

1.1	Virus-host interactions	2
1.1.1	Cytokines	2
1.1.1.1	Type I interferon	2
1.1.1.2	Viral Evasion of IFN Responses	4
1.1.1.3	Other cytokines	6
1.1.2	Chemokines	6
1.1.2.1	Chemokine receptors	6
1.1.2.2	Viral strategies to evade chemokine action	7
1.1.3	Antigen presentation	9
1.1.3.1	MHC Class I Antigen Presentation	9
1.1.3.2	Viral strategies to evade MHC class I antigen presentation	10
1.1.3.3	MHC Class II Antigen Presentation	11
1.1.4	Antibody response and virus antigenic variation	11
1.1.5	Apoptosis	13
1.1.5.1	Viral inhibition of apoptosis	13
1.1.5.2	Viral activation of apoptosis	14
1.1.6	Other virus-host interactions	14
1.1.6.1	Tumor suppressor p53	14
1.1.6.2	Transcription factor NFκB	15
1.1.6.3	Mitogen-activated protein kinases (MAPKs)	15

1.2	Epstein-Barr virus	16
1.2.1	EBV life cycle	19
1.2.2	Primary infection	19
1.2.3	Latent infection	20
1.2.4	Lytic infection	21
1.2.5	EBV induced B cell immortalization	22
1.2.5.1	EBNA1	22
1.2.5.2	EBNA2 and EBNA-LP	23
1.2.5.3	EBNA3A, EBNA3B, and EBNA3C	24
1.2.5.4	LMP1	25
1.2.5.5	<i>Bam</i> HIA Transcripts	26
1.2.5.6	EBERs	27
1.2.6	EBV-associated lymphomas	28
1.2.6.1	Burkitt's lymphoma	28
1.2.6.2	Hodgkin's disease	28
1.2.6.3	Immunosuppression-related lymphoproliferations	29
1.2.7	EBV infection in epithelial cells	29
1.2.8	EBV-associated carcinoma	31
1.2.8.1	Nasopharyngeal carcinoma	31
1.2.8.2	Lymphoepithelial carcinoma	32
1.2.8.3	Gastric adenocarcinoma	32
1.2.8.4	Breast carcinoma	33
1.2.8.5	Hepatocellular carcinoma	33
1.2.9	EBV BARF1	34
1.2.9.1	BARF1 is exclusively expressed in EBV-positive carcinomas	35
1.2.9.2	Functions of EBV BARF1 in oncogenicity and immunomodulation	36
1.3	Coronavirus	39
1.3.1	Avian infectious bronchitis virus	40
1.3.2	Classification	41
1.3.2.1	Serotyping	41

1.3.2.2	Genotyping	41
1.3.2.3	Protectotyping	42
1.3.3	Virion morphology	42
1.3.4	Genomic structure and mRNAs	43
1.3.5	Viral Proteins	46
1.3.5.1	The replicase polyproteins	46
1.3.5.2	Spike protein (S)	47
1.3.5.3	Nucleocapsid protein (N)	49
1.3.5.4	Membrane protein (M)	50
1.3.5.5	Envelope protein (E)	51
1.3.5.6	Non-structural proteins	52
1.3.6	Virus Replication	53
1.3.6.1	Attachment and Penetration	53
1.3.6.2	Viral mRNA transcription	54
1.3.6.3	Viral protein translation	56
1.3.6.4	Virion Assembly and Release	56
1.3.7	Evolution of IBV	57
1.4	Aim of the project	58
1.4.1	EBV BARF1 and its interaction with hTid1	59
1.4.2	IBV cell tropism and pathogenesis	59

Chapter Two: Materials and methods

2.1	Materials	62
2.1.1	General reagents	62
2.1.2	Enzymes	62
2.1.3	Commercial kits	62
2.1.4	DNA vectors	62
2.1.5	Escherichia coli (E. coli)	62
2.1.6	Yeast	63

2.1.7	Mammalian cells	63
2.1.8	Viruses	64
2.1.9	Media	64
2.1.10	Buffers and solutions	65
2.1.11	Antibodies	66
2.2	Methods	66
2.2.1	General methods for DNA and RNA manipulation	66
2.2.1.1	Quantification of DNA	66
2.2.1.2	Restriction endonuclease digestion	67
2.2.1.3	DNA separation by agarose gel electrophoresis	67
2.2.1.4	Purification of DNA fragments by agarose gel electrophoresis	67
2.2.1.5	DNA ligation	68
2.2.1.6	Preparation of <i>E. coli</i> competent cells	68
2.2.1.7	Transformation of competent <i>E. coli</i> cell with plasmid DNA by heat shock	69
2.2.1.8	Transformation of competent <i>E. coli</i> cell with plasmid DNA by electroporation	69
2.2.1.9	Extraction of plasmid DNA	69
2.2.1.10	Polymerase Chain Reaction (PCR)	70
2.2.1.11	Identification of colonies that contain recombinant plasmids of interest	70
2.2.1.12	Extraction of genomic DNA	70
2.2.1.13	Site-directed mutagenesis	71
2.2.1.14	Extraction of total RNA from mammalian cells	71
2.2.1.15	Extraction of viral RNA from culture medium of virus infected cells	71
2.2.1.16	Reverse Transcription PCR (RT-PCR)	72
2.2.1.17	Automated sequencing	72
2.2.2	General methods for cell culture	72
2.2.2.1	Cell storage in Liquid Nitrogen	73
2.2.2.2	Cell Recovery from Liquid Nitrogen	73

2.2.2.3	Culture of Mammalian cells	73
2.2.3	Yeast two hybrid screening	73
2.2.4	Mammalian cell transfection	75
2.2.5	Sodium Dodecyl Sulphate polyacrylamide Gel Electrophoresis (SDS-PAGE)	75
2.2.6	Western blotting	76
2.2.7	Dimerization studies under reducing or non-reducing conditions	76
2.2.8	Co-immunoprecipitation	76
2.2.9	Indirect immunofluorescence	77
2.2.10	Confocal microscopy	77
2.2.11	Staining of ER organelle with R6	78
2.2.12	Staining of mitochondria organelle with Mitotracker Deep Red 633	78
2.2.13	Endoglycosidase Digestions	79
2.2.14	Virus infection and stock preparation	79
2.2.15	Virus purification	79
2.2.16	Plasmid construction	80

Chapter Three: Biochemical and functional characterization of Epstein-Barr virus-encoded BARF1 protein: interaction with human hTid1 protein facilitates its maturation and secretion

3.1	Introduction	84
3.2	Results	86
3.2.1	Expression, post-translational modification and secretion of BARF1	86
3.2.2	Mutational analysis of the four cysteine residues	87
3.2.3	Subcellular localization of BARF1 and secretion-defective mutants	89
3.2.4	Identification of hTid1 as BARF1-binding protein	91
3.2.5	Confirmation of the interaction between BARF1 and hTid1 by co-immunoprecipitation and co-localization studies	95

3.2.6	Promotion of BARF1 maturation by its interaction with hTid1	97
3.2.7	Deletion analysis of hTid-1 domains involved in BARF1 maturation	104
3.2.8	Further characterization of the subcellular localization of wild-type hTid1L and five deletion constructs	107
3.3	Discussion	111
3.3.1	Biochemical characterization of BARF1	111
3.3.2	The interaction between BARF1 and hTid1	113

Chapter Four: Avian Infectious Bronchitis Virus Cell Tropism and Pathogenesis

4.1	Introduction	118
4.2	Results	121
4.2.1	The susceptibility of fifteen cell lines to Vero cell-adapted IBV	121
4.2.2	Expression of IBV structural protein S, N, and M in IBV-infected cell lines	121
4.2.2.1	Lung cell lines susceptible to IBV	124
4.2.2.2	Liver cell lines susceptible to IBV	126
4.2.2.3	Colorectal cell lines susceptible to IBV	127
4.2.2.4	Kidney cell lines susceptible to IBV	128
4.2.2.5	Other cell lines susceptible to IBV	129
4.2.3	Growth profiles of Vero cell-adapted IBV in H1299, Huh7, and HCT116 cells	129
4.2.4	The relative Stability of IBV S gene during infection of human cell lines with the Vero cell-adapted IBV	133
4.2.5	IFN- β induction in IBV-infected cells	133
4.2.6	ISG15 induction in IBV-infected cells	135
4.3	Discussion	139
4.3.1	Coronavirus cell tropism	139

4.3.2	Host factors that restrict the replication of IBV	140
-------	---	-----

Chapter Five: Summary and Discussion

5.1	EBV BARF1 and its interaction with hTid1	144
5.1.1	Biochemical properties of BARF1 and future functional characterization of BARF1	144
5.1.2	hTid1 acts as a chaperone to facilitate the maturation of BARF1	146
5.1.3	Other potential functional implications of the interaction between BARF1 and hTid1	147
5.1.4	Association of hTid1 with its partners influences the subcellular localization of hTid1	149
5.2	Coronavirus cell tropism and pathogenesis	150
5.2.1	IBV cell tropism	150
5.2.2	IBV strategy to evade host innate immune response	150
5.2.3	Host factors that restrict IBV replication	153

Reference

Publication from this study:

Wang, L., Tam, J. P., Liu, D. X. (2006). Biochemical and functional characterization of Epstein-Barr virus-encoded BARF1 protein: interaction with human hTid1 protein facilitates its maturation and secretion. *Oncogene*. 25, 4320-4331.

Abbreviations

BSA	bovine serum albumin
CD	cluster of differentiation
cDNA	complimentary DNA
DMSO	dimethyl sulphoxide
dNTP	deoxynucleotide triphosphate
DTT	dithiothreitol
DMEM	Dulbecco's Modified Eagle's Medium
DNA	deoxyribonucleic acid
ECL	enhanced chemiluminescence
EDTA	ethylene-diamine-tetra acetic acid
ER	endoplasmic reticulum
h	hour(s)
HA	haemagglutination
kbp	kilobase pairs
kDa	kilodaltons
IP	immunoprecipitation
min	minute(s)
RNA	ribonucleic acid
mRNA	messenger ribonucleic acid
OD	optical density
PAGE	polyacrylamide gel electrophoresis
PBS	phosphate buffered saline
RNA	ribonucleic acid
RNP	ribonucleoprotein
rpm	revolutions per minute
RPMI	Roswell Park Memorial Institute
SDS	sodium dodecyl sulphate
TE	Tris- ethylene diamine tetra acetic acid
TEMED	N, N, N', N'-tetramethylethylenediamine
Tris	Tris (hydroxymethyl)-aminoethane
UV	ultraviolet
v/v	volume per volume
w/v	weight per volume

The single-letter and triplet codes for amino acid residues are used. Restriction enzymes are referred to by their three-letter names derived from that of the source microorganism. Other abbreviations are defined in the text where first encountered.

Chapter One
Literature Review

1.1 Virus-host interactions

Almost all living species represent prey for a viral invader. Viruses must be extremely successful predators as they depend on living cells for replication. For millions of years, viruses have coevolved with their hosts, to avoid the host killing and acquire efficient infection. In turn, probably as a result of the constant evolutionary pressure from viruses, higher vertebrates have developed a complex immune system. The nonspecific host defenses function at early stage during infection to prevent or limit infection while the specific host defenses function after infection. Although the virus-host interactions involved in a particular viral infection will vary depending on the virus type, some general principles do exist.

1.1.1 Cytokines

Cytokines play their roles by binding to specific high affinity receptors on target cells (Vilcek and Sen, 1996). This binding switches on a series of intracellular events including signal transduction, protein-protein interaction, gene expression alteration, and cascade activation of other cytokines. As a result, the rate of cell proliferation and/or differentiation increases or decreases. One of the most important cytokines is interferon (IFN).

1.1.1.1 Type I interferon

IFNs are commonly grouped into two types, type I and type II (Biron et al., 2001). Type I IFNs, including IFN- α , IFN- β , and IFN- ω , are also known as viral IFNs as they are induced by virus infection. Type II IFN is also known as immune IFN (IFN- γ) as it is induced by mitogenic or antigenic stimuli. Most types of virally infected cells are capable of synthesizing IFN- α/β in cell culture, while IFN- γ is synthesized only by cells of immune system, including natural killer (NK) cells, CD4⁺ Th1 cells, and CD8⁺ cytotoxic suppressor cells (Young, 1996; Bach et al.,

1997). Therefore, type I IFNs have emerged as pivotal in the conflict of host defense and virus replication.

Pathogen sensing occurs before the interferon production. There are two pathways: Toll-like receptor (TLR) dependent and independent pathways. The Toll-like receptor (TLR) family is composed of membrane proteins with domains to sample the environment for pathogen-associated molecular patterns (PAMPs) (Medzhitov and Janeway Jr, 1998). TLRs become activated and transmit signals through their cytoplasmic domains, resulting in the transcriptional induction of multiple genes involved in innate and adaptive immunity, including type I IFN. Different TLR molecules recognize specific PAMPs and, among these, TLR3, TLR7, TLR8, and TLR9 appear to play important roles in identifying viral products (Hemmi et al., 2000; Alexopoulou et al., 2001; Diebold et al., 2004; Heil et al., 2004; Lund et al., 2004). TLR-independent pathways of sensing viral infections and triggering IFN production exist as well. One such pathway is mediated by cytoplasmic DExD/H box RNA helicase proteins, including the retinoic acid inducible gene I (RIG-I) and the melanoma differentiation associated gene 5 (mda5), which contain caspase-recruiting domains (CARDs) (Yoneyama et al., 2004). These RNA helicases, upon binding to dsRNA, interact with a downstream molecule identified independently by four different groups as mitochondrial antiviral signaling protein (MAVS/IPS-1/VISA/CARDIF) (Seth et al., 2005; Kawai et al., 2005; Xu et al., 2005; Meylan et al., 2005). MAVS interacts with the CARD of RIG-I and recruits and activates, by not yet well-defined mechanisms, IKK ϵ /TBK1, the IKK α / β / γ complex, and MAPK, resulting in activation of IRF3, nuclear factor κ B (NF- κ B), and AP-1 and in IFN- β induction.

After synthesis and secretion, the type I IFNs bind to the cell surface type I IFN receptors (IFNARs) (Biron and Sen, 2001; Brierley and Fish, 2002; Platanias,

2005), resulting in receptor subunit dimerization, activation of kinases that associate with cytoplasmic tails of IFNARs and downstream signal transducers. At last, more than 100 IFN-stimulated genes (ISGs), whose concerted action leads to the generation of an “antiviral state” are transcribed. The myxovirus resistance gene (Mx), the protein kinase stimulated by dsRNA (PKR), and the 2'-5' oligoadenylate synthetases (OAS) are among the best characterized ISGs with antiviral activity (Biron and Sen, 2001). However, even in the absence of these IFN-regulated antiviral pathways, IFN can still induce an effective antiviral response (Zhou et al., 1999), raising the intriguing question of whether hosts have evolved redundant pathways to make it generally difficult for viruses to use any single mechanisms to inhibit the IFN antiviral response.

In addition, type I IFNs may extend their antiviral defense functions to other immune response components. They can also activate natural killer (NK) cells to mediate elevated cytotoxicity (Lee et al., 2000; Nguyen et al., 2002) and induce interleukin-15 (IL-15) to promote NK cell proliferation (Nguyen et al., 2002). At high concentrations, type I IFNs inhibit IL-12 (Karp and Biron, 2000) and NK cell responsiveness for IFN- γ expression (Nguyen et al., 2000).

1.1.1.2 Viral Evasion of IFN Responses

Antagonism of type I IFN induction

Viral inhibition of IRF3, resulting in decreased type I IFN production, has been documented to occur at multiple levels. For example, influenza NS1 and poxviruses E3L prevent IRF3 activation (Talon et al., 2000; Xiang et al., 2002), by sequestering viral dsRNA and preventing stimulation of cellular sensors of dsRNA, such as RIG-I and mda5. Direct binding and inhibition of Mda5 has been engaged by the V protein of several paramyxoviruses (Andrejeva et al., 2004). MAVS is the target

for cleavage by the NS3/4A protease of hepatitis C virus (Meylan et al., 2005). In addition, the P proteins of some negative RNA viruses inhibit the action of TBK1, preventing IRF3 phosphorylation (Unterstab et al., 2005). The human herpesvirus 8 encodes several analogs of IRF, known as viral IRFs (Biron and Sen, 2001), some of which act as dominant negative mutants of IRF3.

Antagonism of type I IFN signaling

The JAK/STAT pathway is also targeted at multiple levels by viral IFN antagonists. Poxviruses secrete a soluble form of the IFNAR that sequesters type I IFN before it can bind to the natural IFNAR (Symons et al., 1995). Inhibition of the JAK kinases has been documented for several viruses (Biron and Sen, 2001). STATs appear to be a preferred target for many paramyxoviruses, whose accessory V and W proteins bind to these factors and prevent their activation in response to IFN (Horvath, 2004).

Antagonism of type I IFN-inducible genes and their products

Among more than 100 ISGs, the PKR product appears to be a common target for many viral IFN antagonists. The ways viruses inhibit the PKR pathway are diverse, ranging from sequestration of the PKR-activating dsRNA, expression of dsRNA mimics, binding to PKR preventing its dimerization and activation, and substrate competitive inhibition (Katze et al., 2002). Finally, activation of cellular proteins involved in negative regulation of IFN response is also a strategy used by several viruses. For example, influenza virus activates a cellular inhibitor of PKR, the p58IPK, and herpesviruses encode a protein, γ 34.5, that recruits a cellular phosphatase for the dephosphorylation of eIF2 α , reverting the PKR-mediated translational block (Katze et al., 2002).

1.1.1.3 Other cytokines

Other cytokines such as tumour necrosis factor (TNF), transforming growth factor beta (TGF- β) and interleukins (ILs) have also been shown to inhibit viral replication through IFN-like mechanisms or through the upregulation of MHC class I or class II antigens (Biron and Sen, 2001). Viruses have developed elaborated ways to circumvent cytokine-mediated host defense. Epstein-Barr virus (EBV) BCRF1 protein, which is homologous to IL-10, binds to IL-10 receptor, thus inhibiting synthesis of IFN- γ , IL-2 and TNF (Moore et al., 1990). Human cytomegalovirus (HCMV) also encodes an IL-10 homolog to attenuate dendritic cells function, thereby subverting the efficient induction of antiviral immune responses (Chang et al., 2004). Cowpox virus crmA inhibits proteolytic activation of IL-1 β by IL-1 β converting enzyme and blocks apoptosis induced by CTLs, TNF and Fas (Ray et al., 1992). HCMV attenuates IL-1 β and TNF α proinflammatory signaling by inhibition of NF- κ B activation (Jarvis et al., 2006).

1.1.2 Chemokines

Chemokines are a homologous superfamily of relatively small proteins ranging from 8 to 17 kDa that probably arose through duplication and modification of an ancestral gene. The superfamily of chemokines is subclassified on the basis of the arrangement of cysteine residues located in the N-terminal region. Virtually every tissue and cell type tested to date can be induced to secrete chemokines.

1.1.2.1 Chemokine receptors

It is well known that chemokines exert their effect through guanosine nucleotide-protein-coupled receptors (GPCR), which are among a superfamily of related receptors that are involved in transducing a broad spectrum of extracellular stimuli such as hormones, neurotransmitters, chemokines, odorants, and light

(Bockaert et al., 1998). In general, the chemokine receptors are between 320 and 380 amino acids in length and show significant sequence homology. Chemokine receptor activation begins with extracellular ligand binding, which triggers interaction with the intracellular quiescent GDP-bearing trimeric G-proteins (Locati et al., 1999; Maghazachi, 1999; Wu et al., 1993). This results in exchange of GDP for GTP, causing the G-protein to dissociate into G- α and G- β/γ subunits. The latter subunit in turn activates enzymes such as phospholipase C and phosphoinositide-3-kinase, which convert phosphatidylinositol-4,5-diphosphate (IP₂) into phosphatidylinositol-1,4,5-triphosphate (IP₃) and diacylglycerol (DAG). IP₃ stimulates the influx of calcium ions, and DAG activates protein kinase C (PKC) isoforms, leading to a cascade of intracellular phosphorylation events involving a series of kinases (e.g., mitogen-activated protein kinase, protein tyrosine kinase) and small GTPases (e.g., Ras and Rho) that ultimately affect cellular events such as adhesion, chemotaxis, degranulation, and respiratory burst (Dikic and Blaukat, 1999; Henning and Cantrell, 1998; Luttrell et al., 1997).

1.1.2.2 Viral strategies to evade chemokine action

Much attention has been focused on the interaction between virus and chemokines. Due to cytopathic effects, virus infected cells probably provide the initial source of chemokines to recruit and activate inflammatory leukocytes, which in turn begin a cascade of events involving induction of cytokines such as IFN- γ and TNF- α that further amplify chemokine synthesis and leukocyte recruitment. Therefore, it is not surprising that viruses have acquired numerous mechanisms to undermine chemokines actions.

Production of chemokine mimics

Human herpesvirus 8 (HHV-8) is the source of a number of chemokine mimics, vMIP-I, vMIP-II, and vMIP-III (Dairaghi et al., 1999; Sozzani et al., 1998; Stine et al., 2000). It is particularly intriguing that several groups have reported that vMIP chemokines have agonistic interactions with CCR8 or CCR4, chemokine receptors expressed by Th2 cells (Dairaghi et al., 1999; Endres et al., 1999; Sozzani et al., 1998; Stine et al., 2000). This activity has provoked the notion that HHV-8 may interfere with the Th1/Th2 immune balance. Murine cytomegalovirus (MCMV) chemokine 1 (MCK-1) activates monocytes *in vitro* and increases monocyte-associated viremia *in vivo* (Saederup et al., 1999). human immunodeficiency virus (HIV) Tat is partially homologous to chemokines and is a potent monocyte chemoattractant (Albini et al., 1998).

Production of chemokine receptor mimics (vCKRs)

HHV-8 ORF74 is a functional GPCR with significant homology to the high-affinity IL-8 receptor, and it appears to promote cell growth. It also appears to promote the formation of Kaposi's sarcoma-like angioproliferative tumors (Rosenkilde et al., 2000; Yang et al., 2000). vCKRs encoded by HCMV and HHV-6 reduce the amount of the factor regulated upon activation normal T-cell expressed and secreted (RANTES) in tissue culture and/or its transcription and might inhibit chemokine activity locally (Lalani et al., 2000; Milne et al., 2000)

Synthesis of chemokine binding proteins (CKBP)

Three soluble vCKBPs have been identified that have no sequence similarity to cellular CKRs (Smith et al., 1997; Nash et al., 1999; Lalani et al., 2000; Alcamì et al., 1998). vCKBP-I is a soluble IFN- γ R encoded by MV, which binds the heparin-binding domain of a wide range of chemokines and might prevent the correct

localization of chemokines *in vivo* by blocking their interaction with proteoglycans. The poxvirus-secreted vCKBP-II (Carfi et al., 1999), binds chemokines with high affinity and blocks their activity. Murine gamma-herpesvirus 68 (MHV-68) has recently been shown to encode a distinct secreted protein (vCKBP-III) that sequesters kinds of chemokines (Parry et al., 2000).

1.1.3 Antigen presentation

Initiation of an immune response requires that antigenic fragments of pathogen-derived proteins be presented by the products of the major histocompatibility complex (MHC). MHC class I products sample the cytosolic compartment and its topological equivalents and present peptides to antigen-specific receptors on CD8⁺ T-lymphocytes⁺. MHC class II products mostly focus on peptides generated in the endocytic pathway.

1.1.3.1 MHC Class I Antigen Presentation

While IFNs represent the first line of host defense against virus, the second wave of the cellular immunity consists of CD8⁺ T-lymphocytes, which are activated via the presentation of viral antigens by professional antigen-presenting cells. Antigen presentation involves not only the processing of viral antigens, but also the biosynthesis and intracellular trafficking of MHC molecules. Typically, viral peptides derived from proteasome-mediated degradation of viral gene products are loaded on MHC class I complexes in the endoplasmic reticulum (ER). Assembled MHC class I complexes are subsequently transported to the cell surface, where they can be recognized by cognate T-cell receptors (TCR) on the surface of CD8⁺ T-lymphocytes. Engagement of the TCR by the viral peptide-MHC class I complex is a prerequisite for activation of the CD8⁺ T-lymphocytes and subsequent cytolysis or control of infected cells. Entry into the class I-restricted pathway of antigen presentation through

other routes is also possible. Phagocytes and dendritic cells, for example, can ingest materials, including host cells that express viral antigens, and have them processed and presented by class I products (Rock et al., 1996).

1.1.3.2 Viral strategies to evade MHC class I antigen presentation

Viruses are known to target every single step in the assembly and trafficking of the MHC class I complex (Ploegh, 1998; Piguet, 2005).

Regulation of expression of components in class I antigen presentation pathway

Transcription of key players of the class I antigen presentation pathway is targeted by a number of viruses. Examples include adenovirus E1A protein, which inhibits transcription of nearly all components of the MHC class I pathway (Friedman and Ricciardi, 1988; Rotem-Yehudar et al., 1994; Vertegaal et al., 2003), HIV-1 Tat protein (Carroll et al., 1998) and the early protein E5 of bovine papillomavirus-1 (Ashrafi et al., 2002). HCMV and MCMV inhibit IFN- γ induced up-regulation of MHC class I genes in a similar fashion (Miller et al., 1999; Khan et al., 2004).

Interference with proteolysis of viral proteins

Viruses are also known to interfere with peptide generation by the proteasome. HCMV phosphoprotein, pp65, inhibits the generation of HCMV-specific T cell epitopes (Gilbert et al, 1996). In EBV, the Gly-Ala repeats present in the EBNA-1 protein interfere with its degradation by the proteasome and antigen presentation (Levitskaya et al., 1997). HIV Tat competes with the IFN- γ -inducible 11S regulator for binding to the 20S proteasome (Seeger et al., 1997; Huang et al., 2002; Apcher et al., 2003). Binding of Tat to the 20S proteasome inhibits the peptidase activity of the latter. Murine leukemia virus (MuLV), an oncogenic retrovirus, prevents generation of immunodominant epitopes (Ossendorp et al., 1996; Beekman et al., 2000).

Blockage of transport of pathogen peptide and MHC class I molecules

Viral mechanisms against the transporting of pathogen peptides and MHC molecules exist at several levels, including inhibiting tapasin to turn off the peptide transport, redirecting MHC class I heavy chains into the cytosol, and retaining MHC class I molecules in the ER or Golgi (Ambagala et al., 2005).

Internalizing MHC class I molecules

The HIV Nef protein downregulates surface MHC class I by increasing endocytosis of these molecules (Schwartz et al., 1996), resulting in escape of HIV infected cells from CD8⁺ CTL mediated killing. Similarly, KSHV selectively down-regulates MHC class I expression at the cell surface by increasing the rate of endocytosis (Coscoy and Ganem, 2000; Ishido et al., 2000; Coscoy et al., 2001).

1.1.3.3 MHC Class II Antigen Presentation

The MHC class II-restricted pathway of antigen presentation focuses largely on events in the endocytic pathway (Wolf and Ploegh, 1995). Endosomal and lysosomal proteases destroy internalized protein antigens and generate peptide fragments appropriate for presentation by MHC class II molecules.

Transcription of class II molecules can be manipulated by viruses. In HCMV infected cells, the Jak/Stat pathway seems compromised and expression of class II molecules cannot be up-regulated (Miller et al., 1998). Besides, the induction of the transcriptional transactivator CIITA in HCMV infected cells is also repressed, hence the class II presentation machinery inhibited (Sedmak et al., 1994).

1.1.4 Antibody response and virus antigenic variation

Virus infection elicits a diverse spectrum of antiviral antibody responses. Antibodies can not only directly neutralize viruses by preventing the attachment of viruses to host receptors and viral entry into cells, but also interfere virus uncoating

and release. Antibodies also act as opsonins and facilitate phagocytosis of viruses either by promoting their uptake via Fc or C3b receptors or by agglutinating viruses. Antibody coated cells will be killed by killer cells thereby preventing the spread of infection.

Since viral surface proteins responsible for entry into the host cell are usually targets of the host antibody response, some viruses encode strategies to escape the antibody neutralization by antigenic variation and drift, which have been more effectively adopted by RNA viruses than DNA viruses because of the higher mutational frequency of RNA replicases compared to most viral DNA polymerases (Elena and Sanjuan, 2005). Examples include neuraminidase and haemagglutinin of influenza virus, gp120 of HIV and spike protein of coronavirus. For these viruses, several different viral genotypes may co-exist in the host as a result of the high mutation rates. The recombination and reassortment between these different genotypes may produce new strains with adaptive mutations, most of which reside in the genes encode for surface proteins, thereby evading recognition by previously produced antibodies. The antigenic drift rate of some RNA virus is so rapid that it effectively outpaces not only development of an effective immune response in the infected host but also confounds the attempts to develop prophylactic vaccines (Cavanagh and Naqi et al., 1997; Bowen and Walker, 2005, Derdeyn and Silvestri, 2005; Thomas et al., 2006). Even DNA viruses can undergo significant levels of mutational drift and thus become subject to immune selection. For example, single-stranded DNA viruses can exhibit mutational frequencies (Shackelton et al., 2005), and even double-stranded DNA viruses with high-fidelity polymerases like cytomegalovirus can still produce a diverse set of progeny to permit selective escape from host innate immunity (French et al., 2004).

1.1.5 Apoptosis

Apoptosis is a process in which cells are induced to commit suicide (White, 1996). The apoptotic bodies are engulfed by nearby phagocytosis cells and thus the entire scavenging action takes place without induction of an inflammatory response. It is an effective way for the organism to sacrifice a few infected cells to limit the spread of infection. It is not surprising that many viruses have evolved mechanisms to suppress or delay early cell death to allow production of high yields of progeny virus at the early stage of virus infection (Teodoro et al., 1997; O'Brien, 1998). The induction of apoptosis during later stage of virus replication cycle enables the dissemination of progeny virions without causing an inflammatory response or exposure to host enzymes and neutralizing antibodies (Teodoro et al., 1997; O'Brien, 1998).

1.1.5.1 Viral inhibition of apoptosis

Human adenovirus E1B-19K protein interacts with Bax and Bak and inhibits the apoptosis induced by different agents (Han et al., 1996a; Han et al., 1996b; Sundararajan et al., 2001). Similar to E1B 19K protein, the vaccinia virus F1L protein and Myxoma virus M11L protein block apoptosis through interaction and inhibition of pro-apoptotic Bax and Bak (Wang et al., 2004; Wasilenko et al., 2005; Su et al., 2006). The adenovirus E3 enhances clearance of Fas from the cell surface, thus inhibiting Fas-induced apoptosis, and blocks TNF-mediated apoptosis by interfering with downstream signaling of TNF receptor (Krajcsi et al., 1996; Shisler et al., 1997). Some viruses encode homologues of anti-apoptotic proteins to prevent apoptosis. For example, EBV BHRF1 and herpesvirus saimiri (HSV) ORF16 proteins which are Bcl-2 homologues protect host cells from apoptosis (Henderson et al., 1993; Nava et al., 1997). The cowpox virus CrmA protein acts as a specific inhibitor of proteases

belonging to the ICE family and thus prevents apoptosis caused by CTLs (Tewari et al., 1995) and Fas signaling (Tewari and Dixit, 1995).

1.1.5.2 Viral activation of apoptosis

During the late stages of infection, many viruses encode proteins that promote apoptosis, causing the cell to die and viral progeny to be spread to neighbouring cells. For example, the adenovirus E3-11.6 K adeno death protein (ADP) is expressed in large amounts during the very late stages of infection (Tollefson et al., 1996) to block the anti-apoptotic action of the adenovirus E1B-19 K protein. The poliovirus 2A protease has recently been shown to be sufficient for inducing apoptosis infected cells (Goldstaub et al., 2000). The HIV regulatory protein Tat downregulates the anti-apoptotic Bcl-2 and increases the pro-apoptotic Bax (Sastry et al., 1996). During apoptosis, the contents of the dying cells are packaged in membrane-bound apoptotic bodies instead of releasing into extracellular. Therefore, apoptosis represents a very efficient mechanism by which the virus can induce cell death and disseminate progeny, while limiting inflammatory and immune responses, especially for nonenveloped and nonlytic viruses.

1.1.6 Other virus-host interactions

1.1.6.1 Tumor suppressor p53

As a key player in the cellular damage response, p53 is stabilized and activated after several potentially harmful events, including UV or gamma irradiation, exposure to extreme heat, hypoxia, or starvation and after viral infection (Ko and Prives, 1996). Activation of p53 can lead either to cell cycle arrest, presumably to allow repair of damaged DNA, or to apoptosis. p53 mediates control of these two outcomes primarily by sequence-specific DNA binding and transactivation of specific target genes such as Rb, p21, Bax, and etc (Sax and El-Deiry, 2003). Tumor viruses always

target tumor suppressor proteins such as p53 and Rb to stimulate the proliferation of their host cells, thereby ensuring their own replication. Examples include the p53-interfering viral proteins: SV40 T antigen, adenovirus E1b and papillomavirus E6 proteins (Elledge and Lee, 2005), or the pRB-interfering proteins: SV40 T antigen, adenovirus E1a and papillomavirus E7 proteins (Helt and Galloway, 2003).

1.1.6.2 Transcription factor NF κ B

Nuclear factor κ B has been implicated in many cellular regulatory pathways, such as transformation, inhibition of cell death, immunoregulation and activation of viral gene expression (Baeuerle and Baltimore, 1996). In resting cells, NF κ B is present as a cytoplasmic complex with an inhibitor, I κ B. Cellular activation triggers phosphorylation of I κ B, its release from NF κ B and subsequent translocation of NF κ B to the nucleus where it can regulate gene expression. Many viral proteins involved in cell proliferation target the NF κ B–I κ B complex (Baeuerle and Baltimore, 1996; Goodkin et al., 2003).

1.1.6.3 Mitogen-activated protein kinases (MAPKs)

MAPKs are serine/threonine kinases that are rapidly activated upon stimulation by mitogen. Activation results in their translocation to the nucleus, where MAPKs control the expression of genes essential for cell growth and differentiation. Viruses which are able to activate this pathway includes hepatitis B virus (HBV) (Benn and Schneider, 1994), herpesvirus saimiri (HVS) (Jung and Desrosiers, 1995), Simian immunodeficiency virus (SIV) and HIV (Popik et al., 1998 and Popik and Pitha, 1998), CMV (Boyle et al., 1999), human papillomavirus (HPV) (Payne et al., 2001), HHV-8 (Naranatt et al., 2003), JC virus (JCV) (Querbes et al., 2004).

1.2 Epstein-Barr virus

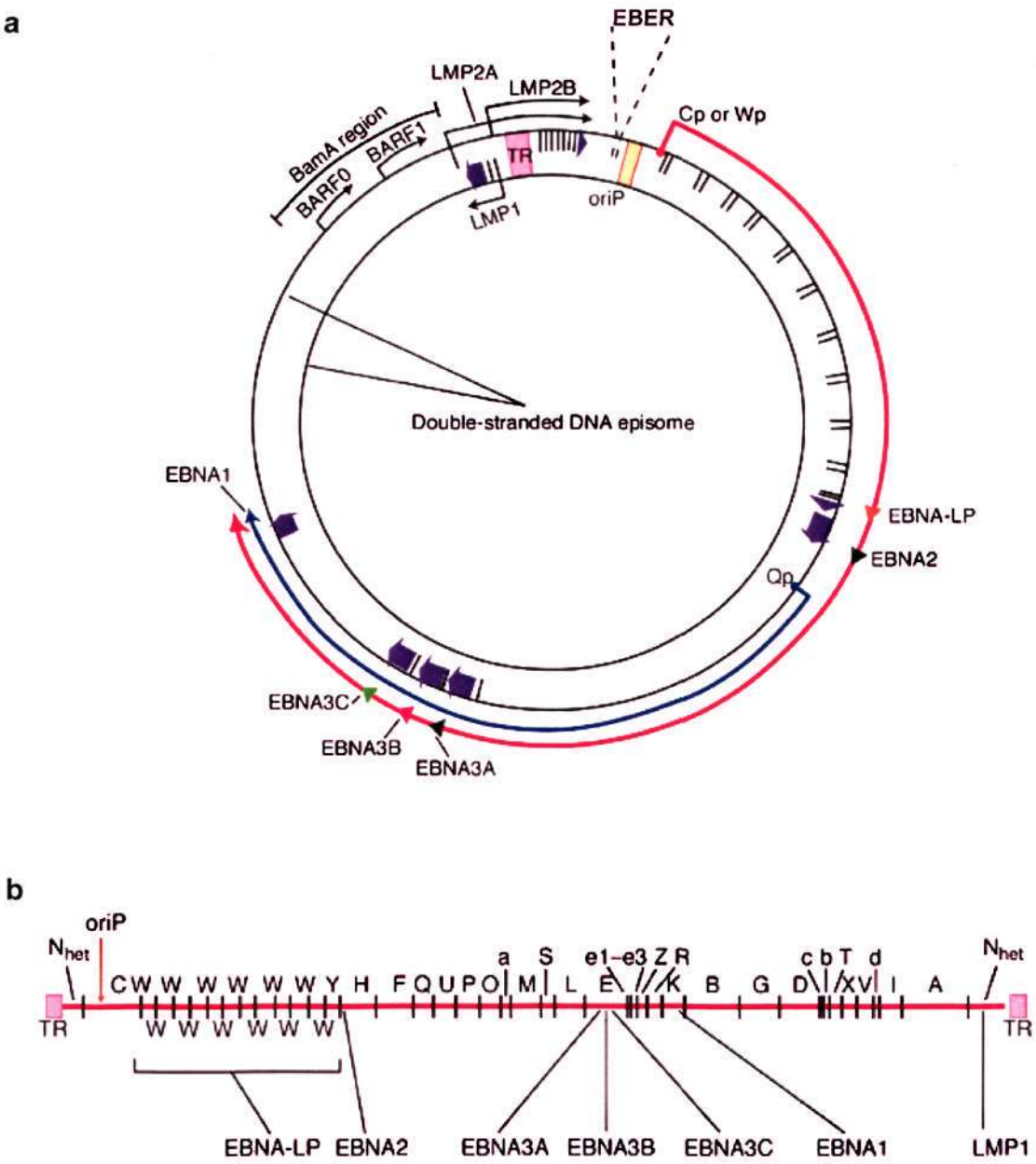
Epstein-Barr virus (EBV) is a member of the herpesvirus family and infects more than 90% of the world's population. Herpesviruses are characterized by the production of nucleic acid metabolism enzymes, nuclear capsid assembly, destruction of infected cells upon production of progeny virus, and the ability to establish a latent infection in host. A distinguished characteristic of EBV includes its ability to infect and transform B-lymphocytes *in vitro* (Henle et al, 1967). Primary B-lymphocytes immortalized by EBV infection are known as lymphoblastoid cell lines (LCLs). EBV can also infect epithelial cells *in vivo* (Rickinson et al, 2001). *In vitro* infection of primary pharyngeal epithelial cells is inefficient, but detectable (Sixbey et al, 1983). Recent studies have demonstrated that EBV can target other cell types including T-lymphocytes, monocytes, endothelial cells and smooth muscle cells (Kikuta et al., 1988; Jones et al., 1995; Savard et al., 2000).

EBV is an enveloped virus with a 172 kilobase pairs (kbps) double-stranded linear DNA genome, containing more than 80 genes that encode structural and regulatory proteins (Fig. 1.1). The genome is characterized by the presence of: 1) tandem repeats of approximately 500 base pairs at each terminus (Hayward and Kieff, 1976; Knitner and Sugden, 1979; Zimmermann and Hammerschmidt, 1995), 2) four clusters of internal direct repeats (IR1-4), 3 kbps in size, reiterated six to twelve times per cluster, and 3) two unique sequence domains, unique short (Us) and unique long (U_L), which are separated by IR1 and contain most of the coding region (Given and Kieff, 1978; Given and Kieff, 1979; Cheung and Kieff, 1981; Cheung and Kieff, 1982).

The EBV genome was the first herpesvirus cloned and sequenced from a *Bam*HI restriction library (Figure. 1.1b). EBV genes are named from the *Bam*HI

fragment from which they were cloned, the orientation of the reading frame, and the number of the frame (Baer et al., 1984). For example, BARF1 was cloned from the *Bam*HI fragment A Rightward Frame 1.

EBV is initially transmitted to the oral epithelium via saliva exchange. Infection of oral epithelium produces progeny virus through lytic replication (Lemon et al., 1977; Lemon et al., 1978; Sixbey et al., 1984). This progeny virus may then infect trafficking resting B-lymphocytes at the oral epithelium or in lymphoid organs such as the tonsils (Babcock et al., 1998; Miyashita et al., 1997; Niedobitek et al., 1997). Entry of EBV into B-lymphocytes occurs through the interaction between EBV envelope protein gp350/220 and the cellular complement 3d receptor, CD21 (Tanner et al., 1987). A second virus-host interaction occurs through the interaction of the viral gp42/gp85/gp25 complex with the MHC class II molecule mediating fusion of virus with cell membrane (Li et al., 1995; Wang et al., 1998). gp85/gp25 are also referred to as the gH/gL heterodimer as they are homologous to the gH and gL components of the herpes simplex virus and CMV membrane fusion complexes (Yaswen et al., 1993). However, the presence of gp42 in the virus envelope impedes infection of epithelial cells (Wang et al., 1998). Thus, the bimolecular gH/gL complex mediates epithelial cell infection, whereas the trimolecular gp42/gH/gL complex is required for infection of B cells. Expression of human leukocyte antigen class II results in reduced levels of gp42 in the virion produced, due to association of these two proteins inside the cell and degradation of gp42 in the endosomal/lysosomal compartment. Thus, EBV replication in epithelial cells generates virions that infect B cells preferentially, thereby establishing the EBV-carrier state in the infected individual, whereas EBV that is produced in B cells may be more efficient at



(Adapted from Young and Rickinson, 2004)

Figure 1.1 EBV genome structure map. **(a)** The EBV episome. Positions of EBV latent genes, transcripts, origin of replication (*oriP*), and terminal repeat (TR) are illustrated. The arrows indicate the direction in which the indicated open reading frames (ORFs) are transcribed. **(b)** The linear EBV genome. Open reading frames for the EBV latent proteins on a *Bam*HI restriction endonuclease map of the prototype B95.8 EBV genome are shown. The *Bam*HI fragments are named according to size, with A being the largest. Lower-case letters denote the smallest fragments. Note that the LMP2 proteins are produced from mRNAs that splice across the terminal repeats (TR) in the circularised EBV genome.

mediating virus spread, due to more efficient infection of epithelial cells (Borza and Hutt-Fletcher, 2002). Compared to B lymphocyte-produced virions, EBV from epithelial cells exhibits a significantly increased capacity to infect monocytes via MHC class II molecules and inhibit their development into dendritic cells (Guerreiro-Cacais et al., 2004).

1.2.1 EBV life cycle

Upon viral entry into B-lymphocytes, the viral genome circularizes to form an episome and is replicated once per cell cycle by the host cell's replication machinery. It initiates restricted latency program through transcription initiated from the Wp latency promoter using the cellular RNA polymerase II (Sample et al., 1986). Latent infection of B-lymphocytes has limited expression of viral proteins, allowing infected cells to evade host immune surveillance and remain infected for life (Tierney et al., 1994; Miyashita et al., 1997; Babcock et al., 2000; Thorley-Lawson, 2001; Hochberg et al., 2004).

Latently infected B-lymphocytes periodically reactivate to lytic replication and produce progeny virus (Anagnostopoulos et al., 1995; Babcock et al., 1998), which can re-infect surrounding cells. If reactivation occurs in trafficking B-lymphocytes in the oropharynx, virus is shed into the saliva, thereby allowing horizontal transmission to a new host. During the lytic cycle, the viral genome is actively amplified by a rolling circle mechanism, followed by packaging of these genomes into capsids to form infectious virions (Rickinson and Kieff, 2001).

1.2.2 Primary infection

Usually the EBV primary infection takes place in the first few years of life as measured by seroconversion, and infection does not result in any recognized disease. However, the dramatic immune response that can occur when primary infection is

delayed until adolescence or adulthood frequently results in infectious mononucleosis (IM). However, symptoms do not usually appear until four to six weeks post infection, and therefore, little is known about early events in primary infection.

During IM, cell-free infectious virus can be isolated from throat washings and saliva. IM patients have elevated infected circulating B-lymphocytes (Pope et al., 1967; Gerber et al., 1972). During acute disease, infectious virus cannot be detected in circulating B-lymphocytes and a large number (0.1-10%) of circulating B-lymphocytes express the EBV latent antigen Epstein-Barr viral nuclear antigen 1 (EBNA1) (Klein et al., 1976; Crawford et al., 1979; Robinson et al., 1980; Prang et al., 1997). Therefore, this acute disease is associated with latent infection of circulating B-lymphocytes. In response to infection, large number of atypical mononuclear cells can be detected in the blood mainly consisting of CD8⁺ lymphoblasts with some CD4⁺ T-lymphocytes and natural killer (NK) cells. During acute disease, T-lymphocyte response is directed against latent EBV antigens (Steven et al., 1997). However, the percentage of T-lymphocytes directed towards EBV latent antigens increase during the four months post-IM before stabilizing while the percentage of CTL directed against the EBV lytic antigen, BZLF1 decreases immediately after IM.

1.2.3 Latent infection

During latent infections, the virus has restricted transcriptional activity and the genes expressed then are referred to as latent genes. There are only eleven or fewer of these proteins are expressed in latently infected cells. Depending on the location and differentiation state of the infected B cell, three distinct form of latency exist, differing in which latent genes are expressed (Thorley-Lawson, 2001).

In the peripheral blood of healthy carriers, the virus is tightly restrained, being found only in resting memory B-lymphocytes. These cells express the putative

Latency 0, also called latency program, characterized by complete silencing of the viral genome, or the Latency I, in which LMP2A alone or together with EBNA1 may be expressed. By adopting these latency types, the virus persists in resting recirculating memory cells in a way that is non-pathogenic and not detectable by the immune system.

In the absence of effective immune surveillance, EBV infected B-lymphocytes express the Latency III, characterized by the expression of six EBV nuclear antigens (EBNAs 1, 2, 3A, 3B, 3C and LP) and three latent membrane proteins (LMP1, 2A and 2B). This expression pattern has also been called growth program due to its association with autonomous B cell proliferation. Activation of the growth program contributes to the expansion of the initial pool of EBV infected B-lymphocytes.

Another latency type, Latency II, also called default program, in which a restricted set of three latent proteins (EBNA1, LMP1 and LMP2A) is used to provide necessary survival signals for infected lymphoblasts to differentiate into memory cells. In addition to having different gene expression patterns, different types of latencies are associated with the different EBV related diseases. While Burkitt lymphoma (BL) and gastric carcinoma are associated with Latency I, Latency II proteins are detected in nasopharyngeal carcinoma (NPC), Hodgkin's disease and certain T cell lymphomas. The Latency III pattern is observed in patients with infectious mononucleosis and in immunocompromised patients with lymphoproliferative diseases.

1.2.4 Lytic infection

Like other herpesviruses, EBV lytic replication maintains temporal gene regulation. Production of lytic genes can be divided into three categories: immediate early (IE), early and late gene expression. Immediate early genes are defined as viral mRNAs that can be transcribed in the presence of a protein synthesis inhibitor

(Packham et al., 1993). Early genes are expressed before viral DNA replication, and late genes need viral DNA synthesis before they are transcribed.

The switch from the latent to the lytic phase is mediated by the expression of two primary IE genes *BZLF1* and *BRLF1*, encoding transactivators Zta and Rta, individually. The two proteins activate viral and certain cellular promoters, leading to an ordered cascade of viral gene expression.

1.2.5 EBV induced B cell immortalization

The ability of Epstein - Barr virus to transform B-lymphocytes into permanent, latently infected lymphoblastoid cell lines (LCLs) *in vitro* was discovered more than thirty years ago (Henle & Henle, 1979; Pope et al., 1968). Relative to the quiescent precursor B lymphocyte, the immortalized cells have an enlarged appearance due to the increased cytoplasmic volume required to support high rates of RNA and protein synthesis. They are typically ovoid or slightly elongated and frequently have a cluster of short villipodia projecting from the surface (Miller, 1990).

In EBV-immortalized LCLs, every cell carries multiple extrachromosomal copies of the viral episome and constitutively expresses a limited set of viral gene products, which comprise six EBV nuclear antigens (EBNAs 1, 2, 3A, 3B, 3C and LP) and three latent membrane proteins (LMPs 1, 2A and 2B). Transcripts from the *BamHIA* region (BARTs) and abundant expression of EBV encoded small RNAs (EBER1 and EBER2) are also detected in LCLs. Six (EBNAs 1, 2, 3A, 3C, LP and LMP1) are implicated directly in the process of B cell immortalization.

1.2.5.1 EBNA1

The EBNA1 protein of Epstein-Barr virus (EBV) enables the persistence of the episomal viral genome in latently infected, cycling B-lymphocytes, which can lead to malignant transformation under some circumstances. EBNA1 makes several

contributions to EBV latent infection. First, EBNA1 is required for the initiation of DNA replication from the EBV latent origin, *oriP* (Yates et al., 1985). This involves the binding of EBNA1 to the dyad symmetry (DS) element of *oriP* and recruitment of cellular replication initiation proteins (Chaudhuri et al., 2001, Schepers et al., 2001). Second, EBNA1 is required for the stable segregation of the viral genomes during cell division. Segregation requires EBNA1 binding to the family of repeats (FR) element of *oriP* and attachment of EBNA1 to the host mitotic chromosomes through an interaction with the cellular hEBP2 protein present on the mitotic chromosomes (Wu et al., 2000; Hung et al., 2001; Kapoor et al., 2005). Third, through binding to the FR element, EBNA1 can activate the transcription of other EBV latency genes, although the mechanism of this activation is not known (Reisman and Sugden, 1986; Gahn and Sugden, 1995). Finally, EBNA1 can counteract the stabilization of p53 by USP7 that occurs in response to DNA damage, thereby decreasing apoptosis and increasing cell survival (Kennedy et al., 2003; Saridakis et al., 2005).

1.2.5.2 EBNA2 and EBNA-LP

EBNA2 and EBNA-LP are only expressed during type III latency. While EBNA2 is necessary for EBV mediated B-lymphocyte transformation, EBNA-LP is not essential, but augments EBNA2 activity (Allan et al., 1992). EBNA-LP and EBNA2 enhance their upstream promoters, Cp or Wp, which results in transcription of not only EBNA-LP and EBNA2 but also EBNA1, EBNA3A, EBNA3B, EBNA3C, LMP1, LMP2A, and LMP2B (Kieff and Rickinson, 2001). Like many transcriptional activator proteins, EBNA2 is able to interact with components of the basal transcription machinery in addition to a number of transcriptional coactivator proteins. So far, EBNA2 has been shown to interact with TFIIB, TAF40, p62 and XPD (p80) subunits of TFIIH, a 100 kDa protein that associates with TFIIIE, hSNF5, p300, CBP

and PCAF, CBF1 (Tong et al., 1995a, 1995b, 1995c; Wu et al., 1996; Wang et al., 2000; Pegman et al., 2006). EBNA2 directly or indirectly up-regulates B lymphocyte CD21, CD23, c-myc, AML2, BATF, IL16, IL18r, c-fgr, cyclin D2, cdk4, TNF- α , lymphotoxin, HES1, G-CSF RNAs and some other RNAs encoding proteins important in cell signaling, cell-cycle regulation, and survival (Kaiser et al., 1999; Kieff and Rickinson, 2001; Spender et al., 2001; Spender et al., 2002; Johansen et al., 2003; Pages et al., 2005; Zhao et al., 2006).

1.2.5.3 EBNA3A, EBNA3B, and EBNA3C

EBNA3A, EBNA3B and EBNA3C share limited but significant amino acid sequence similarity, have the same gene structure (a short 5' exon and a long 3' exon) and are arranged in tandem in the genome (Kieff & Rickinson, 2001). EBNA3A and EBNA3C are essential for B-lymphocyte transformation (Tomkinson et al., 1993), while EBNA3B is not necessary for LCL outgrowth, cell survival, or lytic replication (Tomkinson et al., 1992). All three EBNA3 proteins can interact with complexes of cellular proteins that are involved in transcription regulation (Young and Rickinson, 2004) and bind RBPJ κ (Johannsen et al., 1996; Krauer et al., 1996; Robertson and Kieff, 1995; Waltzer et al., 1996; Zhao et al., 1996). The EBNA3s compete with EBNA2 and cellular Notch for RBPJ κ and limit EBNA2 transactivation of viral and cellular genes (Johannsen et al., 1996; Krauer et al., 1996; Marshall and Sample, 1995; Robertson and Kieff, 1995; Robertson et al., 1996; Waltzer et al., 1996; and Zhao et al., 1996). Despite this activity, EBNA3C coactivates the LMP1 promoter with EBNA2, and this activity is dependent upon the PU.1 site within the promoter (Zhao and Sample, 2000). EBNA3C can also recruit histone deacetylases and binds to the co-repressor C-terminal binding protein (CtBP) via a PLDLS amino acid motif (Radkov et al., 1999; Touitou et al., 2001; Knight et al., 2003). Proteins recently

identified to interact with EBNA3C include cyclin A and C8/ α 7 subunit of the 20S proteasome (Knight et al., 2004; Touitou et al., 2005).

1.2.5.4 LMP1

LMP1 is an integral membrane protein expressed during type II and type III latency that is essential for B lymphocyte transformation (Kaye et al., 1993). LMP1 is considered the EBV oncogene. LMP1 transforms rodent fibroblast (Arrand et al., 1981; Moorthy et al., 1993; Wang et al., 1985), supports anchorage independent growth in soft agar (Baichwal and Sugden, 1988), and when expressed in Rat-1 cells is tumorigenic in nude mice (Wang et al., 1985). LMP1 associates with the cytoplasmic cytoskeleton (Liebowitz et al., 1986; Liebowitz et al., 1987) and is constitutively present in the cholesterol-rich plasma membrane microdomains, lipid rafts without any ligand stimulation (Brown et al., 2001; Higuchi et al., 2001).

The cytoplasmic C-terminal signaling domain of LMP1 contains two main signaling regions. The membrane proximal region is known as C-terminal activating region 1 (CTAR1) and the membrane terminal region is known as C-terminal activating region 2 (CTAR2). It is functionally analogous to a tumor necrosis factor receptor (TNFR) or CD40 (Mosialos et al., 1995). CTAR1 binds TRAFs 1, 2, 3 and 5 (Devergne et al., 1996; Devergne et al., 1998) and CTAR2 binds TNFR associated death domain protein (TRADD) and receptor interacting protein (RIP) (Izumi et al., 1999; Izumi and Kieff, 1997). Unlike TNFR, LMP1 constitutively associates with TRAFs in a ligand-independent fashion (Devergne et al., 1996; Franken et al., 1996). Association of LMP1 with TRAFs results in activation of the NF- κ B family of transcription factors from both CTAR1 and CTAR2 (Hammaraskjold and Simurda, 1992; Laherty et al., 1992). In addition to activation of the NF- κ B pathway, LMP1 activates numerous other signaling pathways including cdc42, p38 pathway, c-jun N-

terminal kinase (JNK) pathway, and the phosphoinositide 3-kinase (PI3K) pathway. LMP1 induces an increase in cell surface expression of CD23, CD39, CD40, CD44, MHC class II, LFA-1, ICAM1, and LFA3 (Wang et al., 1988). LMP1 expression also increases secretion of the cytokine IL-10 and decreases CD10 (Wang et al., 1988). LMP1 also increases expression of anti-apoptotic proteins A20 and bcl-2 (Henderson et al., 1991; Laherty et al., 1992), protects B-lymphocytes from apoptosis, and protects epithelial cells from p53 mediated apoptosis (Gregory et al., 1991; Henderson et al., 1991; Laherty et al., 1992; Martin et al., 1993; Rowe et al., 1994; Fries et al., 1996). Expression in epithelial cells blocks epithelial cell differentiation (Dawson et al., 1990). Furthermore, expression *in vivo* in transgenic mice induces epidermal hyperplasia when expressed in skin and increases the incidence of B-lymphocyte lymphomas when expressed under the control of the immunoglobulin heavy chain promoter (Kulwichit et al., 1998; Wilson et al., 1990).

1.2.5.5 *Bam* HIA Transcripts

The *Bam* HIA transcripts (BARTs) are a family of highly spliced transcripts that are 3' co-terminal. The BARTs can be detected in all three types of latency and have been detected in a variety of EBV associated malignancies (Gilligan et al., 1990; Chen et al., 1992; Brooks et al., 1993; Sadler and Raab-Traub, 1995; Smith et al., 2000; and van Beek et al., 2003). However, BARTs seem not to be essential for B lymphocyte transformation as virus in which BARTs are deleted still transforms B-lymphocytes *in vitro* (Robertson et al., 1994). Three transcripts, *rk-barf0*, *rb2* (A73) and *rk103* (RPMS1), are interesting, as they appear to contain open reading frames and encode proteins. By RNase protection assay, RK103 appears to be the most abundant transcript followed by RB2 (Smith et al., 2000). However, RB2 and RK-BARF0 may be present at high levels in nasopharyngeal carcinoma (NPC) as RT-PCR analysis a

NPC indicated that RB2 and RK-BARF0 were present in the most abundant mRNA (Sadler and Raab-Traub, 1995). Yeast-two hybrid analyses of the proteins encoded by RK-BARF0, RB2, and RK103 have identified important cellular binding partners. RK-BARF0 binds the extracellular portion of Notch 1 and Notch4 and induces nuclear translocation of full-length, unprocessed Notch (Kusano and Raab-Traub, 2001). RK103 binds the downstream Notch transcription factor RBPJ κ and inhibits the transactivating function of both EBNA2 and the intracellular portion of Notch (NotchIC) (Zhang et al., 2001). Furthermore, RB2 binds the receptor for activated protein kinase c (RACK) (Smith et al., 2000). Their interactions with these cellular proteins suggest an important function in viral infection (Fries et al., 1997; Kienzle et al., 1999, van Beek et al., 2003).

1.2.5.6 EBERs

The EBERs are a family of viral-encoded, small, non-polyadenylated RNAs that are the most abundant RNAs in latently infected cells. Although not necessary for EBV-mediated immortalization of B-lymphocytes *in vitro* (Swaminathan et al., 1991), EBERs promote cellular transformation in various systems (Takada and Nanbo, 2001; Yajima et al., 2005) and inhibit apoptosis that is induced by interferon- α (Nanbo et al., 2002; Ruf et al., 2005). These activities were attributed to the binding and inhibition of the double-stranded RNA-dependent protein kinase R (PKR) by some studies (Sharp et al., 1993; Takada and Nanbo, 2001; Nanbo et al., 2002). However, recent results indicate that EBERs do not inhibit PKR activity *in vivo* when cells are challenged with various PKR stimuli (Ruf et al., 2005; Wang et al., 2005). EBERs are located in infected cell nuclei and can be found complexed with the cellular proteins La and human ribosomal protein L22 (Lerner et al., 1981; Toczyski and Steitz, 1991).

1.2.6 EBV-associated lymphomas

1.2.6.1 Burkitt's lymphoma (BL)

BL is endemic in equatorial regions of Africa and Papua-Guinea where it is a common childhood cancer (Burkitt et al., 1965). In Western countries, BL occurs as a sporadic tumour. All BL cases characteristically carry a chromosomal translocation, t(8; 14), t(8; 2), or t(8; 22), placing the *c-myc* oncogene under the control of an immunoglobulin gene, resulting in an inappropriate overexpression of *c-myc* (Klein, 1979). The most compelling evidence of EBV's involvement in BL is the high frequency (98%) of tumors carrying the virus (de-The, 1985) in endemic areas and the presence of clonal EBV in all of the tumor cells (Gulley et al., 1992). However, none of the growth-promoting latent genes are expressed. The only genes expressed encode for EBNA1 (Gregory et al., 1990) and the untranslated RNAs called EBERS and BARTS. Although it was suggested that EBNA1 (Wilson et al., 1996) and the EBERS (Takada and Nanbo, 2001), the findings remain unsubstantiated and there is currently no broadly accepted understanding of the role of EBV in BL (Lenoir and Bornkamm, 1987; Kelly et al., 2002; Niller et al., 2004).

1.2.6.2 Hodgkin's disease (HD)

HD is characterized histologically by the presence of Hodgkin and Reed-Sternberg (HRS) cells admixed with abundant lymphocytes and other reactive cells. Most cases of classical HD are also derived from B-lymphocytes (see below) although a small proportion of T-cell derived HD have been described (Kanzler et al., 1996; Müschen et al., 2000). In western countries, EBV is detectable in the HRS cells of 20–50% of HD cases while in developing countries up to 100% of cases may be associated with the virus (Ambinder et al., 1993; Herbst et al., 1993). In all EBV-associated HD cases, LMP1 and LMP2A are expressed in addition to the EBERS and

EBNA1 (Herbst et al., 1991; Deacon et al., 1993; Grässer et al., 1994; Niedobitek et al., 1997).

1.2.6.3 Immunosuppression-related lymphoproliferations

Immunosuppressed transplant patients are at an increased risk of developing lymphoproliferative disorders (post-transplant lymphoproliferative disorders, PTLD) (Hopwood and Crawford, 2000). The vast majority of these cases are B-cell-derived and EBV-associated. PTLD comprise a spectrum of diseases ranging from polyclonal polymorphic lesions to frankly malignant monomorphic and monoclonal lymphomas which are morphologically indistinguishable from lymphomas occurring in nonimmunosuppressed individuals (Craig et al., 1993). Polymorphic PTLDs tend to display type III latency although there is usually a degree of variability at the single cell level (Oudejans et al., 1995). In monoclonal lymphomas, the expression of viral latent genes is generally more restricted, conforming to latency patterns I or II (Niedobitek et al., 1997). Patients with acquired immunodeficiency syndrome (AIDS) also have an increased risk of developing malignant lymphomas.

1.2.7 EBV infection in epithelial cells

In comparison with the infection of B-lymphocytes, infection of epithelial cells is more difficult *in vitro*. EBV adheres to B-lymphocytes through CD21 molecules expressed on these cells, and this determines the B cell tropism (Fingerhuth et al., 1984). In contrast, epithelial cells are CD21 negative and this was believed to be why infection is not established, especially because they become susceptible to EBV infection when the barrier is overcome by CD21 expression via gene transfer (Li et al., 1992) or membrane implantation (Shapiro et al., 1982). In addition, Fingerhuth *et al* have reported that EBV can infect a human epithelial cell line, 293, in a CD21 dependent manner (Fingerhuth et al., 1999).

However, a viral EBV mutant lacking gp350/220 was shown to still infect the 293 epithelial cell line, as well as B-lymphocytes, albeit with a reduced efficiency (Janz et al., 2000). In line with this assertion, the gp42 glycoprotein encoded by the viral BZLF2 gene is critical for the infection of B-lymphocytes but not of epithelial cells (Wang and Hutt-Fletcher, 1998). Most of the epithelial cell lines that were successfully infected with EBV were CD21 negative, and the infection was not inhibited by anti-CD21 monoclonal antibodies (OKB7) (Yoshiyama et al., 1997). Another CD21 negative cell line, monkey kidney primary epithelial cell, could be infected using EBV particles derived from a nasopharyngeal carcinoma tumor line (Danve et al., 2001). Therefore, besides the CD21 dependent pathway, EBV might be able to infect epithelial cells by other mechanisms. It was reported that in the pathway whereby IgA in the blood is processed into the secreted form by epithelial cells, EBV is incorporated into the epithelial cells in a bound state with IgA antibody against envelope protein (Sixbey and Yao, 1992). This phenomenon could explain the involvement of EBV infection in the development of nasopharyngeal carcinoma and possibly of gastric carcinoma, which are typically preceded and accompanied by the appearance of virus specific IgA in serum (Henle and Henle, 1972; Fukayama et al., 1994; Imai et al., 1994; Levine et al., 1995). Another possible method of EBV infection in vivo is that cell to cell contact because of some evidences for direct infection of various human epithelial cells, which are CD21 receptor negative by EBV in vitro (Yoshiyama et al., 1997; Imai et al., 1998). By comparison, cocultivation with virus producers showed about 800-fold-higher efficiency of infection than cell-free infection did, suggesting the significance of direct cell-to-cell contact as a mode of virus spread in vivo (Imai et al., 1998).

1.2.8 EBV-associated carcinoma

1.2.8.1 Nasopharyngeal carcinoma (NPC)

NPCs are endemic in South-east Asia, northern Africa, and some other regions, while they occur rarely in Western Europe and North America (Niedobitek, 2000). Non-keratinizing undifferentiated NPC, usually associated with a prominent admixture of tumour-infiltrating lymphocytes, represents the most common histological type while conventional squamous cell NPC are less common (Niedobitek et al., 1996). Independently of the geographical origin of the patients, undifferentiated NPCs are always EBV-positive and harbour monoclonal viral episomes (Raab-Traub and Flynn, 1986; Niedobitek et al., 1996). Expression of LMP1 can be detected at the mRNA or protein level in most undifferentiated NPCs (IARC, 1997). LMP2A expression in NPC cells is detectable at the transcriptional level but the protein is usually undetectable by immunohistochemical techniques (Niedobitek, 2000). Expression of another EBV latent gene, BARF1, with possible transforming functions has also been detected in NPCs (Decaussin et al., 2000). The association of undifferentiated NPC with EBV has been well documented. By contrast, an association of the virus with squamous cell NPC is controversial (IARC, 1997). This issue has been resolved by a study demonstrating that EBV is present in all squamous cell NPCs from an endemic area, while the virus is detectable only in about 30% of cases from regions with a low NPC incidence (Nicholls et al., 1997). This suggests that other factors may be able to replace EBV in the pathogenesis of squamous cell NPC. Smoking and infection with human papillomaviruses are likely to be of importance in this respect (Hording et al., 1994; Vaughan et al., 1996).

1.2.8.2 Lymphoepithelial carcinoma

Carcinomas showing morphological features similar to undifferentiated NPCs, called lymphoepithelial carcinomas, can arise at other sites and these tumours have been extensively studied for an association with EBV. These studies have identified three different groups. Lymphoepithelial carcinomas of the stomach are EBV-associated in approximately 80% of cases regardless of the origin of the patients (Osato and Imai, 1996). Lymphoepithelial carcinomas of the salivary glands, the lungs and possibly of the thymus are frequently associated with EBV infection in areas where NPC is endemic whereas similar tumours arising, e.g. in Caucasian patients, appear to be EBV-negative (IARC, 1997). Finally, there is a large group of EBV-negative lymphoepithelial carcinomas, including carcinomas of the cervix uteri, the urinary bladder, the skin, and the larynx (IARC, 1997). It has to be noted, however, that this statement relies largely on single case reports and studies of small series. Systematic comparative studies are lacking, probably owing to the scarcity of these tumours.

1.2.8.3 Gastric adenocarcinoma (GC)

The detection of EBV in gastric lymphoepithelial carcinomas has prompted several groups to study conventional GC, revealing the presence of EBV in 2–16% of cases world-wide (Osato and Imai, 1996; IARC, 1997). Analysis of EBV in tumour biopsies indicates that the carcinoma is formed by the proliferation of a single EBV infected epithelial cell (Imai et al, 1994; Fukayama et al, 1994), thus suggesting that EBV infection had occurred in the very early stage of tumor development. Studies of EBV latent gene expression in gastric carcinomas (lymphoepithelial and adenocarcinomas) have revealed the expression of EBNA1 in the absence of EBNA2

and LMP1 (Osato and Imai, 1996). Expression of LMP2A and of BARF1 has been detected at the transcriptional level (Osato and Imai, 1996; zur Hausen et al., 2000).

1.2.8.4 Breast carcinoma

An association with EBV has also been reported for a proportion of breast carcinomas (Labrecque et al., 1995). EBV genomes can be detected by Q-PCR in about half of breast tumor specimens, although viral load is not high (Arbach et al., 2006). Importantly, most if not all of the EBV DNA detected in the breast cancer biopsy specimens was of epithelial tumor cell origin. However, studies of medullary carcinoma of the breast, which shares some morphological features with undifferentiated NPC have consistently failed to identify the virus (Niedobitek et al., 1991; Kumar and Kumar, 1994; Lespagnard et al., 1995). Through microdissection and isolation of pure tumor cells, it was found that even in EBV-positive tumor samples, many tumor cells do not contain EBV genomes and that the breast carcinomas are highly heterogeneous in terms of genome content and distribution (Arbach et al., 2006). These evidences raise the possibility that although EBV is unlikely to have an etiologic role in the genesis of breast cancer, the virus might contribute to tumor progression. EBNA-1 and BARF1 transcripts were detected in almost all of the EBV-positive breast cancer tumors and LMP-1 was also detected in 20% tumors (Arbach et al., 2006).

1.2.8.5 Hepatocellular carcinoma

EBV has been detected in approximately 35% of hepatocellular carcinomas using Southern blot hybridization (Sugawara et al., 1999). Interestingly, analysis of the terminal repeats of the EBV genome revealed monoclonal viral genomes while immunostaining for the EBNA complex suggested that the virus was present only in a proportion of the tumour cells (Sugawara et al., 1999). The most surprising finding of

this study was the absence of detectable expression of the EBERs suggesting a new type of latency (Sugawara et al., 1999).

1.2.9 EBV BARF1

EBV BARF1 gene, encoding a protein of 221 amino acids (Zhang et al., 1988), is located at nucleotide positions 165,449-166,189 of strain B95.8. BARF1 was so called because it was cloned from the *Bam*HI A Rightward Frame 1 from a *Bam*HI restriction library. It is transcribed just before the onset of EBV DNA synthesis in EBV producer B-lymphocytes and translated into a 33 kDa early protein (p33) which is recognized by high early antigen (EA) titre NPC sera (Zhang et al., 1988). Computer analysis of BARF1 sequence predicted a signal peptide sequence present in the N terminal with a cleavage site after the 20th N-terminal amino acid. The secretion of a 29 kDa BARF1-encoded polypeptide from human B-lymphocytes was already reported by Strockbine et al., 1998 and confirmed from different cells (Sall et al., 2004; Seto et al., 2005; de Turenne-Tessier et al., 2005). The cleavage site was predicted to be 20th amino acid and later on confirmed (de Turenne-Tessier et al., 2005). It was found that EBV-carrying Raji cells in which partial sequence including the BARF1 ORF was not transcribed were incapable of synthesizing viral DNA, indicating that this gene might be involved in viral replication (Hatfull et al., 1988). BARF1 has been thought to be a lytic gene, since it is not expressed in BL tissues and its expression is induced upon induction of the lytic cycle in BL cell lines (Zhang et al., 1988; Decaussin et al., 2000). Until recently, BARF1 gene was suggested to be a latent gene in nasopharyngeal carcinoma and EBV-associated gastric carcinoma tissues (Seto et al., 2005).

1.2.9.1 BARF1 is exclusively expressed in EBV-positive carcinomas

EBV is associated with various epithelioid malignancies such as nasopharyngeal carcinoma (NPC) and gastric carcinoma (GC) (Imai et al., 2001). However, the precise contribution of EBV to the pathogenesis of these malignancies remains unclear as in contrast to B-lymphocytes, it is very difficult to investigate EBV infection and transformation of epithelial cells (Sixbey et al., 1983; Gan et al., 1997). Six genes, *EBNA1*, *EBNA2*, *EBNA3A*, *EBNA3C*, *EBNA-LP*, and *LMP1*, are indispensable for B-cell immortalization (Kieff, 1996). However, EBV genes that are essential for epithelial cell immortalization are not well known yet. It would be interesting to characterize the EBV genes which are involved in epithelioid malignancies.

The strong etiological link between EBV and NPC has been known for over 3 decades (zur Hausen et al., 1970; Spano et al., 2003; Wei and Sham, 2005). Classically, NPC is considered to have a latency type II EBV transcription, with expression of EBV-encoded small RNAs 1 and 2 (EBER1/2), *BamHI* A rightward transcripts (BARTs), Epstein-Barr nuclear antigen 1 (EBNA1) and latent membrane protein 2 (LMP2), while LMP1 is more heterogeneously expressed (IARC, 1997; Middeldorp et al., 2003; Khabir et al., 2005). However, additional transcription of BARF1 was discovered (Hitt et al., 1989; Brink et al., 1998; Hayes et al., 1999). It was also reported that a NPC-derived EBV strain can transform monkey primary cells which are with epithelial origin and these transformed cells express EBNA1 and BARF1, in the absence of detectable LMP1 or lytic proteins (Danve et al., 2001).

Gastric carcinoma cells express a limited number of EBV genomes, similar to those in Burkitt's lymphoma, which are EBNA1, EBER1, EBER2, BARTs, BARF1 and LMP2A positive (Imai et al., 1994; Sugiura et al., 1996). This is different from the

pattern in NPC, in which LMP1 is also expressed in carcinoma cells in about half of the patients (Young et al., 1988; Rickinson and Kieff, 1996).

Among more than 90 genes encoded by EBV (Baer et al., 1984), only LMP1 and BARF1 (or p31) have been shown oncogenic functions in cell culture systems, especially in rodent cells (Wang et al., 1985; Wei and Ooka., 1989). LMP1 induces epidermal hyperplasia in transgenic mice (Wilson et al., 1990), alters keratin gene expression in human keratinocytes (Fahraeus et al., 1990), inhibits cell differentiation in some immortalized epithelial cell lines (Dawson et al., 1990), induces expression of the epidermal growth factor receptor (Miller et al., 1995), and blocks p53-mediated apoptosis through activation of the A20 gene (Fries et al, 1996). However, LMP1 is expressed in only 30 to 50% of NPC (Fahraeus et al., 1988; Young et al., 1988). Moreover, LMP1 is not expressed, in transformed gastric epithelial cells (Nishikawa et al., 1999) and in gastric carcinoma biopsies (zur Hausen et al., 2000). Therefore, BARF1 is very likely to be involved in the oncogenic progression of NPC and GC.

1.2.9.2 Functions of EBV BARF1 in oncogenicity and immunomodulation

Oncogenicity

The first evidence of involvement of BARF1 in the epithelial cell transformation progress came from that a large EBV fragment that includes the BARF1 ORF immortalizes primary monkey kidney epithelial cells. These immortalized cells expressed an EBV-specific 30 kd protein (Griffin and Karran, 1984), which was later on confirmed to be BARF1. Although injection of BARF1 transfectants into nude mice did not induce any tumor, expression of the BARF1 in *Erythrocebus patas*, a primary monkey kidney epithelial cell, led to the establishment of continuously dividing lines with characteristics of immortalized cells: morphological change, short cell doubling time, ability to divide at low cell density

and continuous growth over 50 passages (Wei et al., 1997). In other cells, Balb/c3T3 and NIH/3T3, both of which are established mouse fibroblasts, BARF1 expression induces a loss of contact inhibition, increased multiplication, morphological changes, anchorage-independent growth and tumorigenicity in newborn rats (Wei and Ooka, 1989). The first 54 amino acids of BARF1 were sufficient to both induce rodent fibroblast malignant transformation and activate Bcl-2 expression (Sheng et al., 2001).

Besides epithelial cells, non-tumorigenic Louckes lymphoid cells can be transformed by BARF1 as well (Wei et al., 1994). Activation of the c-myc proto-oncogene and increased expression of the B-cell surface proteins, the transferrin receptor, CD21, and CD23 were found in BARF1 expressing cells. The transformed cell induced a diffuse lymphoma-like tumor in newborn rats, although the tumors regressed after 3-4 weeks (Wei et al., 1994). Again, in EBV-negative Akata cells, BARF1 transfection induced tumor formation when they were injected into SCID mice (Sheng et al., 2003). However, BARF1 is dispensable for B cell transformation (Cohen and Lekstrom, 1999). A EBV mutant with BARF1 deleted transformed B-lymphocytes, and the B-lymphocytes transformed with the BARF1 mutant virus induced tumors in SCID mice with an efficiency similar to that of the wild-type virus (Cohen and Lekstrom, 1999).

Apart from these direct lines of evidence, BARF1 was also proposed to contribute to the epithelioid malignancy by other indirect information. It was noted that lymphocyte-derived EBV like B95.8 or Akata strain was not able to immortalize Patas cells, one type of epithelial cells, while EBV derived from NPC was able to, implying that an EBV isolate derived from an NPC tumor has better molecular equipment to penetrate and stably transform epithelial cells (Danve et al., 2001). It is probable that the products of several viral genes acted in synergy to establish the

growth-transformed phenotype of EBV-infected Patas cells. Among the gene products expressed in the transformed cells, BARF1 gene is likely to play a major role. Not only was the BARF1 protein consistently expressed in all Patas transformed clones (Danve et al., 2001) but it was previously shown that the BARF1 gene by itself can transform Patas epithelial cells (Wei et al., 1997). These EBV-transformed primary epithelial cells might become the prototype of a new type of EBV latency, characterized by coexpression of EBNA1 and BARF1 in the absence of LMP1 and another EBV nuclear protein, EBNA2 (Danve et al., 2001).

A possible mechanism of oncogenic transformation induced by BARF1 gene was proposed to be autocrine/paracrine and cell cycle activation by the secreted form of BARF1. Addition of purified BARF1 to serum-deprived culture medium, resulted in a specific activation of the cell cycle of not only Balb/c3T3 rodent fibroblastes but also human B-cell line and primary monkey kidney epithelial cells, implying that the BARF1 protein might have cell growth factor functions *in vivo* (Sall et al., 2004). Another mechanism called 'hit and run' was also suggested (Gao et al., 2002). Molecular evidence supports integration of viral information into the host chromosome, and an early genotypic alteration involving specific amplification of a sub-component (IR1) of BARF1 DNA, followed by apparent loss of viral DNA from chromosomes. Sporadic reintegration of surviving viral DNA into the host chromosome was also observed. Cellular genes were suggested to be involved in the process of malignancies induced by BARF1 (Gao et al., 2002). In addition, EBV transformed Patas epithelial cells were immortalized but not tumorigenic in nude mice (Wei et al., 1997), implying that a second cellular event will be necessary for inducing a malignant transformation in epithelial cells. So far, only Bcl-2 activation was observed in both EBV-negative human Akata B-lymphocytes and epithelial cells

transfected by BARF1 gene (Sheng et al., 2001; Sheng et al., 2003) and this Bcl-2 activation confers the BARF1 transfected cells resistance to apoptosis (Sheng et al., 2003).

Immunomodulation

BARF1 protein could function as a soluble receptor for human colony-stimulating factor 1 (CSF-1) (Strockbine et al., 1998) and could regulate immune response by inhibiting Alpha interferon secretion from mononuclear cells (Cohen and Lekstrom, 1999). On the other hand, BARF1 has been shown to serve as a target for antibody-dependent cellular cytotoxicity (ADCC) (Tanner et al., 1997). This protein may act in concert with *BCRF1* to inhibit interferon function and promote increased survival of EBV infected cells (Hsu et al., 1990).

1.3 Coronavirus

Coronaviruses are a group of large, enveloped, non-segmented, positive-stranded RNA viruses that replicate by a unique mechanism, which results in a high frequency of recombination (Lai and Holmes, 2001). The coronaviruses were first time recognized as a distinct group in the 1960s, with a typical corona-like morphology in negatively stained preparations (Berry et al., 1964; Almeida and Tyrrell, 1967). Later on, Toroviruses, which share genomic organization and a replication strategy with coronaviruses, were added to the family *Coronaviridae* (Cavanagh and Horzinek, 1993). The *Coronaviridae*, together with the family Arteriviridae, Roniviridae have been included in the order of Nidovirales (Cavanagh, 1997; de Vries et al., 1997; Mayo, 2002). The viruses in this order share a unique feature of synthesizing a nested set of multiple subgenomic (sg) mRNAs during their replication.

Coronaviruses and Toroviruses have several unique properties: 1) linear, non-segmented, positive-sense, single-stranded RNA genomes; 2) genome organization: 5'-replicase gene-structural protein genes-3'; 3) a 3' co-terminal nested set of four or more sg mRNAs; 4) the genomic RNA functions as the mRNA for the translation of gene I; 5) only the 5' unique regions of the mRNAs are translated (Cavanagh, 1997).

Coronaviruses were classified into four antigenic groups based on differences determined primarily by immunofluorescent assay, enzyme-linked immunosorbent assay, and immunoelectron microscopic (IEM) studies (Holmes, 1991). Mammalian group 1 includes human coronavirus 229E, canine coronavirus, feline infectious peritonitis virus (FIPV), transmissible gastroenteritis virus of swine (TGEV), and feline enteric coronavirus (FECV). Mammalian group 2 includes human coronavirus OC43, mouse hepatitis virus (MHV), bovine coronavirus (BCV), rabbit coronavirus (RbCV), porcine hemagglutinating encephalomyelitis virus (HEV) and sialodacryadentis virus (SDAV). IBV is the only member in antigenic group 3, while turkey coronavirus is the only member of antigenic group 4 (Holmes, 1991). Avian infectious bronchitis virus (IBV), the prototype member of the family *Coronaviridae*, was the first coronavirus isolated from the domestic fowl (Schalk and Hawn, 1931). Here IBV is used as a model to describe the replication and pathogenesis of coronavirus.

1.3.1 Avian infectious bronchitis virus

IBV is the etiologic agent of infectious bronchitis (IB) which causes an acute, highly contagious respiratory disease in chickens. The viral infection can affect the upper-respiratory tract, reproductive tract, and renal system. The disease is characterized by coughing, rales, sneezing and nasal discharge in young birds. IBV is

of considerable economic importance to the poultry industry as infection may result in death of young chicks and feed efficiency in older birds (King and Cavanagh, 1991).

1.3.2 Classification

The classification of IBV is useful for disease control, research and better understanding the epidemiology and evolution of this virus. IBV strains are mostly classified based on features of the spike proteins as neutralizing epitopes are located on this protein (Cavanagh, 1995). However, a clear classification of isolates is very difficult because of the high mutation frequency of the RNA genome, recombination, and multiple serologic cross-reactions among IBVs. There are mainly three methods for IBV typing.

1.3.2.1 Serotyping

The traditional method for typing is serotyping, which is based on the reaction between an IBV strain and IBV serotype-specific antibodies raised in chickens. The statistical method of Archetti and Horsfall is applied for differentiation of serotypes (Archetti et al., 1950). The S1 amino acid sequence of different IBV serotypes usually differ from 20% to 48% (Gelb et al., 1997). However, there are still some examples in which the S1 sequences of two serotypes differs only 3% to 7.6%. The main disadvantage of serotyping is the lack of standardization between the different systems and users.

1.3.2.2 Genotyping

Genotyping is based on genetic characterization of the genome. Contrast to serotyping, genotyping is frequently used because it is faster and more convenient. Methods include sequencing, detection of genotype-specific parts of the genome by RT-PCR, or determining the position of enzyme cleavage sites by restriction fragment length polymorphism (RFLP), and RNase T1 fingerprinting (Kusters et al., 1987;

Kwon et al., 1993; Keeler et al., 1998). The S1 subunit of the spike glycoprotein has been sequenced most frequently as the S1 protein determines serotype and plays a major role in the induction of protective immunity. Many S1 gene sequences have been published (Cavanagh and Davis, 1988; Wang et al., 1994; Gelb et al., 1997; Jia et al., 1995; Kingham et al., 2000; Mondal and Naqi, 2001; Mondal and Cardona, 2004). However, direct translation of information about the genome of an IBV strain to biological function or antigenicity of the virus is not possible. Isolates of the same serotype may differ significantly in some genes, while different serotypes can have high similarity between their sequences (Capua et al., 1998).

1.3.2.3 Protectotyping

Strains that induce protection against each other belong to the same protectotypes. To characterize a protectotype, an *in vivo* cross-immunization study has to be performed (Gelb et al., 1997). Although this method is labor intensive, expensive and requires animal facilities, protectotyping is important because it provides direct information about the efficacy of a vaccine.

1.3.3 Virion morphology

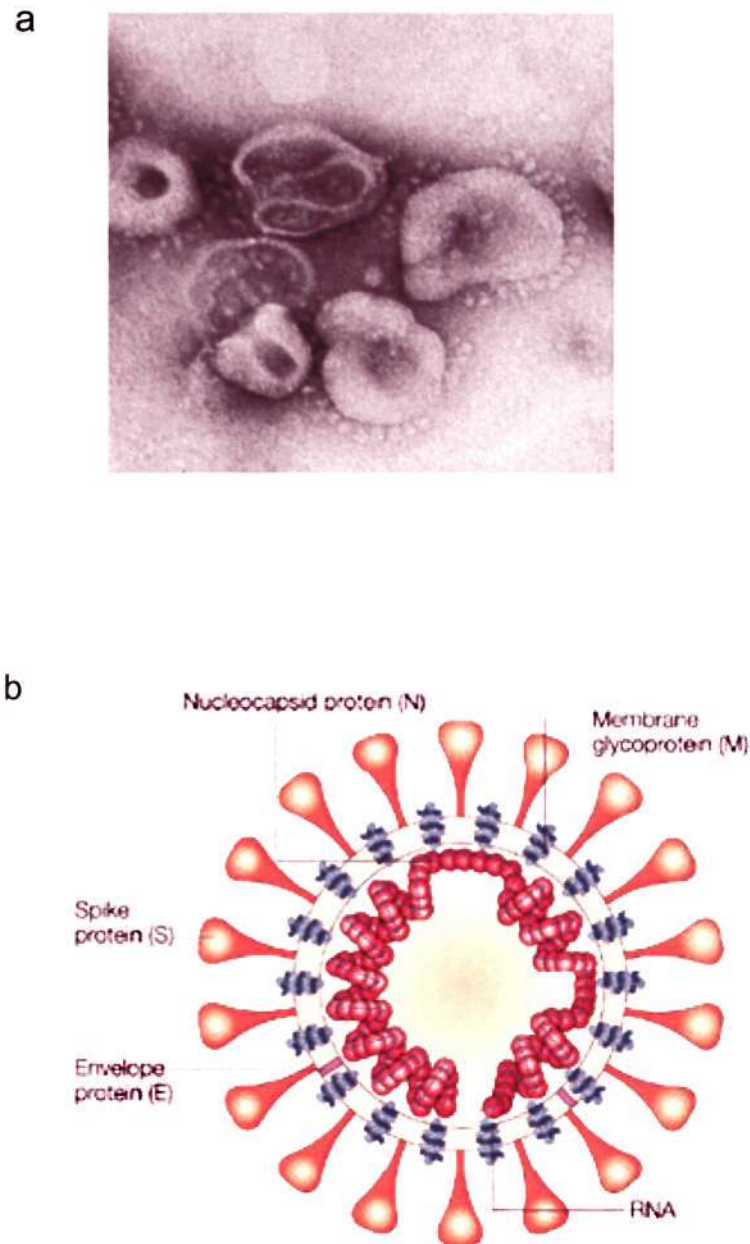
Coronaviridae were first separated from other virus groups based on the morphology examination by electron microscopy (Almeida and Tyrrell, 1967). The shape of IBV virion is more or less spherical, but pleomorphic particles can be seen in negative-stained preparations (Bingham and Almeida, 1977). The virion diameter is about 120 nm. Large club-shaped surface projections approximately 20 nm in length and 10 nm in width, also called spikes, create the distinct corona appearance under electron microscope (McIntosh et al., 1967; McIntosh, 1974). A bilipid layer of cell membrane origin surrounds the nucleocapsid of the virion making the virion sensitive to solvents (Otsuki et al., 1979). The envelope is associated with a membrane (M) and

envelope protein (E). A helical nucleocapsid consisting of the RNA genome and the nucleocapsid (N) protein is inside the envelope. Electron microscopic observation of viral RNP showed a long helix of 10 to 15 nm (Davies et al., 1981). Figure 1.2 shows the electron micrograph and schematic representation of IBV virion.

1.3.4 Genomic structure and mRNAs

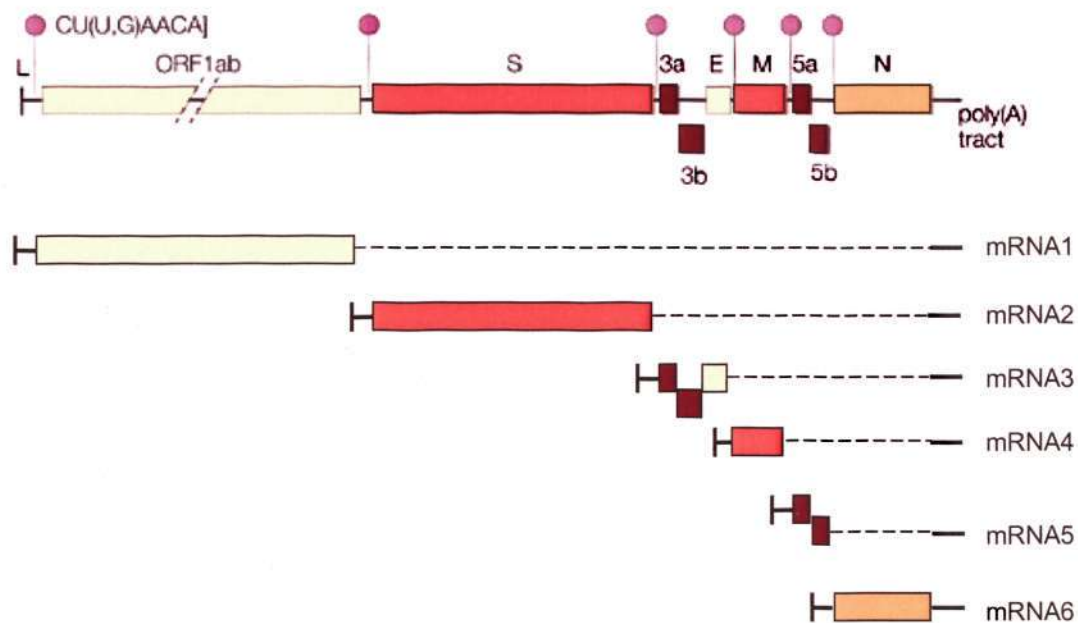
The IBV genome is a single-stranded, capped, polyadenylated, non-segmented linear RNA of approximately 27.6 kb in length (Bournsnell et al., 1984; Binns et al., 1985; Bournsnell et al., 1985a; Bournsnell et al., 1985b; Bournsnell et al., 1987). IBV genome structure is illustrated in Figure 1.3. The genomic RNA is infectious (Lomniczi, 1977), indicating that it can function directly in the infected cell as an RNA dependent polymerase encoding mRNA. In virus infected cells, five sg mRNA species are transcribed from genomic RNA (Stern and Kennedy, 1980a).

The 5' end of the IBV genome has an untranslated region (UTR) consisting of approximately 528 bases (Bournsnell et al., 1987). The 5' terminus of this UTR contains an approximately 64 nt fragment, called leader sequence. Leader sequence is also found at the 5' ends of all the sg mRNAs (Brown et al., 1984; Brown et al., 1986) and are thought to be involved in the regulation of viral replication, and in transcription of genomic and sg mRNAs (Brown and Bournsnell, 1984; Bournsnell et al., 1987). A stretch of consensus sequences (CUUAACAA or CUGAACAA), called intergenic (IG) sequences exist at both the 3' end of the leader sequence and upstream of each of the sg mRNA (Brown and Bournsnell, 1984; Bournsnell et al., 1987). Therefore, the six mRNA species, including one genomic mRNA and five sg mRNAs, starts from a different IG sequence and extends to the 3' end of the genome. They have a 3' co-terminal, nested set structure (Stern and Kennedy, 1980b). The 3' end of



(Adapted from Stadler et al., 2003)

Figure 1.2 (a) Electron micrograph of IBV particles. Large, club-shaped protrusions consisting of spike protein form a crown-like corona. **(b)** Schematic representation of IBV virion. A lipid bilayer comprising the spike protein, the membrane glycoprotein and the envelope protein cloaks the helical nucleocapsid, which consists of the nucleocapsid protein that is associated with the viral RNA.



(Adapted from Stadler et al., 2003)

Figure 1.3 IBV genome structure and mRNAs. The positions of the leader sequence (L) and poly(A) tract are indicated. Boxes of different colours indicate different IBV genes. Circles of purple colour represent group-specific transcription-regulatory sequences (TRS).

the IBV genome contains another UTR consisting of approximately 500 bases followed by poly(A) tail (Boursnell et al., 1985a).

The six mRNAs are named from 1 to 6 according to their size. The IBV genomic RNA serves as the largest mRNA (mRNA1) and five sg mRNA are named as mRNA2-6 according to their sizes (Cavanagh et al., 1990). The products of the IBV genes include both structural and non-structural proteins. mRNA1 encodes two large ORFs (1a and 1b) with ORF1a having the potential to encode a polyprotein of 441 kDa and ORF1b having the potential to encode a polyprotein of 300 kDa (Boursnell et al., 1987). The ORF1b is generated from a ribosomal frameshift as a fusion protein with ORF1a (Brierley et al., 1987; Brierley et al., 1989). This frameshift is mediated by an RNA-pseudoknot structure which causes slippage of the ribosomes on a stretch of adenines and uridines (UUUAAAC) just upstream of the pseudoknot (Brierley et al., 1989). Three structural proteins, the spike (S), membrane (M), and nucleocapsid (N), are encoded by sg mRNAs 2, 4, 6, respectively. The other two mRNAs, mRNA 3 and 5, which contain more than one ORF in their 5'-terminal unique regions, encode three and two viral polypeptides, respectively (Smith et al., 1990; Liu et al., 1991; Liu and Inglis, 1992a, Liu and Inglis, 1992b). Another small structural protein, envelope (E) protein, is encoded by ORF3c, which is in the 3' proximal of mRNA3 (Boursnell et al., 1985a; Smith et al., 1990; Liu and Inglis, 1991).

1.3.5 Viral Proteins

1.3.5.1 The replicase polyproteins

Proteolytic processing of the replicase polyproteins, ORF1a and ORF1a/1b, to smaller cleavage products is mediated by viral proteinases. Three proteinases domains, two overlapping papain-like proteinase (PL^{pro}) domains and a picornavirus 3C-like proteinase (3C-LP) domain, have been predicted in ORF1a (Boursnell et al., 1987;

Gorbalenya et al., 1989; Lee et al., 1991). The PL^{pro} domains encoded in the IBV sequence between nt 4243 and 5553, and the 3C-LP encoded between nt 8937 and 9357, are involved in the production of additional viral proteins required for other aspects of virus replication (Liu et al., 1994; Liu and Brown, 1995; Liu et al., 1995; Liu et al., 1997; Lim et al., 2000).

The IBV PL^{pro} domain-1 (PL1^{pro}), encoded between nt 4243 and 5019 (aa 1239-1497) is responsible for cleavage of the N-terminal regions of ORF1a and ORF1a/1b polyproteins to release an 87-kDa protein and a 195-kDa N-terminal product and a 41-kDa C terminal product in IBV-infected cells (Liu and Brown, 1995; Lim and Liu, 1998; Lim et al., 2000), whereas, the PL^{pro} domain-2 (PL2^{pro}) encoded between nt 4681-5553 (aa 1385-1675) is functionally inactive in IBV. A more important role in the processing of polyproteins is played by the 3C-PL that is responsible for the cleavage of other regions of ORF1a and ORF1a/1b polyproteins, resulting in the release of more than ten proteolysis-derived cleavage products (Liu et al. 1994; Liu and Brown, 1995; Liu et al. 1997; Liu et al. 1998; Ng and Liu, 1998; Tibbles et al., 1999; Ng and Liu, 2000; Ng and Liu, 2002). The processed products constitute a group of replicative enzymes, including the RNA-dependent RNA polymerase (RdRp) and RNA helicase. Because of its key role in replicase gene expression, 3C-LP has been termed the coronavirus main protease (M^{pro}) (Ziebuhr et al., 2000).

1.3.5.2 Spike protein (S)

The surface projections of coronavirus, which form the distinctive corona, are made up by the S protein. S protein is also responsible for attachment to cellular membranes and for fusion of virus envelope with cell membranes (Sturman et al., 1985). The precursor protein, S₀, is post-translationally cleaved into S₁ and S₂

(Cavanagh et al., 1986). The cleavage of S0 into S1 and S2 occurs at an arginine-rich sequence Arg-Arg-Phe-Arg-Arg (Cavanagh et al., 1986). The S1 is derived from the amino terminus of the S0 and consists of about 520 amino acid residues, while S2 is derived from the carboxyl terminus, consisting of about 625 amino acid residues. The S0 glycoprotein is about 180kDa (Niesters et al., 1986). The S1 and S2 are also large glycopolypeptides with the respective molecular weights of 90 and 84 kDa, respectively. Although S protein is responsible for cell fusion, a large portion remains intracellular and the intracellular portion may play roles in pathogenesis (Lontok et al., 2004).

The antigenicity of IBV and other coronaviruses mostly resides in the S protein region as S protein can induce humoral neutralizing and hemagglutination-inhibiting antibody (Cavanagh et al., 1984). The S1 subunit of S protein is the main target for the antigenic variation among different IBV strains. Serotype-specific monoclonal antibodies against S1 neutralize the IBV virus and inhibit hemagglutination (HA) and virus lacking S1 is defective in inducing neutralizing and HA-inhibiting antibodies (Mockett et al., 1984; Cavanagh and Davis, 1986). In addition, purified S1 protein is able to elicit neutralizing antibodies (Cavanagh et al., 1986). From data obtained using monoclonal antibodies, there appears to be at least three to five neutralizing, conformationally dependent epitopes on the S1 subunit in different IBV strains (Karaca et al., 1992; Parr and Collisson, 1993), although S2 also appears to contain one antigenic region (Ignjatovic and Sapats, 2005). One or more of these epitopes are known to be serotypic determinant (Karaca et al., 1992). Based on AA substitutions in monoclonal antibody Neutralization-resistant (NR) mutants, the S1 subunit was divided into three regions (I: residues 38-67, II: residues 91-141, and

III: residues 274-387) associated with neutralizing, conformationally dependent epitopes (Kant et al., 1992).

However, although removal of S1 region abolished the virus infectivity and haemagglutination, the attachment of virus to cells was still observed (Cavanagh and Davis, 1986). It was argued that receptor binding is mediated by S2 and both S1 and S2 are required for infectivity. The S2 subunit is attached to the virus membrane by a small hydrophobic transmembrane segment, in which two long α -helices are located in the C-terminal half of S2, forming a coiled-coil structure. (Cavanagh, 1983a; Cavanagh, 1983b; de Groot et al., 1987). While S2 subunit constitutes the stack of the peplomer, the S1 subunit, which is non-covalently bound to S2, forms the bulb (Cavanagh et al, 1983a, Cavanagh et al., 1983b; de Groot et al, 1987). Comparing to S1, the sequence of S2 subunit is quite conservative, thus it plays little role in the induction of a host immune response (Cavanagh, 1995). Even though, neutralizing, but not serotype specific antibodies were still induced by an immunodominant region localized in the N-terminal half of the S2 subunit (Kusters et al., 1989). Furthermore, secondary structure of the S2 protein from several IBV strains suggested that the S2 subunit can affect binding of S1 subunit specific antibody due to S2 gene variability and subsequent secondary structure differences (Callison et al, 1999).

1.3.5.3 Nucleocapsid protein (N)

The N protein of IBV contains 409 amino acid residues with a predicted molecular weight of about 50 kDa (Stern and Sefton, 1982a; Boursnell et al, 1985b). The protein plays a role in viral replication, assembly, and immunity. The N forms a helical structure with IBV genomic RNA (Lai and Cavanagh, 1997). It also interacts with leader RNA sequences, and is involved in viral mRNA synthesis (Collisson, 1995). Two RNA binding domains for the 3' non-coding terminal RNA, one in the

amino region and the other in the carboxy region, were found in the N protein (Zhou and Collisson, 2000). Dimerization of the C-terminal domain of IBV N protein leads to oligomerization of this protein and viral RNA condensation (Fan et al., 2005; Jayaram et al., 2006). N protein localizes to the cytoplasm and nucleolus both in IBV-infected cells and in cells overexpressing IBV N protein (Hiscox et al., 2001). In nucleolus, N protein interacts with two nucleolar antigens, fibrillarin and nucleolin and these interactions may explain the cell growth inhibition after IBV infection (Chen et al., 2002).

The N protein is immunogenic and induces cross-reactive antibodies (Ignjatovic and Galli, 1993). Linear B-cell epitopes were found in three fragments covering amino acid residues 175-241, 310-370, and 360-409 (Seah et al., 2000). Immunization of chickens with the purified N did not induce protection against virulent challenge whereas the carboxyl-terminal 120 residue polypeptide of N induced cytotoxic T lymphocytes and could protect chickens from acute infection (Ignjatovic and Galli, 1993; Seo et al., 1997).

1.3.5.4 Membrane protein (M)

The M protein is associated with virion membrane, with the major portion embedded in the virion membrane and minor portion projecting outside of the envelope (Cavanagh, 1981). The IBV M protein is also a glycoprotein. The molecular weight of IBV M protein varies from approximately 26-36 kDa depending on the degree of glycosylation (Stern and Sefton, 1982b). The oligosaccharides of IBV M have a high mannose content and are bound to the external amino terminus (Asn-X-Thr/Ser residues) through N- linkages (Rottier, 1995). This differs from MHV M protein, which has O-linked glycosylation (Rottier, 1995). Three distinct hydrophobic regions consisting of 22, 20, and 23 residues, are separated by two short hydrophilic

regions of 9 and 33 residues, respectively according to the computational analysis (Boursnell, 1984). Each of the three hydrophobic regions has the potential to span the envelope membrane once (Boursnell, 1984). The small N-terminal hydrophilic domain is exposed to the outside of the membrane, and the C-terminal hydrophilic domain may extend into the inner surface of the membrane interacting with viral RNA in the nucleocapsid (Boursnell, 1984). Most portion of the protein still lies within the virion membrane as the hydrophilic regions are quite short (Boursnell, 1984). The first 20 amino acids in the N-terminus vary among strains since it encodes for the amino terminus of the M glycoprotein which is on the surface of the virion exposed to the immune system, while the rest sequence is conserved (Cavanagh and Davis, 1988).

The M protein is essential for the formation of viral membrane and virion budding (Stern and Sefton, 1982a). It contains two Golgi retention signals which are required for targeting associated complex to Golgi (Machamer et al., 1993). The M and E protein are essential for viral envelope formation and the release of virus particle. These two protein together can form Virus like particles (VLPs), which are indistinguishable from authentic virions (Corse and Machamer, 2000).

1.3.5.5 Envelope protein (E)

The E protein is produced from the 3' region of sg mRNA 3 and contains approximately 100 amino acids (Boursnell et al., 1985a). It was found that this protein is associated with the viral envelope, and thus represent a new structural protein (Liu and Inglis, 1991). It is an integral membrane protein when expressed in cells with the C terminus in cytoplasm (Corse and Machamer, 2000). Indirect immunofluorescence microscopy showed that E is localized to the Golgi complex in cells transiently expressing IBV E and the cytoplasmic tail is necessary and sufficient for Golgi targeting (Corse and Machamer, 2000; Corse and Machamer, 2002). IBV E physically

interacts with M protein in transfected cells and this two protein can be crosslinked to form VLPs in IBV-infected and transfected cells via their cytoplasmic domains (Lim and Liu, 2001; Corse and Machamer, 2003). Although IBV E is present at low levels in virions, it is apparently expressed at high levels in infected cells near the site of virus assembly (Corse and Machamer, 2000).

Coronavirus E protein plays an essential role in virus assembly (Vennema et al., 1996; Baudoux et al., 1998; Fischer et al., 1998; Maeda et al., 1999). Co-expression of coronavirus M protein and E protein results in the production of virus-like particles (VLPs), while expression of M protein alone does not produce VLPs (Bos et al., 1996; Vennema et al., 1996; Baudoux et al., 1998). Further, E protein alone can drive the production and release of coronavirus envelope in the absence of M protein (Maeda et al., 1999). The coronavirus E protein may also play a role in morphogenesis, because MHV mutants encoding mutated E protein are morphologically aberrant although the replication is not affected (Fischer et al., 1998; Kuo and Masters, 2003).

1.3.5.6 Non-structural proteins

Four small nonstructural proteins, 3a, 3b, 5a, and 5b, are produced by sg mRNAs 3 and 5. Similar small ORFs, interspersed among the structural protein genes are also found in other coronaviruses (de Vries et al., 1997). The 3a, 3b, 5a, and 5b proteins of IBV have been identified in virus infected cells (Liu and Inglis, 1991; Liu and Inglis, 1992a). Neither the RNA nor the proteins of 3a and 3b are essential for IBV replication (Hodgson et al., 2006). IBV 3a is partially targeted to a novel domain of the smooth ER (Pendleton and Machamer, 2005). The normal 3b protein was shown to localize to the nucleus, whereas the truncated form showed a diffuse distribution pattern (Shen et al., 2003). A mutant with a defective 3b gene encoding a C-terminally

truncated product was characterized and the mutant was shown to grow well in cultured cells and in chicken embryos, indicating that the 3b gene is not essential for IBV replication (Shen et al., 2003). Proteins 5a and 5b are also accessory proteins that are not essential for replication (Casais et al., 2005; Youn et al., 2005).

1.3.6 Virus Replication

The replication mechanisms of some coronaviruses has been studied extensively and are clear. However, the precise IBV replication mechanism is not fully studied although there could be many similarities among different coronaviruses (Brian and Baric, 2005). Here, the general mechanism of coronavirus replication is discussed.

1.3.6.1 Attachment and Penetration

The replication cycle of coronaviruses starts with the specific binding of the virion to the membrane of the target cells. Cellular receptors have been identified for several coronaviruses. Aminopeptidase N (APN) acts as the receptor for group 1 coronaviruses including TGEV, HCoV 229E, CCoV, and FIPV (Delmas et al., 1992; Tresnan et al., 1996; Yeager et al., 1992). The APN receptor is widely expressed in on many cell types including respiratory and enteric epithelial cells and neuronal and glial cells (Kusters et al., 1989). The carcinoembryonic antigen-cell adhesion molecular (CEACAM), which is expressed mainly in the liver and gastrointestinal tissues, is the receptor for MHV (Dveksler et al., 1993; Williams et al., 1991; Coutelier et al., 1994; Godfraind et al., 1995). Angiotensin-converting enzyme 2 (ACE2) is employed by SARS-CoV and human coronavirus (HCoV-NL63) as the receptor (Li et al., 2003; Hofmann et al., 2005). CD209L may also serves as the receptor for SARS-CoV (Jeffers et al., 2004). However, although IBV can use APN as the receptor in vitro (Miguel et al., 2002), the IBV receptor in its native or adapted

host cells remains unknown yet. Neuraminidase treatment showed that sialic acid is a receptor determinant for IBV infection during the primary viral attachment to host cells (Winter et al., 2006).

Coronaviruses are generally highly species specific *in vivo* and *in vitro*. The viral protein responsible for binding to the specific cellular receptors and for cell fusion is S protein (Sturman et al., 1985). S protein is the main determinant of the species tropism. A recombinant porcine coronavirus transmissible gastroenteritis virus (TGEV) containing the S gene from an enteric TGEV was shown to have acquired enteric tropism (Sanchez et al., 1999). When the S protein ectodomain of MHV was replaced with the corresponding sequence from coronavirus feline infectious peritonitis virus (FIPV), the resulting virus lost the ability to infect murine cells in tissue culture (Kuo et al., 2000). The reintroduction of the FIPV spike to a mutant FIPV (mFIPV) which has its S region replaced by MHV S gene allowed for regaining the ability to grow in feline cells (Haijema et al., 2003). The role of IBV S glycoprotein in cell tropism was also studied using reverse genetics system. A recombinant IBV, BeauR-M41(S), in which the ectodomain region of the spike gene from IBV M41-CK replaced the corresponding region of the IBV Beaudette genome, acquired the same cell tropism as IBV M41-CK (Casais et al., 2003).

After attachment of virus to the host cell, virus will be internalized and transported to the cytoplasmic organelles where the virus replicates. However, the mechanism by which coronavirus uncoats and releases its genomic RNA is not clear yet.

1.3.6.2 Viral mRNA transcription

Similar to most positive stranded RNA viruses, after releasing the genomic RNA into host cells, the RNA dependent RNA polymerase is translated from the 5'

20kb region of the viral RNA (van der Most and Spaan, 1995). The major difference of coronavirus replication compared to other positive strand RNA viruses are the synthesis of the sg mRNAs as well as sized mRNAs by a leader-body fusion mechanism (Lai et al., 1994; Cavanagh, 1997).

Several models have been proposed to explain the generation of sg RNAs for coronavirus mRNA transcription. A traditional splicing model has been suggested to describe sg RNA synthesis in coronavirus but it has been ruled out (Brayton et al., 1981; Jacobs et al., 1981). Another two discontinuous or quasi-discontinuous transcription models have been suggested (van der Most and Spaan, 1995; Lai and Cavanagh, 1997).

The first model is leader primed transcription. According to this model, discontinuous transcription occurs during positive stranded RNA synthesis. Leader RNAs are transcribed at the 3' end of the negative stranded RNA template and subsequently bind to any IG sequence on the negative stranded RNA template. Leader RNA serves as the primer for sg mRNA transcription. This model was supported by the detection of several small leader sequence related RNA species in the cytoplasm of MHV infected cells (Baric et al., 1985). The second model is the discontinuous extension of negative stranded transcription (Sawicki and Sawicki, 1998). In this model, RdRp pauses at one of the IG sequences and then jumps to the 3' end of the leader sequence on the genomic RNA template during negative stranded RNA synthesis, generating a sg negative stranded RNA with an antisense leader sequence at its 3' end. This incomplete sg sized negative stranded RNA then serves as template for sg mRNA synthesis. Several studies have shown that both genomic and sg sized negative stranded RNAs are present even though positive stranded RNA is present at a higher amount (Sawicki and Sawicki, 1990; Sethna et al., 1991; Schaad and Baric,

1994; Baric and Yount, 2000). Both models are supported by indirect evidence and are still debated.

1.3.6.3 Viral protein translation

After transcription, viral protein is translated from each sg RNA (Luytjes, 1995). All the sg RNAs, except the last smallest one, are polycistronic. But only the 5' first ORF is translated; thus, most of these mRNAs are functionally monocistronic. Most of the structural proteins, including S, M, N, are translated from separate mRNAs by a cap-dependent ribosomal scanning mechanism. Other viral proteins are translated by other mechanisms. mRNA1 is translated into two polyproteins (1a and 1b) by a ribosomal frameshifting mechanism (Brierley et al., 1992). In mRNA3, the third ORF is most efficiently translated as this ORF is preceded by an internal ribosomal entry site sequence, which allows ribosomes to bypass the upstream ORFs and translate the third one by a cap-independent mechanism. (Liu and Inglis, 1992a; Theil and Siddell, 1994). The mRNA5 contains two overlapping ORFs, 5a and 5b, both of which are translated by unknown mechanism (Liu and Inglis, 1992b).

1.3.6.4 Virion Assembly and Release

The exact mechanism of IBV assembly is still unclear. Most of the available information is from studies on MHV. The binding of N protein to viral RNA, forming helical nucleocapsids, is essential for encapsidation, but not enough for RNA packaging into mature virions (Baric et al., 1988). All MHV mRNAs associate with N protein to form RNP complex, but only mRNA1 RNP complex is efficiently packaged into virus particles (Narayanan et al., 2000). It has been suggested that in MHV, N protein and viral genomic RNA forms nucleocapsids and then M protein interact with packaging signal sequence of genomic RNA to generate virion. The MHV M protein can specifically interact with RNA transcripts in the absence of N protein (Narayanan

et al., 2003). M and E protein play important roles in the virion assembly. Co-expression of M and E protein or singly expressing E protein results in the assembly of coronavirus like particles (Bos et al., 1996; Vennema et al., 1996; Baudoux et al., 1998; Maeda et al., 1999; Corse and Machamer, 2000). The interaction of S and M protein draws S protein to the *cis*-Golgi, where the virus obtains its lipid bilayer and buds (Krijnse-Locker et al., 1994). After budding, virus particles may undergo further morphologic changes within the Golgi apparatus, resulting in the appearance of mature virus particles with a compact, electron-dense internal core, as they reach the secretory vesicles (Risco et al., 1998; Salanueva et al., 1999).

1.3.7 Evolution of IBV

IBV evolution can be observed through the occurrence of different variants or serotypes. Since the isolation of IBV in the 1930s, over 50 serotypes or variants have been reported worldwide. The causes of the emerging of variant serotypes are thought to be the quasispecies nature of RNA viruses, immune pressure by wide spread vaccine use, and environmental conditions (Cavanagh and Naqi, 1997).

Mutation rates for RNA viruses have been estimated in the range of 10^{-3} to 10^{-5} substitutions per nucleotide due to the fact that RNA polymerase lacks the 3'→5' exonuclease activity (Garrett and Grisham, 1999; Novella et al., 2003; Moya et al., 2004). IBV genome contains approximately 30,000 nucleotides; therefore, an average of three mutations per template copied will result in mutation rates of 10^{-4} substitutions per nucleotide. Because of their high rates of mutation, genetic drift, a process of accumulation of point mutations in viral genes, usually occurs. If the point mutation accumulates in the antigenic domain of the viral proteins, a virus with slightly changed antigenic structure will appear. In IBV, new serotypes can arise from antigenic drift in the S gene. For example, the S1 glycoprotein of the CU-T2 strain

carries virus-neutralizing and serotype-specific epitopes of two IBV serotypes, Arkansas and Mass (Jia et al., 1995).

Among all IBV genes, the S1 gene is the most variable because it contains serotype specific and virus neutralizing epitopes (Kusters et al., 1989; Wang et al., 1994; Kwon and Jackwood, 1995; Moore et al., 1998). Between strains of different serotypes, S1 region variation may be as low as 2-3% or as high as 49% (148). Hypervariable regions (HVR) among European IBV strains and within the Mass serotype have been identified and were named as HVR I (residues 56-69) and HVR II (residue 117-131) (Cavanagh et al., 1988; Kusters et al., 1989).

Several different viral genotypes will co-exist in the host during the generic or antigenic drift and each genotype probably has different levels of fitness (Domingo et al., 1985). Recombination between these different genotypes, which is a fast and efficient way to create or spread beneficial combinations of mutations, occurs in coronaviruses frequently (Banner et al., 1990; Banner and Lai, 1991; Jia et al., 1995). Recombination can occur in either segmented or unsegmented viruses when donor nucleotide sequence is introduced into a single, contiguous acceptor RNA molecule to produce a new RNA containing genetic information from more than one source (Worobey and Holmes, 1999). By conducting sequence and phylogenetic analysis, many IBV strains are thought to be a recombinant (Kusters et al., 1990; Wang et al., 1993; Wang et al., 1994;). The S1 HVRs are a 'hot spot' for exchanging genetic material between IBV strains (Wang et al., 1993; Wang et al., 1994), but not an exclusive region.

1.4 Aim of the project

In this thesis, EBV and IBV were used as two model systems to investigate the virus-host interactions.

1.4.1 EBV BARF1 and its interaction with hTid1

EBV BARF1 gene encodes a secretory protein with transforming and mitogenic activities. The first purpose of this study is to characterize the biochemical properties of BARF1, including post-translational modification, oligomerization, maturation and secretion of BARF1. The protein was shown to be post-translationally modified by N-linked glycosylation on the asparagine 95 residue. Cysteine 146 and 201 were also essential for proper folding and secretion of the protein. The second purpose of this study is to search for human proteins involved in the maturation process of BARF1. A yeast two-hybrid screening was carried out using the BARF1 as bait, leading to the identification of human hTid1 protein as a potential interacting protein. This interaction was subsequently confirmed by coimmunoprecipitation and dual immunofluorescent labeling of cells coexpressing BARF1 and hTid1. Coexpression of BARF1 with hTid1 demonstrated that hTid1 could promote secretion of BARF1, suggesting that hTid1 may act as a chaperone to facilitate the folding, processing and maturation of BARF1.

1.4.2 IBV cell tropism and pathogenesis

The second part of this thesis is to study IBV cell tropism and pathogenesis. Although coronavirus was thought to be restricted in host range, recently SARS-CoV crossed species from palm civet cats to infect humans (Guan et al., 2003). How a coronavirus breaks the host species barrier to adapt to new host is an intriguing issue. Here IBV is used as a model to study this. Once believed to infect chicken only, IBV has been adapted to Vero cells by serially passage (Shen et al., 2003). In this study, the Vero-adapted IBV was continuously passed to p20 in another five human cell lines, including H1299, HCT116, HepG2, Hep3B and Huh7, but other cell lines with similar organ and tissue origins were more resistant to IBV infection. The purpose of

this project is to study IBV infection in these cells and analyze the determinants of cell susceptibility to IBV infection. Few genotypic changes were found in the IBV spike protein during passage of IBV from Vero cells to these human cell lines. The involvement of two host genes, *IFN- β* and *ISG15*, which are important in anti-viral defense, in IBV infection was also studied.

Chapter Two

Materials and Methods

2.1 Materials

2.1.1 General reagents

General reagents and solvents were analytical grade, and were obtained from Aldrich Chemical Company Ltd., BDH Chemicals Ltd., Becton-Dickenson Ltd., Gibco Ltd., Pierce Ltd., Sigma Chemical Company Ltd., unless otherwise stated. Solutions were sterilized where required, by autoclaving at 15 pounds per square for 20 min, or by passing through a 0.22 μ m filter (Millipore).

2.1.2 Enzymes

All restriction endonucleases and other enzymes were obtained from New England Biolabs, Promega Ltd., Fermentus Ltd., Roche Diagnostics unless other stated and were used according to the manufacturers' instructions.

2.1.3 Commercial kits

ECL Detection Kit	GE Health Care
Plasmid Maxi Kit	QIAGEN Ltd.
QIAprep Spin MINIprep Kit	QIAGEN Ltd.
QIAquick Gel Extraction Kit	QIAGEN Ltd.
QIAquick PCR purification Kit	QIAGEN Ltd.
RNeasy mini Kit	QIAGEN Ltd.
Blood and Cell Culture Mini Kit	QIAGEN Ltd.

2.1.4 DNA vectors

pcDNA3.1(+)	Invitrogen
pGBKT7	Clontech
pACT2	Clontech

2.1.5 Escherichia coli (E. coli)

Strain DH5 α

E. coli strain DH5 α was used for transformation and preparation of plasmids.

Strain MC106

E. coli strain MC106 was used for electroporation of yeast plasmids generated from yeast two hybrid screening.

2.1.6 Yeast

Yeast strain AH109 was used for library screening and to assay for protein and protein interactions. By using this strain, this system employs three nutrition selections: ADE2, HIS3, and MEL1 (or LacZ). The ADE2 reporter alone provides strong nutrition selection, the HIS3 selection reduces the incidence of false positives, and the MEL1 or LacZ that encodes α -galactosidase and β -galactosidase can be assayed directly on X- α -gal or X-gal indicator plates.

2.1.7 Mammalian cells

A549 cell line is a human lung carcinoma cell line derived from a 58 years old Caucasian male. BHK-21 cell line is a baby hamster kidney fibroblast cell line. CHO cell line is a Chinese hamster ovary cell line. Cos-7 cell line is an African green monkey kidney fibroblast cell line derived from CV-1, a simian cell line (*cercopithecus aethiops*), by transformation with an origin-defective mutant of SV-40. DLD-1 and DLD-1A mix are epithelial cancer cell lines derived from a human colorectal adenocarcinoma. HCT116 cell line is an epithelial cell line derived from a human colon carcinoma. HeLa cell line is an epithelial cell line derived from a carcinoma of the cervix of a 31-year-old African-American female. Hep3B, HepG2 and Huh-7 are epithelial cell lines derived from human hepatomas. H1299 cell line is an epithelial cell line derived from a human lung carcinoma. Vero cell line is an epithelial cell line derived from African green monkey kidney. 293T cell line is a

highly transfectable derivative of the 293 cell line into which the temperature sensitive gene for SV40 T-antigen was inserted.

2.1.8 Viruses

The Beaudette strain of IBV was purchased from ATCC and propagated in chicken embryonated eggs for three passages. The viruses were then adapted to grow and passage on Vero cells for 65 passages at 37 °C and used to infect other cell lines.

2.1.9 Media

2.1.9.1 Bacterial media

Luria Broth (LB) was prepared by adding 10 grams of Bacto-tryptone, 5 grams of Bacto-yeast extract and 5 grams of sodium chloride per liter of distilled water. The media was autoclaved and allowed to cool. Ampicillin was added to 50-100ug/ml to select for plasmids carrying the ampicillin resistance gene. For agar plates, 15g/L of agar was added prior to autoclaving.

2.1.9.2 Yeast media

YPD media

YPD media was prepared by adding per 950 ml of distilled water, 20 grams of peptone and 10 grams of yeast extract. After autoclaving, 50 ml of 40% glucose was added to bring the final glucose concentration to 2%. For agar plates, 15 g/L of agar was added prior to autoclaving.

SD synthetic media

SD media was prepared by adding 6.7 grams of yeast nitrogen bases without amino acids to 950 ml of distilled water. Amino acids were added depending on the selectable marker present on the plasmid being transformed. A10x dropout solution of amino acids was prepared with the appropriate amino acid(s) left out. After

autoclaving, 50 ml of 40% glucose was added. The 10 X amino acid dropout solution contained:

Amino acid	mg/l
L-Isoleucine	300
L-Valine	1500
L-Adenosine hemisulfate salt	200
L-Arginine HCl	200
L-Histidine HCl monohydrate	200
L-Leucine	1000
L-Lysine HCl	300
L-Methionine	200
L-Phenylalanine	500
L-Threonine	2000
L-Tryptophan	200
L-Tyrosine	300
L-Uracil	200

2.1.9.3 Mammalian cell culture media

DMEM medium (JRH) with 10% fetal bovine serum (FBS) and 1% penicillin/streptomycin was used for the growth of A549, BHK, CHO, HeLa, HepG2, Hep3B, Huh-7, Vero, 293T cell lines. RPMI 1640 medium (JRH) with 10% FBS and 1% penicillin/streptomycin was used for the growth of Cos-7, DLD-1, DLD-1A mix, H1299 cell lines. MyCoy's 5a medium (Sigma) supplemented with 10% FBS and 1% penicillin/streptomycin was used for the growth of HCT116 cell line.

2.1.10 Buffers and solutions

Cell frozen medium	10% DMSO in FBS
--------------------	-----------------

Western blocking buffer (PBS-T)	1 x PBS containing 5% non-fat milk, 0.1% Tween20
Western transferring buffer	25mM Tris, 250mM Glycine, 15% Methanol
10x SDS Running buffer	0.25M Tris, 1.9M glycine, 1% (w/v) SDS
4x Resolution gel buffer	0.25 Tris, 0.4% (w/v) SDS, pH8.8
4x Stacking gel buffer	0.5M Tris, 0.4% (w/v) SDS, pH6.8
Co-immunoprecipitation lysis buffer	50 mM Tris pH 7.5, 150 mM NaCl, 1% (w/v) NP-40

2.1.11 Antibodies

Rabbit polyclonal and mouse monoclonal HA antibody, hTid-1(RS13) monoclonal antibody were obtained from Santa Cruz. β -actin and His rabbit polyclonal antibodies were purchased from Delta Biolabs. Flag monoclonal antibody and rabbit polyclonal IFN- β antibody were purchased from Sigma. Rabbit polyclonal calnexin antibody was purchased from Abcam. ISG15 polyclonal antibody was purchase from Rockland. Antibodies against IBV S, N, M proteins were raised by injecting purified peptides into rabbit in Institute of Molecular and Cell Biology, Singapore.

2.2 Methods

2.2.1 General methods for DNA and RNA manipulation

2.2.1.1 Quantification of DNA

DNA concentration was determined by its absorbance at wavelength of 260nm based on the calculation: 50mg/ml double-stranded DNA gives an OD₂₆₀ of 1. The OD₂₈₀ was also read and the ratio of OD₂₆₀/OD₂₈₀ was calculated to estimate the purity of the DNA preparations. An OD₂₆₀/OD₂₈₀ ratio between 1.6-2.0 was considered satisfactory.

2.2.1.2 Restriction endonuclease digestion

Restriction endonuclease digestions were usually carried out in a 20-100 μ l reaction volume, with 2-5 U of enzyme used for up to 500 ng DNA, for 1-18 h at an appropriate temperature. Commercially available 10x buffers were used according to the manufacturers' instructions. Digestions with more than one enzyme were carried out simultaneously in a suitable buffer wherever possible. When the buffer requirements were incompatible, restriction digestions were performed sequentially with individual buffer for each enzyme.

2.2.1.3 DNA separation by agarose gel electrophoresis

A 50 ml of 0.8% (w/v) Agarose gel was routinely used for analysis of 0.1-8 kb DNA fragments. Agarose was melt in 1x TBE, cooled to 55°C, before adding ethidium bromide to a final concentration of 1 mg/ml, then casting in a horizontal minigel apparatus. The gel was left to set at room temperature for at least 30 min. electrophoresis was carried out in horizontal apparatus with the gel submerged in 1x TBE, at < 100mA. DNA samples were loaded with one-fifth volume glycerol loading dyes. A standard DNA ladder was also run to allow estimation of the sizes of the sample DNA fragments. DNA fragments were visualized by fluorescence over a UV light (302 nm, UV transilluminator TM-20, UVP), under which DNA/EB complexes fluoresce and the image was recorded.

2.2.1.4 Purification of DNA fragments by agarose gel electrophoresis

When a particular fragment of DNA in a mixture of fragments was required, it was routinely separated from other fragments by agarose gel electrophoresis. Gel slice containing the DNA fragments to be purified were cut from the gel. DNA was extracted using a QIAquick Gel Extraction Kit (Qiagen).

2.2.1.5 DNA ligation

DNA fragments with complementary ends to be ligated were prepared by restriction enzyme digestion and where necessary treated with alkaline phosphatase and/or purified using agarose gel electrophoresis to reduce background ligations. Vector DNA (~ 10 ng) and insert DNA (20-40 ng) were ligated by incubation at RT for 2-3 h, using 1U of T4 DNA ligase in a 20 µl reaction mixture contain 1mM ATP, 50 mM Tris-HCl pH 8.0, 10mM MgCl₂, 20 mM DTT, 50 µl/mg BSA. A reaction without insert DNA was included in the experiments as controls.

2.2.1.6 Preparation of *E. coli* competent cells

The *E.coli* strain DH5α was used to prepare competent cells in advance which were stored at -70°C. A fresh plate of cells was prepared by streaking out cells from frozen stocks and growing overnight at 37°C. On the second day, an individual colony was picked and grown in 10 ml LB broth culture overnight. On the third day, 5 ml of overnight culture was transferred into each of two flasks containing 500 ml LB broth. Incubate at 37°C with aeration until the culture reaches OD₅₅₀ of 0.5. This should take approximately 2 h. The cells were transferred to centrifuge bottles and spin at 4°C for 8 min at 8000 rpm. Pellets were gently resuspended in 250 ml ice cold 0.1 M CaCl₂ and combined into a single bottle. Cells were resuspended again in 250 ml ice cold 0.1 M CaCl₂ and centrifuged at 8000 rpm for 8 min at 4°C. Finally the pellet was resuspended in 43 ml ice cold 0.1 M CaCl₂ in ddH₂O with 7 ml sterile glycerol. Competent cells were distributed into convenient aliquots (0.2 ml) in cold micro-centrifuge tubes. Cells were store at -70°C. A portion of the cells was saved to assay for viability, purity and competence.

2.2.1.7 Transformation of competent *E. coli* cell with plasmid DNA by heat shock

For each transformation, only 50-100 μ l of competent cells are necessary. Competent cells thaw on ice. DNA was added to cells (the volume of DNA should not exceed 40% of the cell volume). The mixture was incubated on ice for 20-30 min followed by a heat shock in a 42°C water bath for 2 min. 1 ml LB broth was added to the tube. The tube was incubated at 37°C with constant shaking for 30 min to 1h. 50-500 μ l of the mixture was streaked out onto plates containing the appropriate antibiotics.

2.2.1.8 Transformation of competent *E. coli* cell with plasmid DNA by electroporation

1 μ g yeast plasmid was gently mixed with 100 μ l of frozen competent cells and transferred to a disposable PulserTM Cuvette (Bio-rad), before pulsing at 1.8 kV(EasyJect, Iwaki). After electroporation, the DNA-cell mixture was transferred to a sterile eppendorf tube containing 100 μ l of LB media, and incubated at 37 °C with shaking for 1 h before plating onto LB plates containing the appropriate selective agent.

2.2.1.9 Extraction of plasmid DNA

For small scale purification of plasmid DNA, 3ml LB with appropriate antibiotics was inoculated with a single colony from an agar plate and incubated at 37°C with constant shaking overnight. Plasmids were extracted by using Qiagen Mini Plasmid kit. For large scale purification of plasmid DNA, a Plasmid Maxi Kit (QIAGEN) was used according to the manufacturers' instructions. This kit routinely yielded between 200-750 μ g DNA from 100 ml of overnight bacterial cultures.

2.2.1.10 Polymerase chain reaction (PCR)

PCR was routinely performed in a 50 μ l reaction volume containing less than 1 μ g template DNA, 1 μ M of each oligonucleotide primer, 200 μ M of each dNTP and 1 U DNA polymerase. Taq polymerase was used for PCR colony screening. Pfu DNA polymerase, which possesses a 3'-5' proofreading activity resulting in a twelve fold increase in fidelity of DNA synthesis over Taq DNA polymerase, was used for high fidelity DNA synthesis. Each polymerase has its own reaction buffer, normally supplied by the manufacturer. The reaction mixtures were subjected to a varying number of cycles of amplification in the DNA Thermal Cycler automated machine (MJ research).

2.2.1.11 Identification of colonies that contain recombinant plasmids of interest

After transformation of competent cells, colonies of interest were identified using either PCR screening or restriction endonuclease digestion, depending on the availability of suitable PCR primers for screening and the degree of background indicated by the control plates. Each colony to be tested was used to inoculate 15 μ l LB. 1 μ l of this inoculated LBA broth was added to a 25 μ l PCR reaction containing 0.5 U Taq polymerase. A negative control and, where possible, a positive control were included in the experiment. Colonies containing the recombinant plasmid of interest were identified by the size of their PCR products using agarose gel electrophoresis. Positives from PCR screening were confirmed using restriction endonuclease digestion.

2.2.1.12 Extraction of genomic DNA

After rinsing 3 times with ice-cold PBS, 1×10^7 cells were scraped off the culture dishes using a cell scraper in PBS and pelleted by centrifugation at 14,000 g for 5 min. High molecular weight genomic DNA was isolated using Blood and Cell

Culture Mini Kit (Qiagen) according to the manufacturer's instructions. 50 µl of sterile distilled water was used to resuspend the purified genomic DNA.

2.2.1.13 Site-directed mutagenesis

Point mutations were made using two rounds of PCR. Two pairs of primers were designed; the first pair being the cloning primers (primer 1 and 2), were used to amplify the full-length fragment, while the second pair carried the respective mutations (primers 3 and 4). The first round of PCR was performed in 2 separate reactions. Each tube contains the appropriate DNA template and primer combinations of primer 1 / primer 4 or primer 3/ primer2. The two PCR fragments were subjected to electrophoresis before they were gel purified. Equal amounts of the gel purified PCR products were mixed and subjected to a second round of PCR using cloning primers 1 and 2.

2.2.1.14 Extraction of total RNA from mammalian cells

After rinsing 3 times with ice-cold PBS, the cells were scraped off the culture dishes using a cell scraper in PBS and pelleted by centrifugation at 14,000 g for 5 min. The total RNA was extracted using the RNeasy Mini kits (Qiagen) according to the manufacturer's instructions. 50 µl of RNase free water was used to resuspend the purified RNA.

2.2.1.15 Extraction of viral RNA from culture medium of virus infected cells

Viral RNA was extracted from virions in cell cultures supernatant using the TRIzol reagent (Invitrogen) according to the manufacturer's instructions. Virions in the cell culture medium were lysed by adding the same volume of TRIzol reagent and passing the lysate several times through a pipette. The homogenized samples were incubated at room temperature to permit the complete dissociation of nucleoprotein complexes. 200ul of chloroform was added in per 1ml of TRIzol reagent. The sample

was vigorously mixed before centrifugation. After centrifugation, RNA remains exclusively in the aqueous phase. RNA was recovered by isopropyl alcohol precipitation.

2.2.1.16 Reverse transcription PCR (RT-PCR)

2.5 μ l (approximately 1 μ g) of total RNA was added to 2 μ l of 10 pmoles of an appropriate primer in a sterile PCR tube. After denaturation at 65 °C for 10 min, the tubes were immediately cooled on ice. The denatured RNA-primer mixture was then added to a 20 μ l of reaction mixture containing 10mM of dNTPs, 20 units of ribonuclease inhibitor, 5 X reverse transcriptase buffer and 1 μ l Expand Reverse Transcriptase (Roche). The first strand cDNA was synthesized at 42 °C for 1h, and reaction was terminated by heating at 65 °C for 10 min. The first strand cDNA was used as the PCR template to amplify desired fragments by using Turbo pfu polymerase (Stratagene) according the manufacturer's instructions.

2.2.1.17 Automated sequencing

1 μ g of Qiagen purified DNA was used in a 20 μ l reaction system containing 15 pmol of appropriate primer, 8 μ l big dye termination mix (1st Base) and ddH₂O was used to make total reaction volume of 20 μ l. The reaction mix was subjected to thermal cycle sequencing: denaturing at 96 °C for 10 sec; annealing at 42 °C for 5 sec and extension at 65 °C for 4 min. 25 cycles of PCR was performed. The PCR product subjected to Perkin Elmer automated sequencing (Civitello et al., 1992).

2.2.2 General methods for cell culture

Cell lines were cultured in 5% CO₂ at 37°C in a humidified tissue culture incubator using Nunc tissue culture flasks.

2.2.2.1 Cell storage in liquid nitrogen

Cells were sedimented at 400 g for 5 min, resuspending in freezing mixture (heat inactivated FBS (GIBCO) + 10% DMSO (Sigma)) at a concentration of 5×10^6 cells/ml and aliquotted into Cryo Vials (Greiner). Cells were frozen in an NALGENTM Cryo 1°C Freezing Container (Nalgen) for 24 h at -70°C, to achieve a 1°C/min rate of cooling, after which the vials were transferred to liquid nitrogen.

2.2.2.2 Cell Recovery from liquid nitrogen

Cells were removed from the liquid nitrogen, quickly brought to 37°C, and washed with 10 ml media to remove DMSO. Each cell pellet was then resuspended in complete media and cultured in 75 cm² flask.

2.2.2.3 Culture of Mammalian cells

Cells were maintained in appropriate media in a humidified tissue culture incubator at 37°C, 5% CO₂. Cells were split 1/6 when they were subconfluent. Cells were washed twice in PBS, detached by 0.25% (w/v) trypsin (GIBCO) for 5 min at RT, followed by tapping of each flask. Trypsin was inactivated by adding full media and directly seeded into fresh flasks at desired concentrations. Cells were propagated indefinitely without any adverse effect on transfection efficiency.

2.2.3 Yeast two hybrid screening

The Matchmaker GAL4 two-hybrid system 3 was used. All yeast two-hybrid system materials except HeLa cDNA library were obtained from Clontech. The HeLa cDNA library in vector pACT2 which contains the LEU2 selectable marker was a gift from Dr. Huang Mei from Institute of Molecular and Cell Biology, Singapore. Plasmid pGBKT7-BARF1Δ was used as bait in a yeast two-hybrid screening.

Large scale library transformation of yeast strain AH109 was performed sequentially as follows. The yeast strain AH109 was transformed by lithium acetate

method (Fields et al., 1993). Bait plasmid containing the interested gene was first transformed into AH109. Expression of the bait protein was confirmed by Western blot before screening. Two flasks containing 500 ml of SD(-Trp) media were inoculated with enough culture of pre-transformed yeast to yield an OD₆₀₀ of 0.2-0.3, then grown at 30°C for 4 h with shaking at 230 rpm. Cells were pelleted at 4°C by centrifugation at 1000 x g for 10 min. Pellets were washed in 500 ml of TE (10mM Tris.HCl, pH7.5, 1 mM EDTA), re-centrifuged as above, then re-suspended in 8 ml of 1 x LiAc/TE solution (0.1 M lithium acetate in filter-sterilized TE buffer). The resuspended cells were added to a DNA mixture which contained 1 mg of plasmid pACT2-HeLa and 5 mg of salmon testis DNA as a carrier. 60 ml of PEG/LiAc (40%[w/v] polyethyleneglycol 4000 in 1 x LiAc/TE) solution was added to this mixture and mixed by inversion. Cells and DNA in the PEG/LiAc were incubated at 30°C for 1 hour, DMSO was added to 10% with swirling and the mixture incubated at 42°C with gentle agitation for 15 min. After the incubation, cells were pelleted as above, re-suspended in 50 ml of TE buffer and repelleted. This last pellet of the transformation mixture was re-suspended in 10 ml of TE buffer. To determine the transformation efficiency, 10 µl of the transformation mixture was plated onto agar media lacking Trp and Leu. Based on this titer, 4x10⁶ transformants were screened. Aliquots of the transformation mixture (200 µl) were plated onto agar media lacking leucine, tryptophan and histidine and containing 25 mM 3-aminotriazole (3-AT) to isolate colonies containing both plasmids and activating the HIS3 reporter gene. After 7 days at 30°C, colonies with 2-6 mm in diameter were selected and re-streaked onto plate lacking leucine and tryptophan, histidine and Adenine. The survived clones were assayed for β-galactosidase expression with the paper filter assay (Fields et al., 1993).

Colonies which showed β -galactosidase expression were regarded as putative positive colonies.

Subsequently, constructs containing the interacting prey proteins were isolated from positive yeast colonies, transformed into *E. coli* strain MC106 by electroporation, and the positive inserts were determined by restriction enzyme digestion and sequencing. The cDNA sequences obtained were entered into the nucleotide sequence database (<http://www.ncbi.nlm.nih.gov/blast>), which is provided by the National Center for Biotechnology Information (NCBI), to determine if they matched any known sequences. The potentially interesting interactions were further verified by switching the bait and prey constructs and re-checking by growing on -Trp, -Leu, -His, and -Ade plates and by testing the β -galactosidase activity.

2.2.4 Mammalian cell transfection

80% confluent monolayers of HeLa cells grown on 35mm-dishes were infected with 10 PFU of the vaccinia/T7 recombinant virus (vTF7) per cell and transfected with 0.5 μ g of plasmid DNAs with 10 μ l Effectene transfection reagent according to the instructions of the manufacturer (Qiagen). 24-48 h after transfection, the cells in each plate were washed in PBS and scraped using a scraper. Cells were spun down and resuspended in an appropriate solution.

2.2.5 Sodium dodecyl sulphate polyacrylamide gel electrophoresis (SDS-PAGE)

Crude cell lysates or IP samples were run in SDS-polyacrylamide gels using a Bio-Rad mini gel apparatus. The protein samples were electrophoresed at a constant voltage of 180 V for 1 h, until the dye marker had run off the bottom of the gel. The gel was subsequently used for staining or western blot.

2.2.6 Western blotting

Proteins separated by SDS-PAGE were transferred onto a PVDF membrane (Bio-rad) by Western blotting. The PVDF membrane was prepared according the manufacturer's instructions: the membrane was equilibrated by washing in methanol for 10 sec, then water for 10 min until miscible, and then in transfer buffer for 5 - 10 min. The SDS-polyacrylamide gel was equilibrated by washing in transfer buffer for 15 min. One western blot thick filter paper, the PVDF membrane, the SDS-PAGE gel and finally the second sponge, was assembled and placed in a Bio-rad semi-dry Western Blot Apparatus, bubbles between each layer were removed carefully, and was Western blotted at 20 V for 30 min. After protein transfer, the membranes were blocked overnight at 4°C in blocking buffer containing 5% non-fat milk in PBS-T, incubated with specific antiserum diluted in blocking buffer (1:500 to 1:2000) at room temperature for 2 h, washed three times with PBS-T, and incubated with horseradish peroxidase-conjugated anti-rabbit or anti-mouse immunoglobulin (DAKO) diluted in blocking buffer (1:2000) at room temperature for 1 h. The proteins were detected using the ECL detection reagents (Amersham).

2.2.7 Dimerization studies under reducing or non-reducing conditions

The transfected HeLa cells were harvested and divided into two parts. One set was resuspended in SDS loading buffer containing 200mM DTT, while the duplicate set was resuspended in SDS loading buffer lacking the reducing reagent DTT.

2.2.8 Co-immunoprecipitation

HeLa cells transfected with appropriate plasmids were lysed on ice to inhibit protein degradation by co-ip lysis buffer (30mM Tris-HCl pH7.4, 150mM NaCl, 1% NP-40, and 10% glycerol) in the presence of 1 x protease inhibitor mixture (Sigma) at 24 h post-transfection. Total cell lysates were immunoprecipitated with appropriate

antibodies for 2 h at 4°C and further incubated for 2 h at 4°C after adding buffer-balanced protein A agarose beads. The beads were washed three times and subjected to electrophoresis on SDS-12% polyacrylamide gel.

2.2.9 Indirect immunofluorescence

HeLa cells were grown on 4-well chamber slides (Iwaki), infected with vTF7 and transfected with appropriate plasmid DNAs. After 3 washes with PBS, the cells were fixed with 4% paraformaldehyde in PBS for 15 min at room temperature. For immunofluorescence of permeabilized cells, cells were incubated in 0.2% Triton X-100 (BDH) for a further 10 min, before they were rinsed three times by PBS. Primary antisera were diluted according to the manufacturer's recommendations or concentrations experimentally optimized, in a fluorescence dilution buffer (5% FBS in 1 x PBS) and incubated for 2 h at room temperature. The usual dilution for polyclonal antisera was 1:50. Cells were then subjected to three washes with PBS and incubated with anti-rabbit or anti-mouse IgG conjugated to fluorescence isothiocyanate (FITC, Dako), tetramethylrhodamine isothiocyanate (TRITC, Dako), or AlexFlour 405 (Molecular probes) diluted in fluorescence dilution buffer for 2 h at 4°C. After three washes with PBS, cells were mounted with glass coverslips using fluorescence mounting medium containing 15mM NaN₃ (Dako).

2.2.10 Confocal microscopy

Confocal microscopy was performed on a Zeiss Axioplan microscope. For co-localization study, dual labeled cells were viewed for co-localization by superimposing the green, red and/or blue fluorescence image. The region of overlap in the merged image was displayed as yellow (dual labeling of green and red) or white (triple labeling of green, red and blue).

2.2.11 Staining of ER organelle with R6

Rhodamine B is a lipophilic dye that stains a reticular network in cells. At low concentration, the largely positively charged Rhodamine B stains mitochondria by their negative membrane potential, but stains intracellular membranes when concentration is raised. The reticular network that Rhodamine B stains is ER (Yang et al., 1997). Cells were first stained with primary and secondary antibodies. After washing in PBS, the cells were stained in the hexyl ester of rhodamine B at 1 $\mu\text{g/ml}$ (Molecular Probes, Inc., Eugene) for endoplasmic reticulum. Stained cells were viewed and photographed using a confocal laser scanning microscope (LSM 510, Carl Zeiss, Gottingen, Germany).

2.2.12 Staining of mitochondria organelle with Mitotracker Deep Red 633

Prepare Mitotracker Deep Red 633 in cell culture grade DMSO to stock concentration of 1 mM. Dilute the Mitotracker Deep Red 633 stock solution to the final working concentration (200nM) in DMEM supplemented with serum to match the medium that the cells were grown in.

HeLa cells were grown in 4-well chamber slides and transfected with desired DNAs. 12 h after transfection, remove the medium from the dish and add the prewarmed (37°C) growth medium containing the MitoTracker Deep Red. Incubate the cells for 15-45 min under growth conditions.

Deep Red 633 probes can be used to stain cells fixed in formaldehyde. After staining live cells, wash the cells in fresh, pre-warmed growth medium. Carefully remove the growth medium covering the cells, and replace it with freshly prepared, pre-warmed growth medium containing 3.7% formaldehyde. Incubate at 37°C for 15 min. After fixation, rinse the cells several times in PBS. Incubate the fixed cells in PBS containing 0.2% Triton X-100 at room temperature for 5 min. Following

permeabilization, rinse the cells in PBS. Alternatively, the cells may be permeabilized by incubating in ice-cold acetone for 5 min, and then washed in PBS. Even when cells are not going to be labeled with an antibody, this acetone-permeabilization step may be useful because it appears to improve signal retention. Stained cells were viewed and photographed using a confocal laser scanning microscope (LSM 510, Carl Zeiss, Gottingen, Germany).

2.2.13 Endoglycosidase digestions

Proteins in the total cell lysates or eluted from immunoprecipitation were pre-denatured in 1x Glycoprotein Denaturing Buffer at 100 °C for 10 min. The denatured samples were supplemented with 1% NP-40 and 1 x reaction buffer, followed by treating with PNGase F (New England Biolabs) at 37°C for 2 h, according to the instructions of the manufacturers. The digested proteins were separated on 12% SDS-PAGE and analyzed by Western blotting assay.

2.2.14 Virus infection and stock preparation

Following 3 washes of the confluent Vero cells with PBS, IBV was inoculated at a multiplicity of infection (m.o.i) of approximately 1 plaque forming units (PFU)/cell in serum free medium. Presence of serum will reduce IBV infectivity in all cell lines. Cells were then incubated for 48 h at 37°C in 5% humidified CO₂, until cytopathic effect (CPE) was observed. Both culture medium and cells were harvested and aliquoted in appropriate amounts.

2.2.15 Virus purification

200 µl of 10-fold serial dilutions of virus was added drop wise to the monolayer of cells grown on 6-well plates, with gentle swirling. The viruses were allowed to infect the cells for 1 h at 37 °C, 5% humidified CO₂, with occasional shaking. After the inoculum was removed, the cells were washed twice with 1 x PBS.

The monolayer cells were overlaid with 1.5ml DMEM containing 1% PS and 1% cell culture grade, low temperature melting agarose. The plates were left at room temperature for about 15 min until the agarose became solidified and incubated at 37 °C, 5% humidified CO₂ for 4-7 days until the plaques grew up. Plaques were inoculated to individual dishes to amplify viruses.

2.1.16 Plasmid construction

Plasmid pGBKT7-BARF1 Δ

Genomic DNA of EBV positive cell line B95.8 was extracted using the Blood and Cell Culture Mini Kit (Qiagen). BARF1Δ (amino acids from 21-221) were amplified from the genomic DNA from B95.8 cells by PCR. The two primers used to generate BARF1Δ fragment were (5'-GCGAGAATTCGTCACCGCTTTCTTGG-3') and (5'-GGGATCCTTATTGCGACAAGTATC-3'). BARF1Δ PCR fragment was digested with *EcoRI* and *BamHI* and cloned into *EcoRI* /*BamHI* digested pGBKT7 to generate pGBKT7-BARF1Δ.

Plasmid pBARF1-HA and mutants

BARF1 PCR fragment was amplified by primers (5'-GCAGAATTCATGGCCAGGTTTCATCGC-3') and (5'-GATCCTCGAGTTGCGACAAGTATC-3') using genomic DNA from B95.8, digested with *EcoRI* and *XhoI* and ligated into *EcoRI/XhoI* digested pcDNAHA (modified from pcDNA3.1(+) from invitrogen) to generate pBARF1-HA.

Plasmids coding for mutant BARF1 proteins were constructed by replacing wild-type fragments with the same fragments containing the desired mutations by PCR using Pfu polymerase (Stratagene) (Liu et al., 1997). The primers used are as follows:

C14A,	5'-GTTGGCCTCCGCCGTGGCCG-3',	5'-
CGGCCACGGCGGAGGCCAAC-3';	C104A,	5'-GCA

ACTACCTGGCCCGCATGAAAC-3', 5'-GTTTCATGCGGGCCAGGTAGTTGC-3'; C146A, 5'-CCTTACTGTGACAGCCACCGTGAATG-3', 5'-CATTACGGTGGCTGTCACAGTAAG G-3'; C201A, 5'-CTGCCAGTGACCGCCGTTGGGAAA-3', 5'-TTTCCCAACGGCGGTTCAC TGGCAG-3'; N95A, 5'-CCGCTGCCGCCATCTCCCATG-3' and 5'-CATGGGAGATGGC GGCAGCGG-3'.

Plasmid phTid1L/S

hTid1L and hTid1S were amplified from human total RNA from HeLa cells by RT-PCR. The primers used for generating hTid1L PCR fragment were (5'-GCGAATTCATGGCTGCGCGGTGCTC-3') and (5'-CCGCTCGAGTGAGGTAAACATTTTCTTAAG-3'). The 5' primer used for generating hTidS PCR fragment was the same as the one for hTidL and the 3' primer was (5'-CCGCTCGAGGTTTCCAGTGGATC-3'). The purified PCR products were digested with *EcoRI* and *XhoI* and cloned into *EcoRI*/*XhoI* digested pcDNAHA and pcDNA3.1(+) to generate phTid1L/S-HA and phTid1L/S.

Plasmid phTidΔ1-HA, phTidΔ2-HA, phTidΔ3-HA, phTidΔ4-HA

The PCR fragment for TΔ1 was amplified by using primer 5'-GGGATCCCCATGGCCAAAGAAGATTATTATC-3' and the 3' primer for hTid1L. The PCR fragment for TΔ4 was generated by using the 5' primer for hTid1L and the 3' primer 5'-GACCTCGAGCACAGGGATCATCACTCGC-3'. The deletion constructs TΔ2 and TΔ3 were made by two rounds of PCR as described above. The primers used for TΔ2 are 5'-ATTTGTACTCATAGCTACTGGAAGGGA-3' and 5'-GTAGCTATGAGTACAAATGAAAGGG-3'. The primers for TΔ3 are 5'-GGCTCTGCACCTGTGGGAAAAAGGGAAAT-3' and 5'-TCCCACAGGTGCAGAGCCGTAGGCATC-3'. The PCR products were generated,

digested with *EcoRI* and *XhoI* and cloned into *EcoRI* /*XhoI* digested pcDNAHA to generate phTid Δ 1-HA, phTid Δ 2-HA, phTid Δ 3-HA, phTid Δ 4-HA.

Plasmid pcDNAHis-T Δ 2, pcDNAHis- Δ HPD

T Δ 2-His and Δ HPD-His PCR fragment was obtained by using (5'-GCGAATTCATGGCTGCGCGGTGCTC-3') as the 5' primer and (5'-CCGCTCGAGTGAATGATGATGATGATGATGGGTAAACATTTTCTTAAG-3') as the 3' primer. The template of PCR for T Δ 2-His is phTid Δ 2-HA and that for Δ HPD-His is phTid Δ HPD-HA

All constructs were confirmed by automated nucleotide sequencing. All the sequences are correct as expected.

Chapter Three

Biochemical and functional characterization of Epstein-Barr virus-encoded BARF1 protein: interaction with human hTid1 protein facilitates its maturation and secretion

3.1 Introduction

EBV is normally restricted to B-lymphocytes and epithelial cells. EBV infection is associated with several cancers of lymphocytic or epithelial origins, including NPC, BL and Hodgkin's lymphoma. Six EBV genes, *EBNA1*, *EBNA2*, *EBNA3A*, *EBNA3C*, *EBNA-LP*, and *LMP-1*, are essential for immortalization of B-lymphocytes (Kieff, 1996). In EBV-immortalized epithelial cells, the expression of five genes, *EBNA1*, *EBERs*, *LMP2A*, *BARF1* and *BARF0*, was reported (Nishikawa et al., 1999; Danve et al., 2001).

BARF1 gene is located at nucleotide positions 165,449-166,189 of strain B95.8, encoding a protein of 221 amino acids with a calculated molecular mass of 24.47 kDa (Zhang et al., 1988). This protein may play diverse functions in immunomodulation and oncogenicity, including as a functional receptor for hCSF-1 (Strockbine et al., 1998), inhibition of interferon alpha secretion from mononuclear cells (Cohen and Lekstrom, 1999), and induction of malignant transformation in Balb/c3T3 cell line (Wei and Ooka, 1989) as well as in EBV negative human Louckes and Akata B cell lines (Wei et al., 1994; Sheng et al., 2003). In addition, primary monkey epithelial cells were shown to be immortalized by *BARF1* (Wei et al., 1997).

BARF1 was expressed in EBV-immortalized epithelial cells in the absence of the expression of *LMP-1* (Danve et al., 2001), which is essential for B cell immortalization (Kieff, 1996). In rodent fibroblasts, the first 54 amino acids of *BARF1* were shown to be able to transform cells and activate Bcl-2 expression (Sheng et al., 2001). Although *BARF1* was a lytic gene in B-lymphocytes (Zhang et al., 1988; Decaussin et al., 2000), its expression was detected in NPC and EBV-positive GC tissues in the absence of the expression of other lytic genes (Seto et al., 2005). It suggests that *BARF1* may be expressed as a latent gene in these carcinoma

tissues. The secreted form of BARF1 can act as a growth factor *in vivo* (Sall et al., 2004). It could inhibit alpha interferon secretion from mononuclear cells (Cohen and Lekstrom, 1999) and has mitogenic activity *in vivo* (Sall et al., 2004).

In this study, we show that BARF1 is posttranslationally modified by N-linked glycosylation on the asparagine 95 residue. This modification was confirmed to be essential for the maturation and secretion of the protein. Analysis of the four cysteine residues by site-directed mutagenesis demonstrated that cysteine 146 and 201 residues were also essential for proper folding and secretion of the protein. Furthermore, human hTid1 protein was identified as a potential interacting protein of BARF1 by yeast two-hybrid screening, and the interaction was subsequently confirmed by coimmunoprecipitation and dual immunofluorescent labeling of cells co-expressing the two proteins. Interestingly, co-expression of BARF1 with hTid1 demonstrated that hTid1 could promote secretion of BARF1, suggesting that hTid1 may act as a chaperone to facilitate the folding, processing and maturation of BARF1.

3.2 Results

3.2.1 Expression, post-translational modification and secretion of BARF1

BARF1 encodes a protein of 221 amino acids (Figure 3.1a). Analysis of its amino-acid sequence shows that the protein contains four cysteine residues, an N-terminal signal peptide and a potential N-linked glycosylation site at residue 95 (Figure 3.1a). To systematically study the expression and post-translational modification of this protein, a C-terminally HA-tagged construct (pBARF1-HA) was made and expressed in HeLa cells using the recombinant vaccinia/T7 virus expression system. Proteins in total cell lysates were separated by SDS-PAGE under either reducing or nonreducing conditions, and analyzed by Western-blotting with anti-HA antibodies (Santa Cruz). Proteins secreted to the culture medium were immunoprecipitated with anti-HA antibodies and analyzed by Western blotting with anti-HA. Under nonreducing conditions, a protein band with an apparent molecular mass of approximately 26 kDa, representing the monomer of BARF1, was observed (Figure 3.1b, lane 1). In addition, protein bands with apparent molecular masses of 50, 80 kDa and above were detected (Figure 3.1b, lane 1); they may represent dimers and other higher-order oligomers/aggregates of the protein. Under reducing conditions, three bands ranging from 26 to 28 kDa that may represent isoforms of the protein, the 50-kDa dimer and other higher order oligomers were detected (Figure 3.1b, lane 2). Immunoprecipitation and Western blotting analyses of the culture media were then carried out, showing the detection of the 28-kDa monomer and trace amounts of the 50-kDa dimer (Figure 3.1b, lanes 3 and 4). These results demonstrate that BARF1 can be post-translationally modified and secreted into the culture medium.

BARF1 is predicted to be modified by N-linked glycosylation on the N95 residue (Figure 3.1a). To define if this modification does occur, treatment of the

intracellular forms of the protein with PNGaseF, a glycosidase which cleaves all N-linked oligosaccharide structures from the substrate, showed that the 28-kDa species of the three isoforms of the monomers was sensitive to PNGaseF treatment (Figure 3.1c, lanes 1 and 2), suggesting that the protein has indeed undergone post-translational modification by N-linked glycosylation, and the 28-kDa species represents the glycosylated form of the protein. The other two bands which migrated slower are both unglycosylated forms as they were shown to be resistant to PNGaseF treatment (Figure 3.1c, lanes 1 and 2). The 27-kDa species may represent the full length unglycosylated BARF1 protein, while the 26-kDa one may be the product after signal peptide cleavage of the 27-kDa species. To determine if the predicted N95 residue is the site for N-glycosylation, mutation of N95 to A (N95A) was made by site-directed mutagenesis. Expression of the construct showed the detection of the 26- and 27-kDa species only (Figure 3.1c, lanes 3 and 4), confirming that the N95 residue is indeed the site for N-linked glycosylation of the protein. Analysis of the culture medium showed much less, if any, secretion of the mutant protein (Figure 3.1c, lanes 5–8).

3.2.2 Mutational analysis of the four cysteine residues

BARF1 contains four cysteine residues at position 14, 103, 146 and 201 (Figure 3.1a). The detection of dimers and higher-order oligomers in cells expressing BARF1 under both reducing and nonreducing conditions suggests that these cysteine residues may play certain roles in the folding, oligomerization and subsequent secretion of the protein. To assess their functions, these cysteine residues were individually mutated to alanine, giving rise to the mutant constructs C14A, C103A, C146A and C201A. Expression and analysis of wild type and mutants under reducing conditions showed the detection of the 26- and 28-kDa monomers (Figure 3.2a, lanes

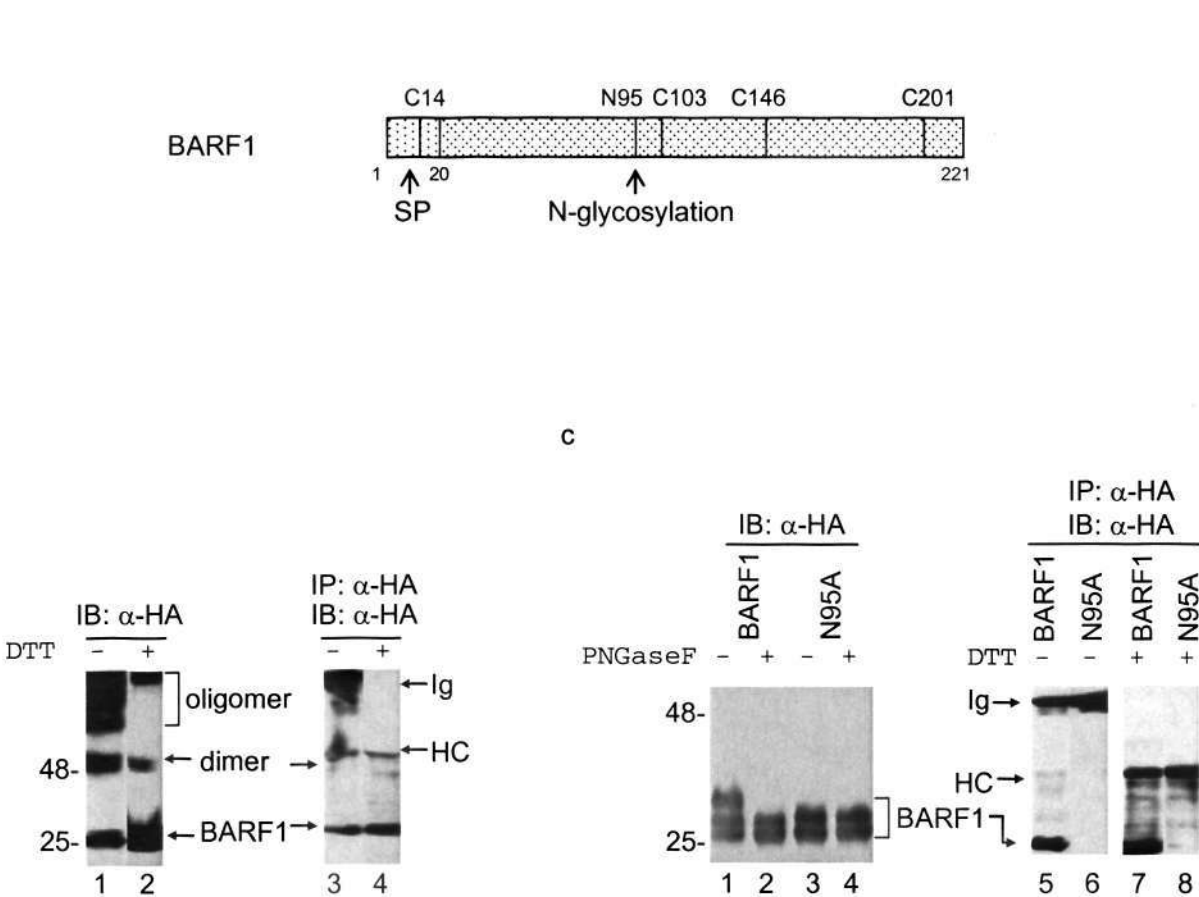


Figure 3.1(a) Diagram showing the positions of the signal peptide, N-linked glycosylation site and the four cysteine residues in BARF1 protein. **(b)** Expression and secretion of BARF1 protein. HeLa cells were transfected with the HA-tagged BARF1 construct and harvested at 24 h post-transfection. Cell lysates were prepared and the expression of BARF1 protein was detected by Western blot with anti-HA antibodies after proteins were separated by 12% SDS-PAGE under either reducing (lane 2) or nonreducing conditions (lane 1). Proteins secreted into the culture medium were immunoprecipitated with anti-HA antibodies, separated by 12% SDS-PAGE under either reducing (lane 4) or nonreducing conditions (lane 3), and analyzed by Western blot with anti-HA antibodies. Numbers on the left indicate molecular masses in kilodaltons. Ig and HC indicate immunoglobulin (Ig) and heavy chain (HC) of antibodies. **(c)** N-linked glycosylation of BARF1 protein. Total cell lysates prepared from HeLa cells expressing the HA-tagged wild type (lanes 1 and 2) and N95A mutant (lanes 3 and 4) BARF1 protein were treated either with (lanes 2 and 4) or without (lanes 1 and 3) PNGase F. Polypeptides were separated by 12% SDS-PAGE under reducing conditions and analyzed by Western blot with anti-HA antibodies. Proteins secreted into the culture medium were immunoprecipitated with anti-HA antibodies, separated by 12% SDS-PAGE under either reducing (lanes 7 and 8) or nonreducing conditions (lanes 5 and 6), and analyzed by Western blot with anti-HA antibodies. Numbers on the left indicate molecular masses in kilodaltons. Ig and HC indicate immunoglobulin (Ig) and heavy chain (HC) of antibodies.

1–5). The 50-kDa dimer was also detected in cells expressing wild type and three mutants, C14A, C103A and C201A (Figure 3.2a, lanes 1–3 and 5), but not detected in cells expressing mutant C146A (Figure 3.2a, lane 4). The detection of dimer under reducing conditions suggests that the hydrophobic BARF1 may form oligomers via hydrophobic interaction. It also suggests that cysteine 146 may be involved in the formation of BARF1 homodimer by hydrophobic interaction, but is not involved in the formation of disulfide bond. Under nonreducing conditions, the monomers and dimers were detected in cells expressing wild type and all four mutants (Figure 3.2a, lanes 6–10). Significant amounts (even more abundant in some cases) of protein aggregation were also detected in cells expressing mutants C103A, C146A and C201A (Figure 3.2a, lanes 8–10). It suggests that these residues may be involved in the folding and maturation of the protein.

The secretion of wild type and mutant BARF1 constructs was analyzed by immunoprecipitation and Western blotting. Secretion of the protein to the culture medium was detected in cells expressing wild type and mutants C14A and C103A, but not detected in cells expressing C146A and C201A (Figure 3.2b). Interestingly, other abundant aggregates were detected in cells expressing these two mutants (Figure 3.2a, lanes 9 and 10), implying that proper folding of the protein is essential for its secretion.

3.2.3 Subcellular localization of BARF1 and secretion-defective mutants

The subcellular localization of wild type and three secretion-defective mutants C146A, C201A and N95A was studied by indirect immunofluorescence. HeLa cells expressing the HA-tagged wild type and mutants were fixed with 4% paraformaldehyde at 12 h post-infection and stained with anti-HA monoclonal antibodies. In nonpermeabilized cells, positive staining was observed in cells

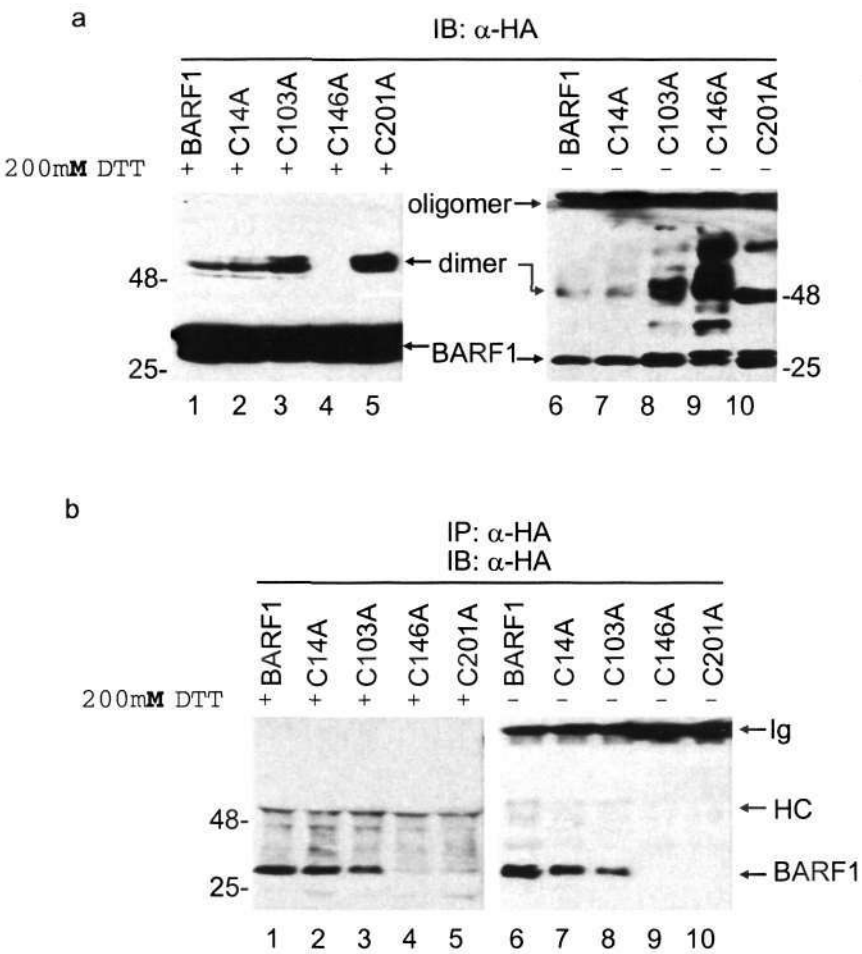


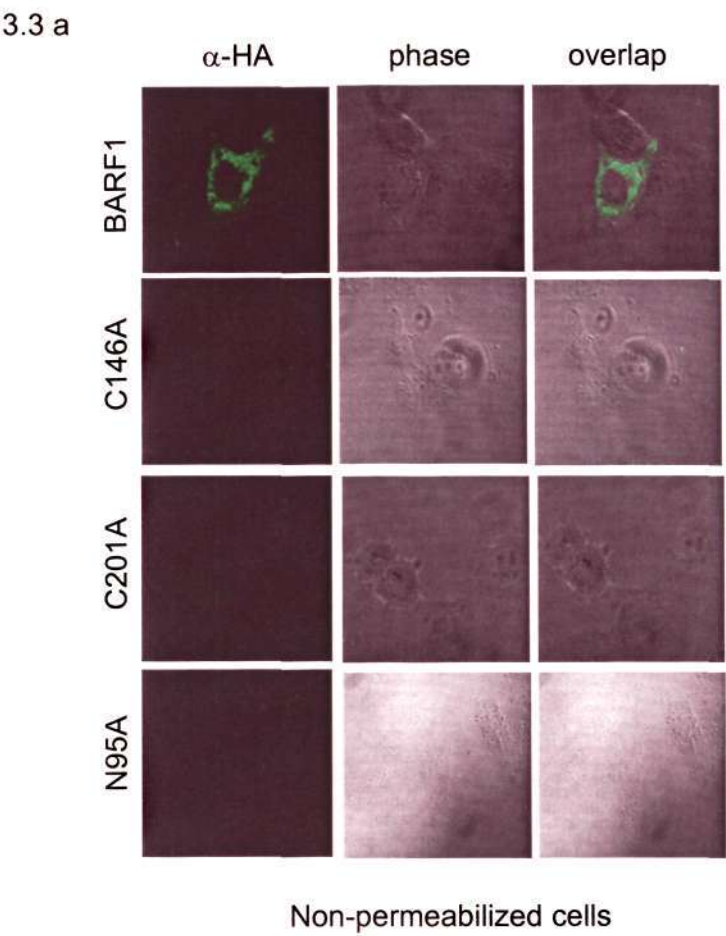
Figure 3.2 Mutational analysis of the four cysteines residues in BARF1 protein. **(a)** HeLa cells were transfected with the HA-tagged wild type and four mutant BARF1 constructs, harvested at 24 h post-transfection, and cell lysates were prepared. Polypeptides were separated by 12% SDS–PAGE under either reducing (lanes 1–5) or nonreducing (lanes 6–10) conditions, and analyzed by Western blot using anti-HA antibodies. Numbers on the left and right indicate molecular masses in kilodaltons. **(b)** Proteins secreted into the culture medium were immunoprecipitated with anti-HA antibodies, separated by 12% SDS–PAGE under either reducing (lanes 1 and 5) or nonreducing (lanes 6 and 10) conditions, and analyzed by Western blot with anti-HA antibodies. Numbers on the left indicate molecular masses in kilodaltons. Ig and HC indicate immunoglobulin (Ig) and heavy chain (HC) of antibodies.

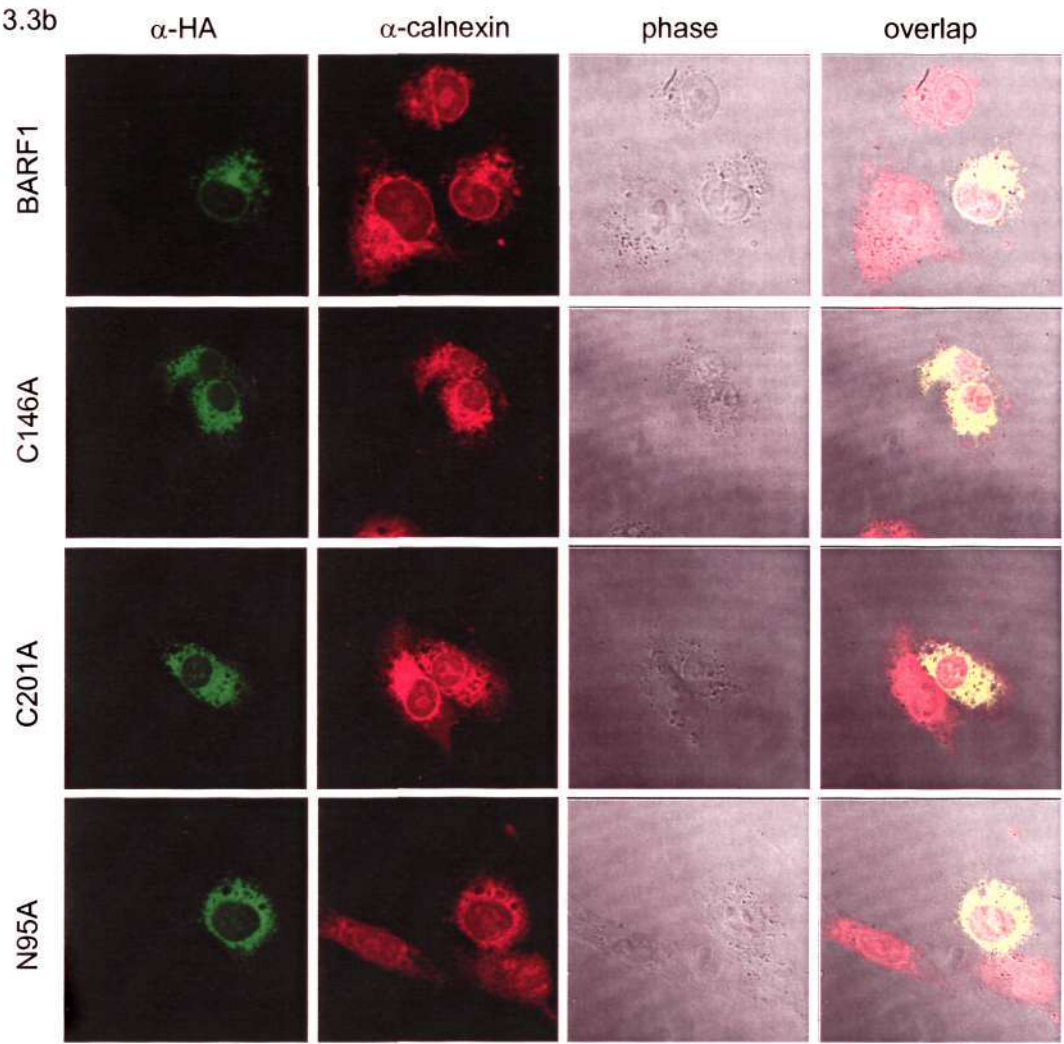
expressing wild-type BARF1 only (Figure 3.3a). No staining was observed in cells expressing all three mutants (Figure 3.3a). In cells permeabilized with 0.2% Triton X-100, the protein was mainly localized to the perinuclear regions of the cells expressing wild-type and mutant constructs (Figure 3.3b). The staining patterns overlap well with the ER staining patterns (Figure 3.3b) shown by staining with an anti-calnexin antibody (Abcam).

A time-course experiment was then carried out to study the translocation of wild type and the secretion-defective mutant N95A by incubation of the transfected cells in the presence of 100 µg/ml of cycloheximide for 30 min at 6 h post-transfection to stop new protein synthesis. The cells were then chased and fixed at 7, 10, and 16 h post-transfection, respectively, and the subcellular localization patterns were viewed by indirect immunofluorescent staining. As shown in Figure 3.3c, typical ER localization pattern of wild-type BARF1 was observed at 7 h post-transfection; translocation of the protein to the Golgi apparatus and the cell surface was observed at 10 and 16 h post-transfection (Figure 3.3c). In cells transfected with N95A mutant, the protein was observed in the ER throughout the time-course experiment (Figure 3.3c).

3.2.4 Identification of hTid1 as BARF1-binding protein

The detection of multiple forms of aggregates that are secretion-defective in cells overexpressing wild type and several mutant BARF1 constructs and the fact that mutation of the N-linked glycosylation blocks the secretion of the protein suggest that proper folding, oligomerization and maturation are essential for the functions of the protein. To identify cellular proteins that may interact with BARF1 and potentially modulate the maturation process of the protein, cDNA sequence coding for amino





Permeabilized cells

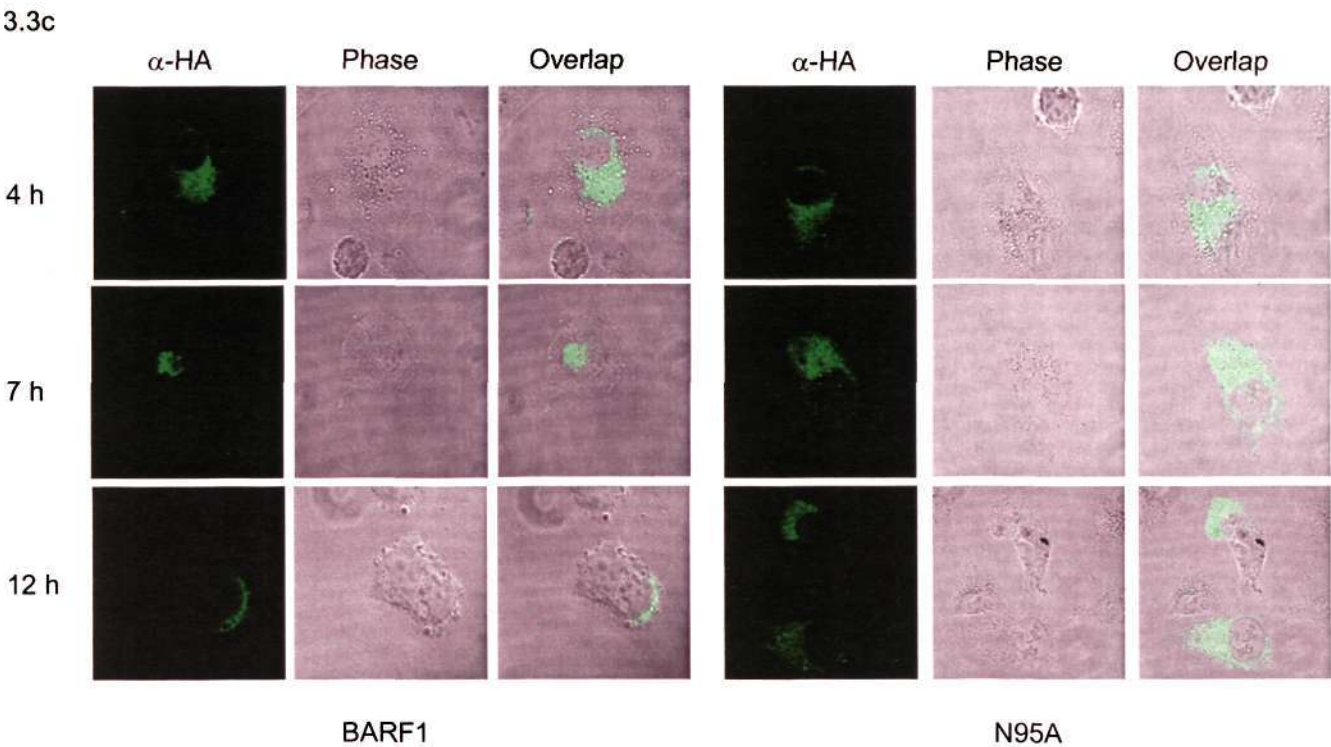


Figure 3.3 Subcellular localization of BARF1 protein. (a) HeLa cells expressing the HA-tagged wild type and C146A, C201A and N95A mutants were stained with anti-HA antibodies at 12 h post-transfection under non-permeabilizing conditions. Images of cell surface staining, phase-contrast images and the overlapping images are shown. (b) HeLa cells expressing the HA-tagged wild type and C146A, C201A and N95A mutant BARF1 protein were permeabilized with 0.2% Triton X-100 and stained with anti-HA antibodies at 12 h post-transfection. The same cells were also stained with an anti-calnexin antibody for the ER. (c) Subcellular translocation of the HA-tagged wild type and N95A mutant BARF1 protein. HeLa cells were transfected with the HA-tagged wild type and N95A mutant BARF1 constructs and incubated in the presence of 100 μ g/ml of cycloheximide for 30 min at 6 h post-transfection. The cells were fixed at 7, 10 and 16 h post-transfection, respectively, permeabilized with 0.2% Triton X-100 and stained with anti-HA antibodies.

acids 21–221 of BARF1 was fused with the GAL4 DNA-binding domain, giving rise to pGBKT7- BARF1 Δ . The N-terminal signal peptide was excluded in this construct. Plasmid pGBKT7-BARF1 Δ was then used as bait in a yeast two-hybrid system to screen a cDNA library derived from HeLa cells. Clones were selected on Trp-, Leu-, His-triple drop out medium containing 25 mM 3-aminotriazol (3-AT) and then transferred to Trp-, Leu-, His- and Ade-drop out medium. The survived clones were subjected to X-gal filter lift assay, and positive clones were verified through re-transformation using switched bait and prey constructs, re-selected by drop out medium, and re-analyzed by X-gal filter lift assay. A total of 74 positive clones were identified by this process. Sequence analysis and BLAST searches of GenBank™ revealed that a clone contains partial sequence encoding amino acids 146–392 of hTid1, a human homolog of the *Drosophila* tumor suppressor protein Tid56. In this report, hTid1 was chosen for further analysis, as it was reported to be involved in the interaction with Hsp70 and may act as a chaperone (Cheng et al., 2001; Kim et al., 2004).

3.2.5 Confirmation of the interaction between BARF1 and hTid1 by co-immunoprecipitation and co-localization studies

The full-length hTid1L was cloned into pcDNA3.1 by RT-PCR. HeLa cells were cotransfected with plasmids that express HA-tagged BARF1 (pBARF1-HA) and hTid1L (pTid1L), lysates were prepared at 24 h post-transfection, and were immunoprecipitated with anti-HA antibodies. The precipitates were resolved by 12% SDS-PAGE and subjected to Western blotting using anti-hTid1 (Santa Cruz) antibodies, showing that hTid1L was detected in cells coexpressing BARF1 and hTid1L but not in cells expressing BARF1 alone (Figure 3.4a, lanes 3 and 4). The same lysates were then immunoprecipitated with anti-hTid1 antibodies. Western-

blotting analysis of the precipitates with anti-HA antibodies showed the detection of BARF1 protein in cells coexpressing BARF1 and hTid1L (Figure 3.4a, lane 8), but not in cells expressing BARF1 alone (Figure 3.4a, lane 7). These data confirm the yeast two-hybrid screening results that BARF1 indeed interacts with hTid1.

To further determine if the two proteins colocalize in cells, HA-tagged BARF1 and hTid1L were transfected into HeLa cells. BARF1 was detected using rabbit polyclonal anti-HA antibody and hTid1L was visualized with mouse monoclonal anti-hTid1 antibody. The results showed that both proteins were localized to the perinuclear region of the cells, and the two staining patterns coaligned well (Figure 3.4b). Similar staining patterns and colocalization were also observed in cells coexpressing hTid1L and the three secretion-defective mutants C146A, C201A and N95A (Figure 3.4b).

As hTid1 protein contains a mitochondria processing signal in the N-terminal region and was reported to be localized to the mitochondrial matrix (Syken et al., 1999), we next examined if BARF1 and hTid1 colocalize in the same subcellular compartment. In this experiment, Mitotracker Deep Red (Molecular Probes) which stains the mitochondria and an ER marker were used. As shown in Figure 3.4c, the staining images of the two proteins were not completely merged with either marker in cells coexpressing BARF1 and hTid1L, but relatively better co-alignment of the two proteins with the ER marker was observed. These data suggest that BARF1 could sequester hTid1L to the ER.

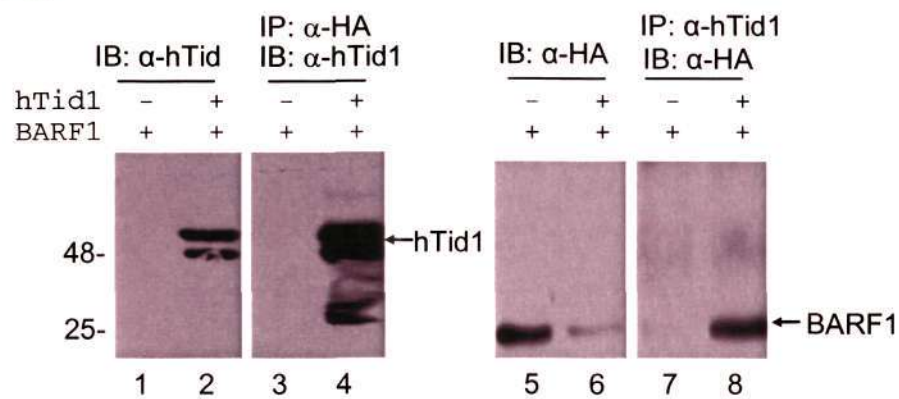
To map the interacting domain on hTid1, three fragments covering hTid1 sequences from amino acids 149–320, 303–453 and 303–480 were cloned into the activating plasmid pACT2, and co-transformed into yeast cells with the bait construct pGBKT7-BARF1 Δ . As shown in Figure 3.4c, no growth of the transformed yeast in

Trp-, Leu- and His-drop out plate was observed only when fragment covering amino acids 303–480 was used. Normal growth of the transformed yeast was observed when other fragments were used (Figure 3.4d). These results demonstrate that the interacting domain may locate in the region from amino acids 149–320 in hTid1L, but one additional interacting domain may exist in the region 303–453 in hTid1S.

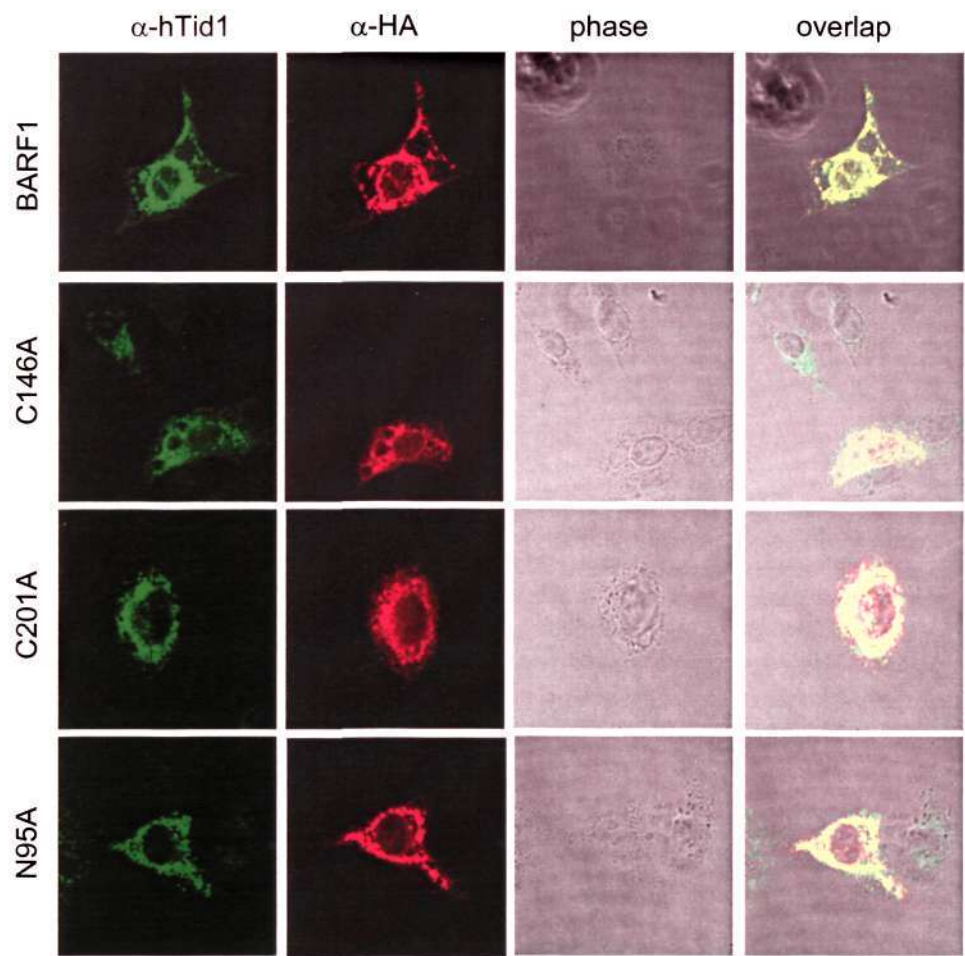
3.2.6 Promotion of BARF1 maturation by its interaction with hTid1

Over the course of studying the expression of BARF1 and hTid1 and characterization of their interaction, it was noted that coexpression of hTid1 could reduce the accumulation of higher-molecular-weight aggregates of BARF1, indicating that hTid1 may be involved in the maturation of BARF1. To confirm and further characterize this observation, cells expressing either hTid1L or BARF1 alone or coexpressing two proteins were first radiolabelled with [³⁵S] methionine and cysteine. Proteins expressed in cells and secreted into the culture medium were analyzed by immunoprecipitation under mild washing conditions. To simplify the assay and meanwhile allow more precise comparison of the expression levels of the two proteins, both BARF1 and hTid1L were tagged with HA and detected by immunoprecipitation with anti-HA antibodies. As shown in Figure 3.5a, immunoprecipitation of total cell lysates with anti-HA antibodies showed the detection of BARF1 monomers and dimers in cells expressing BARF1 alone or coexpressing BARF1 and hTid1L (Figure 3.5a, lanes 1 and 2). Interestingly, in cells expressing BARF1 alone, the majority of the species identified was at the dimer position (Figure 3.5a, lane 1). However, in cells coexpressing BARF1 and hTid1L, the major species was the monomer forms (Figure 3.5a, lane 2). Similar expression levels of hTid1L were detected in cells either expressing hTid1L alone or coexpressing hTid1L and BARF1 (Figure 3.5a, lanes 2

3.4a



3.4b



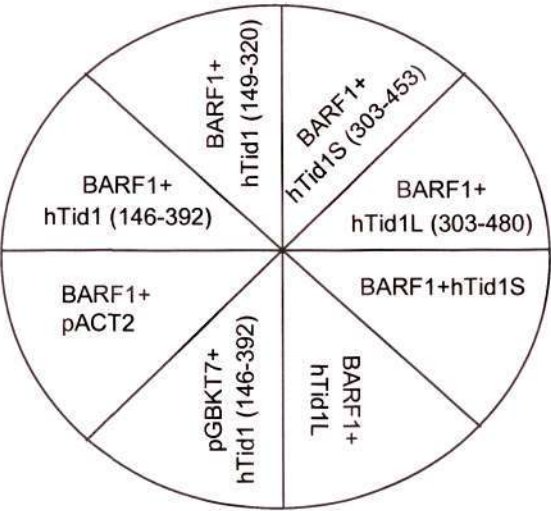
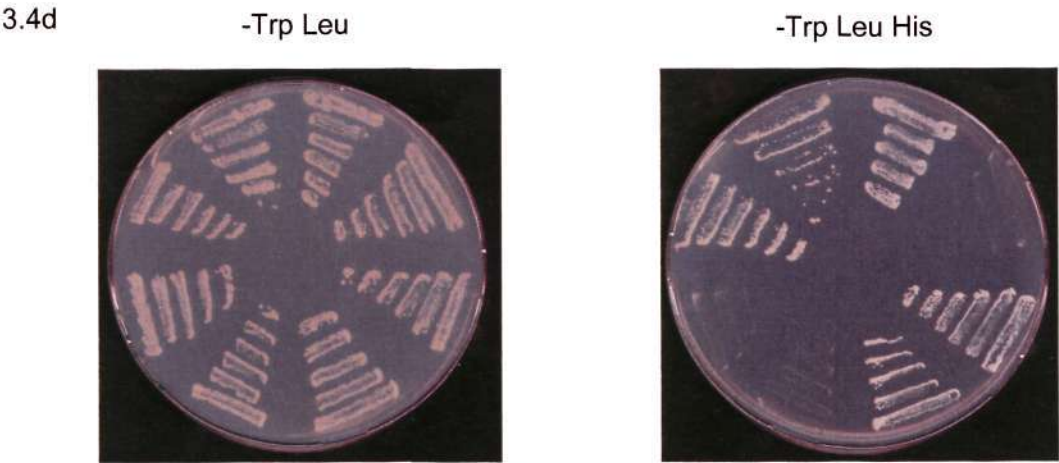
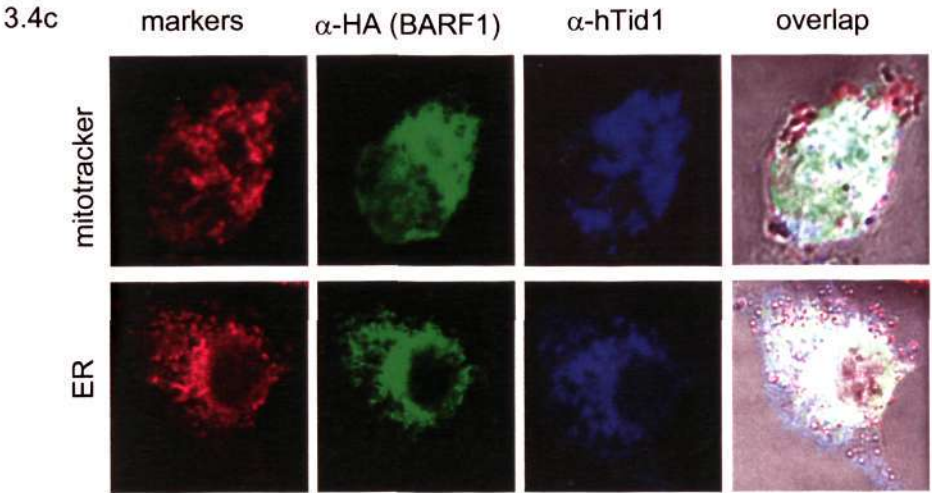


Figure 3.4 Interaction of BARF1 protein with human hTid1 protein. **(a)** HeLa cells were either transfected with the HA-tagged BARF1 alone (lanes 1, 3, 5 and 7) or cotransfected with hTid1L (lanes 2, 4, 6 and 8), and harvested at 24 h post-transfection. Polypeptides were either separated directly by 12% SDS-PAGE (lanes 1, 2, 5 and 6) or immunoprecipitated with either anti-HA (lanes 3 and 4) or anti-hTid1 (lanes 7 and 8) antibodies before separated by 12% SDS-PAGE, and analyzed by Western blot using anti-hTid1 (lanes 1–4) or anti-HA (lanes 5–8) antibodies. Numbers on the left indicate molecular masses in kilodaltons. **(b)** Colocalization of wild type and mutant BARF1 protein with hTid1L protein. HeLa cells coexpressing hTid1L with the HA-tagged wild type and C146A, C201A and N95A mutant BARF1 protein, respectively, were permeabilized with 0.2% Triton X-100 and stained with anti-HA and anti-hTid1 antibodies at 12 h post-transfection. **(c)** Subcellular localization and colocalization of BARF1 and hTid1L proteins. HeLa cells coexpressing hTid1L with the HA-tagged-wild type BARF1 protein were permeabilized with 0.2% Triton X-100 and stained with anti-HA and anti-hTid1 antibodies at 12 h post-transfection. The same cells were also stained with Mitotracker Deep Red and R6, a vital ER dye. **(d)** Mapping the region in hTid1 responsible for interaction with BARF1 protein. The full-length and four fragments covering hTid1 sequences from amino acids 149–392, 149–320, 303–453 and 303–480 were cloned into plasmid pACT2 and co-transformed into yeast cells with the bait construct pGBKT7-BARF1 (as shown). The growth of the yeast cells on either Trp- and Leu-minus plate or Trp-, Leu- and His-minus plate is shown. Two negative controls, pGBKT7-BARF1 plus empty pACT2 and hTid1 (149–392) plus empty pGBKT7, were also included.

and 3). No detection of BARF1 and hTid1L in mock-transfected control cells was obtained (Figure 3.5a, lane 4). Immunoprecipitation of the culture media with anti-HA antibodies showed the detection of the BARF1 monomers in the culture media collecting from cells either expressing BARF1 alone or coexpressing BARF1 and hTid1L, but the amount of the protein detected in the culture medium collecting from cells coexpressing BARF1 and hTid1L was much higher than that from expressing BARF1 alone (Figure 3.5a, lanes 5 and 6).

BARF1 maturation and secretion were then analyzed by Western blotting and immunoprecipitation of non-radiolabelled total cell lysates and culture media. Western-blotting analysis of total cell lysates with anti-HA antibodies showed the detection of BARF1 monomers, dimers and other higher-order oligomers in cells expressing BARF1 alone or coexpressing BARF1 and hTid1L (Figure 3.5b, lanes 1 and 2). However, detection of much more dimers and other higher-order oligomers was obtained in cells expressing BARF1 alone (Figure 3.5b, lanes 1 and 2). Once again, similar expression levels of hTid1L were detected in cells either expressing hTid1L alone or coexpressing hTid1L and BARF1 (Figure 3.5b, lanes 2 and 3). Immunoprecipitation of the culture medium showed the detection of the BARF1 monomers in the medium collecting from cells coexpressing BARF1 and hTid1L (Figure 3.5b, lane 6); the protein was barely detected in the same volume of the culture medium collecting from cells expressing BARF1 alone (Figure 3.5b, lane 5). These results confirm that coexpression of BARF1 with hTid1 facilitates its maturation process and promotes its secretion to the culture medium.

Coexpression of hTid1L with the two secretion-defective BARF1 mutants, C146A and N95A, was then carried out to test if hTid1 can promote maturation and secretion of the mutant proteins. As shown in Figure 3.5c, coexpression of hTid1L did

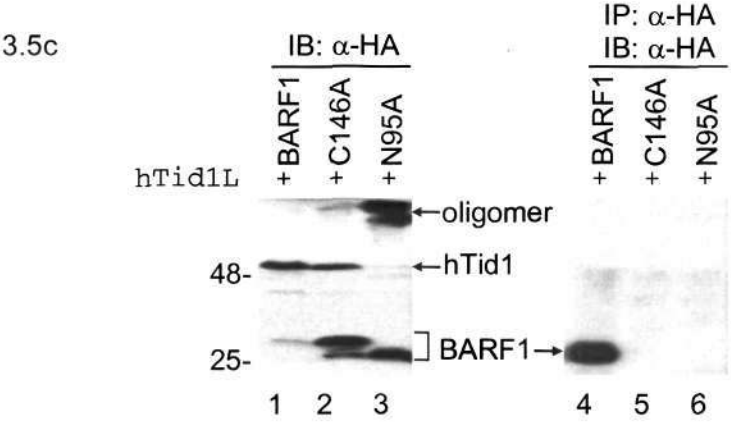
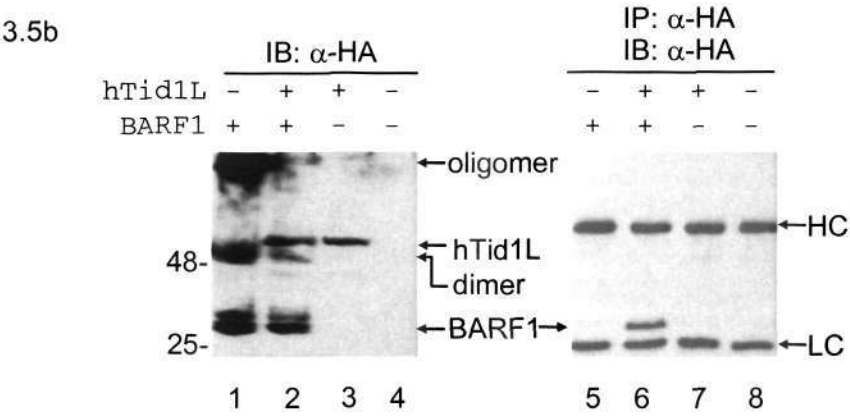
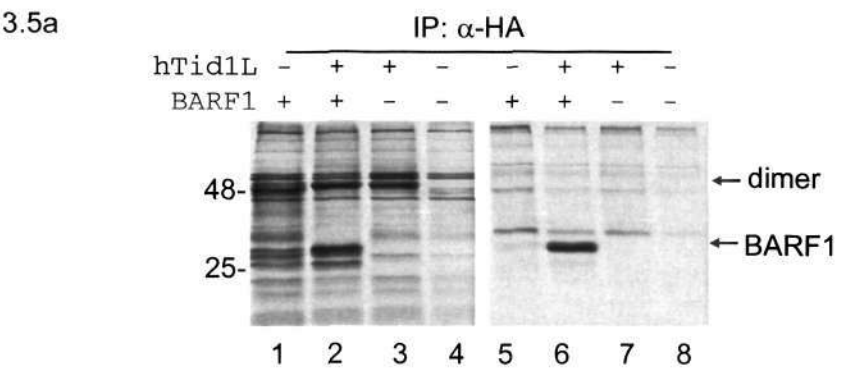


Figure 3.5 Enhanced secretion of BARF1 protein into the culture medium by coexpression with hTid1. **(a)** HeLa cells were transfected with BARF1 (lanes 1 and 5), BARF1+hTid1L (lanes 2 and 6), hTid1L (lanes 3 and 7) and empty vectors (lanes 4 and 8), radiolabeled with [³⁵S] methionine-cysteine for 3 h and harvested at 24 h post-transfection. Proteins in the total cell lysates (lanes 1–4) and culture medium (lanes 5–8) were immunoprecipitated with anti-HA antibodies, separated on 12% SDS–PAGE and visualized by autoradiography. Numbers on the left indicate molecular masses in kilodaltons. **(b)** HeLa cells were transfected with BARF1 (lanes 1 and 5), BARF1+hTid1L (lanes 2 and 6), hTid1L (lanes 3 and 7) and empty vectors (lanes 4 and 8), and harvested at 24 h post-transfection. Proteins in the total cell lysates (lanes 1–4) were separated by 12% SDS–PAGE and analyzed by Western blot with anti-HA antibodies. Proteins in the culture medium (lanes 5–8) were immunoprecipitated with anti-HA antibodies, separated by 12% SDS–PAGE and analyzed by Western blot with anti-HA antibodies. Numbers on the left indicate molecular masses in kilodaltons. HC and LC indicate heavy chain (HC) and light chain (LC) of antibodies. **(c)** HeLa cells were transfected with BARF1+hTid1L (lanes 1 and 4), C146A+hTid1L (lanes 2 and 5) and N95A+hTid1L (lanes 3 and 6), and harvested at 24 h post-transfection. Proteins in the total cell lysates (lanes 1–3) were separated by 12% SDS–PAGE and analyzed by Western blot with anti-HA antibodies. Proteins in the culture medium (lanes 4–6) were immunoprecipitated with anti-HA antibodies, separated by 12% SDS–PAGE and analyzed by Western blot with anti-HA antibodies. Numbers on the left indicate molecular masses in kilodaltons.

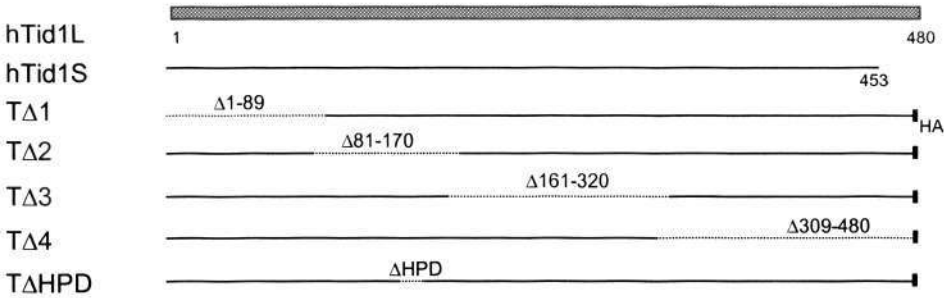
not alter the maturation process and secretion of the two mutants. Accumulation of significantly more higher-order oligomers was observed in cells expressing both mutants (Figure 3.5c, lanes 1–3); this was especially more obvious in cells expressing N95A (Figure 3.5c, lane 3). No secretion of the two mutants to the cultured medium was observed (Figure 3.5, lanes 4–6).

3.2.7 Deletion analysis of hTid1 domains involved in BARF1 maturation

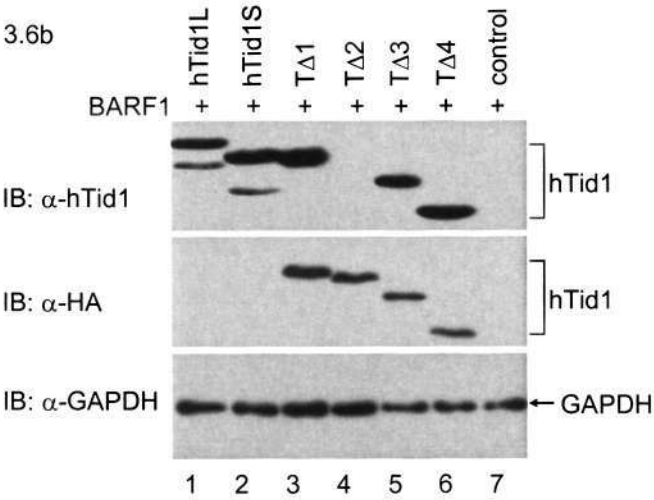
Four constructs, hTid1 Δ 1, hTid1 Δ 2, hTid1 Δ 3 and hTid1 Δ 4, which contain deletions of hTid1L sequences from amino acids 1–89, 81–170, 161–320 and 309–480, respectively, were made (Figure 3.6a), and co-transfected into HeLa cells with BARF1. Western-blotting analysis showed that similar levels of wild type and all mutant hTid1 proteins were expressed (Figure 3.6b, lanes 1–7). Immunoprecipitation and Western-blotting analysis of the culture medium showed that two deletion constructs, hTid1 Δ 3 and hTid1 Δ 4, lost the ability to promote secretion of BARF1 (Figure 3.6c, lane 5 and 7).

Human Tid1 belongs to DnaJ family containing a signature J domain through which it interacts with the heat shock protein 70 (Hsp70). In hTid1 Δ 2, the J domain was completely deleted, but the deleted protein could still promote the secretion of BARF1. As mutation of the H₁₂₁P₁₂₂D₁₂₃ motif present in the J domains was previously shown to abolish its stimulation of the ATPase activity of Hsp70 (Bork *et al.*, 1992; Cheetham and Caplan, 1998), a new deletion construct, hTid1 Δ HPD, with deletion of the conserved HPD motif was constructed. Coexpression of this deletion construct with BARF1 showed the detection of similar amounts of BARF1 in the culture medium as wild-type hTid1 (Figure 3.6d, lane 2, 3, 7, and 8). To further exclude the possibility that the observed promotion of BARF1 secretion by hTid1 may be a nonspecific effect, BARF1 was coexpressed with the vesicle-associated

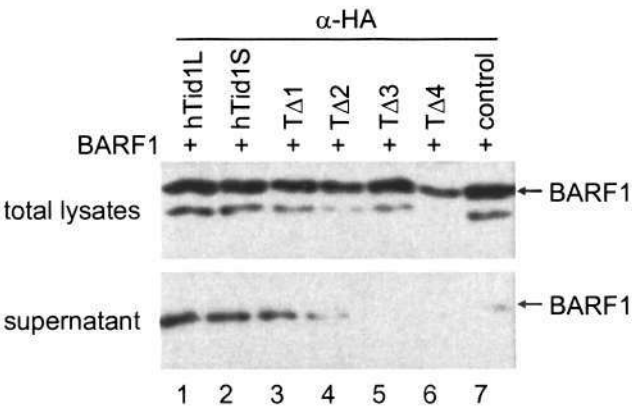
3.6a



3.6b



3.6c



3.6d

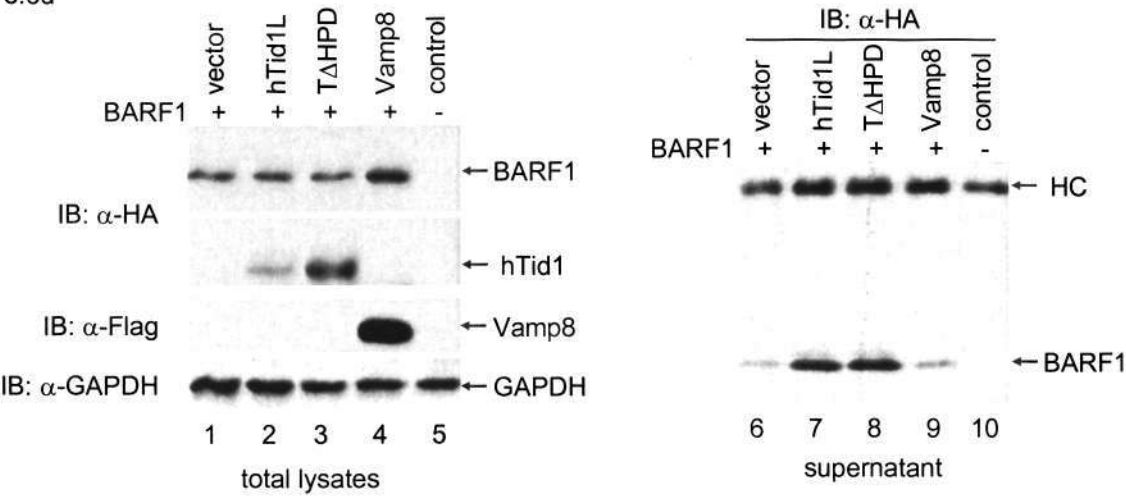


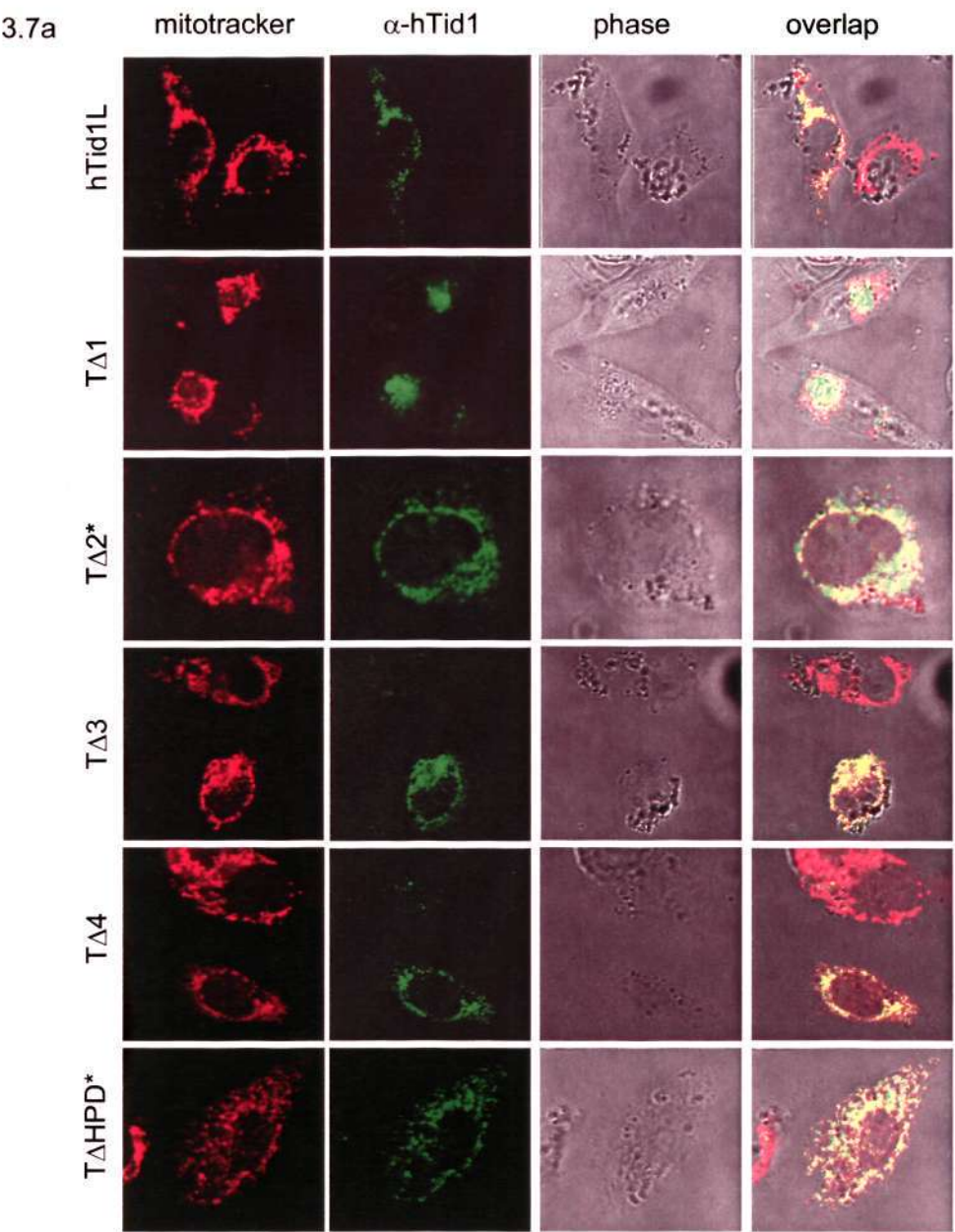
Figure 3.6 Effects of deletions of hTid1 on the maturation and secretion of BARF1. **(a)** Diagram showing wild-type hTid1L, hTid1S, and five deletion constructs. **(b)** Expression of wild type hTid1L, hTid1S, and four deletion constructs. HeLa cells were transfected with BARF1+hTid1L (lane 1), BARF1+hTid1S (lane 2), BARF1+hTid1 Δ 1 (lane 3), BARF1+hTid1 Δ 2 (lane 4), BARF1+hTid1 Δ 3 (lane 5), BARF1+hTid1 Δ 4 (lane 6), and BARF1+empty vectors (lane 7), and harvested at 24 h posttransfection. Proteins in the total cell lysates were separated by 12% SDS–PAGE and analyzed by Western blot with anti-hTid1 (upper panel) and anti-HA (middle panel) and anti-GAPDH (lower panel) antibodies. **(c)** HeLa cells were transfected with BARF1+hTid1L (lane 1), BARF1+hTid1S (lane 2), BARF1+hTid1 Δ 1 (lane 3), BARF1+hTid1 Δ 2 (lane 4), BARF1+hTid1 Δ 3 (lane 5), BARF1+hTid1 Δ 4 (lane 6) and empty vectors (lane 7), and harvested at 24 h post-transfection. Proteins in the total cell lysates (upper panel) were separated by 12% SDS–PAGE and analyzed by Western blot with anti-HA antibodies. Proteins in the culture medium (lower panel) were immunoprecipitated with anti-HA antibodies, separated by 12% SDS–PAGE and analyzed by Western blot with anti-HA antibodies. **(d)** HeLa cells were transfected with BARF1+empty vector (lanes 1 and 6), BARF1+hTid1L (lanes 2 and 7), BARF1+hTid1 Δ HPD (lanes 3 and 8), BARF1+Vamp8 (lanes 4 and 9) and empty vectors (lanes 5 and 10), respectively, and harvested at 24 h post-transfection. Proteins in the total cell lysates (lanes 1–5) were analyzed by Western blot with either anti-HA, anti-Flag, or anti-GAPDH antibodies. Proteins in the culture medium (lanes 6–10) were first immunoprecipitated with anti-HA antibodies, and analyzed by Western blot with anti-HA antibodies. HC indicates heavy chain (HC) of antibodies.

membrane protein 8 (Vamp8), a protein involved in the secretory pathway of cells (Wang et al., 2004), and the secretion of BARF1 to the culture medium was detected and compared with that from cells coexpressing BARF1 and hTid1L. As shown, coexpression of Vamp8 did not promote the secretion of BARF1 (Figure 3.6d, lane 2, 4, 7 and 9).

3.2.8 Further characterization of the subcellular localization of wild-type hTid1L and five deletion constructs

The subcellular localization of wild type hTid1L and the five deletion constructs, hTid1 Δ 1, hTid1 Δ 2, hTid1 Δ 3, hTid1 Δ 4 and hTid1 Δ HPD, was first determined by staining cells expressing the individual constructs with anti-hTid1 antibody (anti-His antibody in the case of hTid1 Δ 2 and hTid1 Δ HPD, as they cannot be recognized by anti-hTid1 antibody). The cells were also co-stained with Mitotracker Deep Red. As shown in Figure 3.7a, the staining patterns of hTid1L, hTid1 Δ 2, hTid1 Δ 3, hTid1 Δ 4 and hTid1 Δ HPD were overlapped reasonably well with the Mitotracker dye. However, very little co-alignment with the same dye was observed in cells expressing hTid1 Δ 1 (Figure 3.7a).

Coexpression of BARF1 with wild-type hTid1L and the five deletion constructs was carried out to test the effects of deletion on the colocalization of the two proteins. As shown in Figure 3.7b, relatively good colocalization of the two proteins was observed in cells coexpressing BARF1 with wild type hTid1, hTid1 Δ 1, hTid1 Δ 2 and hTid1 Δ HPD, respectively. However, in cells coexpressing BARF1 with hTid1 Δ 3 or hTid1 Δ 4, very little colocalization of the two proteins was observed (Figure 3.7b). These data support the conclusion that the mitochondria localization of hTid1 is not required for its interaction with BARF1, but the C-terminal region of the protein is essential for its physical and functional association with BARF1.



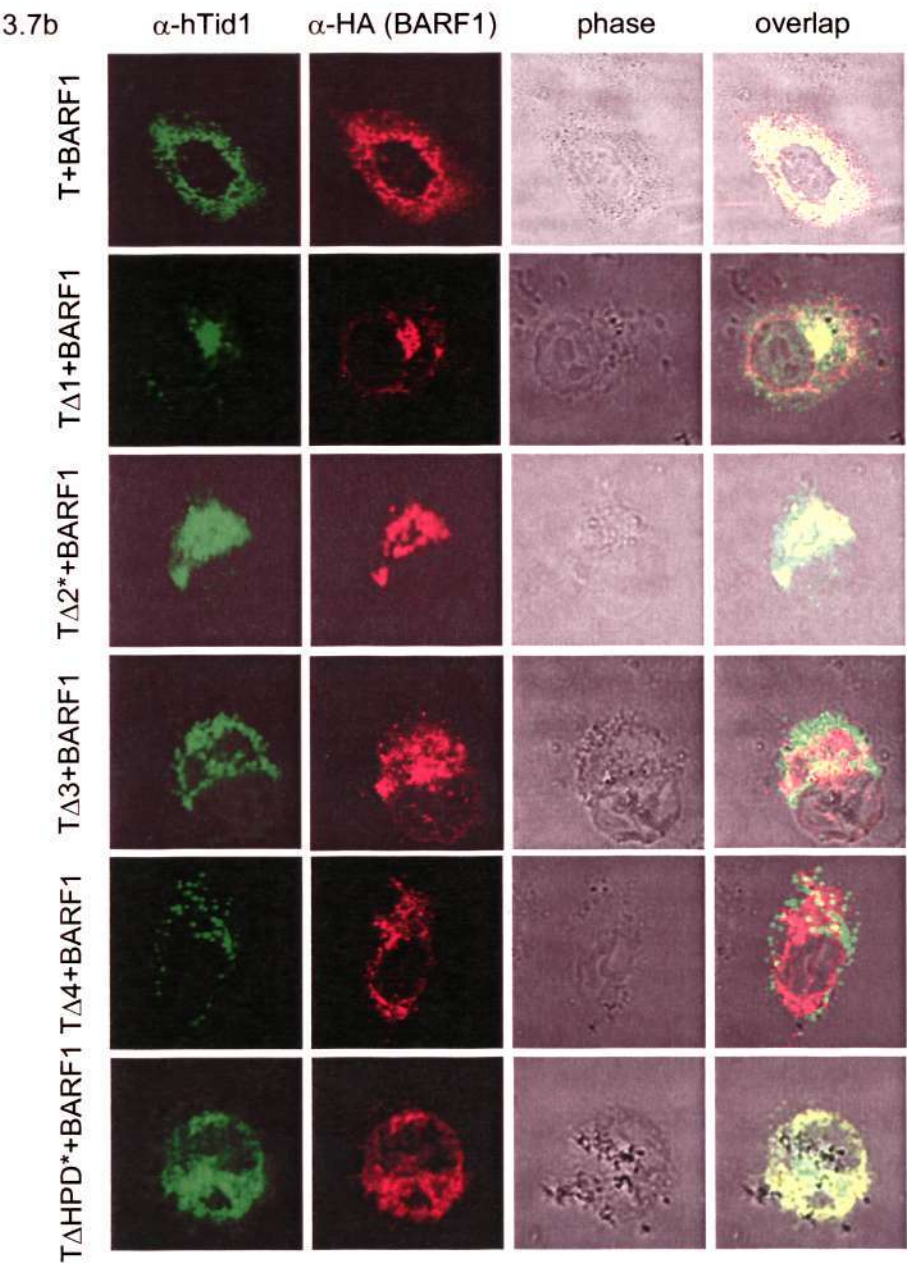


Figure 3.7 Subcellular localization of wild type hTid1 protein and five deletion constructs, and their colocalization with BARF1. **(a)** Subcellular localization of hTid1 protein and the deletion constructs. HeLa cells expressing hTid1 Δ 1, His-tagged hTid1 Δ 2, hTid1 Δ 3, hTid1 Δ 4 and His-tagged hTid1 Δ HPD were permeabilized with 0.2% Triton X-100 and stained with anti-HA antibodies (*anti-His antibodies for the His-tagged hTid1 Δ 2 and His-tagged hTid1 Δ HPD) at 12 h post-transfection. The same cells were also stained with Mitotracker Deep Red before fixation and permeabilization. **(b)** Colocalization of BARF1 protein with wild-type hTid1L and the deletion constructs. HeLa cells coexpressing HA-tagged BARF1 with hTid1L, hTid1 Δ 1, His-tagged hTid1 Δ 2, hTid1 Δ 3, hTid1 Δ 4 and His-tagged hTid1 Δ HPD, respectively, were permeabilized with 0.2% Triton X-100 and stained with anti-HA and anti-hTid1 antibodies (*anti-His antibodies in the case of His-tagged hTid1 Δ 2 and His-tagged hTid1 Δ HPD) at 12 h post-transfection.

3.3 Discussion

3.3.1 Biochemical characterization of BARF1

EBV BARF1 gene encodes a secretory protein with transforming and mitogenic activities. In this study, detailed characterization of the biochemical properties, including post-translational modification, folding, maturation and secretion, of BARF1 protein was initially carried out by expression of the protein in mammalian cells using the vaccinia/T7 expression system. Data presented showed that the monomeric BARF1 protein migrated as three major bands with approximately molecular masses of 26, 27, and 28 kDa on SDS-PAGE under reducing conditions, suggesting that post-translational modifications may occur on the mature form of the protein. Computer-aided prediction, glycosidase treatment and site-directed mutagenesis confirmed that the protein was post-translationally modified by N-linked glycosylation and that asparagine 95 was the site for this modification. Immunofluorescent staining of cells expressing wild-type and N95A mutant BARF1 protein showed that the mutant protein failed to translocate to the Golgi apparatus and the plasma membrane. No secretion of the protein into the culture medium was detected. These results demonstrated that N-linked glycosylation of BARF1 protein is essential for the folding, subcellular translocation and efficient secretion of the protein.

BARF1 protein contains a total of four cysteine residues in its amino-acid sequence. Site-directed mutagenesis of the four cysteine residues demonstrated that cysteine residues 146 and 201 were also essential for proper folding and secretion of the protein. Under nonreducing conditions, intracellular BARF1 protein migrated as monomers, dimers and other higher-order oligomers/aggregates, whereas the secreted form was detected as almost uniform monomers. As the secreted BARF1 was shown to possess mitogenic activities, the functionally active BARF1 protein may be

monomeric when analyzed by denaturing SDS–PAGE under both reducing and nonreducing conditions. This is consistent with the reported results (Sall et al., 2004; De Turenne-Tessier et al., 2005). However, the secreted BARF1 protein was demonstrated to be in the macromolecular state with a molecular mass in the range of 150–240 kDa under native conditions (De Turenne-Tessier et al., 2005). As this macromolecular complex was disassociated under denaturing conditions, it is unlikely linked by covalent bonds. The significance of dimerization/oligomerization of BARF1 protein by the formation of interchain disulfide bonds in the biological activities of the protein is currently unclear. It is plausible that the higher-order oligomers/aggregates detected by the denaturing SDS–PAGE used in this study may represent functionally inactive BARF1 protein. On the other hand, detection of dimers from cells expressing wild-type and C14A, C103A and C201A mutants under reducing conditions suggests that the formation of BARF1 oligomers is partially due to other interactions, including hydrophobic interaction, between BARF1 molecules. Interestingly, no detection of dimers and other oligomers was obtained in cells expressing mutant C146A under reducing conditions. However, multiple forms of aggregates were detected under nonreducing conditions in cells expressing C146A and C201A mutants. These results indicate that cysteine 146 and 201 may play essential roles in maintaining the overall conformation of BARF1 either via formation of intrachain disulfide bonds and/or by hydrophobic interaction.

In this study, overexpression of BARF1 on its own in cells was shown to induce the formation of massive aggregates/higher-order oligomers with a wide range of molecular masses. The majority of these aggregates/oligomers formed in cells overexpressing the HA-tagged BARF1 was undetectable by immunoprecipitation with anti-HA antibody, though efficient detection of these forms was achieved by Western-

blot analysis with the same antibody. This provides an additional line of supportive evidence that aggregates/higher-order oligomers may represent functionally inactive BARF1 with distorted conformation.

3.3.2 The interaction between BARF1 and hTid1

In an attempt to search for host proteins that may promote the folding, processing, maturation and secretion of BARF1 protein by yeast two-hybrid screening, human hTid1 protein was identified as an interacting protein of BARF1. This interaction was shown to reduce the formation of aggregates/higher-order oligomers and to promote secretion of BARF1. The specificity of this secretion-promoting effect rendered by the association of BARF1 with hTid1 was further supported by the observation that coexpression of BARF1 with Vamp8 did not affect the secretion of BARF1. These results suggest that hTid1 may act as a chaperone to facilitate the maturation process of BARF1.

The human homologue of the *Drosophila* tumor suppressor lethal (2) tumorous imaginal disc 1 (*l(2)tid*) gene, hTid1, encodes two proteins (hTiDL and hTiDS) of 43 and 40 kDa by alternative mRNA splicing (Syken et al., 1999). Human hTid1 protein interacts with a diverse of viral and cellular proteins, and regulates the functions of these partner proteins. Examples include its interaction with a molecular chaperone complex containing Tax and Hsp70 (Cheng et al., 2001) and repression of the Tax-induced transactivation of NF- κ B (Cheng et al., 2002), interaction with herpes simplex virus type 1 (HSV-1) nuclear protein UL9 and enhancement of the binding of UL9 to the viral genome (Eom et al., 2002). It is also a cellular target of the oncogenic protein E7 of HPV16 (Schilling et al., 1998) and viral transforming protein Tax of human T-cell leukemia virus type 1 (HTLV-1). Cellular proteins that were identified to interact with hTid1 include Jak2 tyrosine kinase (Sarkar et al., 2001), Erb-2

receptor tyrosine kinase (Kim et al., 2004) and TPR/MET tyrosine kinase (Schaaf et al., 2005).

Molecular chaperones are proteins that associate specifically with incompletely folded or unassembled proteins and increase the efficiency of acquiring correct three-dimensional structures of these proteins. Protein chaperones and cochaperones are usually involved in the synthesis and maturation of viral proteins (Mayer, 2005). Human hTid1 protein was found to be able to interact with several other viral and cellular proteins (Schilling et al., 1998; Eom and Lehman, 2002; Kim et al., 2004; Schaaf et al., 2005). As hTid1 could form complex with Hsp70 (Cheng et al., 2001; Sarkar et al., 2001; Kim et al., 2004), attempts were made to detect the interaction between BARF1 and Hsp70. However, no direct interaction between the two proteins was detected. As deletion of the conserved HPD motif within the J domain of hTid1 was reported to impair its association with Hsp70 (Cheng et al., 2001), construct with the same deletion was made and coexpressed with BARF1. Interestingly, it was observed that, similar to the results obtained from coexpression of BARF1 and hTid1 Δ 2 (with deletion of the whole J domain), deletion of this motif did not affect the secretion-promoting activity of the hTid1 protein, implying that association of hTid1 with Hsp70 may be not necessary for the involvement of hTid1 in the maturation and secretion of BARF1. At present, however, we cannot rule out the possibilities that BARF1, hTid1, and Hsp70 might be able to form a weak multi-protein complex, and that other chaperone proteins may be also involved.

Deletion studies revealed that two domains located at amino acids 149–320 and 303–453, respectively, in hTid1S may contribute to its interaction with BARF1. As the extreme C-terminal region of hTidL may block the binding of the second domain to BARF1, it is likely that only the first domain from amino acids 149–320 is

responsible for the interaction of hTid1L with BARF1. However, the full-length hTid1L showed similar binding affinity as hTid1S, and both isoforms could promote the secretion of BARF1. Coexpression of two deletion mutants of hTid1L, hTid1 Δ 3 and hTid1 Δ 4, with BARF1 showed that no enhanced secretion of BARF1 was detected. Instead, they may have certain inhibitory effect on the secretion of BARF1. These results indicate that binding of hTid1 to BARF1 *per se* is not sufficient to promote secretion of BARF1. To reinforce this conclusion, it was observed that all three secretion-defective BARF1 mutants were able to interact with hTid1. However, this interaction cannot restore the secretion of the mutant proteins even in the presence of hTid1.

Human Tid1 was shown to be localized to the mitochondria and its function as a chaperone is also associated with this localization pattern (Cheng et al., 2001; Sarkar et al., 2001). The presence of BARF1 protein partially sequesters hTid1 from the mitochondria to the ER. In fact, the hTid1 protein is not completely merged with a mitochondria marker even when it was expressed on its own. Interestingly, deletion (hTid1 Δ 1) that removes the mitochondria-localization signal did not affect the secretion-promoting activity of hTid1. On the contrary, deletions (hTid1 Δ 3 and hTid1 Δ 4) that maintain the mitochondria-localization signal but abrogate the association of hTid1 with BARF1 abolished the secretion-promoting activity of hTid1. Coincidentally, when BARF1 was coexpressed with wild type hTid1, hTid1 Δ 1, hTid1 Δ 2 and hTid1 Δ HPD, respectively, the two proteins were found to assume ER- and/or Golgi-localization patterns and the staining patterns of the two proteins are largely overlapped. When hTid1 Δ 3 or hTid1 Δ 4 was coexpressed with BARF1, however, very little co-alignment of the staining patterns of the two proteins was found. It suggests that physical association between BARF1 and hTid1 that sequesters the later to the

ER and/or the Golgi apparatus would be a prerequisite for the functional interaction of the two proteins. In conclusion, this study has revealed a mitochondria-independent function of hTid1 protein that is essential for promoting the maturation and secretion of a viral transforming and mitogenic protein.

Chapter Four

Avian Infectious Bronchitis Virus Cell Tropism and Pathogenesis

4.1 Introduction

Successful replication of virus in its host is a complex process involving virus-host interactions. The viral pathogen must gain entry into the host cell, replicate with the assistance of host factors, evade the inhibitory effects of host products, exit the initially infected cells and spread to neighboring cells. Viruses can also transmit from the initial host to a new host. Each of these processes may require adaptive changes in the pathogen. It is beneficial and interesting to understand the molecular changes that enable viruses to adapt to a new host.

Entry of viruses into the host cell by crossing the cell membrane is a prerequisite to replication. This process is initially mediated by the interaction of a virus protein with its corresponding host receptor and this interaction is one of the prime determinants for the host specificity. Cellular receptors have been identified for several coronaviruses. For example, aminopeptidase N (APN) acts as the receptor for group 1 coronaviruses including TGEV, HCoV 229E, CCoV, and FIPV (Delmas et al., 1992; Tresnan et al., 1996; Yeager et al., 1992). The carcinoembryonic antigen-cell adhesion molecular (CEACAM), which is expressed mainly in the liver and gastrointestinal tissues, is the receptor for MHV (Dveksler et al., 1993; Williams et al., 1991; Coutelier et al., 1994; Godfraind et al., 1995). Angiotensin-converting enzyme 2 (ACE2) and CD209L are employed by SARS-CoV and human coronavirus (HCoV-NL63) as the receptor (Li et al., 2003; Hofmann et al., 2005; Jeffers et al., 2004). CD209L was initially identified as a human immunodeficiency virus (HIV) co-receptor (Curtis et al., 1992; Geijtenbeek et al., 2000) but has been found to be a co-receptor for hepatitis C virus (Pohlmann et al., 2003), cytomegalovirus (Halary et al., 2002), dengue virus (Tassaneetrithep et al., 2003), and Sars-CoV (Jeffers et al., 2004).

The IBV receptor in its native or adapted host cells remains unknown yet, although IBV might use APN as the receptor in vitro (Miguel et al., 2002). The widely distributed sialic acid was suggested to be important for primary attachment of IBV to host cells (Winter et al., 2006).

In addition to the presence of a suitable host cell receptor, virus must find ways to overcome host cell innate immune system, the first line of anti-viral defense, to ensure the successful infection. In tissue cells, transcription of the IFN- β gene represents the primary response to virus infection (Deonarain et al., 2000). Infected cells synthesize and secrete alpha/beta interferon (IFN- α/β), which causes neighboring cells to express antiviral factors, thereby limiting viral spread (Stark et al., 1998). The biological response to IFN is mediated by its binding to cell type specific receptors, activation of the Jak-Stat signaling pathway and stimulation of transcription of several hundreds of IFN-induced genes (ISG) (de Veer et al., 2001). Viruses have evolved effective strategies to evade the IFN system (Goodbourn et al., 2000; Levy and Garcia-Sastre, 2001; Weber et al., 2003). However, the interaction between coronavirus and IFN system has not been extensively studied, although coronaviruses are known to be sensitive to the antiviral action of IFNs (Cinatl et al., 2003, Kawamoto et al., 2003; Pei et al., 2001). It was recently reported that SARS-CoV was able to prevent induction of IFN in infected cells by inhibiting the nuclear localization of IRF3, which is required for IFN- β induction (Spiegel et al., 2005).

Coronaviruses generally have a limited host range. The novel SARS-CoV was found to cross host species from palm civet cats to humans (Guan et al., 2003). In addition, HCoV-OC43 was able to infect cells from a large number of mammalian species, although the virus was passed exclusively in suckling mouse brains (Butler et al., 2006). How a coronavirus breaks the host barrier and become zoonotic would be

very interesting. Here, IBV was used to study the mechanisms underlying the specificity of coronavirus and coronavirus-host interactions.

For a long time, chicken is believed to be the only natural host for IBV. However, the Beaudette strain of IBV from chicken embryo was continuously propagated in a monkey kidney cell line, Vero, for 65 passages (Shen et al., 2003). This adaptation was accompanied by dramatic changes in the S protein (Fang et al., 2005). In this study, a total of fifteen cell lines with different species and tissue origins were found to be susceptible to the Vero cell-adapted IBV, and five out of the fifteen were able to support continuous IBV propagation. It would be interesting to characterize mechanisms by which IBV successfully replicate in these new cell lines. IBV infection in these fifteen cell lines was studied and whether genotypic changes in IBV S gene occur during the replication were also examined. The expression of host innate immune genes, *IFN- β* and *ISG15*, in cells infected with IBV was also analyzed.

4.2 Results

4.2.1 The susceptibility of fifteen cell lines to Vero cell-adapted IBV

The Beaudette strain of IBV from chicken embryo has been serially propagated in a monkey kidney cell line, Vero, for 65 passages (Shen et al., 2003). A dominant Vero cell-adapted strain was generated by either dramatic changes in S gene or rapid selection of a fitter strain from some minor variants during this adaptation (Fang et al., 2005). In this study, the susceptibility of various cell lines to IBV was tested by infecting them with the 65th passage (p65) of Vero cell-adapted IBV (Vero-p65). The tissue and species origins of each cell line were listed in Table 4.1. The cytopathic effect (CPE) caused by IBV infection in each cell line was visualized under microscopy 12 h post-infection (Figure 4.1). Similar to Vero cell line, infection of cell lines H1299, Huh7, and Hep3B with IBV generated giant syncytial cells, leading to the destruction of the entire monolayers and death of the infected cells (Figure 4.1, left panel). In these three cell lines, IBV could be continuously passed to passage 20 (p20), indicating that IBV was readily adapted to these cells. Another two cell lines in which IBV was passed to p20 were HepG2 and HCT116. It was noted that CPE was not obvious in HepG2 and even not visible in HCT116 (Figure 4.1). For cell lines A549, BHK, CHO, CHOHT3, Cos-7, DLD1Amix, HeLa, and 293T, IBV infection caused formation of some syncytial cells at 12 h post-infection (Figure 4.1). These fusion cells died after longer incubation and the viruses did not spread to neighboring cells. CPE was rarely observed in MRC-5 and DLD1 cell lines (Figure 4.1).

4.2.2 Expression of IBV structural protein S, N, and M in IBV-infected cell lines

As described, CPE was observed in some but not in others of the fifteen cell lines. To confirm the infection in these cells, a time course experiment was carried out

Cell line	Organ and cell type	Organism	Continuous propagation
H1299	Lung epithelial cell	Human	Yes
A549	Lung epithelial cell	Human	No
MRC-5	Lung fibroblast	Human	No
Huh7	Liver epithelial cell	Human	Yes
HepG2	Liver epithelial cell	Human	Yes
Hep3B	Liver epithelial cell	Human	Yes
HCT116	Colon epithelial cell	Human	Yes
DLD-1	Colon epithelial cell	Human	No
DLD-1A Mix	Colon epithelial cell	Human	No
Vero	Kidney epithelial cell	Monkey	Yes
BHK	Kidney fibroblast	Hamster	No
293T	Kidney epithelial cell	Human	No
Cos-7	Kidney fibroblast	monkey	No
CHO	Ovary epithelial cell	Hamster	No
CHOHT3	Ovary epithelial cell	Hamster	No
HeLa	Cervix epithelial cell	Human	No

Table 4.1 Different cell lines which are susceptible to IBV.

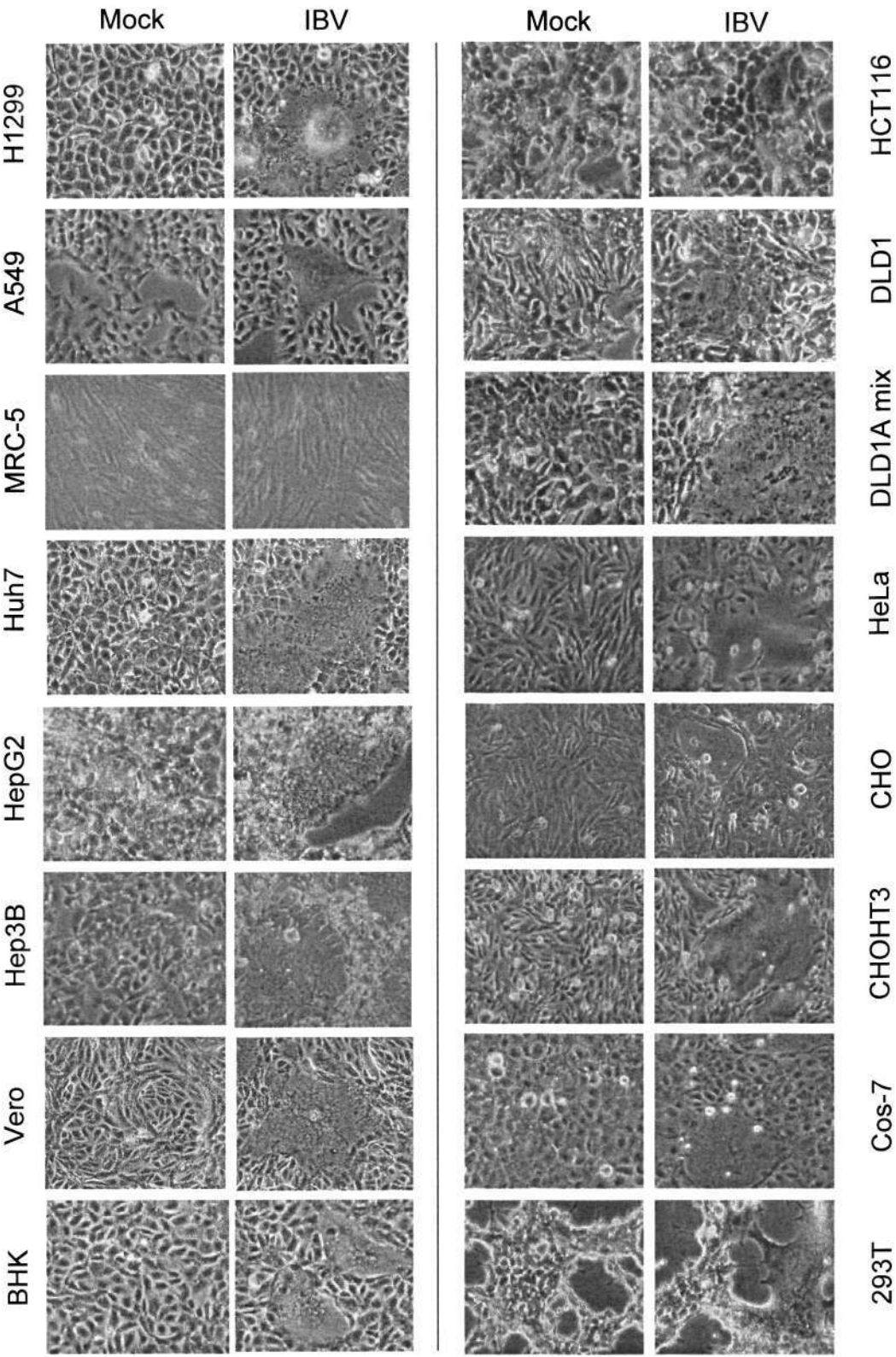


Figure 4.1 Morphological change of different cell lines infected with Vero-p65. Cells were infected with Vero-p65 and observed by phase-contrast microscopy at 12 h post-infection.

in each cell line. Cells were infected with IBV and harvested at different time points post-infection. IBV structural proteins, S, N, and M, were analyzed by Western blot using polyclonal antibodies against S, N, and M, respectively. β -actin was included as the loading control. To allow better understanding of tissue tropism of IBV, the fifteen cell lines were classified into five groups according to their tissue origins.

4.2.2.1 Lung cell lines susceptible to IBV

Cell lines A549, H1299, and MRC-5 are originated from lung tissue. A549 and H1299 cell lines are derived from human lung carcinomas. MRC-5 is a human lung fibroblast cell line. As A549 and MRC-5 cells are much more resistant to IBV infection than H1299 cells, 1×10^4 PFU/ml of IBV was used to infect H1299 while 3×10^4 PFU/ml of IBV was used to infect the other two cell lines.

In IBV-infected H1299 cells, S and N proteins were detectable at as early as 12 h post-infection (Figure 4.2a, top panel, lane 2), and M protein was detectable from 16 h post-infection (Figure 4.2a, top panel, lane 3-6). The expression level of all three proteins increased with the infection time. IBV S antibodies detected three protein species of approximately 180, 150, 90 kDa (Figure 4.2a, top panel, lane 4 and 5). The 180- and 150-kDa bands represent the glycosylated and unglycosylated forms of precursor protein S0, respectively. The 90-kDa band represents the post-translationally cleaved S1/S2 protein. The molecular weight of S1 is similar to that of S2. The two bands were not separated in this experiment. For N protein, a major protein species of approximately 48 kDa and three less abundant bands, which migrated more rapidly than the 48-kDa band, were detected (Figure 4.2a, top panel, lane 4-6). The four isoforms may represent the full length and post-translationally modified forms of the IBV N protein. IBV M antibodies detected two protein bands of

approximately 30 kDa and 25 kDa, representing the glycosylated and nascent M protein (Figure 4.2a, top panel, lane 4-6).

In IBV-infected A549 cells, S and N proteins were detectable from 16 h post-infection (Figure 4.2a, middle panel, lane 3-6), and M protein was detectable from 36 h post-infection (Figure 4.2a, middle panel, lane 5). The expression level of all three proteins increased with the infection time. IBV S antibodies detected only two protein species, the unglycosylated S0 protein and the cleaved S1/S2 protein (Figure 4.2a, middle panel, lane 3-6). For IBV N protein, the full length form and one additionally modified form were detected (Figure 4.2a, middle panel, lane 5 and 6). IBV M antibodies detected one single band of approximately 30 kDa, which represents the glycosylated M protein (Figure 4.2a, middle panel, lane 5 and 6).

In IBV-infected MRC-5 cells, S, N and M proteins were all detectable from 12 h post-infection but the expression level did not increase much with infection time (Figure 4.2a, bottom panel, lane 2-6). IBV S antibodies detected three protein species, the unglycosylated S0 protein and the cleaved S1 and S2 proteins (Figure 4.2a, bottom panel, lane 3-6). S1 protein was shown to migrated a bit slower than S2 protein (Figure 4.2a, bottom panel, lane 3-6). IBV N antibodies detected the 48-kDa full length species only (Figure 4.2a, bottom panel, lane 2-6). IBV M antibodies detected the glycosylated M protein, which is approximately 30 kDa (Figure 4.2a, bottom panel, lane 2-6).

Although two folds more infectious viruses were used to infect A549 and MRC-5 cells, the expression levels of IBV structural protein S, N and M in these two cell lines were much lower than those in H1299 cells, suggesting that IBV replicated much more efficiently in H1299 cells than in A549 and MRC-5 cells.

4.2.2.2 Liver cell lines susceptible to IBV

Hep3B, HepG2 and Huh-7 are three liver cancer cell lines derived from human hepatomas. The same amount of IBV, 1×10^4 PFU/ml, was used to infect the three cell lines. Huh7 cells showed comparatively better capability to support the replication of IBV than HepG2 and Hep3B cells from the expression levels of viral proteins S, N, and M at different time points post-infection (Figure 4.2b).

In IBV-infected Huh7 cells, S, N and M proteins were detectable from 16 h post-infection and expression levels increased with the infection time (Figure 4.2b, top panel). The glycosylated form of S0 protein and the cleaved S1/S2 protein with molecular mass of 80-90 kDa were detected by IBV S antibodies (Figure 4.2b, top panel, lane 4 and 5). For IBV N protein, the full length 48-kDa band and about six post-translationally modified bands were detected (Figure 4.2b, top panel, lane 4-6). IBV M antibodies detected two major bands of approximately 32 kDa and 30 kDa and one weak band of approximately 25 kDa (Figure 4.2b, top panel, lane 4-6). The 32-kDa and 30-kDa species of M protein may represent the glycosylated forms. All three IBV structural proteins expressed in IBV-infected Huh7 cells were much more heavily translationally modified than that in H1299 cells and other cells, as evidenced from the detection of more isoforms for each protein (Figure 4.2b, top panel).

In IBV-infected HepG2 cells, S protein was able to be detected from 16 h post-infection (Figure 4.2b, middle panel, lane 3-6), and N protein was detected from 12 h post-infection (Figure 4.2b, middle panel, lane 2-6). The glycosylated and unglycosylated S0 proteins and the cleaved S1/S2 protein were detected by IBV S antibodies (Figure 4.2b, middle panel, lane 6). The full length N protein and two less abundant species which are post-translationally modified N proteins were detected by IBV N antibodies ((Figure 4.2b, middle panel, lane 2-6). IBV M protein was not

detected in IBV-infected HepG2 cells up to 36 h post-infection and only tiny amount was detected at 48 h post-infection (Figure 4.2b, middle panel, lane 6). This is probably due to the inefficient solubilization of this protein as IBV M protein is highly hydrophobic and membrane associated. The poor expression of M protein in HepG2 cells may also suggest that IBV replication in this cell line is not very efficient.

In IBV-infected Hep3B cells, IBV S, N and M proteins were all detectable from 12 h post-infection (Figure 4.2b, bottom panel, lane 2-6). The expression level of S protein peaked at 16 h post-infection and decreased marginally with longer time infection. The expression level of N protein increased with the infection time. IBV S antibodies detected the glycosylated S0 protein and the cleaved S1 and S2 proteins (Figure 4.2b, bottom panel, lane 3-6). The expression level of N protein increased with the infection time. The 48-kDa full length N protein and two post-translationally modified species were detected by IBV N antibodies (Figure 4.2b, bottom panel, lane 4-6). The expression level of M protein did not increase much with the infection time and IBV M antibodies detected one single band of approximately 30 kDa, which is the glycosylated M protein (Figure 4.2b, bottom panel, lane 2-6).

4.2.2.3 Colorectal cell lines susceptible to IBV

HCT116 cell line is derived from a human colon carcinoma. DLD-1 and DLD-1Amix are cell lines derived from human colorectal adenocarcinomas. The starting amount of IBV used to infect was 3×10^4 PFU/ml for all these three cell lines. The expression profiles of IBV S and N proteins in IBV-infected DLD-1, DLD-1Amix and HCT116 cells were similar. IBV S and N proteins were detectable at as early as 12 h post-infection and increased with infection time (Figure 4.2c, lane 2). Two protein species, which are the unglycosylated S0 protein and the cleaved S1/S2 protein, were detected by IBV S antibodies (Figure 4.2c, lane 2-6). IBV N protein antibodies

detected the full length form and two post-translationally modified forms (Figure 4.2c, lane 5 and 6). In IBV-infected HCT116 cells, M protein was not detected throughout the whole time course (Figure 4.2c, top panel, lane 2-6), indicating the inefficient IBV replication in this cell line. In IBV-infected DLD1 and DLD1Amix cells, M protein was detectable at 16 and 12 h post-infection respectively, and increased with infection time (Figure 4.2c, middle and bottom panels, lane 2-6).

4.2.2.4 Kidney cell lines susceptible to IBV

Similar to Vero cell line, BHK-21, a baby hamster fibroblast cell line and 293T, a human epithelial cell line, are both with kidney tissue origin. 3×10^4 PFU/ml of IBV was used to infect BHK-21 and 293T cells while 1×10^4 PFU/ml of IBV was used to infect Vero cells.

In IBV-infected Vero cells, N protein was detected from 12 h post-infection and increased with infection time (Figure 4.2d, top panel, lane 2-6). IBV S and M proteins were detectable from 24 h post-infection and increased with infection time (Figure 4.2d, top panel, lane 4-6). Three protein species, which are the unglycosylated and glycosylated S0 proteins and the cleaved S1/S2 protein, were detected by IBV S antibodies (Figure 4.2d, top panel, lane 4-6). For IBV N protein, the full length form and more than four post-translationally modified forms were detected (Figure 4.2d, top panel, lane 5 and 6). IBV M antibodies detected two protein species, the glycosylated and unglycosylated M proteins (Figure 4.2d, top panel, lane 5 and 6).

In IBV-infected 293T cells, IBV S and N proteins were detectable at as early as 12 h post-infection (Figure 4.2d, middle panel, lane 2-6). Three protein species, which are the unglycosylated and glycosylated S0 proteins and cleaved S1/S2 protein, were detected by IBV S antibodies (Figure 4.2d, middle panel, lane 4-6). The full length N protein and more than four post-translationally modified bands were detected

by IBV N antibodies (Figure 4.2d, middle panel, lane 3-6). M protein was not detectable in IBV-infected 293T cells (Figure 4.2d, middle panel, lane 2-6)

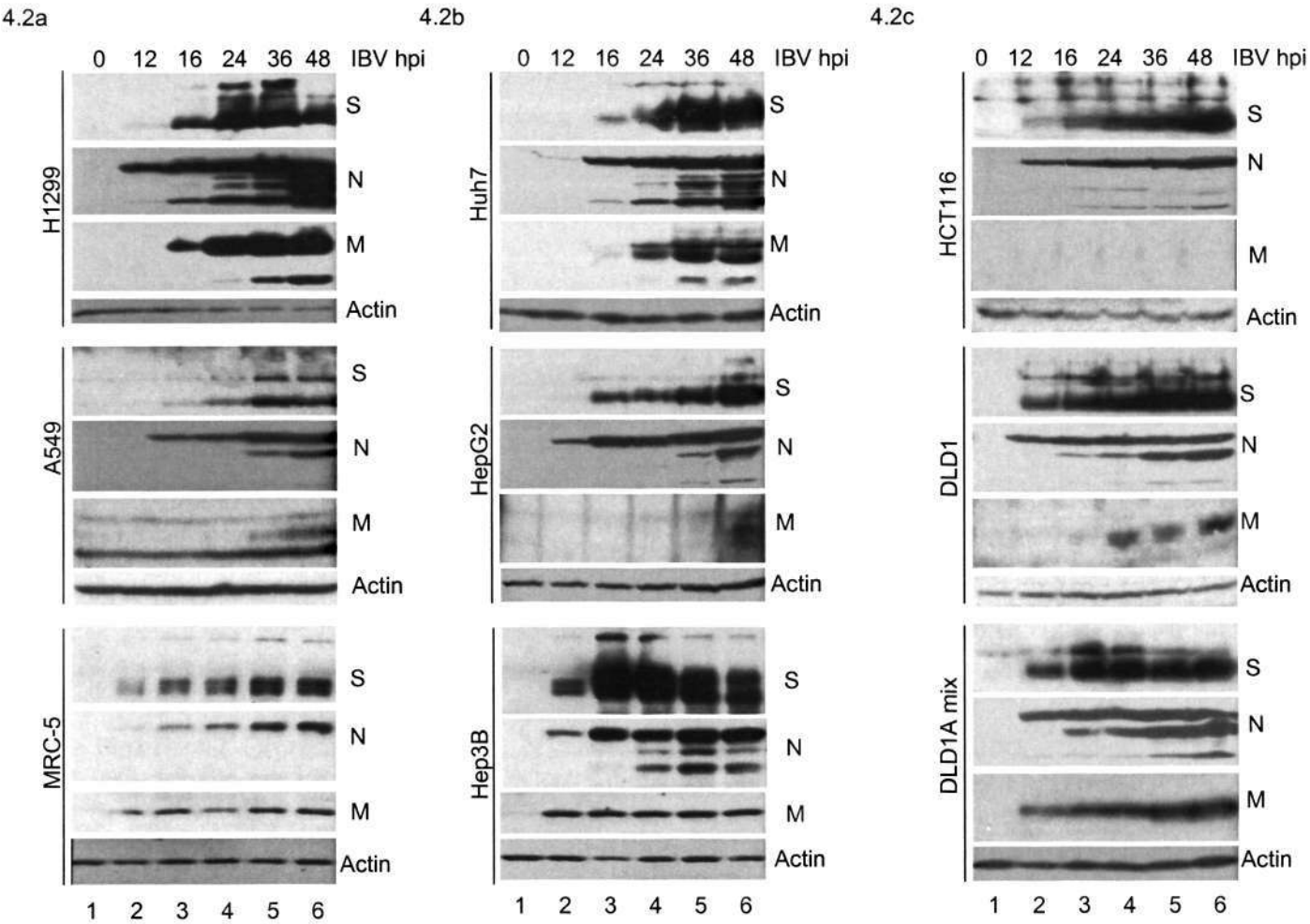
In IBV-infected BHK cells, the expression levels of all three viral proteins increased with infection time. IBV S and M proteins were detectable from 16 h post-infection and IBV N protein was detected from 12 h post-infection (Figure 4.2d, bottom panel, lane 3-6). Three protein species, which are the unglycosylated and glycosylated S0 proteins and the cleaved S1/S2 protein, were detected by IBV S antibodies (Figure 4.2d, bottom panel, lane 3-6). IBV N antibodies detected the full length isoform and four or five post-translationally modified isoforms (Figure 4.2d, bottom panel, lane 5 and 6). IBV M antibodies detected the glycosylated M protein (Figure 4.2d, bottom panel, lane 5 and 6).

4.2.2.5 Other cell lines susceptible to IBV

The expression of IBV structural proteins in IBV-infected Cos-7, CHO, CHOHT3, and HeLa cells were also analyzed by Western blot, but not shown here, as no time course infection was done.

4.2.3 Growth profiles of Vero cell-adapted IBV in H1299, Huh7, and HCT116 cells

Although IBV structural proteins were detectable in all fifteen cell lines infected with IBV (Figure 4.2), IBV was continuously passaged to p20 in only five human cell lines including H1299, HepG2, Hep3B, Huh7, and HCT116. In the other nine cell lines, viruses were hardly recovered after only one or a few passages. The growth profiles of p1, p5, and p20 IBV from H1299, Huh7 and HCT116 cell lines were studied by TCID₅₀ assay. Approximately 1×10^4 PFU/ml of p1, p5 and p20 IBV from H1299 or Huh7 cells were used to infect H1299 or Huh7 cells, respectively. The titer of progeny virus was determined over a 36 h period. Approximately 1×10^4



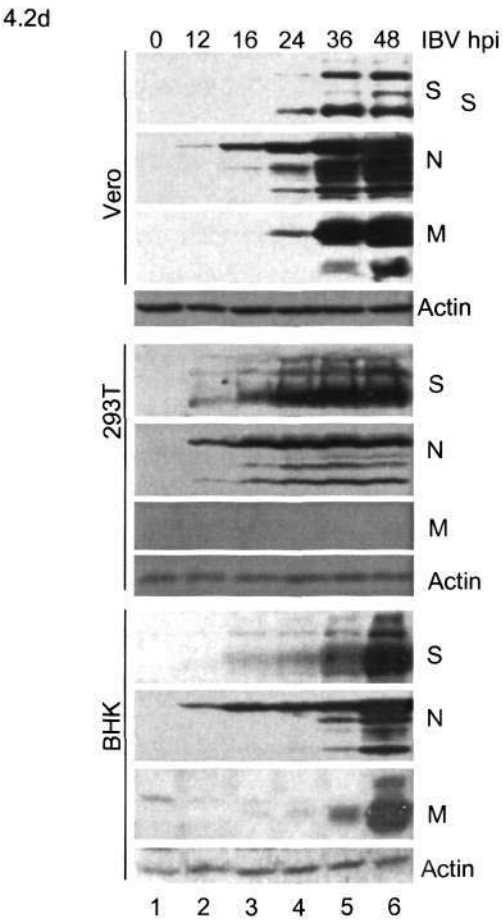


Figure 4.2 Expression of IBV S, N, and M proteins in different cell lines infected with IBV. (a) H1299, A549, and MRC-5 cells were infected with IBV and harvested at 12, 16, 24, 36, and 48 h post-transfection. Cell lysates were prepared and the expression of IBV S, N, and M proteins was detected by Western blot with anti-S, -N, and -M antibodies after proteins were separated by 8% SDS-PAGE. (b) Huh7, HepG2, and Hep3B cells were infected with IBV and harvested at 12, 16, 24, 36, and 48 h post-transfection. Cell lysates were prepared and the expression of IBV S, N, and M proteins was detected by Western blot with anti-S, -N, and -M antibodies after proteins were separated by 8% SDS-PAGE. (c) HCT116, DLD1, and DLD1Amix cells were infected with IBV and harvested at 12, 16, 24, 36, and 48 h post-transfection. Cell lysates were prepared and the expression of IBV S, N, and M proteins was detected by Western blot with anti-S, -N, and -M antibodies after proteins were separated by 8% SDS-PAGE. (d) Vero, 293T, and BHK cells were infected with IBV and harvested at 12, 16, 24, 36, and 48 h post-transfection. Cell lysates were prepared and the expression of IBV S, N, and M proteins was detected by Western blot with anti-S, -N, and -M antibodies after proteins were separated by 8% SDS-PAGE.

PFU/ml of p1, p5 and p20 IBV from HCT116 cells were used to infect Vero cells to determine the titer of progeny virus, because CPE was hardly observed in HCT116 cells (Figure 4.1, right panel).

The titer of p1 IBV from H1299 cells (H1299-p1) dropped to approximately 1×10^2 PFU/ml at 6 h post-infection, increased afterwards, peaked to 5×10^5 PFU/ml at 16 h post-infection and declined afterwards (Figure 4.3a, dark blue line). The titer of p5 IBV from H1299 cells (H1299-p5) dropped to approximately 1×10^3 PFU/ml at 6 h post-infection, increased afterwards, peaked to 5×10^5 PFU/ml at 24 h post-infection and declined slowly afterwards (Figure 4.3a, red line). The virus titer of p20 IBV from H1299 cells (H1299-p20) dropped to 5×10^2 PFU/ml at 6 h post-infection, increased at 10 h post-infection, dropped slightly again at 16 h post-infection and peaked at 24 h post-infection to 1×10^5 PFU/ml (Figure 4.3a, green line).

The p1 and p5 IBV from Huh7 cells (Huh7-p1 and Huh7-p5) were shown to display similar growth characteristics. The titers of these two viruses dropped at 6 h post-infection, increased at 10 h post-infection, and peaked at 16 h post-infection (Figure 4.3b, dark blue and red lines). The titer of p20 IBV from Huh7 cells (Huh7-p20) dropped to 1×10^2 PFU/ml at 6 h post-infection, increased afterwards, and peaked at 24 h post-infection to 1×10^6 PFU/ml (Figure 4.3b, green line).

The virus titer of p1 IBV from HCT116 cells (HCT116-p1) dropped to 5×10^2 PFU/ml at 6 h post-infection, increased afterwards, and peaked at 36 h post-infection with the titer of 5×10^6 PFU/ml (Figure 4.3c, dark blue line). The virus titer of p5 IBV from HCT116 cells (HCT116-p5) dropped to 1×10^3 PFU/ml at 6 h post-infection, increased afterwards, and peaked at 24 h post-infection with the titer of 1×10^7 PFU/ml (Figure 4.3c, red line). The growth curve of p20 IBV from HCT116 cells (HCT116-p20) is slightly different from that of HCT116-p1 and HCT116-p5; the virus titer

dropped to 1×10^3 PFU/ml at 6 h post-infection, increased afterwards, and peaked at 18 h post-infection with the titer of 5×10^6 PFU/ml (Figure 4.3b, green line). The growth curves of viruses of different passages from H1299, Huh7, and HCT116 cells suggest that IBV infectivity did not change much during passage, implying that Vero cell-adapted IBV readily infected these three cell lines.

4.2.4 The relative stability of IBV S gene during infection of human cell lines by the Vero cell-adapted IBV

Rapid changes in virus genome allowed the adaptation of the IBV Beaudette strain from chicken embryo to Vero cells (Fang et al., 2005). More than 53.06% mutations were located in the S gene (Fang et al., 2005). To study the genotypic changes which may occur during the infection of human cell lines with Vero cell-adapted IBV, S genes of Huh7-p1, -p5, and -p20 were amplified from IBV virions in the cell culture media by RT-PCR, sequenced and compared to the published sequence of p65 IBV from Vero cells. As different IBV genotypes may co-exist in the infected cells, five isolates of each virus were purified by plaque purification and sequenced. Only one mutation, which is from A to C in nucleotide 23565, was found in S2 region of two virus isolates from Huh7-p5. No mutation was found in any isolate from Huh7-p1 and Huh7-p20. The occurrence of rare mutation in IBV S genes suggests that the Vero cell-adapted IBV strain probably has acquired the potential to infect some human cell lines. However, genetic changes in other viral genes which are implicated in IBV tropism may also account for the IBV adaptation. This would be characterized in future studies.

4.2.5 IFN- β induction in IBV-infected cells

IBV was successfully adapted to Vero cells from chicken embryo (Shen et al., 2003). One of the reasons for the susceptibility of Vero cells to IBV was thought to be

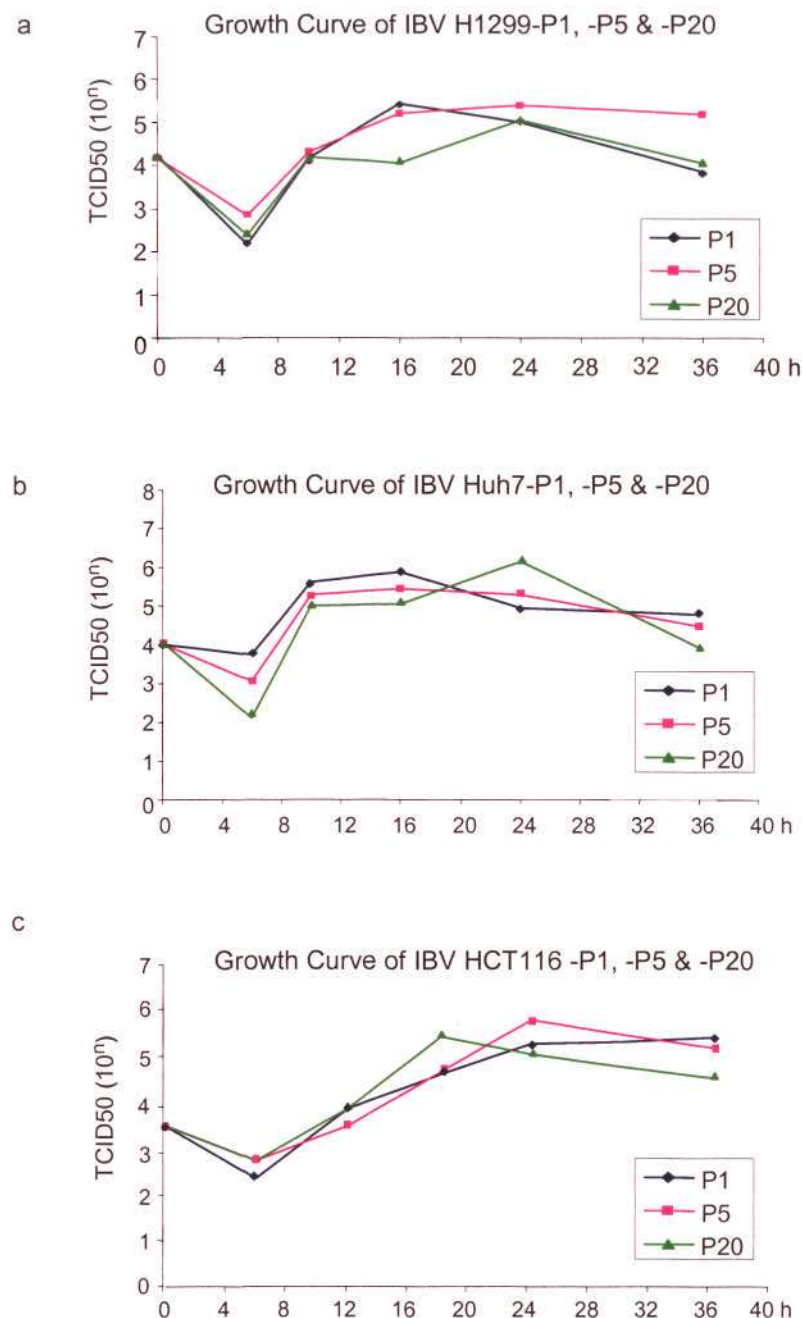


Figure 4.3 Growth Curves of p1, p5, and p20 IBV produced by passaging Vero cell-adapted IBV (Vero-p65) in H1299, Huh7, and HCT116 cells. **(a)** H1299 cells were infected with H1299-p1, H1299-p5, or H1299-p20 separately and harvested at 0 to 36 h post-infection. Total cell lysates were analyzed for progeny virus by TCID50 assay in H1299 cells. **(b)** Huh7 cells were infected with Huh7-p1, Huh7-p5, or Huh7-p20 separately and harvested at 0 to 36 h post-infection. Total cell lysates were analyzed for progeny virus by TCID50 assay in Huh7 cells. **(c)** HCT116 cells were infected with HCT116-p1, HCT116-p5, or HCT116-p20 separately and harvested at 0 to 36 h post-infection. Total cell lysates were analyzed for progeny virus by TCID50 assay in Vero cells.

the deletion of IFN- β gene from the Vero cell genome. However, cell lines Huh7, Hep3B, HepG2 and HCT116, which are able to support continuous IBV propagation, do have intact IFN- β gene. Whether these cell lines would produce IFN- β upon IBV infection appears to be an interesting issue. To test this possibility, different cell lines were infected with IBV and intracellular IFN- β protein expressions were analyzed by Western blot using polyclonal IFN- β antibody (Sigma) (Figure 4.4). A positive control of purified human IFN- β sample was included. IFN- β stimulation upon IBV infection was observed in Huh7, Hep3B, HepG2, and HCT116 cells but not in DLD1 and DLD1Amix cells (Figure 4.4). In IBV-infected Huh7 cells, IFN- β expression was detectable at as early as 8 h post-infection and increased with infection time (Figure 4.4a, lane 2-6). In IBV-infected Hep3B cells, IFN- β expression was detectable from 12 h post-infection, peaked at 24 h post-infection, and remained unchanged up to 48 h (Figure 4.4b, lane 3-6). The IFN- β expression pattern in IBV-infected HepG2 and HCT116 cells were similar; cells began to express IFN- β at 12 h post-infection and the expression level increased with infection time (Figure 4.4c and 4.4d, lane 3-6). However, no IFN- β was detected in IBV-infected DLD1 and DLD1A cells (Figure 4.4e and 4.4f). As described, Huh7, Hep3B, HepG2, and HCT116 cells supported continuous IBV growth. The susceptibility of these cell lines to IBV in the presence of IFN- β induction gives us a clue that IBV may encode certain mechanism to evade the IFN- β action.

4.2.6 ISG15 induction in IBV-infected cells

ISG15 was one of the first recognized ISGs (Farrell et al., 1979). The antiviral activity of ISG15 has been documented (Malakhova et al., 2003; Dao and Zhang, 2005; Okumura et al., 2006). To study the ISG15 induction after IBV infection, total RNA from mock infected and IBV-infected Vero cells was analyzed by Northern blot.

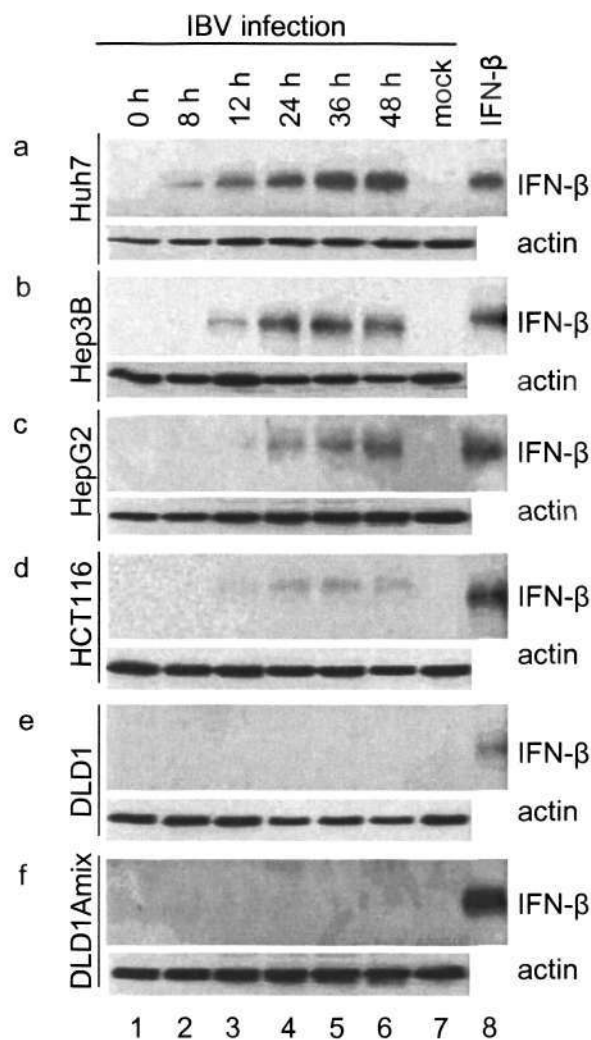


Figure 4.4 Expression of IFN-β in IBV infected cells. Huh7, Hep3B, HepG2, HCT116, DLD1, and DLD1Amix cells were infected with IBV and harvested at 8, 12, 24, 36, and 48 h post-transfection. Cell lysates were prepared and the expression of IFN-β was detected by Western blot with IFN-β antibody (Sigma) after proteins were separated by 15% SDS-PAGE.

The ISG15 in Vero cells stimulated by 1000 international unit (IU)/ml. IFN- β was included as a positive control. ISG15 mRNA in mock infected Vero cells was not detectable (Figure 4.5a, lane 1), but it was stimulated significantly from 16 h post-infection and peaked at 24 h post-infection (Figure 4.5a, lane 3 and 4). However, the ISG15 protein remained undetectable throughout the time course (Figure 4.5a, lane 1-6). This is contradictory with the ISG15 induction in Vero cells with IFN- β treatment shown in Figure 4.5b. The ISG15 mRNA was detectable at 3 h post-treatment and peaked at 10 h post-treatment, while ISG15 protein was detectable at 10 h post-treatment and peaked at 24 h post-treatment (Figure 4.5b). ISG15 protein accumulation paralleled the mRNA increase under the treatment of 1000 IU/ml IFN- β . This result suggests that the translation of antiviral ISG15 may be inhibited by IBV. ISG15 induction in HCT116 cells was also examined. ISG15 mRNA in IBV-infected HCT116 cells increases with infection time (Figure 4.5c, lane 1-6). ISG15 protein in mock infected cells was detectable but decreased upon IBV infection (Figure 4.5c, lane 1-6). Taken together, our results suggest that induction of ISG15 might be suppressed at the translational level, but not the transcriptional level in IBV-infected cells. Whether the ISG15 inhibition by IBV applies to other susceptible cells will be characterized in the future work.

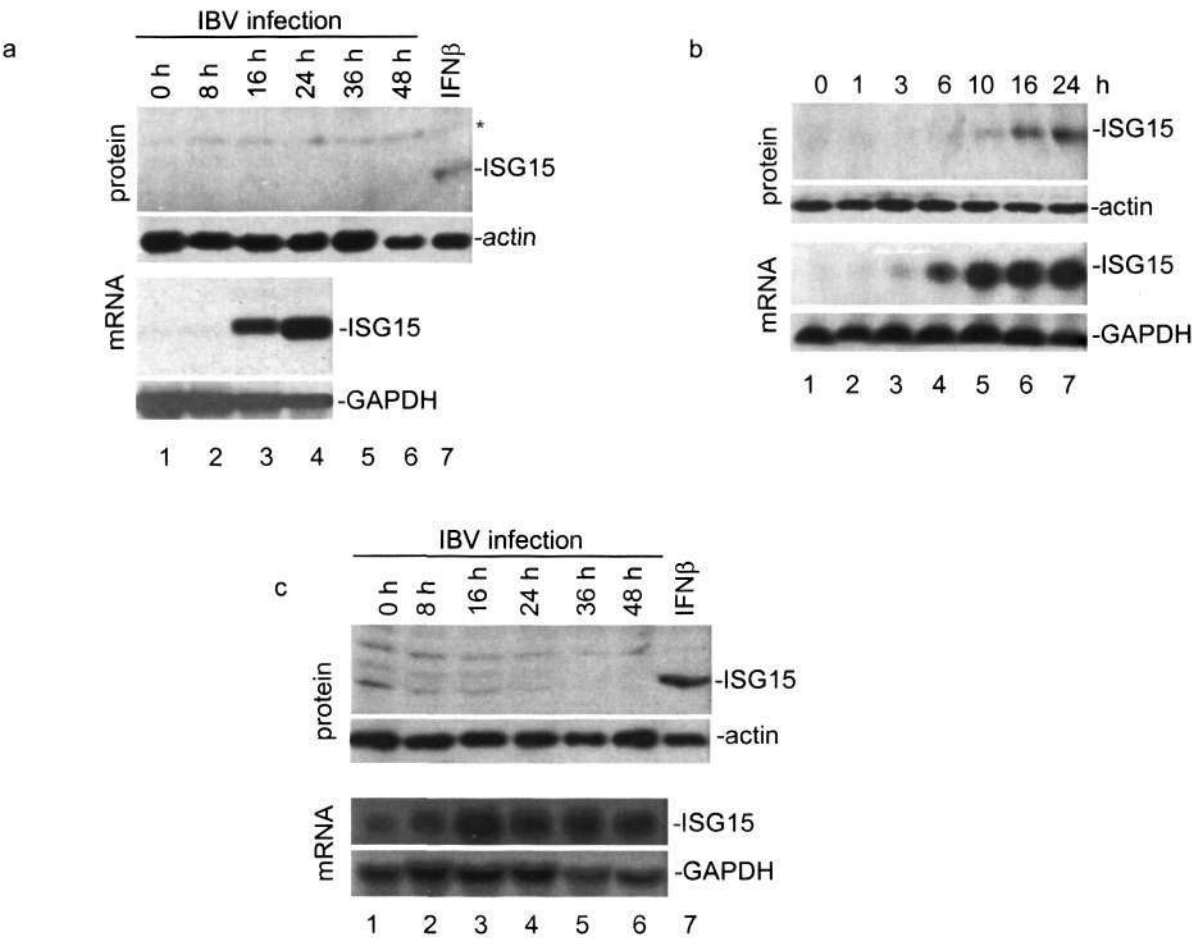


Figure 4.5 Induction of ISG15 in Vero and HCT116 cells. **(a)** Vero cells were infected with IBV and harvested 0-48 h post-infection. Total RNA was extracted and ISG15 mRNA was detected by Northern blot with DIG labeled ISG15 probe. Cell lysates were prepared and the expression of ISG15 was detected by Western blot with ISG15 antibody after proteins were separated by 15% SDS-PAGE. **(b)** Vero cells were stimulated with 1000 IU/ml IFN- β and harvested 0-24 h after treatment. Total RNA was prepared and ISG15 mRNA expression was analyzed by Northern blot. Expression of ISG15 protein was detected by Western blot with ISG15 antibody (Rockland). **(c)** HCT116 cells were infected with IBV and harvested 0-48 h post-infection. Total RNA was extracted and ISG15 mRNA was detected by Northern blot with DIG labeled ISG15 probe. Cell lysates were prepared and the expression of ISG15 was detected by Western blot with ISG15 antibody after proteins were separated by 15% SDS-PAGE.

4.3 Discussion

4.3.1 Coronavirus cell tropism

Chicken is generally believed to be the only natural host for IBV, although IBV was reported to be isolated from pheasants as well (Gough et al., 1996). *In vitro*, IBV Beaudette-42 and Holte strains grew in BHK-21 cell line (Otsuki et al., 1979). The Beaudette strain of IBV from chicken embryo was serially propagated in a monkey kidney cell line, Vero, for 65 passages (Shen et al., 2003). However, the susceptibilities of other cell lines to IBV have not been documented yet. In this study, fifteen cell lines with different tissue origins and host species were shown to be susceptible to Vero cell-adapted IBV. The susceptibility of fifteen cell lines to IBV allows us to investigate the IBV pathogenesis in cultured cells. IBV was passaged to at least p20 in five human cell lines, including H1299, HepG2, Hep3B, Huh7, and HCT116. HepG2, Hep3B, and Huh7 cell lines are derived from hepatoma, while H1299 and HCT116 are cancer cells with lung and intestine tissue origin, respectively. The Vero cell-adapted IBV crossed not only species but also tissue barriers to infect these five human cell lines.

The S protein can determine the tissue and species tropism of coronavirus. A recombinant porcine coronavirus transmissible gastroenteritis virus (TGEV) containing the S gene from an enteric TGEV was shown to have acquired enteric tropism (Sanchez et al., 1999). When the S protein ectodomain of MHV was replaced with the corresponding sequence from coronavirus feline infectious peritonitis virus (FIPV), the resultant virus acquired the ability to infect murine cells in tissue culture (Kuo et al., 2000). Reintroduction of the FIPV spike allowed for regaining the ability to grow in feline cells (Haijema et al., 2003). Only a relatively few mutations in its spike protein allow the MHV to switch from a murine restricted tropism to an

extended host range by being passaged in vitro (de Haan et al., 2005), while mutations in the Feline Coronavirus spike protein determines the acquisition of macrophage tropism (Rottier et al., 2005). A recombinant IBV, BeauR-M41(S), in which the ectodomain region of the spike gene from IBV M41-CK replaced the corresponding region of the IBV Beaudette genome, acquired the same cell tropism as IBV M41-CK (Casais et al., 2003). Dramatic changes in IBV S protein also occurred during the virus adaptation from chicken embryo to a monkey kidney cell line (Fang et al., 2005). However, the sequencing of S gene of IBV of different passages from Huh7, a human liver cancer cell line, showed that in this region only one mutation, which is from A to C in nucleic acid and Q to H in amino acid, occurred in p5. However, this mutation was only found in two isolates of Huh-p5, but not found in all five isolates of Huh7-p20, suggesting that this mutation probably exists only in a minor variant and this minor variant was discarded during further selection. In another word, IBV has gained the ability to infect human cell lines once adapted to Vero cell line; therefore, no significant change in S protein is required. This was further evidenced from the virus growth characteristics result that the viral infectivity did not change much during IBV passage in three newly infected H1299, Huh7, and HCT116 cell lines (Figure 4.3).

4.3.2 Host factors that restrict the replication of IBV

IBV was shown to cause typical CPE in most cell lines and viral structural proteins were detected in these cells (Figure 4.1 and 4.2). Five human cell lines, including H1299, HepG2, Hep3B, Huh7, and HCT116, were demonstrated to support continuous IBV propagation. In cell lines such as A549 and Cos-7, however, IBV was not able to continuously replicate. It seems that IBV initiated infection in some cells and caused cell-cell fusion, but the initially infected cells died later on. Therefore, IBV could not spread to the neighboring cells. Characterization of the differences

between resistant and susceptible cell lines would help reveal host factors restricting IBV replication. For example, both H199 and A549 are cell lines derived from human lung tissue, but A549 was much more resistant to IBV infection than H1299. In A549 cells, IBV could not spread infection to the whole monolayer and be propagated continuously. But in H1299 cells, the virus was able to do so. One obvious reason would be the absence of tumor suppressor p53 in H1299 cells. H1299 cell lines stably expressing two transactivation defective mutants of p53 (H175 and H273) were established. However, introducing p53 wild type gene to H1299 cells is very difficult and we only managed to obtain one cell line which expresses the N-terminal 220 amino acids of p53 wild type gene (p53N). H1299 cells expressing H175, H273, and p53N were still susceptible to IBV, suggesting that other components may also be targeted by this virus. Another example is the comparison of Vero and Cos-7 cells. They are both derived from monkey kidney, but Cos-7 cell line is more resistant to IBV infection than Vero cell line. It is probably due to the absence of IFN- β gene in Vero cell line.

An important host factor involved in the anti-viral mechanism is IFN- β , which is the first line of host defense. IFN- β induction in different cell lines after IBV infection was examined. At least four cell lines, including HepG2, Hep3B, Huh7 and HCT116, produced and secreted IFN- β upon IBV infection (Figure 4.4). However, all these cell lines support continuous growth of IBV. The mechanism(s) that IBV employed to survive and replicate under the IFN- β challenging will help to elucidate the pathogenesis of IBV in various cell lines. In this study, ISG15, one of the interferon-stimulated genes (ISGs), was used as the main focus. IBV infection in Vero cells stimulated ISG15 mRNA induction dramatically, but the ISG15 protein level remained undetectable (Figure 4.6a), raising the postulation that the translation of

ISG15 may be suppressed by IBV. This phenomenon was also observed in HCT116 cell line. As ISG15 has been suggested to play certain roles in anti-viral activities (Malakhova et al., 2003; Dao and Zhang, 2005; Okumura et al., 2006), it is not surprising that it became targeted by IBV. This putative mechanism will be investigated further. The causes of ISG15 induction can be examined by using irradiated IBV. If virus replication is required, ISG15 would not be stimulated in either transcriptional or translational level after infection with irradiated IBV. If binding of virus to cell surface is sufficient to cause the stimulation, ISG15 would be induced in both transcriptional and translational levels, as irradiated IBV can not replicate within susceptible cells to generate viral proteins which are responsible for suppressing ISG15. Specific antibody neutralization will help to study the virus elements which are implicated in ISG15 induction. Furthermore, IBV may exploit different mechanisms to antagonize specific anti-viral actions in different cell lines. IFN- β and ISG15 inductions in more cell lines infected with IBV (both resistant and susceptible cells) will be analyzed in future studies to elucidate IBV pathogenesis in various cell lines.

Chapter Five

Summary and Discussion

5.1 EBV BARF1 and its interaction with hTid1

In chapter three, the post-translational modification, folding, maturation and secretion of BARF1 were systematically studied by site-directed mutagenesis and overexpression of the protein in mammalian cells using the vaccinia/T7 system. The protein was shown to be post-translationally modified by N-linked glycosylation on the asparagine 95 residue. This modification was confirmed to be essential for the maturation and secretion of the protein. Analysis of the four cysteine residues by site-directed mutagenesis demonstrated that cysteine 146 and 201 were essential for proper folding and secretion of the protein. To search for human proteins involved in the maturation process of the protein, a yeast two-hybrid screening was carried out using the BARF1 sequence from amino acids 21–221 (BARF1 Δ) as bait, leading to the identification of human hTid1 protein as a potential interacting protein. This interaction was subsequently confirmed by coimmunoprecipitation and dual immunofluorescent labeling of cells coexpressing BARF1 and hTid1. Interestingly, coexpression of BARF1 with hTid1 demonstrated that hTid1 could promote secretion of BARF1, suggesting that hTid1 may act as a molecular chaperone.

5.1.1 Biochemical properties of BARF1 and future functional characterization of BARF1

The secretion of BARF1 from human B-lymphocytes overexpressing this protein was reported (Strockbine et al. 1998) and confirmed from different cells in other reports (Seto et al., 2005; Sall et al., 2004; de Turenne-Tessier et al., 2005). The purified BARF1 protein was able to activate DNA synthesis and cell growth *in vitro*, suggesting that the secreted BARF1 may have mitogenic activity. As the N95A, C145A, and C201A mutants of BARF1 were demonstrated to be defective in secretion by our data, these mutants might lose the function as a growth factor if the

mechanism of oncogenic transformation induced by BARF1 were autocrine/paracrine cell cycle activation. Proper folding must be important to a mitogenic protein as downstream events are mediated by specific binding of the mitogen to its receptor. From our result, the mutant C103A was suggested to be not correctly folded as a lot of high-order aggregates of this protein was detected in cell lysates, suggesting that although this mutant was successfully secreted to extracellular, the secreted form might be not in its right structure and not function normally. Therefore, analysis of transformation/immortalization activities of three secretion defective mutants (N95A, C146A, and C201A) and the other two cysteine mutants (C14A and C103A) might be a helpful study to verify if the mitogenic activity of BARF1 accounts for its induced transformation/immortalization. In the future investigation, the growth characteristics of NIH/3T3 cells stably expressing all five mutants will be examined. The secreted form of C14A and C103A mutants will be purified and subjected to *in vitro* cell proliferation assay to determine if these two cysteines are relevant to the structure of the functionally active BARF1. The biochemical characterization of BARF1 in this thesis and functional study of improperly folded mutants in the future may lead to a better understanding of the mechanism of oncogenic transformation induced by BARF1.

Our data demonstrated the crucial role of N-linked glycosylation of BARF1 during its trafficking in the intracellular compartments and subsequent secretion to extracellular compartment. This is in line with the widely accepted notion that N-linked glycosylation is a common step in the maturation of viral glycoproteins and is often necessary for proper folding of such proteins (Doms et al., 1993). Besides assisting in the protein folding, N-linked glycosylation may help to mask proteins from reactivity with virus-specific antibodies, facilitate escape from neutralization by

antibodies, or complement, and interfere with antigen processing (Hounsell et al., 1996; Lisowska, 2002). The anti-BARF1 antibody was shown to be present in the sera from patients with EBV-associated NPC (Tanner et al., 1997). BARF1 might exploit certain mechanisms to disarm the antibody neutralization as BARF1 was suggested to play a positive role in development of EBV associated epithelioid malignancies such as NPC and GC. Whether the N-linked glycosylation of BARF1 plays any role in assisting EBV to evade host antibody response is a question worthy to be investigated in the future. Again, as the cysteine residues were shown to be important for the proper folding of BARF1 and the antibody recognition is structure-based, the investigation of the roles of these four cysteine residues in antibody neutralization might enrich our knowledge of the immunomodulation by BARF1.

5.1.2 hTid1 acts as a chaperone to facilitate the maturation of BARF1

It is known that both the *Drosophila melanogaster* Tid56 and human homolog hTid1 belong to the DnaJ family, which serves as cochaperones and regulatory factors for the heat shock protein 70 (Hsp70) family of molecular chaperones (Silver and Way, 1993). Hsp70 proteins and their associated DnaJ co-chaperone mediate a variety of cellular activities, including the folding of newly synthesized polypeptides, the translocation of proteins across membranes and assembly of multimeric protein complexes (Hartl, 1996). A recent study showed that either hTid1L or hTid1S was able to substitute for the mitochondrial DnaJ-like protein Mdj1p in yeast (Lu et al., 2006), which is one essential component of a chaperone system for quality control of matrix proteins (Germaniuk et al., 2002; Duchniewicz et al., 1999). However, the direct association of hTid1 with other proteins to facilitate their maturation has not been documented yet. In our study, hTid1 was identified to interact with BARF1 and

promote the secretion of BARF1. This is the first report to confirm hTid1 as a molecular chaperone to assist the folding and maturation of its interacting partner.

The host chaperone system plays important role in virus replication. Viruses need cellular chaperones to ensure proper folding of viral proteins because a large number of proteins are synthesized in a short time. Chaperones are also involved in the control of cellular processes including signal transduction, cell cycle regulation and induction of apoptosis. Therefore, some viruses reprogram their host cell by interacting with them (Mayer, 2005). Our data demonstrated that hTid1 was engaged by a viral protein to act as a molecular chaperone. Other studies on hTid1 suggest that it is a protein with a few functions, including modulation of IFN- γ signaling pathway (Sarkar et al., 2001), regulation of apoptosis induced by exogenous stimuli (Syken et al., 1999), regulation of NF- κ B activity (Cheng et al., 2002; Cheng et al., 2005), and suppression of malignant transformation (Cheng et al., 2001). The functional multiplicity of hTid1 suggests that this chaperone might participate in other virus-host interactions during EBV infection. Further functional study of the interaction between BARF1 and hTid1 is in need to elicit some insights on involvement of hTid1 in the EBV pathogenesis and carcinogenesis in EBV related cancers.

5.1.3 Other potential functional implications of the interaction between BARF1 and hTid1

Although dispensable for B-cell transformation (Cohen and Lekstrom, 1999), BARF1 was demonstrated to immortalize and transform a few epithelial cells and B-lymphocytes (Wei and Ooka, 1989; Wei et al., 1994; Wei et al., 1997; Sheng et al., 2003). The transformation or immortalization induced by an oncogenic protein is a complicated process and must involve multiple cellular proteins. hCSF-1 was reported to interact with BARF1 (Strockbine et al., 1998). But this interaction appears to be

employed by BARF1 to induce local immune suppression rather than oncogenic progression. The binding of BARF1 to hCSF-1 expressed on macrophage progenitor cells reduced macrophage proliferation due to the sequestration of hCSF-1 from its receptor (Strockbine et al., 1998). hTid1, which was identified to interact with BARF1 in our study, might be one potential candidate implicated in the transformation or immortalization process induced by BARF1. The function of hTid1 as a tumor suppressor has been reported. Expression of hTid-1 inhibited the transformation phenotype of two human lung adenocarcinoma cell lines (Cheng et al., 2001). It is possible that hTid1 or/and other unknown partner are recruited by BARF1 to modulate the cell growth transformation. A 'hit and run' mechanism was proposed to explain the oncogenic potential of BARF1 (Gao et al., 2002). The secreted form of BARF1 could act as a growth factor *in vivo* (Sall et al., 2004). This mitogenic activity might contribute to the immortalization induced by BARF1 as well. However, the exact mechanism is still undefined. The further investigation of relationship between growth transformation and the interaction of BARF1 with hTid1 might help to elucidate the mechanism(s) of BARF1 induced transformation, and EBV pathogenesis in EBV positive tumors, especially those with epithelial origin. It will also help to resolve the paradox that hTid1 on one hand facilitate the production of oncogenic BARF1 and on the other hand worked as a tumor suppressor by reducing the colony formation of cancer cells (Cheng et al., 2001).

The anti-apoptotic role of BARF1 in gastric cancer cells was reported (Wang et al., 2006). The resistance of BARF1 expressing cells to apoptosis induced by anticancer drug was associated with increased Bcl-2 and Bax ratio and decreased expression of cleaved PARP (Wang et al., 2006). hTid1L promote while hTid1S inhibit apoptosis induced by exogenous stimuli (Syken et al., 1999; Syken et al.,

2003). The apoptosis enhanced by hTid1 was accompanied by mitochondrial cytochrome C release and caspase activation (Syken et al., 1999; Trentin et al., 2004). Whether BARF1 and hTid1 antagonize each other to balance the cell survival and cell death in EBV positive cancer cells remains to be studied in the future.

5.1.4 Association of hTid1 with its partners influences the subcellular localization of hTid1

hTid1 has been shown to interact directly with a few viral and cellular proteins. They include HPV E7 (Schilling et al., 1998), HTLV Tax (Cheng et al., 2001), HSV-1 UL9 (Eom and Lehman, 2002), Jak2 (Sarkar et al., 2001), Trk receptor tyrosine kinases (Schaaf et al., 2005), and hRFI (Sasaki et al., 2004). These proteins are non-mitochondrial, either cytosolic or nuclear. Our study also revealed the interaction between hTid1 and a non-mitochondrial viral protein, EBV BARF1. However, endogenous and overexpressed hTid1 was shown to be primarily localized to mitochondria by different methods (Cheng et al., 2001 Sarkar et al., 2001). hTid1 must encode certain mechanism to solve the paradox of mitochondrial localization and non-mitochondrial interaction and function. hTid1 was shown to have a long residency time in cytosol prior to mitochondrial import (Lu et al., 2006). During the intermediate residency in cytosol, hTid1 may interact with cytosolic or nuclear proteins and these interactions may increase the cytosolic residency time of hTid1. Our observation that physical association between BARF1 and hTid1 sequesters the latter to the ER and/or the Golgi apparatus reinforces the notion that the fate and function of hTid1 inside and outside of mitochondria are influenced by cytosolic or nuclear protein interactions.

In conclusion, the biochemical properties of BARF1, the interaction between EBV BARF1 and cellular hTid1, and the chaperone function of hTid1 were

characterized in this study. Our work presented in this thesis will definitely lead to a better understanding of EBV protein maturation, host chaperone system employed during EBV infection and multiple functions of hTid1. Further investigations of the interaction between BARF1 and hTid1 described above might help to elucidate the mechanism for the role of EBV infection in associated tumors.

5.2 Coronavirus cell tropism and pathogenesis

In chapter four, a total of fifteen cell lines with different species and tissue origins were shown to be susceptible to the Vero cell-adapted IBV strain. IBV can be continuously passaged to p20 in five human cell lines. Sequencing of the S gene of different passages from different cell lines suggests that it is relatively stable during the passage from Vero cells to human cells. The viral infectivity did not increase during continuous passage of the virus in human cell lines. To study the relationship between host response and susceptibility to IBV, the expression of IFN- β and ISG15 in IBV infected cells was analyzed. The induction of IFN- β in IBV-infected cells implies that certain mechanisms must be employed by IBV to counteract the IFN- β action. ISG15, an IFN- β stimulated gene was shown to be suppressed at the translational level in IBV-infected Vero and HCT116 cells.

5.2.1 IBV cell tropism

The host spectrum of a specific coronavirus is largely determined by its S protein. A recombinant IBV, BeauR-M41(S), in which the ectodomain region of the spike gene from IBV M41-CK replaced the corresponding region, acquired the same cell tropism as IBV M41-CK (Casais et al., 2003). Rapid and dramatic changes occurred in S protein during the adaptation of IBV Beaudette strain from chicken embryo to monkey kidney cells (Fang et al., 2005). In our study, however, sequencing of the S gene of IBV during passage of the virus from Vero cells to H1299, Huh-7 and

HCT116 cell lines revealed that genetic variation, at least in S gene, is not required for IBV to transmit from a monkey kidney cell line to human cell lines. The readily adaptation of IBV from Vero cell line to human cells lines and the stability of IBV S genes during the passage suggest that that IBV has extended its host range specificity after its adaptation to Vero cells. This could be probably due to the closeness of monkey and human in species and distribution of similar receptors on the cell surface. However, cell lines originated from hamster such as CHO and BHK were also permissive for Vero cell-adapted IBV, suggesting that IBV might broaden its narrow host specificity by utilizing a relatively nonspecific moiety as the entry receptor, which has been documented for MHV (de Haan et al., 2005). So far, IBV receptor in its native or adapted host cells remains unknown yet. The broadened host range specificity of IBV demonstrated in our study underscores the need for the identification of the host receptors engaged by IBV and better characterization of IBV pathogenesis in its natural hosts and adapted cultured cells. The acquisition of the capability to infect human cell lines by IBV reminds us the importance of investigating and characterizing zoonotic transmission of coronavirus in order to anticipate and avoid next SARS.

An alternative method of cloning IBV S gene into vector and sequencing different colonies will be used in the future to avoid inaccuracy of sequencing PCR product because subtle alterations in S protein are sufficient to extend or alter the host range of some coronaviruses (Kuo et al, 2000; Casais et al, 2003; Haijema et al, 2003; Schickli et al, 2004). In addition, we are also interested in characterization of changes in other viral proteins that are necessary for IBV to adapt from chicken embryo to cultured cells. The widely distributed sialic acid, which was suggested to be important for primary attachment of IBV to host cells (Winter et al., 2006), will be

included in our further identification of IBV receptors in its natural host and adapted cell lines.

5.2.2 IBV strategy to evade host innate immune response

The innate immune responses of different cell lines after IBV infection were revealed by the examination of the expression profiles of two genes, *IFN- β* and *ISG15*. Our data suggest that IBV might encode certain strategy to circumvent the *IFN- β* action but not induction. *ISG15*, an *IFN- β* stimulated gene, was shown to be induced significantly at the transcriptional level but not the translational level, suggesting that the expression of *IFN- β* stimulated gene rather than that of *IFN- β* itself was suppressed. These data provide a plausible explanation for the efficient replication of IBV in some cell lines in the presence of *IFN- β* induction. IBV may circumvent the innate immune system by suppressing the expression of *IFN- β* stimulated genes, buying time to spread during the initial phase of infection. To our knowledge, such a mechanism has not yet been described, suggesting that IBV may use a unique strategy to bypass *IFN* action. The exact mechanism that IBV exploits to block *ISG15* translation is presently unknown. Our further investigation will focus on the mechanism of action, e.g., inhibition of host translational machinery or degradation of *ISG15*. In addition, experiments will be performed to identify the viral protein(s) responsible for the *IFN*-antagonistic effect. Similar studies in the six cell lines (Vero, H1299, HepG2, and Hep3B, Huh7, and HCT116), which supported efficient replication of IBV, will tell us whether the same strategy was exploited by IBV ubiquitously or different strategies were employed specifically in different cell lines to counteract *IFN- β* action. The characterization of IBV immune invasion strategies will allow better understanding of coronavirus pathogenesis and help to control coronavirus-related disease.

5.2.3 Host factors that restrict IBV replication

The six cultured cell lines, H1299, HepG2, and Hep3B, Huh7, HCT116 and Vero, can support continuous propagation of IBV. However, other cell lines with similar organ and tissue origins were shown to be more resistant to IBV infection as evidenced by the observation that IBV was hardly recovered from these cell lines after only one or a few passages. A prominent example is the comparison between H1299 and A549. They are both human lung cancer cell lines, but H1299 can support efficient replication of IBV while A549 cannot. Tumor suppressor p53 becomes an intriguing candidate for studying the host restricting factors, as one obvious difference between the two cell lines is the presence or absence of the p53 gene. The differences between the cell lines susceptible to IBV and the cell lines resistant to IBV infection will provide us valuable information for identifying and characterizing more host factors implicated in IBV infection in future studies.

In summary, susceptibility of a total of fifteen cell lines to Vero cell-adapted IBV, extended host range specificity of IBV, stability of IBV S protein during the adaptation, and the immune invasion mechanism encoded by IBV were demonstrated in our study. The study of IBV adaptation to new cell lines or hosts is critical to understanding fundamental aspects of virus pathogenesis, species transmission, and emerging disease caused by zoonotic viruses. Identifying the underlying virulence mechanism may be helpful for the rational design of specific antiviral therapies and engineering of attenuated vaccines.

References

Albini, A., Ferrini, S., Benelli, R., Sforzini, S., Giunciuglio, D., Aluigi, M. G., Proudfoot, A. E., Alouani, S., Wells, T. N., Mariani, G., Rabin, R. L., Farber, J. M., Noonan, D. M. (1998). HIV-1 Tat protein mimicry of chemokines. *Proc. Natl. Acad. Sci. U. S. A.* 95, 13153–13158.

Alcami, A. (1998). Poxviruses: capturing cytokines and chemokines. *Sem. Virol.* 8, 419–427.

Alexopoulou, L., Holt, A. C., Medzhitov, R., Flavell, R. A. (2001). Recognition of double-stranded RNA and activation of NF-kappaB by Toll-like receptor 3. *Nature.* 413, 732–738.

Allan, G. J., Inman, G. J., Parker, B. D., Rowe, D. T., Farrell, P. J. (1992). Cell growth effects of Epstein-Barr virus leader protein. *J. Gen. Virol.* 73, 1547–1551.

Almeida, J. D., Tyrrell, D. A. (1967). The morphology of three previously uncharacterized human respiratory viruses that grow in organ culture. *J. Gen. Virol.* 1, 175–178.

Ambagala, A. P., Solheim, J. C., Srikumaran, S. (2005). Viral interference with MHC class I antigen presentation pathway: the battle continues. *Vet. Immunol. Immunopathol.* 107, 1–15.

Ambinder, R. F., Browning, P. J., Lorenzana, I., Leventhal, B. G., Cosenza, H., Mann, R. B., MacMahon, E. M., Medina, R., Cardona, V., Grufferman, S., Olshan, A., Levin, A., Petersen, E. A., Blattner, W. and Levine, P. H. (1993). Epstein-Barr virus and childhood Hodgkin's disease in Honduras and the United States. *Blood.* 81, 462–467.

Anagnostopoulos, I., Hummel, M., Kreschel, C., Stein, H. (1995). Morphology, immunophenotype, and distribution of latently and/or productively Epstein-Barr virus-infected cells in acute infectious mononucleosis: implications for the interindividual infection route of Epstein-Barr virus. *Blood.* 85, 744–750.

Andrejeva, J., Childs, K. S., Young, D. F., Carlos, T. S., Stock, N., Goodbourn, S., Randall, R. E. (2004). The V proteins of paramyxoviruses bind the IFN-inducible RNA helicase, mda-5, and inhibit its activation of the IFN-beta promoter. *Proc. Natl. Acad. Sci. USA* 101, 17264–17269.

Apcher, G. S., Heink, S., Zantopf, D., Kloetzel, P. M., Schmid, H. P., Mayer, R. J. and Kruger, E. (2003). Human immunodeficiency virus-1 Tat protein interacts with distinct proteasomal alpha and beta subunits. *FEBS. Lett.* 553, 200–204.

Arbach, H., Viglasky, V., Lefeu, F., Guinebretiere, J. M., Ramirez, V., Bride, N., Boualaga, N., Bauchet, T., Peyrat, J. P., Mathieu, M. C., Mourah, S., Podgorniak, M. P., Seignerin, J. M., Takada, K., Joab, I. (2006). Epstein-Barr virus (EBV) genome and expression in breast cancer tissue: effect of EBV infection of breast cancer cells on resistance to paclitaxel (Taxol). *J. Virol.* 80, 845-853.

Archetti, I., Horsfall, F. L. Jr. (1950). Persistent antigenic variation of influenza A viruses after incomplete neutralization in ovo with heterologous immune serum. *J. Exp. Med.* 92, 441-462.

Arrand, J. R., Rymo, L., Walsh, J. E., Bjorck, E., Lindahl, T., Griffin, B. E. (1981). Molecular cloning of the complete Epstein-Barr virus genome as a set of overlapping restriction endonuclease fragments. *Nucleic Acids Res.* 9, 2999-3014.

Ashrafi, G. H., Tsirimonaki, E., Marchetti, B., O'Brien, P. M., Sibbet, G. J., Andrew, L. and Campo, M. S. (2003). Down-regulation of MHC class I by bovine papillomavirus E5 oncoproteins. *Oncogene.* 21, 248-259.

Babcock, G. J., Decker, L. L., Volk, M., Thorley-Lawson, D. A. (1998). EBV persistence in memory B cells in vivo. *Immunity.* 9, 395-404.

Babcock, G. J., Hochberg, D., Thorley-Lawson, A. D. (2000) The expression pattern of Epstein-Barr virus latent genes in vivo is dependent upon the differentiation stage of the infected B cell. *Immunity.* 13, 497-506.

Baer, R., Bankier, A. T., Biggin, M. D., Deininger, P. L., Farrell, P. J., Gibson, T. J., Hatfull, G., Hudson, G. S., Satchwell, S. C., Seguin, C. et al. (1984). DNA sequence and expression of the B95-8 Epstein-Barr virus genome. *Nature.* 310, 207-211.

Baeuerle, P. A., Baltimore, D. (1996). NF-kappa B: ten years after. *Cell.* 87, 13-20.

Baichwal, V. R., Sugden, B. (1988). Transformation of Balb 3T3 cells by the BNLF-1 gene of Epstein-Barr virus. *Oncogene.* 2, 461-467.

Bairoch, A., Bucher, P. and Hofmann, K. (1995). The PROSITE database, its status in 1995. *Nucleic Acids Res.* 24, 189-196.

Banner, L. R., Keck, J. G., Lai, M. M. (1990). A clustering of RNA recombination sites adjacent to a hypervariable region of the peplomer gene of murine coronavirus. *Virology.* 175, 548-555.

Banner, L. R., Lai, M. M. (1991). Random nature of coronavirus RNA recombination in the absence of selection pressure. *Virology.* 185, 441-445.

Baudoux, P., Carrat, C., Besnardeau, L., Charley, B., Laude, H. (1998). Coronavirus pseudoparticles formed with recombinant M and E proteins induce alpha interferon synthesis by leukocytes. *J. Virol.* 72, 8636-8643.

Beekman, N. J., van Veelen, P. A., van Hall, T., Neisig, A., Sijts, A., Camps, M., Kloetzel, P. M., Neefjes, J. J., Melief, C. J. and Ossendorp, F. (2000). Abrogation of CTL epitope processing by single amino acid substitution flanking the C-terminal proteasome cleavage site. *J. Immunol.* 164, 1898-1905.

Benn, J., Schneider, R. J. (1994). Hepatitis B virus HBx protein activates Ras-GTP complex formation and establishes a Ras, Raf, MAP kinase signaling cascade. *Proc. Natl. Acad. Sci. USA.* 91, 10350-10354.

Berry, D. M., Cruickshank, J. G., Chu, H. P., Wells R. J. (1964). The structure of infectious bronchitis virus. *Virology.* 23, 403-407.

Bingham, R. W., Almeida, J. D. (1977). Studies on the structure of a coronavirus-avian infectious bronchitis virus. *J. Gen. Virol.* 36, 495-502.

Binns, M. M., Boursnell, M. E., Cavanagh, D., Pappin, D. J., Brown, T. D. (1985). Cloning and sequencing of the gene encoding the spike protein of the coronavirus IBV. *J. Gen. Virol.* 66, 719-726.

Biron, C. A., Sen, G. C. (2001) in *Fields Virology*, Fourth Edition, D. M. Knipe et al., Eds. Lippincott, Williams, and Wilkins, Philadelphia, PA. pp321-351.

Bockaert, J., and Pin, J. P. (1998). Use of a G-protein-coupled receptor to communicate. An evolutionary success. *C. Rend. Acad. Sci. Ser. Iii* 321, 529-551.

Bork, P., Sander, C., Valencia, A. (1992). An ATPase domain common to prokaryotic cell cycle proteins, sugar kinases, actin, and hsp70 heat shock proteins. *Proc. Natl. Acad. Sci.* 89, 7290-7294.

Borza, C. M. and Hutt-Fletcher, L. M. (2002). Alternate replication in B cells and epithelial cells switches tropism of Epstein-Barr virus. *Nat Med* 8, 594-599.

Bos, E. C., Luytjes, W., van der Meulen, H. V., Koerten, H. K., Spaan, W. J. (1996). The production of recombinant infectious DI-particles of a murine coronavirus in the absence of helper virus. *Virology.* 218, 52-60.

Boursnell, M. E., Binns, M. M., Brown, T. D. (1985a). Sequencing of coronavirus IBV genomic RNA: three open reading frames in the 5' 'unique' region of mRNA D. *J. Gen. Virol.* 66, 2253-2258.

Bournsnell, M. E., Binns, M. M., Foulds, I. J., Brown, T. D. (1985b). Sequences of the nucleocapsid genes from two strains of avian infectious bronchitis virus. *J. Gen. Virol.* 66, 573-580.

Bournsnell, M. E., Brown, T. D., Binns, M. M. (1984). Sequence of the membrane protein gene from avian coronavirus IBV. *Virus Res.* 1, 303-313.

Bournsnell, M. E., Brown, T. D., Foulds, I. J., Green, P. F., Tomley, F. M., Binns, M. M. (1987). Completion of the sequence of the genome of the coronavirus avian infectious bronchitis virus. *J. Gen. Virol.* 68, 57-77.

Bowen, D. G. and Walker, C. M. (2005). Adaptive immune responses in acute and chronic hepatitis C virus infection. *Nature.* 436, 946-952.

Boyle, K. A., Pietropaolo, R. L. and Compton, T. (1999). Engagement of the cellular receptor for glycoprotein B of human cytomegalovirus activates the interferon-responsive pathway. *Mol. Cell. Biol.* 19, 3607-3613.

Brayton, P. R., Ganges, R. G., Stohlman, S. A. (1981). Host cell nuclear function and murine hepatitis virus replication. *J. Gen. Virol.* 56, 457-460.

Brian, D. A., Baric, R. S. (2005). Coronavirus genome structure and replication. *Curr. Top. Microbiol. Immunol.* 287, 1-30.

Brierley, I., Boursnell, M. E., Binns, M. M., Bilimoria, B., Blok, V. C, Brown, T. D., Inglis, S. C. (1987). An efficient ribosomal frame-shifting signal in the polymerase-encoding region of the coronavirus IBV. *EMBO. J.* 6, 3779-3785.

Brierley, M. M., Fish, E. N. (2002). IFN-alpha/beta receptor interactions to biologic outcomes: understanding the circuitry. *J. Interferon Cytokine Res.* 22, 835-845.

Brierley, I., Jenner, A. J., Inglis, S. C. (1992). Mutational analysis of the "slippery-sequence" component of a coronavirus ribosomal frameshifting signal. *J. Mol. Biol.* 227, 463-479.

Brierley, I., Digard, P., Inglis, S. C. (1989). Characterization of an efficient coronavirus ribosomal frameshifting signal: requirement for an RNA pseudoknot. *Cell.* 57, 537-547.

Brink, A. A., Vervoort, M. B., Middeldorp, J. M., Meijer, C. J., van den Brule, A. J. (1998). Nucleic acid sequence-based amplification, a new method for analysis of spliced and unspliced Epstein-Barr virus latent transcripts, and its comparison with reverse transcriptase PCR. *J. Clin. Microbiol.* 36, 3164-3169.

Brooks, L. A., Lear, A. L., Young, L. S., Rickinson, A. B. (1993). Transcripts from the Epstein-Barr virus BamHI A fragment are detectable in all three forms of virus latency. *J. Virol.* 67, 3182-3190.

Brown, K. D., Hostager, B. S., Bishop, G. A. (2001). Differential signaling and tumor necrosis factor receptor-associated factor (TRAF) degradation mediated by CD40 and the Epstein-Barr virus oncoprotein latent membrane protein 1 (LMP1). *J. Exp. Med.* *193*, 943-954.

Brown, T. D., Boursnell, M. E., Binns, M. M. (1984). A leader sequence is present on mRNA A of avian infectious bronchitis virus. *J. Gen. Virol.* *65*, 1437-1442.

Brown, T. D., Boursnell, M. E., Binns, M. M., Tomley, F. M. (1986). Cloning and sequencing of 5' terminal sequences from avian infectious bronchitis virus genomic RNA. *J. Gen. Virol.* *67*, 221-228.

Brown, T. D. and Boursnell, M. E. (1984). DNA sequencing studies of genomic cDNA clones of avian infectious bronchitis virus. *Adv. Exp. Med. Biol.* *173*, 215-224

Butler, N., Pewe, L., Trandem, K., Perlman, S. (2006). Murine encephalitis caused by HCoV-OC43, a human coronavirus with broad species specificity, is partly immune-mediated. *Virology.* *347*, 410-421.

Burkitt, D., Hutt, M. S. R., Wright, D. H. (1965). The African lymphoma. Preliminary observations on response to therapy. *Cancer* *18*, 399-410.

Callison, S. A., Jackwood, M. W., Hilt, D. A. (1999). Infectious bronchitis virus S2 gene sequence variability may affect S1 subunit specific antibody binding. *Virus Genes.* *19*, 143-151.

Carfi, A., Smith, C.A., Smolak, P. J., McGrew, J., Wiley, D. C. (1999). Structure of a soluble secreted chemokine inhibitor vCCI (p35) from cowpox virus. *Proc. Natl. Acad. Sci. U. S. A.* *96*, 12379-12383.

Carroll, I. R., Wang, J., Howcroft, T. K. and Singer, D. S. (1998). HIV Tat represses transcription of the beta 2-microglobulin promoter. *Mol. Immunol.* *35*, 1171-1178.

Casais, R., Davies, M., Cavanagh, D. and Britton, P. (2005). Gene 5 of the avian coronavirus infectious bronchitis virus is not essential for replication. *J. Virol.* *79*, 8065-8078.

Casais, R., Dove, B., Cavanagh, D., Britton, P. (2003). Recombinant avian infectious bronchitis virus expressing a heterologous spike gene demonstrates that the spike protein is a determinant of cell tropism. *J. Virol.* *77*, 9084-9089.

Cavanagh, D. (1981). Structural polypeptides of coronavirus IBV. *J. Gen. Virol.* *53*, 93-103.

Cavanagh, D. (1983a). Coronavirus IBV: structural characterization of the spike protein. *J. Gen. Virol.* *64*, 2577-2583.

Cavanagh, D. (1983b). Coronavirus IBV: further evidence that the surface projections are associated with two glycopolypeptides. *J. Gen. Virol.* 64, 1787-1791.

Cavanagh, D. (1995). The coronavirus surface glycoprotein. In: Siddell, S.G.(Ed.), *The coronaviridae*. Plenum Press, New York, pp. 73-113.

Cavanagh, D. (1997). Nidovirales: a new order comprising Coronaviridae and Arteriviridae. *Arch. Virol.* 142, 629-633.

Cavanagh, D., Darbyshire, J. H., Davis, P. J. and Peters, R.W. (1984). Induction of humoral neutralizing and hemagglutination-inhibiting antibody by the spike protein of infectious bronchitis virus. *Avian Pathol.* 13, 573-583.

Cavanagh, D., Davis, P. J. (1986). Coronavirus IBV: removal of spike glycopolypeptide S1 by urea abolishes infectivity and haemagglutination but not attachment to cells. *J. Gen. Virol.* 67, 1443-1448.

Cavanagh, D., Davis, P. J. (1988). Evolution of avian coronavirus IBV: sequence of the matrix glycoprotein gene and intergenic region of several serotypes. *J. Gen. Virol.* 69, 621-629.

Cavanagh, D., Davis, P., Cook, J., Li, D. (1990). Molecular basis of the variation exhibited by avian infectious bronchitis coronavirus (IBV). *Adv. Exp. Med. Biol.* 276, 369-372.

Cavanagh, D., Davis, P. J., Mockett, A. P. (1988). Amino acids within hypervariable region 1 of avian coronavirus IBV (Massachusetts serotype) spike glycoprotein are associated with neutralization epitopes. *Virus Res.* 11, 141-150.

Cavanagh, D., Davis, P. J., Pappin, D. J., Binns, M. M., Boursnell, M. E., Brown, T. D. (1986). Coronavirus IBV: partial amino terminal sequencing of spike polypeptide S2 identifies the sequence Arg-Arg-Phe-Arg-Arg at the cleavage site of the spike precursor polypeptide of IBV strains Beaudette and M41. *Virus Res.* 4, 133-143.

Cavanagh, D., Horzinek, M. C. (1993). Genus Torovirus assigned to the Coronaviridae. *Arch. Virol.* 128, 395-396.

Cavanagh, D. and Naqi, S. A. (1997). Infectious Bronchitis. In: *Disease of poultry*, 10th ed. B. W. Calnek, H.J. Barnes, C.W. Beard, W.M. Reid, and H.W. Yoder, eds. Iowa State University Press, Ames, Iowa. pp. 511-526.

Chang, W. L., Baumgarth, N., Yu, D., Barry, P. A. (2004). Human cytomegalovirus-encoded interleukin-10 homolog inhibits maturation of dendritic cells and alters their functionality. *J. Virol.* 78, 8720-8731.

Chaudhuri, B., Xu, H., Todorov, I., Dutta, A. and Yates, J. L. (2001). Human DNA replication initiation factors, ORC and MCM, associate with *oriP* of Epstein-Barr virus. *Proc. Natl. Acad. Sci. USA* 98, 10085-10089.

Cheetham, M. E., Caplan, A. J. (1998). Structure, function and evolution of DnaJ: conservation and adaptation of chaperone function. *Cell Stress Chaperones*. 3, 28-36.

Chen, H. L., Lung, M. M., Sham, J. S., Choy, D. T., Griffin, B. E., Ng, M. H. (1992). Transcription of BamHI-A region of the EBV genome in NPC tissues and B cells. *Virology*. 191, 193-201.

Chen, H., Wurm, T., Britton, P., Brooks, G., Hiscox, J. A. (2002). Interaction of the coronavirus nucleoprotein with nucleolar antigens and the host cell. *J. Virol.* 76, 5233-5250.

Cheng, H., Cenciarelli, C., Nelkin, G., Tsan, R., Fan, D., Cheng-Mayer, C., Fidler, I. J. (2005). Molecular mechanism of hTid-1, the human homolog of *Drosophila* tumor suppressor l(2)Tid, in the regulation of NF-kappaB activity and suppression of tumor growth. *Mol Cell Biol.* 25, 44-59.

Cheng, H., Cenciarelli, C., Tao, M., Parks, W. P., and Cheng-Mayer, C. (2002). HTLV-1 Tax-associated hTid-1, a human DnaJ protein, is a repressor of I κ B kinase beta subunit. *J. Biol. Chem.* 277, 20605-20610.

Cheng, H., Cenciarelli, C., Shao, Z., Vidal, M., Parks, W. P., Pagano, M., and Cheng-Mayer, C. (2001). Human T-cell leukemia virus type 1 Tax associates with a molecular chaperone complex containing hTid-1 and Hsp70. *Curr. Biol.* 11, 1771-1775.

Cheung, A., Kieff, E. (1981). Epstein-Barr virus DNA. X. Direct repeat within the internal direct repeat of Epstein-Barr virus DNA. *J. Virol.* 40, 501-507.

Cheung, A., Kieff, E. (1982). Long internal direct repeat in Epstein-Barr virus DNA. *J. Virol.* 44, 286-294.

Cinatl, J., Morgenstern, B., Bauer, G., Chandra, P., Rabenau, H., Doerr, H. W. (2003). Treatment of SARS with human interferons. *Lancet* 362, 293-294.

Civitello, A. B., Richards, S., Gibbs, R. A. (1992). A simple protocol for the automation of DNA cycle sequencing reactions and polymerase chain reactions. *DNA Seq.* 3, 17-23.

Cohen, J. I., and Lekstrom, K. (1999). Epstein-Barr virus BARF1 protein is dispensable for B-cell transformation and inhibits alpha interferon secretion from mononuclear cells. *J. Virol.* 73, 7627-7632.

Collisson, E. W., Williams, A. K., Chung, S. I., Zhou, M. (1995). Interactions between the IBV nucleocapsid protein and RNA sequences specific for the 3' end of the genome. *Adv. Exp. Med. Biol.* 380, 523-528.

Corse, E., Machamer, C. E. (2000). Infectious bronchitis virus E protein is targeted to the Golgi complex and directs release of virus-like particles. *J. Virol.* 74, 4319-4326.

Corse, E., Machamer, C. E. (2002). The cytoplasmic tail of infectious bronchitis virus E protein directs Golgi targeting. *J. Virol.* 76, 1273-1284.

Corse, E., Machamer, C. E. (2003). The cytoplasmic tails of infectious bronchitis virus E and M proteins mediate their interaction. *Virology.* 312, 25-34.

Coscoy, L. and Ganem, D. (2001). A viral protein that selectively downregulates ICAM-1 and B7-2 and modulates T cell costimulation. *J. Clin. Invest.* 107, 1599-1606.

Coscoy, D., Sanchez, J. and Ganem, D. (2001). A novel class of herpesvirus-encoded membrane-bound E3 ubiquitin ligases regulates endocytosis of proteins involved in immune recognition. *J. Cell Biol.* 155, 1265-1273.

Coutelier, J. P., Godfraind, C., Dveksler, G. S., Wysocka, M., Cardellicchio, C. B., Noel, H., Holmes, K. V. (1994). B lymphocyte and macrophage expression of carcinoembryonic antigen-related adhesion molecules that serve as receptors for murine coronavirus. *Eur. J. Immunol.* 24, 1383-1390.

Craig, F. E., Gulley, M. L., Banks, P. M. (1993). Posttransplantation lymphoproliferative disorders. *Am. J. Clin. Pathol.* 99, 265-276.

Crawford, D. H., Epstein, M. A., Bornkamm, G. W., Achong, B. G., Finerty, S., Thompson, J. L. (1979). Biological and biochemical observations on isolates of EB virus from the malignant epithelial cells of two nasopharyngeal carcinomas. *Int. J. Cancer.* 24, 294-302.

Curtis, B. M., Scharnowski, S., and Watson, A. J. (1992). Sequence and expression of a membrane-associated C-type lectin that exhibits CD4-independent binding of human immunodeficiency virus envelope glycoprotein gp120. *Proc. Natl. Acad. Sci. USA* 89, 8356-8360.

Dairaghi, D. J., Fan, R. A., McMaster, B. E., Hanley, M. R., and Schall, T. J. (1999). HHV8-encoded vMIP-1 selectively engages chemokine receptor CCR8. Agonist and antagonist profiles of viral chemokines. *J. Biol. Chem.* 274, 21569-21574.

Danve, C., Decaussin, G., Busson, P., Ooka, T. (2001). Growth transformation of primary epithelial cells with a NPC-derived Epstein-Barr virus strain. *Virology.* 288, 223-235.

Dao, C. T., and Zhang, D. E. (2005). ISG15: a ubiquitin-like enigma. *Front. Biosci.* 10, 2701-2722.

Davies, H. A., Dourmashkin, R. R., Macnaughton, M. R. (1981). Ribonucleoprotein of avian infectious bronchitis virus. *J. Gen. Virol.* 53, 67-74.

Dawson, C. W., Rickinson, A. B., Young, L. S. (1990). Epstein-Barr virus latent membrane protein inhibits human epithelial cell differentiation. *Nature.* 344, 777-780.

Deacon, E. M., Pallesen, G., Niedobitek, G., Crocker, J., Brooks, L., Rickinson, A. B., Young, L. S. (1993). Epstein-Barr virus and Hodgkin's disease: transcriptional analysis of virus latency in the malignant cells. *J. Exp. Med.* 177, 339-349.

Decaussin, G., Sbih-Lammali, F., de Turenne-Tessier, M., Bouguermouh A., Ooka T. (2000). Expression of BARF1 gene excoded by Epstein-Barr virus in nasopharyngeal carcinoma. *Cancer Res.* 60, 5584-5588.

de Groot, R. J., Luytjes, W., Horzinek MC, van der Zeijst BA, Spaan WJ, Lenstra JA. (1987). Evidence for a coiled-coil structure in the spike proteins of coronaviruses. *J Mol Biol.* 196, 963-966.

Delmas, B., Gelfi, J., L'Haridon, R., Vogel, L. K., Sjostrom, H., Noren, O., Laude, H. (1992). Aminopeptidase N is a major receptor for the entero-pathogenic coronavirus TGEV. *Nature.* 357, 417-420.

de Haan, C. A., Li, Z., te Lintelo, E., Bosch, B. J., Haijema, B. J., Rottier, P. J. (2005). Murine coronavirus with an extended host range uses heparan sulfate as an entry receptor. *J Virol.* 79, 14451-14456.

Deonarain, R., Alcamì, A., Alexiou, M., Dallman, M. J., Gewert, D. R., Porter, A. C. (2000). Impaired antiviral response and alpha/β interferon induction in mice lacking beta interferon. *J. Virol.* 74, 3404-3409.

Derdeyn, C. A. and Silvestri, G. (2005). Viral and host factors in the pathogenesis of HIV infection. *Curr. Opin. Immunol.* 17, 366-373.

de-The, G. (1985). Epstein-Barr virus and Burkitt's lymphoma worldwide: the causal relationship revisited. *IARC Sci Publ.* 60, 165-176.

de Turenne-Tessier, M., Jolicoeur, P., Middeldorp, J. M., Ooka, T. (2005). Expression and analysis of the Epstein-Barr virus BARF1-encoded protein from a tetracycline-regulatable adenovirus system. *Virus Res.* 109, 9-18.

de Veer, M. J., Holko, M., Frevel, M., Walker, E., Der, S., Paranjape, J. M., Silverman, R. H., Williams, B. R. (2001) *J. Leukoc. Biol.* 69, 912-920.

Devergne, O., Cahir McFarland, E. D., Mosialos, G., Izumi, K. M., Ware, C. F., Kieff, E. (1998). Role of the TRAF binding site and NF-kappaB activation in Epstein-Barr virus latent membrane protein 1-induced cell gene expression. *J. Virol.* 72, 7900-7908.

Devergne, O., Hatzivassiliou, E., Izumi, K. M., Kaye, K. M., Kleijnen, M. F., Kieff, E., Mosialos, G. (1996). Association of TRAF1, TRAF2, and TRAF3 with an Epstein-Barr virus LMP1 domain important for B-lymphocyte transformation: role in NF-kappaB activation. *Mol. Cell. Biol.* 16, 7098-7108.

de Vries, A. A. F., Horzinek, M. C.; Rottier, P. J. M., de Groot, R. J. (1997). The Genome Organization of the Nidovirales: Similarities and Differences between Arteri-, Toro-, and Coronaviruses. *Semin. Virol.* 8: 33-47.

Diebold, S. S., Kaisho, T., Hemmi, H., Akira, S., Reis e Sousa, C. (2004). Innate Antiviral Responses by Means of TLR7-Mediated Recognition of Single-Stranded RNA. *Science.* 303, 1529-1531.

Dikic, I., and Blaukat, A. (1999). Protein tyrosine kinase-mediated pathways in G protein-coupled receptor signaling. *Cell Biochem. Biophys.* 30, 369-387.

Domingo, E., Martinez-Salas, E., Sobrino, F., de la Torre, J. C., Portela, A., Ortin, J., Lopez-Galindez, C., Perez-Brena, P., Villanueva, N., Najera, R., et al. (1985). The quasispecies (extremely heterogeneous) nature of viral RNA genome populations: biological relevance--a review. *Gene.* 40, 1-8.

Doms, R. W., Lamb, R. A., Rose, J. K., Helenius, A. (1993). Folding and assembly of viral membrane proteins. *Virology.* 193, 545-562.

Duchniewicz, M., Germaniuk, A., Westermann, B., Neupert, W., Schwarz, E., and Marszalek, J. (1999). Dual Role of the Mitochondrial Chaperone Mdj1p in Inheritance of Mitochondrial DNA in Yeast. *Mol. Cell. Biol.* 19, 8201-8210.

Dveksler, G. S., Pensiero, M. N., Dieffenbach, C. W., Cardellichio, C. B., Basile, A. A., Elia, P. E., Holmes, K. V. (1993). Mouse hepatitis virus strain A59 and blocking antireceptor monoclonal antibody bind to the N-terminal domain of cellular receptor. *Proc. Natl. Acad. Sci. USA.* 90, 1716-1720.

Eom, C. Y., and Lehman, I. R. (2002). The human DnaJ protein, hTid-1, enhances binding of a multimer of the herpes simplex virus type 1 UL9 protein to oris, an origin of viral DNA replication. *Proc. Natl. Acad. Sci.* 99, 1894-1898.

Elena, S. F., Sanjuan, R. (2005). Adaptive value of high mutation rates of RNA viruses: separating causes from consequences. *J. Virol.* 79, 11555-11558.

Elledge, R. M., Lee, W. H. (1995). Life and death by p53. *Bioessays.* 17, 923-930.

Endres, M. J., Garlisi, C. G., Xiao, H., Shan, L., and Hedrick, J. A. (1999). The Kaposi's sarcoma-related herpesvirus (KSHV)-encoded chemokine vMIP-I is a specific agonist for the CC chemokine receptor (CCR)8. *J. Exp. Med.* 189, 1993-1998.

Fahraeus, R., Jansson, A., Ricksten, A., Sjoblom, A., Rymo, L. (1990). Epstein-Barr virus-encoded nuclear antigen 2 activates the viral latent membrane protein promoter by modulating the activity of a negative regulatory element. *Proc. Natl. Acad. Sci. USA.* 87, 7390-7394.

Fahraeus, R., Fu, H. L., Ernberg, I., Finke, J., Rowe, M., Klein, G., Falk, K., Nilsson, E., Yadav, M., Busson, P., et al. (1988). Expression of Epstein-Barr virus-encoded proteins in nasopharyngeal carcinoma. *Int. J. Cancer.* 42, 329-338.

Fan, H., Ooi, A., Tan, Y. W., Wang, S., Fang, S., Liu, D. X., Lescar, J. (2005). The nucleocapsid protein of coronavirus infectious bronchitis virus: crystal structure of its N-terminal domain and multimerization properties. *Structure.* 13, 1859-1868.

Fang, S. G., Shen, S., Tay, F. P., Liu, D. X. (2005). Selection of and recombination between minor variants lead to the adaptation of an avian coronavirus to primate cells. *Biochem Biophys Res Commun.* 336, 417-423.

Farrell, P. J., Broeze, R. J., Lengyel, P. (1979). Accumulation of an mRNA and protein in interferon-treated Ehrlich ascites tumour cells. *Nature* 279, 523-525.

Fingerroth, J. D., Diamond, M. E., Sage, D. R., Hayman, J., Yates, J. L. (1999). CD21-dependent infection of an epithelial cell line, 293, by Epstein-Barr virus. *J. Virol.* 73, 2115-2125.

Fingerroth, J. D., Weis, J. J., Tedder, T. F., *et al.* (1984). Epstein-Barr virus receptor of human B lymphocytes is the C3d receptor CR2. *Proc. Natl. Acad. Sci.* 81, 4510-4514.

Fischer, F., Stegen, C. F., Masters, P. S., Samsonoff, W. A. (1998). Analysis of constructed E gene mutants of mouse hepatitis virus confirms a pivotal role for E protein in coronavirus assembly. *J. Virol.* 72, 7885-7894.

Franken, M., Devergne, O., Rosenzweig, M., Annis, B., Kieff, E., Wang, F. (1996). Comparative analysis identifies conserved tumor necrosis factor receptor-associated factor 3 binding sites in the human and simian Epstein-Barr virus oncogene LMP1. *J. Virol.* 70, 7819-7826.

French, A. R., Pingel, J. T., Wagner, M., Bubic, I., Yang, L., Kim, S., Koszinowski, U., Jonjic, S. and Yokoyama, W. M. (2004). Escape of mutant double-stranded DNA virus from innate immune control. *Immunity.* 20, 747-756.

Friedman, D. J. and Ricciardi, R. P. (1988). Adenovirus type 12 E1A gene represses accumulation of MHC class I mRNAs at the level of transcription, *Virology*. 165, 303–305.

Fries, K. L., Miller, W. E., Raab-Traub, N. (1996). Epstein-Barr virus latent membrane protein 1 blocks p53-mediated apoptosis through the induction of the A20 gene. *J. Virol.* 70, 8653-8659.

Fries, K. L., Sculley, T. B., Webster-Cyriaque, J., Rajadurai, P., Sadler, R. H., Raab-Traub, N. (1997). Identification of a novel protein encoded by the BamHI A region of the Epstein-Barr virus. *J. Virol.* 71, 2765-2771.

Fukayama, M., Hayashi, Y., Iwasaki, Y., Chong, J., Ooba, T., Takizawa, T., Koike, M., Mizutani, S., Miyaki, M., Hira, K. (1994). Epstein-Barr virus-associated gastric carcinoma: Epstein-Barr virus infection of the stomach. *Lab. Invest.* 71, 73–81.

Gahn, T. and Sugden, B. (1995). An EBNA1-dependent enhancer acts from a distance of 10 kilobase pairs to increase expression of the Epstein-Barr virus LMP gene. *J. Virol.* 69, 2633-2636.

Gan YJ, Chodosh J, Morgan A, Sixbey JW. (1997). Epithelial cell polarization is a determinant in the infectious outcome of immunoglobulin A-mediated entry by Epstein-Barr virus. *J Virol.* 71, 519-526.

Gao, Y., Lu, Y. J., Xue, S. A., Chen, H., Wedderburn, N., Griffin, B. E. (2002). Hypothesis: a novel route for immortalization of epithelial cells by Epstein-Barr virus. *Oncogene*. 21, 825-835.

Garrett, R. and Grisham, C. (1999) *Biochemistry*, 2nd ed. Saunders college publishing. Orlando, F. L.

Geijtenbeek, T. B. H., Kwon, D. S., Torensma, R., van Vliet, S. J., van Duijnhoven, G. C. F., Middel, J., Cornelissen, I. L. M. H., Nottet, H. S. L. M., KewalRamani, V. N., and Littman, D. R. (2000). DC-SIGN, a dendritic cell-specific HIV-1-binding protein that enhances trans-infection of T Cells. *Cell* 100, 587-597.

Gelb, J. Jr, Keeler, C. L. Jr, Nix, W. A., Rosenberger, J. K., Cloud, S. S. (1997). Antigenic and S-1 genomic characterization of the Delaware variant serotype of infectious bronchitis virus. *Avian. Dis.* 41, 661-669.

Gerber, P., Lucas, S., Nonoyama, M., Perlin, E., Goldstein, L. I. (1972). Oral excretion of Epstein-Barr virus by healthy subjects and patients with infectious mononucleosis. *Lancet*. 2, 988-989.

Germaniuk, A., Liberek, K., and Marszalek, J. (2002). A Bichaperone (Hsp70-Hsp78) System Restores Mitochondrial DNA Synthesis following Thermal Inactivation of Mip1p Polymerase. *J. Biol. Chem.* 277, 27801–27808.

Gilbert, M. J., Riddell, S. R., Plachter, B., Greenberg, P. D. (1996). Cytomegalovirus selectively blocks antigen processing and presentation of its immediate-early gene product. *Nature.* 383, 720-722.

Gilligan, K., Sato, H., Rajadurai, P., Busson, P., Young, L., Rickinson, A., Tursz, T., Raab-Traub, N. (1990). Novel transcription from the Epstein-Barr virus terminal EcoRI fragment, DIJhet, in a nasopharyngeal carcinoma. *J. Virol.* 64, 4948-4956.

Given, D., Kieff, E. (1978). DNA of Epstein-Barr virus. IV. Linkage map of restriction enzyme fragments of the B95-8 and W91 strains of Epstein-Barr Virus. *J. Virol.* 28, 524-542.

Given, D., Kieff, E. (1979). DNA of Epstein-Barr virus. VI. Mapping of the internal tandem reiteration. *J. Virol.* 31, 315-324.

Godfraind, C., Langreth, S. G., Cardellichio, C. B., Knobler, R., Coutelier, J. P., Dubois-Dalcq, M., Holmes, K. V. (1995). Tissue and cellular distribution of an adhesion molecule in the carcinoembryonic antigen family that serves as a receptor for mouse hepatitis virus. *Lab Invest.* 73, 615-627.

Goldstaub, D., Gradi, A., Bercovitch, Z., Grosman, Z., Nophar, Y., Luria, S., Sonenberg, N., Kahana, C. (2000). Poliovirus 2A protease induces apoptotic cell death. *Mol. Cell. Biol.* 20, 1271-1277.

Goodbourn, S., Didcock, L., Randall, R. E. (2000). Interferons: cell signalling, immune modulation, antiviral response and virus countermeasures. *J. Gen. Virol.* 81, 2341-2364.

Goodkin, M. L., Ting, A. T. and Blaho, J. A. (2003). NF- κ B is required for apoptosis prevention during herpes simplex virus type 1 infection. *J. Virol.* 77, 7261-7280.

Gorbalenya, A. E., Koonin, E. V., Donchenko, A. P., Blinov, V. M. (1989). Coronavirus genome: prediction of putative functional domains in the non-structural polyprotein by comparative amino acid sequence analysis. *Nucleic Acids Res.* 17, 4847-4861.

Gough, R. E., Cox, W. J., Winkler, C. E., Sharp, M. W., Spackman, D. (1996). Isolation and identification of infectious bronchitis virus from pheasants. *Vet. Rec.* 138, 208–209.

Grasser, F. A., Murray, P. G., Kremmer, E., Klein, K., Remberger, K., Feiden, W., Reynolds, G., Niedobitek, G., Young, L. S, Mueller-Lantzsch, N. (1994). Monoclonal antibodies directed against the Epstein-Barr virus-encoded nuclear antigen 1 (EBNA1): immunohistologic detection of EBNA1 in the malignant cells of Hodgkin's disease. *Blood.* 84, 3792–3798.

Gregory, C. D., Dive, C., Henderson, S., Smith, C. A., Williams, G. T., Gordon, J., Rickinson, A. B. (1991). Activation of Epstein-Barr virus latent genes protects human B cells from death by apoptosis. *Nature*. *349*, 612-614.

Gregory, C. D., Rowe, M. and Rickinson, A. B. (1990). Different Epstein-Barr virus-B cell interactions in phenotypically distinct clones of a Burkitt's lymphoma cell line. *J. Gen. Virol.* *71*, 1481-1495.

Griffin, B. E., Karran, L. (1984). immortalization of monkey epithelial cells by specific fragments of Epstein-Barr virus DNA. *Nature*. *309*, 78-82.

Guan, Y., Zheng, B. J., He, Y. Q., Liu, X. L., Zhuang, Z. X., Cheung, C. L., Luo, S. W., Li, P. H., Zhang, L. J., Guan, Y. J., Butt, K. M., Wong, K. L., Chan, K. W., Lim, W., Shortridge, K. F., Yuen, K. Y., Peiris, J. S., Poon, L. L. (2003). Isolation and characterization of viruses related to the SARS coronavirus from animals in southern China. *Science*. *302*, 276-278.

Guerreiro-Cacais, A. O., Li, L., Donati, D., Bejarano, M. T., Morgan, A., Masucci, M. G., Hutt-Fletcher, L., Levitsky, V. (2004). Capacity of Epstein-Barr virus to infect monocytes and inhibit their development into dendritic cells is affected by the cell type supporting virus replication. *J Gen Virol.* *85*, 2767-2778.

Gulley, M. L., Raphael, M., Lutz, C. T., Ross, D. W. and Raab-Traub, N. (1992). Epstein-Barr virus integration in human lymphomas and lymphoid cell lines, *Cancer*. *70*, 185-191.

Haijema, B. J., Volders, H., Rottier, P. J. (2003). Switching species tropism: an effective way to manipulate the feline coronavirus genome. *J. Virol.* *77*, 4528-4538.

Halary, F., Amara, A., Lortat-Jacob, H., Messerle, M., Delaunay, T., Houles, C., Fieschi, F., Renzana-Seisdedos, F., Moreau, J. F., and Chanet-Merville, J. (2002). Human cytomegalovirus binding to DC-SIGN is required for dendritic cell infection and target cell trans-infection. *Immunity* *17*, 653-664.

Hammariskjold, M. L., Simurda, M. C. (1992). Epstein-Barr virus latent membrane protein transactivates the human immunodeficiency virus type 1 long terminal repeat through induction of NF-kappa B activity. *J. Virol.* *66*, 6496-6501.

Han, J., Sabbatini, P., White, E. (1996). Induction of apoptosis by human Nbk/Bik, a BH3-containing protein that interacts with E1B 19K. *Mol. Cell Biol.* *16*, 5857-5864.

Han, J., Sabbatini, P., Perez, D., Rao, L., Modha, D., White, E. (1996). The E1B 19K protein blocks apoptosis by interacting with and inhibiting the p53-inducible and death-promoting Bax protein. *Genes Dev.* *10*, 461-77.

Hartl, F. U. (1996). Molecular chaperones in cellular protein folding. *Nature*. 381, 571-579.

Hatfull, G., Bankier, A. T., Barrell, B. G., Farrell, P. J. (1988). Sequence analysis of Raji Epstein-Barr virus DNA. *Virology*. 164, 334-340.

Hayes, D. P., Brink, A. A., Vervoort, M. B., Middeldorp, J. M., Meijer, C. J., van den Brule, A. J. (1999). Expression of Epstein-Barr virus (EBV) transcripts encoding homologues to important human proteins in diverse EBV associated diseases. *Mol. Pathol.* 52, 97-103.

Hayward, S. D., Kieff, E. D. (1976). Epstein-Barr virus-specific RNA. I. Analysis of viral RNA in cellular extracts and in the polyribosomal fraction of permissive and nonpermissive lymphoblastoid cell lines. *J. Virol.* 18, 518-25.

Heil, F., Hemmi, H., Hochrein, H., Ampenberger, F., Kirschning, C., Akira, S., Lipford, G., Wagner, H., Bauer, S. (2004). Species-Specific Recognition of Single-Stranded RNA via Toll-like Receptor 7 and 8. *Science*. 303, 1526-1529.

Helt, A. M., Galloway, D. A. (2003). Mechanisms by which DNA tumor virus oncoproteins target the Rb family of pocket proteins. Mechanisms by which DNA tumor virus oncoproteins target the Rb family of pocket proteins. *Carcinogenesis*. 24, 159-169.

Hemmi, H., Takeuchi, O., Kawai, T., Kaisho, T., Sato, S., Sanjo, H., Matsumoto, M., Hoshino, K., Wagner, H., Takeda, K., Akira, S. (2000). *Nature*. 408, 740-745.

Henderson, S., Huen, D., Rowe, M., Dawson, C., Johnson, G., Rickinson, A. (1993). Epstein-Barr virus-coded BHRF1 protein, a viral homologue of Bcl-2, protects human B cells from programmed cell death. *Proc. Natl. Acad. Sci. USA*. 90, 8479-8483.

Henderson, S., Rowe, M., Gregory, C., Croom-Carter, D., Wang, F., Longnecker, R., Kieff, E., Rickinson, A. (1991). Induction of bcl-2 expression by Epstein-Barr virus latent membrane protein 1 protects infected B cells from programmed cell death. *Cell*. 65, 1107-1115.

Henle, W., Diehl, V., Kohn, G., Zui, Hausen, H. and G. Henle. (1967). Herpes-type virus and chromosome marker in normal leukocytes after growth with irradiated Burkitt cells. *Science*. 157, 1064-1065.

Henle, G., Henle, W. (1972). Epstein-Barr virus-specific IgA serum antibodies as an outstanding feature of nasopharyngeal carcinoma. *Int. J. Cancer*. 17, 1-7.

Henle, W., Henle, G. (1979). Seroepidemiology of the virus. In M. Epstein & B. Achong (Eds.) *The Epstein-Barr Virus* (Springer-Berlag, Berlin):61-78.

Henning, S. W., and Cantrell, D. A. (1998). GTPases in antigen receptor signalling. *Curr. Opin. Immunol.* 10, 322-329.

Herbst, H., Dallenbach, F., Hummel, M., Niedobitek, G., Pileri, S., Muller-Lantzsch, N., Stein, H. (1991). Epstein-Barr virus latent membrane protein expression in Hodgkin and Reed-Sternberg cells. *Proc. Natl. Acad. Sci. USA* 88, 4766-4770.

Herbst, H., Stein, H., Niedobitek, G. (1993). Epstein-Barr virus in CD30+ malignant lymphomas. *Crit. Rev. Oncogenesis.* 4, 191-239.

Higuchi, M., Izumi, K. M., Kieff, E. (2001). Epstein-Barr virus latent-infection membrane proteins are palmitoylated and raft-associated: protein 1 binds to the cytoskeleton through TNF receptor cytoplasmic factors. *Proc. Natl. Acad. Sci.* 98, 4675-4680.

Hiscox, J. A., Wurm, T., Wilson, L., Cavanagh, D., Britton, P. and Brooks, G. (2001). The coronavirus infectious bronchitis virus nucleoprotein localizes to the nucleolus. *J. Virol.* 75, 506-512.

Hitt, M. M., Allday, M. J., Hara, T., Karran, L., Jones, M. D., Busson, P., Tursz, T., Ernberg, I., Griffin, B. E. (1989). EBV gene expression in an NPC-related tumour. *EMBO. J.* 8, 2639-2651.

Hochberg, D., Middeldorp, J. M., Catalina, M., Sullivan, J. L., Luzuriaga, K., Thorley-Lawson, D. A. (2004). Demonstration of the Burkitt's lymphoma Epstein-Barr virus phenotype in dividing latently infected memory cells in vivo. *Proc. Natl. Acad. Sci. USA.* 101, 239-244.

Hodgson, T., Britton, P., Cavanagh, D. (2006). Neither the RNA nor the proteins of open reading frames 3a and 3b of the coronavirus infectious bronchitis virus are essential for replication. *J. Virol.* 80, 296-305.

Hofmann, H., Pyrc, K., van der Hoek, L., Geier, M., Berkhout, B., Pohlmann, S. (2005). Human coronavirus NL63 employs the severe acute respiratory syndrome coronavirus receptor for cellular entry. *Proc. Natl. Acad. Sci. USA.* 102, 7988-7993.

Holmes, K.V. (1991). Coronaviridae and their replication. In *Fundamental Virology*, 2nd edn, pp.471-486.

Hopwood, P. and Crawford, D. H. (2000). The role of EBV in post-transplant malignancies: a review. *J. Clin. Pathol.* 53, 248-254.

Hording, U., Nielsen, W. H., Daugaard, S., Albeck, H. (1994). Human papillomavirus types 11 and 16 detected in nasopharyngeal carcinomas by the polymerase chain reaction. *Laryngoscope.* 104, 99-102.

Horvath, C.M. (2004). Weapons of STAT destruction. Interferon evasion by paramyxovirus V protein. *Eur J Biochem.* 271, 4621-4628.

Hounsell, E. F., Davies, M. J., Renouf, D. V. (1996). O-linked protein glycosylation structure and function. *Glycoconj J.* 13, 19-26.

Hsu, D. H., de Waal Malefyt, R., Fiorentino, D. F., Dang, M. N., Vieira, P., de Vries, J., Spits, H., Mosmann, T. R., Moore, K. W. (1990). Expression of interleukin-10 activity by Epstein-Barr virus protein BCRF1. *Science.* 250, 830-832.

Huang, X., Seifert, U., Salzmann, U., Henklein, P., Preissner, R., Henke, W., Sijts, A. J., Kloetzel, P. M. and Dubiel, W. (2002). The RTP site shared by the HIV-1 Tat protein and the 11S regulator subunit alpha is crucial for their effects on proteasome function including antigen processing. *J. Mol. Biol.* 323, 771-782.

Hung, S. C., Kang, M. S. and Kieff, E. (2001). Maintenance of Epstein-Barr virus (EBV) oriP-based episomes requires EBV-encoded nuclear antigen-1 chromosome-binding domains, which can be replaced by high-mobility group-I or histone H1. *Proc. Natl. Acad. Sci. USA* 98, 1865-1870.

IARC 1997. Epstein-Barr Virus and Kaposi's Sarcoma Herpesvirus/Human Herpesvirus 8. Lyon, France: World Health Organization.

Ignjatovic, J., Galli, L. (1993). Structural proteins of avian infectious bronchitis virus: role in immunity and protection. *Adv. Exp. Med. Biol.* 342, 449-453.

Ignjatovic, J., Sapats, S. (2005). Identification of previously unknown antigenic epitopes on the S and N proteins of avian infectious bronchitis virus. *Arch. Virol.* 150, 1813-1831.

Imai, S., Koizumi, S., Sugiura, M., Tokunaga, M., Uemura, Y., Yamamoto, N., Tanaka, S., Sato, E., Osato, T. (1994). Gastric carcinoma: monoclonal epithelial malignant cells expressing Epstein-Barr virus latent infection protein. *Proc. Natl. Acad. Sci. USA* 91, 9131-9135.

Imai, S., Nishikawa, J., Kuroda, M., Takada, K. (2001). Epstein-Barr virus infection of human epithelial cells. *Curr. Top. Microbiol. Immunol.* 258, 161-184.

Imai, S., Nishikawa, J., Takada, K. (1998). Cell-to-cell contact as an efficient mode of Epstein-Barr virus infection of diverse human epithelial cells. *J. Virol.* 72, 4371-4378.

Ishido, S., Wang, C., Lee, B. S., Cohen, G. B. and Jung, J. U. (2000). Downregulation of major histocompatibility complex class I molecules by Kaposi's sarcoma-associated herpesvirus K3 and K5 proteins. *J. Virol.* 74, 5300-5309.

Izumi, K. M., Cahir McFarland, E. D., Ting, A. T., Riley, E. A., Seed, B., Kieff, E. D. (1999). The Epstein-Barr virus oncoprotein latent membrane protein 1 engages the tumor

necrosis factor receptor-associated proteins TRADD and receptor-interacting protein (RIP) but does not induce apoptosis or require RIP for NF-kappaB activation. *Mol. Cell. Biol.* 19, 5759-5767.

Izumi, K. M., Kieff, E. D. (1997). The Epstein-Barr virus oncogene product latent membrane protein 1 engages the tumor necrosis factor receptor-associated death domain protein to mediate B lymphocyte growth transformation and activate NF-kappaB. *Proc. Natl. Acad. Sci. USA.* 94, 12592-12597

Jacobs, L., Spaan, W. J., Horzinek, M. C., van der Zeijst, B. A. (1981). Synthesis of subgenomic mRNA's of mouse hepatitis virus is initiated independently: evidence from UV transcription mapping. *J. Virol.* 39, 401-406.

Janz A., Oezel, M., Kurzeder, C., Mautner, J., Pich, D., Kost, M., Hammerschmidt, W., Delecluse, H. J. (2000). Infectious Epstein-Barr virus lacking major glykoprotein BLLF1 (gp350/220) demonstrates the existence of additional viral ligands. *J. Virol.* 74, 10142-10152.

Jarvis, M. A., Borton, J. A., Keech, A. M., Wong, J., Britt, W. J., Magun, B. E., Nelson, J. A. (2006). Human cytomegalovirus attenuates interleukin-1beta and tumor necrosis factor alpha proinflammatory signaling by inhibition of NF-kappaB activation. *J. Virol.* 80, 5588-5598.

Jayaram, H., Fan, H., Bowman, B. R., Ooi, A., Jayaram, J., Collisson, E. W., Lescar, J., Prasad, B. V. (2006). X-ray structures of the N- and C-terminal domains of a coronavirus nucleocapsid protein: implications for nucleocapsid formation. *J. Virol.* 80, 6612-6620.

Jeffers, S. A., Tusell, S. M., Gillim-Ross, L., Hemmila, E. M., Achenbach, J. E., Babcock, G. J., Thomas, W. D. Jr, Thackray, L. B., Young, M. D., Mason, R. J., Ambrosino, D. M., Wentworth, D. E., Demartini, J. C., Holmes, K. V. (2004). CD209L (L-SIGN) is a receptor for severe acute respiratory syndrome coronavirus. *Proc. Natl. Acad. Sci. USA.* 101, 15748-15753.

Jia, W., Karaca, K., Parrish, C. R., Naqi, S. A. (1995). A novel variant of avian infectious bronchitis virus resulting from recombination among three different strains. *Arch. Virol.* 140, 259-271.

Johannsen, E., Miller, C. L., Grossman, S. R., Kieff, E. (1996). EBNA-2 and EBNA-3C extensively and mutually exclusively associate with RBPJkappa in Epstein-Barr virus-transformed B lymphocytes. *J. Virol.* 70, 4179-4183.

Johansen, L. M., Deppmann, C. D., Erickson, K. D., Coffin, W. F., Thornton, T. M., Humphrey, S. E., Martin, J. M., Taparowsky, E. J. (2003). EBNA2 and activated Notch induce expression of BATF. *J. Virol.* 77, 6029-6040.

Jones, K., Rivera, C., Sgadari, C., Franklin, J., Max, E. E., Bhatia, K., Tosato, G. (1995). Infection of human endothelial cells with Epstein-Barr virus. *J. Exp. Med.* 182, 1213-1221.

Jung, J. U. (1995). Desrosiers RC. Association of the viral oncoprotein STP-C488 with cellular ras. *Mol. Cell Biol.* 15, 6506-6512.

Kaiser, C., Laux, G., Eick, D., Jochner, N., Bornkamm, G. W., Kempkes, B. (1999). The proto-oncogene c-myc is a direct target gene of Epstein-Barr virus nuclear antigen 2. *J. Virol.* 73, 4481-4484.

Kanzler H, Küppers R, Hansmann ML, Rajewski K. (1996). Hodgkin and Reed-Sternberg cells in Hodgkin's disease represent the outgrowth of a dominant tumor clone derived from (crippled) germinal center B cells. *J. Exp. Med.* 184, 1495-1505.

Kapoor, P., Lavoie, B. D. and Frappier, L. (2005). EBP2 plays a key role in Epstein-Barr virus mitotic segregation and is regulated by aurora family kinases. *Mol. Cell. Biol.* 25, 4934-4945.

Karp, C. L., Biron, C. A., Irani, D. N. (2000). Interferon beta in multiple sclerosis: is IL-12 suppression the key? *Immunol. Today.* 21, 24-28.

Katze, M. G., He, Y., Gale, M. Jr. (2002). Viruses and interferon: a fight for supremacy. *Nat. Rev. Immunol.* 2, 675-687.

Kaye, K. M., Izumi, K. M., Kieff, E. (1993). Epstein-Barr virus latent membrane protein 1 is essential for B-lymphocyte growth transformation. *Proc. Natl. Acad. Sci. USA.* 90, 9150-9154.

Kawai, T., Takahashi, K., Sato, S., Coban, C., Kumar, H., Kato, H., Ishii, K. J., Takeuchi, O., Akira, S. (2005). IPS-1, an adaptor triggering RIG-I- and Mda5-mediated type I interferon induction. *Nat. Immunol.* 6, 981-988.

Kawamoto, S., Oritani, K., Asada, H., Takahashi, I., Ishikawa, J., Yoshida, H., Yamada, M., Ishida, N., Ujiie, H., Masaie, H., Tomiyama, Y., Matsuzawa, Y. (2003). Antiviral activity of limitin against encephalomyocarditis virus, herpes simplex virus, and mouse hepatitis virus: diverse requirements by limitin and alpha interferon for interferon regulatory factor 1. *J. Virol.* 77, 9622-9631.

Keeler, C. L. Jr, Reed, K. L., Nix, W. A., Gelb, J. Jr. (1998). Serotype identification of avian infectious bronchitis virus by RT-PCR of the peplomer (S-1) gene. *Avian. Dis.* 42, 275-284.

Kelly, G., Bell, A. and Rickinson, A. (2002). Epstein-Barr virus-associated Burkitt lymphomagenesis selects for downregulation of the nuclear antigen EBNA2. *Nat. Med.* 8, 1098-1104.

Kennedy, G., Komano, J. and Sugden, B. (2003). Epstein-Barr virus provide a survival factor to Burkitt's lymphomas. *Proc. Natl. Acad. Sci. USA* 100, 14269-14274.

Khabir, A., Karray, H., Rodriguez, S., Rose, M., Daoud, J., Frikha, M., Boudawara, T., Middeldorp, J., Jlidi, R., Busson, P. (2005). EBV latent membrane protein 1 abundance correlates with patient age but not with metastatic behavior in north African nasopharyngeal carcinomas. *Viol. J.* 2, 39.

Khan, A. Zimmermann, M. Basler, M. Groettrup and Hengel, H. (2004). A cytomegalovirus inhibitor of gamma interferon signaling controls immunoproteasome induction. *J. Virol.* 78, 1831-1842.

Kieff, E. (1996). *Fields Virology*, Fields BN, Knipe DM and Howley PM (eds.) 3rd edn. Lippincott-Raven Publishers: Philadelphia, PA (chapter 74), pp2343-2394.

Kienzle, N., Buck, M., Greco, S., Krauer, K., Sculley, T. B. (1999). Epstein-Barr virus-encoded RK-BARF0 protein expression. *J. Virol.* 73, 8902-8906.

Kikuta, H., Taguchi, Y., Tomizawa, K., Kojima, K., Kawamura, N., Ishizaka, A., Sakiyama, Y., Matsumoto, S., Imai, S., Kinoshita, T., et al. Epstein-Barr virus genome-positive T lymphocytes in a boy with chronic active EBV infection associated with Kawasaki-like disease. *Nature.* 333, 455-457.

Kim, S. W., Chao, T. H., Xiang, R., Lo, J. F., Campbell, M. J., Fearn, C. and Lee, J. D. (2004). Tid1, the human homologue of a Drosophila tumor suppressor, reduces the malignant activity of ErbB-2 in carcinoma cells. *Cancer Res.* 64, 7732-7739.

King, D. J. and Cavanagh, D. (1991). Infectious bronchitis. In *Disease of Poultry*, 9 edn, pp471-484.

Kingham, B. F., Keeler, C. L. Jr, Nix, W. A., Ladman, B. S., Gelb, J. Jr. (2000). Identification of avian infectious bronchitis virus by direct automated cycle sequencing of the S-1 gene. *Avian. Dis.* 44, 325-335.

Kintner, C. R., Sugden, B. (1979). The structure of the termini of the DNA of Epstein-Barr virus. *Cell.* 17, 661-671.

Klein, G. (1979). Lymphoma development in mice and humans: diversity of initiation is followed by convergent cytogenetic evolution. *Proc. Natl. Acad. Sci.* 76, 2442-2446.

Klein, G., Svedmyr, E., Jondal, M., Persson, P. O. (1976). EBV-determined nuclear antigen (EBNA)-positive cells in the peripheral blood of infectious mononucleosis patients. *Int. J. Cancer.* 17, 21-26.

Knight, J. S., Lan, K., Subramanian, C. and Robertson, E. S. (2003). Epstein-Barr virus nuclear antigen 3C recruits histone deacetylase activity and associates with the corepressors mSin3A and NCoR in human B-cell lines. *J. Virol.* 77, 4261–4272.

Knight, J. S., Sharma, N., Kalman, D. E., Robertson, E. S. (2004). A cyclin-binding motif within the amino-terminal homology domain of EBNA3C binds cyclin A and modulates cyclin A-dependent kinase activity in Epstein-Barr virus-infected cells. *J. Virol.* 78, 12857-12867.

Ko, L. J., and Prives, C. (1996). p53: puzzle and paradigm. *Genes Dev.* 10, 1054-1072

Krajcsi, P., Dimitrov, T., Hermiston, T. W., Tollefson, A. E., Ranheim, T. S., Van de Pol, S. B., Stephenson, A. H., Wold, W. S. (1996). The adenovirus E3-14.7K protein and the E3-10.4K/14.5K complex of proteins, which independently inhibit tumor necrosis factor (TNF)-induced apoptosis, also independently inhibit TNF-induced release of arachidonic acid. *J. Virol.* 70, 4904-4913.

Krauer, K. G., Kienzle, N., Young, D. B., Sculley, T. B. (1996). Epstein-Barr nuclear antigen-3 and -4 interact with RBP-2N, a major isoform of RBP-J kappa in B lymphocytes. *Virology.* 226, 346-353.

Kulwichit, W., Edwards, R. H., Davenport, E. M., Baskar, J. F., Godfrey, V., Raab-Traub, N. (1998). Expression of the Epstein-Barr virus latent membrane protein 1 induces B cell lymphoma in transgenic mice. *Proc. Natl. Acad. Sci. USA.* 95, 11963-11968.

Kumar, S. and Kumar, D. (1994). Lymphoepithelioma-like carcinoma of the breast. *Mod. Pathol.* 7, 129–131.

Kuo, L., Godeke, G. J., Raamsman, M. J., Masters, P. S., Rottier, P. J. (2000). Retargeting of coronavirus by substitution of the spike glycoprotein ectodomain: crossing the host cell species barrier. *J. Virol.* 74, 1393-1406.

Kuo, L., Masters, P. S. (2003). The small envelope protein E is not essential for murine coronavirus replication. *J. Virol.* 77, 4597-4608.

Kusano, S., Raab-Traub, N. (2001). An Epstein-Barr virus protein interacts with Notch. *J. Virol.* 75, 384-395.

Kusters, J. G., Jager, E. J., Niesters, H. G., van der Zeijst, B. A. (1990). Sequence evidence for RNA recombination in field isolates of avian coronavirus infectious bronchitis virus. *Vaccine.* 8, 605-608.

Kusters, J. G., Niesters, H. G., Bleumink-Pluym, N. M., Davelaar, F. G., Horzinek, M. C., Van der Zeijst, B. A. (1987). Molecular epidemiology of infectious bronchitis virus in The Netherlands. *J. Gen. Virol.* 68, 343-352.

Kusters, J. G., Niesters, H. G., Lenstra, J. A., Horzinek, M. C., van der Zeijst, B. A. (1989). Phylogeny of antigenic variants of avian coronavirus IBV. *Virology*. 169, 217-221.

Kwon, H. M., Jackwood, M. W. (1995). Molecular cloning and sequence comparison of the S1 glycoprotein of the Gray and JMK strains of avian infectious bronchitis virus. *Virus Genes*. 9, 219-229.

Kwon, H. M., Jackwood, M. W., Gelb, J. Jr. (1993). Differentiation of infectious bronchitis virus serotypes using polymerase chain reaction and restriction fragment length polymorphism analysis. *Avian. Dis.* 37, 194-202.

Labrecque, L. G., Barnes, D. M., Fentiman, I. S., Griffin, B. E. (1995). Epstein-Barr virus in epithelial cell tumors: a breast cancer study. *Cancer Res.* 55, 39-45.

Laherty, C. D., Hu, H. M., Opipari, A. W., Wang, F., Dixit, V. M. (1992). The Epstein-Barr virus LMP1 gene product induces A20 zinc finger protein expression by activating nuclear factor kappa B. *J. Biol. Chem.* 267, 24157-24160.

Lai, M. M., Cavanagh, D. (1997). The molecular biology of coronaviruses. *Adv. Virus. Res.* 48, 1-100.

Lai, M. M. C., and Holmes, K. V. (2001). Coronaviridae: The Viruses and their Replication. *Fields Virology*. Lippincott-Wilkins publishers, Philadelphia, PA. pp: 1163-1185.

Lai, M. M., Liao, C. L., Lin, Y. J., Zhang, X. (1994). Coronavirus: how a large RNA viral genome is replicated and transcribed. *Infect. Agents. Dis.* 3, 98-105.

Lalani, A. S., Barrett, J. W., McFadden, G. (2000). Modulating chemokines: more lessons from viruses. *Immunol. Today* 21, 100-106.

Lee, C. K., Rao, D. T., Gertner, R., Gimeno, R., Frey, A. B., Levy, D. E. (2000). Distinct requirements for IFNs and STAT1 in NK cell function. *J. Immunol.* 165, 3571-3577.

Lee, H. J., Shieh, C. K., Gorbalenya, A. E., Koonin, E. V., La Monica, N., Tuler, J., Bagdzhadzhyan, A., Lai, M. M. (1991). The complete sequence (22 kilobases) of murine coronavirus gene 1 encoding the putative proteases and RNA polymerase. *Virology*. 180, 567-582.

Lemon, S. M., Hutt, L. M., Shaw, J. E., Li, J. L., Pagano, J. S. (1977). Replication of EBV in epithelial cells during infectious mononucleosis. *Nature*. 268, 268-270.

Lemon, S. M., Hutt, L. M., Shaw, J. E., Li, J. L., Pagano, J. S. (1978). Replication of Epstein-Barr virus DNA in epithelial cells in vivo. *IARC Sci. Pub.* 1, 739-744.

Lenoir, G. M. and Bornkamm, G. W. (1987). Burkitt lymphoma a human cancer model for the study of the multistep development of cancer: a new scenario. In: G. Klein, Editor, *Advances in viral oncology*, Raven Press, New York. pp173–206.

Lerner, M. R., Andrews, N. C., Miller, G., Steitz, J. A. (1981). Two small RNAs encoded by Epstein-Barr virus and complexed with protein are precipitated by antibodies from patients with systemic lupus erythematosus. *Proc. Natl. Acad. Sci. USA.* 78, 805-809.

Lespagnard, L., Cochaux, P., Larsimont, D. Degeyter, M., Velu, T., Heimann, R. (1995). Absence of Epstein-Barr virus in medullary carcinoma of the breast as demonstrated by immunophenotyping, in situ hybridization and polymerase chain reaction. *Am. J. Clin. Pathol.* 103, 449–452.

Levine, P. H., G. Stemmermann, E. T. Lennette, A. Hildesheim, Shibata, D. and Nomura, A. (1995). Elevated antibody titers to Epstein-Barr virus prior to the diagnosis of Epstein-Barr-virus-associated gastric adenocarcinoma. *Int. J. Cancer.* 60, 642-644.

Levitskaya, J., Sharipo, A., Leonchiks, A., Ciechanover, A., Masucci, M. G. (1997). Inhibition of ubiquitin/proteasome-dependent protein degradation by the Gly-Ala repeat domain of the Epstein-Barr virus nuclear antigen 1. *Proc. Natl. Acad. Sci. USA.* 94, 12616-12621.

Levy, D. E., and Garcia-Sastre, A. (2001). The virus battles: IFN induction of the antiviral state and mechanisms of viral evasion. *Cytokine Growth Factor Rev.* 12, 143-156.

Lisowska, E. (2002). The role of glycosylation in protein antigenic properties. *Cell Mol Life Sci.* 59, 445-55. Review.

Li, Q. X., Young, L. S., Niedobitek, G., Dawson, C. W., Birkenbach, M., Wang, F., Rickinson, A. B. (1992). Epstein-Barr virus infection and replication in a human epithelial cell system. *Nature.* 356, 347–350.

Li, Q., Turk, S. M., Hutt-Fletcher, L. M. (1995). The Epstein-Barr virus (EBV) BZLF2 gene product associates with the gH and gL homologs of EBV and carries an epitope critical to infection of B cells but not of epithelial cells. *J. Virol.* 69, 3987-3994.

Li, W., Moore, M. J., Vasilieva, N., Sui, J., Wong, S. K., Berne, M. A., Somasundaran, M., Sullivan, J. L., Luzuriaga, K., Greenough, T. C., Choe, H., Farzan, M. (2003). Angiotensin-converting enzyme 2 is a functional receptor for the SARS coronavirus. *Nature.* 426, 450-454.

Liebowitz, D., Kopan, R., Fuchs, E., Sample, J., Kieff, E. (1987). An Epstein-Barr virus transforming protein associates with vimentin in lymphocytes. *Mol. Cell. Biol.* 7, 2299-2308.

Liebowitz, D., Wang, D., Kieff, E. (1986). Orientation and patching of the latent infection membrane protein encoded by Epstein-Barr virus. *J. Virol.* 58, 233-237.

Lim, K. P., Liu, D. X. (1998). Characterization of the two overlapping papain-like proteinase domains encoded in gene 1 of the coronavirus infectious bronchitis virus and determination of the C-terminal cleavage site of an 87-kDa protein. *Virology.* 245, 303-312.

Lim, K. P., Liu, D. X. (2001). The missing link in coronavirus assembly. Retention of the avian coronavirus infectious bronchitis virus envelope protein in the pre-Golgi compartments and physical interaction between the envelope and membrane proteins. *J. Biol. Chem.* 276, 17515-17523.

Lim, K. P., Ng, L. F., Liu, D. X. (2000). Identification of a novel cleavage activity of the first papain-like proteinase domain encoded by open reading frame 1a of the coronavirus Avian infectious bronchitis virus and characterization of the cleavage products. *J. Virol.* 74, 1674-1685.

Liu, D. X., Brierley, I., Tibbles, K. W., Brown, T. D. (1994). A 100-kilodalton polypeptide encoded by open reading frame (ORF) 1b of the coronavirus infectious bronchitis virus is processed by ORF 1a products. *J. Virol.* 68, 5772-5780.

Liu, D. X., Brown, T. D. (1995). Characterisation and mutational analysis of an ORF 1a-encoding proteinase domain responsible for proteolytic processing of the infectious bronchitis virus 1a/1b polyprotein. *Virology.* 209, 420-427.

Liu, D. X., Cavanagh, D., Green, P., Inglis, S. C. (1991). A polycistronic mRNA specified by the coronavirus infectious bronchitis virus. *Virology.* 184, 531-544.

Liu, D. X., Inglis, S. C. (1991). Association of the infectious bronchitis virus 3c protein with the virion envelope. *Virology.* 185, 911-917.

Liu, D. X., Inglis, S. C. (1992a). Internal entry of ribosomes on a tricistronic mRNA encoded by infectious bronchitis virus. *J. Virol.* 66, 6143-6154.

Liu, D. X., Inglis, S. C. (1992b). Identification of two new polypeptides encoded by mRNA5 of the coronavirus infectious bronchitis virus. *Virology.* 186, 342-347.

Liu, D. X., Tibbles, K. W., Cavanagh, D., Brown, T. D., Brierley, I. (1995). Identification, expression, and processing of an 87-kDa polypeptide encoded by ORF 1a of the coronavirus infectious bronchitis virus. *Virology.* 208, 48-57.

Liu, D. X., Xu, H. Y., Brown, T. D. (1997). Proteolytic processing of the coronavirus infectious bronchitis virus 1a polyprotein: identification of a 10-kilodalton polypeptide and determination of its cleavage sites. *J. Virol.* 71, 1814-1820.

Liu, D. X., Xu, H. Y., Lim, K. P. (1998). Regulation of mRNA 1 expression by the 5'-untranslated region (5'-UTR) of the coronavirus infectious bronchitis virus (IBV). *Adv. Exp. Med. Biol.* 440, 303-311.

Locati, M., and Murphy, P. M. (1999). Chemokines and chemokine receptors: biology and clinical relevance in inflammation and AIDS. *Annu. Rev. Med.* 50, 425-440.

Lomniczi, B. (1977). Biological properties of avian coronavirus RNA. *J. Gen. Virol.* 36, 531-533.

Lontok, E., Corse, E., Machamer, C. E. (2004). Intracellular targeting signals contribute to localization of coronavirus spike proteins near the virus assembly site. *J. Virol.* 78, 5913-5922.

Lu, B., Garrido, N., Spelbrink, J. N., Suzuki, C. K. (2006). Tid1 isoforms are mitochondrial DnaJ-like chaperones with unique carboxyl termini that determine cytosolic fate. *J Biol Chem.* 281, 13150-13158.

Lund, J. M., Alexopoulou, L., Sato, A., Karow, M., Adams, N. C., Gale, N. W., Iwasaki, A., Flavell, R. A. (2004). *Proc. Natl. Acad. Sci. USA.* 101, 5598-5603.

Luttrell, L. M., van Biesen, T., Hawes, B. E., Koch, W. J., Krueger, K. M., Touhara, K., and Lefkowitz, R. J. (1997). G-protein-coupled receptors and their regulation: activation of the MAP kinase signaling pathway by G-protein-coupled receptors. *Adv. Second Messenger Phosphoprotein Res.* 31, 263-277.

Luytjes, W. (1995). Coronavirus gene expression. Genome organization and protein synthesis. In: Siddell, S.G. (Ed), *The coronaviridae*. Plenum Press, New York, pp33-54.

Machamer, C. E., Grim, M. G., Esquela, A., Chung, S. W., Rolls, M., Ryan, K., Swift, A. M. (1993). Retention of a cis Golgi protein requires polar residues on one face of a predicted alpha-helix in the transmembrane domain. *Mol. Biol. Cell.* 4, 695-704.

Maeda, J., Maeda, A., Makino, S. (1999). Release of coronavirus E protein in membrane vesicles from virus-infected cells and E protein-expressing cells. *Virology.* 263, 265-272.

Maghazachi, A. A. (1999). Intracellular signalling pathways induced by chemokines in natural killer cells. *Cell. Signalling* 11, 385-390.

Malakhova, O. A., Yan, M., Malakhov, M. P., Yuan, Y., Ritchie, K. J., Kim, K. I., Peterson, L. F., Shuai, K., Zhang, D. E. (2003). *Genes Dev.* 17, 455-460.

Marshall, D., Sample, C. (1995). Epstein-Barr virus nuclear antigen 3C is a transcriptional regulator. *J. Virol.* 69, 3624-3630.

Martin, J. M., Veis, D., Korsmeyer, S. J., Sugden, B. (1993). Latent membrane protein of Epstein-Barr virus induces cellular phenotypes independently of expression of Bcl-2. *J. Virol.* 67, 5269-5278.

Mayer, M. P. (2005). Recruitment of Hsp70 chaperones: a crucial part of viral survival strategies. *Rev. Physiol. Biochem. Pharmacol.* 153, 1-46.

Mayo, M. A. (2002). A summary of taxonomic changes recently approved by ICTV. *Arch. Virol.* 147, 1655-1663.

McIntosh, K. (1974). Coronaviruses. A comparative review. *Curr. Top. Microbiol. Immunol.* 6, 85-129.

McIntosh, K., Dees, J. H., Becker, W. B., Kapikian, A. Z., Chanock, R. M. (1967). Recovery in tracheal organ cultures of novel viruses from patients with respiratory disease. *Proc. Natl. Acad. Sci. USA.* 57, 933-940.

Medzhitov, R., Janeway, C. A. Jr. (1998). Innate immune recognition and control of adaptive immune responses. *Semin. Immunol.* 10, 351-353.

Meylan, E., Curran, J., Hofmann, K., Moradpour, D., Binder, M., Bartenschlager, R., Tschopp, J. (2005). *Nature.* 437, 1167-1172.

Middeldorp, J. M., Brink, A. A., van den Brule, A. J., Meijer, C. J. (2003). Pathogenic role for Epstein-Barr virus (EBV) gene products in EBV-associated proliferative disorders. *Crit. Rev. Oncol. Hematol.* 45, 1-36.

Miguel, B., Pharr, G. T., Wang, C. (2002). The role of feline aminopeptidase N as a receptor for infectious bronchitis virus. Brief review. *Arch. Virol.* 147, 2047-2056.

Miller, G. Epstein-Barr virus: biology, pathogenesis, and medical aspects. (1990) In: Fields BN, Knipe DM, eds. *Virology*. Second edition. New York: Raven Press. pp1921-1958.

Miller, W. E., Earp, H. S., Raab-Traub, N. (1995). The Epstein-Barr virus latent membrane protein 1 induces expression of the epidermal growth factor receptor. *J. Virol.* 69, 4390-4398.

Miller, D. M., Zhang, Y., Rahill, B. M., Waldman, W. J. and Sedmak, D. D. (1999). Human cytomegalovirus inhibits IFN- α -stimulated antiviral and immunoregulatory responses by blocking multiple levels of IFN- α signal transduction. *J. Immunol.* 162, 6107-6113.

Miller, D. M., Rahill, B. M., Boss, J. M., Lairmore, M. D., Durbin, J. E., Waldman, J. W., Sedmak, D. D. (1998). Human cytomegalovirus inhibits major histocompatibility

complex class II expression by disruption of the Jak/Stat pathway. *J. Exp. Med.* 187, 675-683.

Milne, R.S. (2000). RANTES binding and down-regulation by a novel human herpesvirus-6 beta chemokine receptor. *J. Immunol.* 164, 2396-2404.

Miyashita, E. M., Yang, B., Babcock, G. J., Thorley-Lawson, D. A. (1997). Identification of the site of Epstein-Barr virus persistence in vivo as a resting B cell. *J. Virol.* 71, 4882-4891.

Mockett, A. P., Cavanagh, D., Brown, T. D. (1984). Monoclonal antibodies to the S1 spike and membrane proteins of avian infectious bronchitis coronavirus strain Massachusetts M41. *65*, 2281-2286.

Mondal, S. P., Cardona, C. J. (2004). Comparison of four regions in the replicase gene of heterologous infectious bronchitis virus strains. *Virology.* 324, 238-248.

Mondal, S. P., Naqi, S. A. (2001). Maternal antibody to infectious bronchitis virus: its role in protection against infection and development of active immunity to vaccine. *Vet. Immunol. Immunopathol.* 79, 31-40.

Moore, K. M., Bennett, J. D., Seal, B. S., Jackwood, M. W. (1998). Sequence comparison of avian infectious bronchitis virus S1 glycoproteins of the Florida serotype and five variant isolates from Georgia and California. *Virus Genes.* 17, 63-83.

Moore, K. W., Vieira, P., Fiorentino, D. F., Trounstein, M. L., Khan, T. A., Mosmann, T. R. (1990). Homology of cytokine synthesis inhibitory factor (IL-10) to the Epstein-Barr virus gene BCRF1. *Science.* 248, 1230-1234.

Moorthy, R. K., Thorley-Lawson, D. A. (1993). All three domains of the Epstein-Barr virus-encoded latent membrane protein LMP-1 are required for transformation of rat-1 fibroblasts. *J. Virol.* 67, 1638-1646.

Mosialos, G., Birkenbach, M., Yalamanchili, R., VanArsdale, T., Ware, C., Kieff, E. (1995). The Epstein-Barr virus transforming protein LMP1 engages signaling proteins for the tumor necrosis factor receptor family. *Cell.* 80, 389-399.

Moya, A., Holmes, E. C. and Gonzalez-Candelas, F. (2004). The population genetics and evolutionary epidemiology of RNA viruses, *Nat. Rev. Microbiol.* 2, 279-288.

Muschen, M., Rajewsky, K., Brauninger, A., Baur, A. S., Oudejans, J. J., Roers, A., Hansmann, M. L., Kuppers, R. (2000). Rare occurrence of classical Hodgkin's disease as a T cell lymphoma. *J. Exp. Med.* 191, 387-394.

Nanbo, A., Inoue, K., Adachi-Takasawa, K. and Takada, K. (2002). Epstein-Barr virus RNA confers resistance to interferon-alpha-induced apoptosis in Burkitt's lymphoma. *EMBO. J.* 21, 954–965.

Nash, P., Barrett, J., Cao, J. X., Hota-Mitchell, S., Lalani, A. S., Everett, H., Xu, X. M., Robichaud, J., Hnatiuk, S., Ainslie, C., Seet, B. T., McFadden, G. (1999). Immunomodulation by viruses: the myxoma virus story. *Immunol. Rev.* 168, 103–120.

Naranatt, P. P., Akula, S. M., Zien, C. A., Krishnan, H. H. and Chandran, B. (2003). Kaposi's sarcoma-associated herpesvirus induces the phosphatidylinositol 3-kinase-PKC-zeta-MEK-ERK signaling pathway in target cells early during infection: implications for infectivity. *J. Virol.* 77, 1524–1539.

Nava, V. E., Cheng, E. H., Veluona, M., Zou, S., Clem, R. J., Mayer, M. L., Hardwick, J. M. (1997). Herpesvirus saimiri encodes a functional homolog of the human bcl-2 oncogene. *J. Virol.* 71, 4118–4122.

Ng, L. F., Liu, D. X. (1998). Identification of a 24-kDa polypeptide processed from the coronavirus infectious bronchitis virus 1a polyprotein by the 3C-like proteinase and determination of its cleavage sites. *Virology.* 243, 388–395.

Ng, L. F., Liu, D. X. (2000). Further characterization of the coronavirus infectious bronchitis virus 3C-like proteinase and determination of a new cleavage site. *Virology.* 272, 27–39.

Ng, L. F., Liu, D. X. (2002). Membrane association and dimerization of a cysteine-rich, 16-kilodalton polypeptide released from the C-terminal region of the coronavirus infectious bronchitis virus 1a polyprotein. *J. Virol.* 76, 6257–6267.

Nguyen, K. B., Cousens, L. P., Doughty, L. A., Pien, G. C., Durbin, J. E., Biron, C. A. (2000). Interferon alpha/beta-mediated inhibition and promotion of interferon gamma: STAT1 resolves a paradox. *Nat. Immunol.* 1, 70–76.

Nguyen, K. B., Salazar-Mather, T. P., Dalod, M. Y., Van Deusen, J. B., Wei, X. Q., Liew, F. Y., Caligiuri, M. A., Durbin, J. E., Biron, C. A. (2002). Coordinated and distinct roles for IFN-alpha beta, IL-12, and IL-15 regulation of NK cell responses to viral infection. *J. Immunol.* 169, 4279–4287.

Nicholls, J. M., Agathangelou, A., Fung, K., Xianggou, Z., Niedobitek, G. (1997). The association of squamous cell carcinomas of the nasopharynx with Epstein-Barr virus shows geographic variation reminiscent of Burkitt's lymphoma. *J. Pathol.* 183, 164–168.

Niesters, H. G., Lenstra, J. A., Spaan, W. J., Zijderveld, A. J., Bleumink-Pluym, N. M., Hong, F., van Scharrenburg, G. J., Horzinek, M. C., van der Zeijst, B. A. (1986). The peplomer protein sequence of the M41 strain of coronavirus IBV and its comparison with Beaudette strains. *Virus Res.* 5, 253–263.

Niedobitek, G., Hansmann, M. L., Herbst, H., et al. (1991). Epstein-Barr virus and carcinomas: undifferentiated carcinomas but not squamous cell carcinomas of the nasopharynx are regularly associated with the virus. *J. Pathol.* 165, 17–24.

Niedobitek, G., Agathangelou, A., Herbst, H., Whitehead, L., Wright, D. H., Young, L. S. (1997). Epstein-Barr virus (EBV) infection in infectious mononucleosis: virus latency, replication and phenotype of EBV-infected cells. *J. Pathol.* 182, 151–159.

Niedobitek, G., Agathangelou, A., Steven, N., Young, L. S. (2000). Epstein-Barr virus (EBV) in infectious mononucleosis: detection of the virus in tonsillar B lymphocytes but not in desquamated oropharyngeal epithelial cells. *Mol. Pathol.* 53, 37–42.

Niedobitek, G., Agathangelou, A., Nicholls, J. M. (1996). Epstein-Barr virus infection and the pathogenesis of nasopharyngeal carcinoma: viral gene expression, tumour cell phenotype, and the role of the lymphoid stroma. *Sem. Cancer Biol.* 7, 165–174.

Niller, H. H., Salamon, D., Banati, F., Schwarzmann, F., Wolf, H. and Minarovits, J. (2004). The LCR of EBV makes Burkitt's lymphoma endemic. *Trends Microbiol.* 12, 495–499.

Nishikawa, J., Imai, S., Oda, T., Kojima, T., Okita, K., Takada, K. (1999). Epstein-Barr virus promotes epithelial growth in the absence of EBNA2 and LMP1 expression. *J. Virol.* 73, 1286–1292.

Novella, I. S. (2003). Contribution of vesicular stomatitis virus to the understanding of RNA virus evolution, *Curr. Opin. Microbiol.* 6, 399–405.

O'Brien, V. (1998). Viruses and apoptosis. *J. Gen. Virol.* 79, 1833–1845.

Okumura, A., Lu, G., Pitha-Rowe, I., Pitha, P. M. (2006). Innate antiviral response targets HIV-1 release by the induction of ubiquitin-like protein ISG15. *Proc Natl Acad Sci U S A.* 103, 1440–1445.

Osato, T. and Imai, S. (1996). Epstein-Barr virus and gastric carcinoma. *Sem. Cancer Biol.* 7, 175–182.

Ossendorp, F., Eggers, M., Neisig, A., Ruppert, T., Groettrup, M., Sijts, A., Mengede, E., Kloetzel, P. M., Neefjes, J., Koszinowski, U. and Melief, C. (1996). A single residue exchange within a viral CTL epitope alters proteasome-mediated degradation resulting in lack of antigen presentation. *Immunity.* 5, 115–124.

Otsuki, K., Yamamoto, H., Tsubokura, M. (1979). Studies on avian infectious bronchitis virus (IBV). I. Resistance of IBV to chemical and physical treatments. *Arch. Virol.* 60, 25–32.

Otsuki, K., Noro, K., Yamamoto, H., Tsubokura, M. (1979). Studies on avian infectious bronchitis virus (IBV). II. Propagation of IBV in several cultured cells. *Arch Virol.* 60, 115-122.

Oudejans, J. J., Jiwa, M., van den Brule, A. J., Grasser, F. A., Horstman, A., Vos, W., Kluin, P. M., van der Valk, P., Walboomers, J. M., Meijer, C. J. (1995). Detection of heterogeneous Epstein-Barr virus gene expression patterns within individual post-transplant lymphoproliferative disorders. *Am. J. Pathol.* 147, 923-933.

Packham, G., Brimmell, M., Cook, D., Sinclair, A. J., Farrell, P. J. (1993). Strain variation in Epstein-Barr virus immediate early genes. *Virology.* 192, 541-550.

Pages, F., Galon, J., Karaschuk, G., Dudziak, D., Camus, M., Lazar V., Camilleri-Broet, S., Lagorce-Pages, C., Lebel-Binay, S., Laux, G., Fridman, W. H., Henglein, B. (2005). Epstein-Barr virus nuclear antigen 2 induces interleukin-18 receptor expression in B cells. *Blood.* 105, 1632-1639.

Parry, C. M., Simas, J. P., Smith, V. P., Stewart, C. A., Minson, A. C., Efstathiou, S., Alcamí, A. (2000). A broad spectrum secreted chemokine binding protein encoded by a herpesvirus. *J. Exp. Med.* 191, 573-578.

Payne, E., Bowles, M. R., Don, A., Hancock, J. F. and McMillan, N A. (2001). Human papillomavirus type 6b virus-like particles are able to activate the Ras-MAP kinase pathway and induce cell proliferation. *J. Virol.* 75, 4150-4157.

Pegman, P. M., Smith, S. M., D'Souza, B. N., Loughran, S. T., Maier, S., Kempkes, B., Cahill, P. A., Simmons, M. J., Gelinas, C., Walls, D. (2006). Epstein-Barr virus nuclear antigen 2 trans-activates the cellular antiapoptotic bfl-1 gene by a CBF1/RBPJ kappa-dependent pathway. *J. Virol.* 80, 8133-8144.

Pei, J., Sekellick, M. J., Marcus, P. I., Choi, I. S., Collisson, E. W. (2001). Chicken interferon type I inhibits infectious bronchitis virus replication and associated respiratory illness. *J. Interferon Cytokine Res.* 21, 1071-1077.

Pendleton, A. R., Machamer, C. E. (2005). Infectious bronchitis virus 3a protein localizes to a novel domain of the smooth endoplasmic reticulum. *J. Virol.* 79, 6142-6151.

Piguet, V. (2005). Receptor modulation in viral replication: HIV, HSV, HHV-8 and HPV: same goal, different techniques to interfere with MHC-I antigen presentation. *Curr. Top. Microbiol. Immunol.* 285, 199-217.

Platanias, L. C. (2005). Mechanisms of type-I- and type-II-interferon-mediated signalling. *Nat. Rev. Immunol.* 5, 375-386.

Pohlmann, S., Zhang, J., Baribaud, F., Chen, Z., Leslie, G. J., Lin, G., Granelli-Piperno, A., Doms, R. W., Rice, C. M., and McKeating, J. A. (2003). Hepatitis C virus glycoproteins interact with DC-SIGN and DC-SIGNR. *J. Virol.* 77, 4070-4080.

Pope, J. H., Horne, M. K., Scott, W. (1968). Transformation of foetal human leukocytes in vitro by filtrates of a human leukaemic cell line containing herpes-like virus. *Int. J. Cancer.* 3, 857-866.

Pope, J. H. (1967). Establishment of cell lines from peripheral leucocytes in infectious mononucleosis. *Nature.* 216, 810-811.

Popik, W., Hesselgesser, J. E. and Pitha, P. M. (1998). Binding of human immunodeficiency virus type 1 to CD4 and CXCR4 receptors differentially regulates expression of inflammatory genes and activates the MEK/ERK signaling pathway. *J. Virol.* 72, 6406-6413.

Popik, W. and Pitha, P. M. (1998). Early activation of mitogen-activated protein kinase kinase, extracellular signal-regulated kinase, p38 mitogen-activated protein kinase, and c-Jun N-terminal kinase in response to binding of simian immunodeficiency virus to Jurkat T cells expressing CCR5 receptor. *Virology.* 252, 210-217.

Prang, N. S., Hornef, M. W., Jager, M., Wagner, H. J., Wolf, H., Schwarzmann, F. M. (1997). Lytic replication of Epstein-Barr virus in the peripheral blood: analysis of viral gene expression in B lymphocytes during infectious mononucleosis and in the normal carrier state. *Blood.* 89, 1665-1677.

Querbes, W., Benmerah, A., Tosoni, D., Di Fiore, P. P. and Atwood, W. J. (2004). A JC virus-induced signal is required for infection of glial cells by a clathrin- and eps15-dependent pathway. *J. Virol.* 78, 250-256.

Raab-Traub, N. and Flynn, K. (1986). The structure of the termini of the Epstein-Barr virus as a marker of clonal cellular proliferation. *Cell* 47, 883-889.

Radkov, S. A., Touitou, R., Brehm, A., Rowe, M., West, M., Kouzarides, T. and Allday, M. J. (1999). Epstein-Barr virus nuclear antigen 3C interacts with histone deacetylase to repress transcription. *J. Virol.* 73, 5688-5697.

Ray, C. A., Black, R. A., Kronheim, S. R., Greenstreet, T. A., Sleath, P. R., Salvesen, G. S., Pickup, D. J. (1992). Viral inhibition of inflammation: cowpox virus encodes an inhibitor of the interleukin-1 beta converting enzyme. *Cell.* 69, 597-604.

Reisman, D. and B. Sugden. (1986). *trans* activation of an Epstein-Barr viral transcriptional enhancer by the Epstein-Barr viral nuclear antigen 1. *Mol. Cell. Biol.* 6, 3838-3846.

Rickinson, A. B. and Kieff E. (1996). Epstein-Barr virus, pp2397-2446. In B. N. Fields, D. M. Knipe, and P. M. Howley (ed.), *Virology*, 3rd ed. Lippincott-Raven, Philadelphia, PA.

Rickinson, A. B. and E. Kieff. (2001). Epstein-Barr Virus, pp2511-2627. *Fields Virology*, Fourth edition, vol.2. Lippincott Williams & Wilkins Publishers, Philadelphia, PA.

Robertson, E., Kieff, E. (1995). Reducing the complexity of the transforming Epstein-Barr virus genome to 64 kilobase pairs. *J. Virol.* 69, 983-993.

Robertson, E. S., Lin, J., Kieff, E. (1996). The amino-terminal domains of Epstein-Barr virus nuclear proteins 3A, 3B, and 3C interact with RBPJ(kappa). *J. Virol.* 70, 3068-3074.

Robertson, E. S., Tomkinson, B., Kieff, E. (1994). An Epstein-Barr virus with a 58-kilobase-pair deletion that includes BARF0 transforms B lymphocytes in vitro. *J Virol.* 68, 1449-1458.

Robinson, J., Smith, D., Niederman, J. (1980). Mitotic EBNA-positive lymphocytes in peripheral blood during infectious mononucleosis. *Nature.* 287, 334-335.

Rock, K. L. (1996). A new foreign policy: MHC class I molecules monitor the outside world. *Immunol. Today* 17, 131-137.

Rosenkilde, M. M., Kledal, T. N., Holst, P. J., and Schwartz, T. W. (2000). Selective elimination of high constitutive activity or chemokine binding in the human herpesvirus 8 encoded seven transmembrane oncogene ORF74. *J. Biol. Chem.* 275, 26309-26315.

Rotem-Yehudar, R., Winograd, S., Sela, S., Coligan, J. E. and Ehrlich, R. (1994). Downregulation of peptide transporter genes in cell lines transformed with the highly oncogenic adenovirus 12. *J. Exp. Med.* 180, 477-488.

Rottier, P. J. M. (1995). The coronavirus membrane glycoprotein. In: Siddell, S.G. (Ed.), *The coronaviridae*. Plenum Press, New York, pp115-139.

Rottier, P. J., Nakamura, K., Schellen, P., Volders, H., Haijema, B. J. (2005). Acquisition of macrophage tropism during the pathogenesis of feline infectious peritonitis is determined by mutations in the feline coronavirus spike protein. *J Virol.* 79, 14122-14130.

Rowe, M., Peng-Pilon, M., Huen, D. S., Hardy, R., Croom-Carter, D., Lundgren, E., Rickinson, A. B. (1994). Upregulation of bcl-2 by the Epstein-Barr virus latent membrane protein LMP1: a B-cell-specific response that is delayed relative to NF-kappa B activation and to induction of cell surface markers. *J Virol.* 68, 5602-5612.

Ruf, I. K., Lackey, K.A., Warudkar, S. and Sample, J. T. (2005). Protection from interferon-induced apoptosis by Epstein-Barr virus small RNAs is not mediated by inhibition of PKR. *J. Virol.* 79, 14562-14569.

Sadler, R. H., Raab-Traub, N. (1995). Structural analyses of the Epstein-Barr virus BamHI A transcripts. *J. Virol.* 69, 1132-1141.

Saederup, N., Lin, Y. C., Dairaghi, D. J., Schall, T. J., Mocarski, E. S. (1999). Cytomegalovirus-encoded beta chemokine promotes monocyte-associated viremia in the host. *Proc. Natl. Acad. Sci. U. S. A.* 96, 10881-10886.

Sall, A. S. Caserta, P., Jolicoeur, L. Franqueville, M., de Turenne-Tessier, and Ooka, T. (2004). Mitogenic activity of Epstein-Barr virus-encoded BARF1 protein. *Oncogene* 23, 4938-4944.

Sample, J., Hummel, M., Braun, D., Birkenbach, M., Kieff, E. (1986). Nucleotide sequences of RNAs encoding Epstein-Barr virus nuclear proteins: a probable transcriptional initiation site. *Proc. Natl. Acad. Sci. USA.* 83, 5096-5100.

Sanchez, C. M., Izeta, A., Sanchez-Morgado, J. M., Alonso, S., Sola, I., Balasch, M., Plana-Duran, J., Enjuanes, L. (1999). Targeted recombination demonstrates that the spike gene of transmissible gastroenteritis coronavirus is a determinant of its enteric tropism and virulence. *J. Virol.* 73, 7607-7618.

Sarkar, S., Pollack, B. P., Lin, K. T., Kotenko, S. V., Cook, J. R., Lewis, A., and Pestka, S. (2001). hTid-1, a human DnaJ protein, modulates the interferon signaling pathway. *J. Biol. Chem.* 276, 49034-49042.

Saridakis, V., Y. Sheng, F. Sarkari, M. N. Holowaty, K. Shire, T. Nguyen, R. G. Zhang, J. Liao, W., Lee, A. M. Edwards, Arrowsmith, C. H. and Frappier, L. (2005). Structure of the p53 binding domain of HAUSP/USP7 bound to Epstein-Barr nuclear antigen 1 implications for EBV-mediated immortalization. *Mol. Cell.* 18, 25-36.

Sasaki, S., Watanabe, T., Konishi, T., Kitayama, J., Nagawa, H. (2004). Effects of expression of hRFI on adenoma formation and tumor progression in colorectal adenoma-carcinoma sequence. *J Exp Clin Cancer Res.* 23:507-512.

Sastry, K. J., Marin, M. C., Nehete, P. N., McConnell, K., el-Naggar, A. K., McDonnell, T. J. (1996). Expression of human immunodeficiency virus type I tat results in down-regulation of bcl-2 and induction of apoptosis in hematopoietic cells. *Oncogene.* 13, 487-493.

Savard, M., Belanger, C., Tardif, M., Gourde, P., Flamand, L., Gosselin, J. (2000). Infection of primary human monocytes by Epstein-Barr virus. *J. Virol.* 74, 2612-2619.

Sax, J. K. and El-Deiry, W. S. (2003). p53 downstream targets and chemosensitivity. *Cell Death Differ.* 10, 413-417.

Schaaf, C. P., Benzing, J., Schmitt, T., Erz, D. H., Tewes, M., Bartram, C. R., and Janssen, J. W. (2005). Novel interaction partners of the TPR/MET tyrosine kinase. *FASEB J.* 19, 267-269.

Schalk, A. F., and Hawn, M. C. (1931). An apparently new respiratory disease of chicks. *A. Am. Vet. Med. Assoc.* 78, 413-422.

Schepers, A., Ritzi, M., Bousset, K., Kremmer, E., Yates, J. L., Harwood, J., Diffley, J. F. X. and. Hammerschmidt, W. (2001). Human origin recognition complex binds to the region of the latent origin of DNA replication of Epstein-Barr virus. *EMBO. J.* 20, 4588-4602.

Schickli, J. H., Thackray, L. B., Sawicki, S. G., Holmes, K. V. (2004). The N-terminal region of the murine coronavirus spike glycoprotein is associated with the extended host range of viruses from persistently infected murine cells. *J Virol.* 78, 9073-9083.

Schilling, B., De-Medina, T., Syken, J., Vidal, M., and Munger, K. (1998). A novel human DnaJ protein, hTid-1, a homolog of the *Drosophila* tumor suppressor protein Tid56, can interact with the human papillomavirus type 16 E7 oncoprotein. *Virology* 247, 74-85.

Schwartz, O., Marechal, V., Le Gall, S., Lemonnier, F. and Heard, J. M. (1996). Endocytosis of major histocompatibility complex class I molecules is induced by the HIV-1 Nef protein. *Nat. Med.* 2, 338-342.

Seah, J. N., Yu, L., Kwang, J. (2000). Localization of linear B-cell epitopes on infectious bronchitis virus nucleocapsid protein. *Vet. Microbiol.* 75, 11-16.

Sedmak, D. D., Guglielmo, A. M., Knight, D. A., Birmingham, D. J., Huang, E. H., Waldman, W. J. (1994). Cytomegalovirus inhibits major histocompatibility class II expression on infected endothelial cells. *Am. J. Pathol.* 144, 683-692.

Seeger, M., Ferrell, K., Frank, R. and Dubiel, W. (1997). HIV-1 tat inhibits the 20 S proteasome and its 11 S regulator-mediated activation. *J. Biol. Chem.* 272, 8145-8148.

Seo, S. H., Wang, L., Smith, R., Collisson, E. W. (1997). The carboxyl-terminal 120-residue polypeptide of infectious bronchitis virus nucleocapsid induces cytotoxic T lymphocytes and protects chickens from acute infection. *J. Virol.* 71, 7889-7894.

Seth, R. B., Sun, L., Ea, C. K., Chen, Z. J. (2005). Identification and characterization of MAVS, a mitochondrial antiviral signaling protein that activates NF-kappaB and IRF 3. *Cell.* 122, 669-682.

Seto, E., Yang, L., Middeldorp, J., Sheen, T. S., Chen, J. Y., Fukayama, M., Eizuru, Y., Ooka, T., Takada, K. (2005). Epstein-Barr virus (EBV)-encoded BARF1 gene is

expressed in nasopharyngeal carcinoma and EBV-associated gastric carcinoma tissues in the absence of lytic gene expression. *J. Med. Virol.* 76, 82-88.

Shackelton, L. A., Parrish, C. R., Truyen, U. and Holmes, E. C. (2005). High rate of viral evolution associated with the emergence of carnivore parvovirus. *Proc. Natl. Acad. Sci. USA.* 102, 379-384.

Shapiro, I. M., Volsky, D. J. (1982). Infection of normal human epithelial cells by Epstein-Barr virus. *Science.* 219, 1225-1229.

Sharp, T. V., Schwemmle, M., Jeffrey, I., Laing, K., Mellor, H., Proud, C. G., Hilse, K., Clemens, M. J. (1993). Comparative analysis of the regulation of the interferon-inducible protein kinase PKR by Epstein-Barr virus RNAs EBER-1 and EBER-2 and adenovirus VAI RNA. *Nucleic Acids Res.* 21, 4483-4490.

Shen, S., Wen, Z. L., Liu, D. X. (2003). Emergence of a coronavirus infectious bronchitis virus mutant with a truncated 3b gene: functional characterization of the 3b protein in pathogenesis and replication. *Virology.* 311, 16-27.

Sheng, W., Decaussin, G., Sumner, S. and Ooka, T. (2001). N-terminal domain of BARF1 gene encoded by Epstein-Barr virus is essential for malignant transformation of rodent fibroblasts and activation of BCL-2. *Oncogene.* 20, 1176-1185.

Sheng, W., Decaussin, G., Ligout, A., Takada, K. and Ooka, T. (2003). Malignant transformation of Epstein-Barr virus-negative Akata cells by introduction of the BARF1 gene carried by Epstein-Barr virus. *J. Virol.* 77, 3859-3865.

Silver, P. A., and Way, J. C. (1993). Eukaryotic DnaJ homologs and the specificity of Hsp70 activity. *Cell.* 74, 5-6.

Sixbey, J. W., Nedrud, J. G., Raab-Traub, N., Hanes, R. A., Pagano, J. S. (1984). Epstein-Barr virus replication in oropharyngeal epithelial cells. *N. Engl. J. Med.* 310, 1225-1230.

Sixbey, J. W., Vesterinen, E. H., Nedrud, J. G., Raab-Traub, N., Walton, L. A., Pagano, J. (1983). Replication of Epstein-Barr virus in human epithelial cells infected in vitro. *Nature.* 306, 480-483.

Sixbey, J. W., Yao, Q. (1992). Immunoglobulin A-induced shift of Epstein-Barr virus tissue tropism. *Science.* 255, 1578-1580.

Smith, A. R., Boursnell, M. E., Binns, M. M., Brown, T. D., Inglis, S. C. (1990). Identification of a new membrane-associated polypeptide specified by the coronavirus infectious bronchitis virus. *J. Gen. Virol.* 71, 3-11.

Smith, G. L., Symons, J. A., Khanna, A., Vanderplasschen, A., Alcami, A. (1997). Vaccinia virus immune evasion. *Immunol. Rev.* 159, 137-154.

Smith, P. R., de Jesus, O., Turner, D., Hollyoake, M., Karstegl, C. E., Griffin, B. E., Karran, L., Wang, Y., Hayward, S. D., Farrell, P. J. (2000). Structure and coding content of CST (BART) family RNAs of Epstein-Barr virus. *J. Virol.* 74, 3082-3092.

Sozzani, S., Luini, W., Bianchi, G., Allavena, P., Wells, T. N., Napolitano, M., Bernardini, G., Vecchi, A., D'Ambrosio, D., Mazzeo, D., Sinigaglia, F., Santoni, A., Maggi, E., Romagnani, S., and Mantovani, A. (1998). The viral chemokine macrophage inflammatory protein-II is a selective Th2 chemoattractant. *Blood* 92, 4036-4039.

Spano, J. P., Busson, P., Atlan, D., Bourhis, J., Pignon, J. P., Esteban, C., Armand, J. P. (2003). Nasopharyngeal carcinomas: an update. *Eur. J. Cancer.* 39, 2121-2135.

Spender L. C., Cornish G. H., Rowland B., Kempkes B., Farrell P. J. (2001). Direct and indirect regulation of cytokine and cell cycle proteins by EBNA-2 during Epstein-Barr virus infection. *J. Virol.* 75, 3537-3546.

Spender L. C., Cornish G. H., Sullivan A., Farrell P. J. (2002). Expression of transcription factor AML-2 (RUNX3, CBF(alpha)-3) is induced by Epstein-Barr virus EBNA-2 and correlates with the B-cell activation phenotype. *J. Virol.* 76, 4919-4927.

Spiegel, M., Pichlmair, A., Martinez-Sobrido, L., Cros, J., Garcia-Sastre, A., Haller, O., Weber, F. (2005). Inhibition of Beta Interferon Induction by Severe Acute Respiratory Syndrome Coronavirus Suggests a Two-Step Model for Activation of Interferon Regulatory Factor 3. *J Virol.* 79, 2079-2086.

Stadler, K., Massignani, V., Eickmann, M., Becker, S., Abrignani, S., Klenk, H. D., Rappuoli, R. (2003). SARS--beginning to understand a new virus. *Nat Rev Microbiol.* 1, 209-218.

Stark, G. R., Kerr, I. M., Williams, B. R., Silverman, R. H., Schreiber, R. D. (1998). How cells respond to interferons. *Annu. Rev. Biochem.* 67, 227-264.

Stern, D. F., Kennedy, S. I. (1980a). Coronavirus multiplication strategy. I. Identification and characterization of virus-specified RNA. *J. Virol.* 34, 665-674.

Stern, D. F., Kennedy, S. I. (1980b). Coronavirus multiplication strategy. II. Mapping the avian infectious bronchitis virus intracellular RNA species to the genome. *J. Virol.* 36, 440-449.

Stern, D. F., Sefton, B. M. (1982a). Coronavirus proteins: biogenesis of avian infectious bronchitis virus virion proteins. *J. Virol.* 44, 794-803.

Stern, D. F., Sefton, B. M. (1982b). Coronavirus proteins: structure and function of the oligosaccharides of the avian infectious bronchitis virus glycoproteins. *J. Virol.* 44, 804-812.

Steven, N. M., Annels, N. E., Kumar, A., Leese, A. M., Kurilla, M. G., Rickinson, A. B. (1997). Immediate early and early lytic cycle proteins are frequent targets of the Epstein-Barr virus-induced cytotoxic T cell response. *J. Exp. Med.* 185, 1605-1617.

Stine, J. T., Wood, C., Hill, M., Epp, A., Raport, C. J., Schweickart, V. L., Endo, Y., Sasaki, T., Simmons, G., Boshoff, C., Clapham, P., Chang, Y., Moore, P., Gray, P. W., and Chantry, D. (2000). KSHV-encoded CC chemokine vMIP-III is a CCR4 agonist, stimulates angiogenesis, and selectively chemoattracts TH2 cells. *Blood* 95, 1151-1157.

Strockbine, L. D., Cohen, J. I., Farrah, T., Lyman, S. D., Wagener, F., DuBose, R. F., Armitage, R. J. and Spriggs, M. K. (1998). The Epstein-Barr virus BARF1 gene encodes a novel, soluble colony-stimulating factor-1 receptor. *J Virol.* 72:4015-4021.

Sturman, L. S., Ricard, C. S., Holmes, K. V. (1985). Proteolytic cleavage of the E2 glycoprotein of murine coronavirus: activation of cell-fusing activity of virions by trypsin and separation of two different 90K cleavage fragments. *J. Virol.* 56, 904-911.

Su, J., Wang, G., Barrett, J. W., Irvine, T. S., Gao, X. and McFadden, G. (2006) Myxoma virus M11L blocks apoptosis through inhibition of conformational activation of Bax at the mitochondria. *J. Virol.* 80, 1140-1151.

Sugawara, Y., Mizugaki, Y., Uchida, T., Torii, T., Imai, S., Makuuchi, M., Takada, K. (1999). Detection of Epstein Barr virus (EBV) in hepatocellular carcinoma tissue: a novel EBV latency characterized by the absence of EBV-encoded small RNA expression. *Virology* 256, 196-202.

Sugiura, M., Imai, S., Tokunaga, M., Koizumi, S., Uchizawa, M., Okamoto, K. and Osato, T. (1996). Transcriptional analysis of Epstein-Barr virus gene expression in EBV-positive gastric carcinoma: unique viral latency in the tumour cells. *Br. J. Cancer* 74, 625-631.

Sundararajan, R., Cuconati, A., Nelson, D., White, E. (2001). Tumor necrosis factor- α induces Bax-Bak interaction and apoptosis, which is inhibited by adenovirus E1B 19K. *J. Biol. Chem.* 276, 45120-45127.

Swaminathan, S., Tomkinson, B., Kieff, E. (1991). Recombinant Epstein-Barr virus with small RNA (EBER) genes deleted transforms lymphocytes and replicates in vitro. *Proc. Natl. Acad. Sci. USA.* 88, 1546-1550.

Syken, J., De-Medina, T., and Munger, K. (1999). *TID1*, a human homolog of the *Drosophila* tumor suppressor *l(2)tid*, encodes two mitochondrial modulators of apoptosis with opposing functions. *Proc. Natl. Acad. Sci.* 96, 8499-9504.

Syken, J., Macian, F., Agarwal, S., Rao, A., Munger, K. (2003). TID1, a mammalian homologue of the drosophila tumor suppressor lethal(2) tumorous imaginal discs, regulates activation-induced cell death in Th2 cells. *Oncogene.* 22, 4636-4641.

Symons, J. A., Alcamí, A., Smith, G. L. (1995). Vaccinia virus encodes a soluble type I interferon receptor of novel structure and broad species specificity. *Cell*. 81, 551-560.

Takada, K. and Nanbo, A. (2001). The role of EBERs in oncogenesis. *Semin. Cancer Biol.* 11, 461-467.

Talon, J., Salvatore, M., O'Neill, R. E., Nakaya, Y., Zheng, H., Muster, T., Garcia-Sastre, A., Palese, P. (2000). Influenza A and B viruses expressing altered NS1 proteins: A vaccine approach. *Proc. Natl. Acad. Sci. USA* 97, 4309-4314.

Tanner, J., Weis, J., Fearon, D., Whang, Y., Kieff, E. (1987). Epstein-Barr virus gp350/220 binding to the B lymphocyte C3d receptor mediates adsorption, capping, and endocytosis. *Cell*. 50, 203-213.

Tanner, J. E., Wei, M. X., Ahamad, A., Alfieri, C., Tailor, P., Ooka, T. and Menezes, J. (1997). Antibody and antibody-dependent cellular cytotoxicity responses against the BamHI A rightward open-reading frame-1 protein of Epstein-Barr virus (EBV) in EBV-associated disorders. *J. Infect. Dis.* 175, 38-46.

Tassaneetrithep, B., Burgess, T. H., Granelli-Piperno, A., Trumpfheller, C., Finke, J., Sun, W., Eller, M. A., Pattanapanyasat, K., Sarasombath, S., Birx, D. L., Steinman, R. M., Schlesinger, S., and Marovich, M. A. (2003). DC-SIGN (CD209) mediates Dengue virus infection of human dendritic cells. *J. Exp. Med.* 197, 823-829.

Teodoro, J. G., Branton, P. E. (1997). Regulation of apoptosis by viral gene products. *J. Virol.* 71, 1739-1746.

Tewari, M., Dixit, V. M. (1995). Fas- and tumor necrosis factor-induced apoptosis is inhibited by the poxvirus crmA gene product. *J. Biol. Chem.* 270, 3255-3260.

Tewari, M., Telford, W. G., Miller, R. A., Dixit, V. M. (1995). CrmA, a poxvirus-encoded serpin, inhibits cytotoxic T-lymphocyte-mediated apoptosis. *J. Biol Chem.* 270, 22705-22708.

Thiel, V., Siddell, S. G. (1994). Internal ribosome entry in the coding region of murine hepatitis virus mRNA 5. *J. Gen. Virol.* 75, 3041-3046.

Thomas, P. G., Keating, R., Hulse-Post, D. J., Doherty, P. C. (2006). Cell-mediated protection in influenza infection. *Emerg. Infect. Dis.* 12, 48-54.

Tierney, R. J., Steven, N., Young, L. S., Rickinson, A. B. (1994). Epstein-Barr virus latency in blood mononuclear cells: analysis of viral gene transcription during primary infection and in the carrier state. *J. Virol.* 68, 7374-7385.

Tibbles, K. W., Cavanagh, D., Brown, T. D. (1999). Activity of a purified His-tagged 3C-like proteinase from the coronavirus infectious bronchitis virus. *Virus Res.* 60, 137-145.

Toczyski, D. P., Steitz, J. A. (1991). EAP, a highly conserved cellular protein associated with Epstein-Barr virus small RNAs (EBERs). *EMBO. J.* 10, 459-466.

Tollefson, A. E., Scaria, A., Hermiston, T. W., Ryerse, J. S., Wold, L. J., Wold, W. S. (1996). The adenovirus death protein (E3-11.6K) is required at very late stages of infection for efficient cell lysis and release of adenovirus from infected cells. *J. Virol.* 70, 2296-2306.

Tomkinson, B., Kieff, E. (1992). Second-site homologous recombination in Epstein-Barr virus: insertion of type 1 EBNA 3 genes in place of type 2 has no effect on in vitro infection. *J. Virol.* 66, 780-789.

Tomkinson, B., Robertson, E., Kieff, E. (1993). Epstein-Barr virus nuclear proteins EBNA-3A and EBNA-3C are essential for B-lymphocyte growth transformation. *J. Virol.* 67, 2014-2025.

Tong, X., Drapkin, R., Reinberg, D., Kieff, E. (1995a). The 62- and 80-kDa subunits of transcription factor IIH mediate the interaction with Epstein-Barr virus nuclear protein 2. *Proc. Natl. Acad. Sci. USA.* 92, 3259-3263.

Tong, X., Drapkin, R., Yalamanchili, R., Mosialos, G., Kieff, E. (1995b). The Epstein-Barr virus nuclear protein 2 acidic domain forms a complex with a novel cellular coactivator that can interact with TFIIE. *Mol. Cell. Biol.* 15, 4735-4744.

Tong, X., Wang, F., Thut, C. J., Kieff, E. (1995c). The Epstein-Barr virus nuclear protein 2 acidic domain can interact with TFIIB, TAF40, and RPA70 but not with TATA-binding protein. *J. Virol.* 69, 585-588.

Thorley-Lawson, D. A. (2001). Epstein-Barr virus: exploiting the immune system. *Nat. Rev. Immunol.* 1, 75-82.

Touitou, R., O'Nions, J., Heaney, J., Allday, M. J. (2005). Epstein-Barr virus EBNA3 proteins bind to the C8/alpha7 subunit of the 20S proteasome and are degraded by 20S proteasomes in vitro, but are very stable in latently infected B cells. *J. Gen. Virol.* 86, 1269-1277.

Touitou, R., Hickabottom, M., Parker, G., Crook, T. and Allday, M. J. (2001). Physical and functional interactions between the corepressor CtBP and the Epstein-Barr virus nuclear antigen EBNA3C. *J. Virol.* 75, 7749-7755.

Trentin, G. A., He, Y., Wu, D. C., Tang, D., Rozakis-Adcock, M. (2004). Identification of a hTid-1 mutation which sensitizes gliomas to apoptosis. *FEBS Lett.* 578, 323-330.

Tresnan, D. B., Levis, R., Holmes, K. V. (1996). Feline aminopeptidase N serves as a receptor for feline, canine, porcine, and human coronaviruses in serogroup I. *J. Virol.* 70, 8669-8674.

Unterstab, G., Ludwig, S., Anton, A., Planz, O., Dauber, B., Krappmann, D., Heins, G., Ehrhardt, C., Wolff, T. (2005). Viral targeting of the interferon- β -inducing Traf family member-associated NF- κ B activator (TANK)-binding kinase-1. *Proc. Natl. Acad. Sci. USA.* 102, 13640-13645.

van Beek, J., Brink, A. A., Vervoort, M. B., van Zijp, M. J., Meijer, C. J., van den Brule, A. J., Middeldorp, J. M. (2003). In vivo transcription of the Epstein-Barr virus (EBV) BamHI-A region without associated in vivo BARF0 protein expression in multiple EBV-associated disorders. *J. Gen. Virol.* 84, 2647-2659.

van der Most, R.G. and Spaan, W. J. M. (1995). Coronavirus replication, transcription, and RNA recombination. In: Siddell, S.G. (Ed), *The coronaviridae*. Plenum Press, New York, pp11-31.

Vaughan, T. L., Shapiro, J. A., Burt, R. D., Swanson, G. M., Berwick, M., Lynch, C. F., Lyon, J. L. (1996). Nasopharyngeal cancer in a low-risk population-Defining risk factors by histological type. *Cancer Epidemiol. Biomark. Prev.* 5, 587-593.

Vennema, H., Godeke, G. J., Rossen, J. W., Voorhout, W. F., Horzinek, M. C., Opstelten, D. J., Rottier, P. J. (1996). Nucleocapsid-independent assembly of coronavirus-like particles by co-expression of viral envelope protein genes. *EMBO. J.* 15, 2020-2028.

Vertegaal, A. C., Kuiperij, H. B., Houweling, A., Verlaan, M., van der Eb, A. J. and Zantema, A. (2003). Differential expression of tapasin and immunoproteasome subunits in adenovirus type 5- versus type 12-transformed cells. *J. Biol. Chem.* 278, 139-146.

Waltzer, L., Perricaudet, M., Sergeant, A., Manet, E. (1996). Epstein-Barr virus EBNA3A and EBNA3C proteins both repress RBP-J κ -EBNA2-activated transcription by inhibiting the binding of RBP-J κ to DNA. *J. Virol.* 70, 5909-5915.

Wang, C. C., Ng, C. P., Lu, L., Atlashkin, V., Zhang, W., Seet, L. F., Hong, W. (2004). A role of VAMP8/endobrevin in regulated exocytosis of pancreatic acinar cells. *Dev Cell.* 7, 359-371.

Wang, D., Liebowitz, D., Kieff, E. (1985). An EBV membrane protein expressed in immortalized lymphocytes transforms established rodent cells. *Cell.* 43, 831-840.

Wang, D., Liebowitz, D., Kieff, E. (1988). The truncated form of the Epstein-Barr virus latent-infection membrane protein expressed in virus replication does not transform rodent fibroblasts. *J. Virol.* 62, 2337-2346.

Wang, G., Barrett, J. W., Nazarian, S. H., Everett, H., Gao, X., Bleackley, C., Colwill, K., Moran, M. F. and McFadden, G. (2004). Myxoma virus M11L prevents apoptosis through constitutive interaction with Bak. *J. Virol.* 78, 7097-7111.

Wang, L., Grossman, S. R., Kieff, E. (2000). Epstein-Barr virus nuclear protein 2 interacts with p300, CBP, and PCAF histone acetyltransferases in activation of the LMP1 promoter. *Proc. Natl. Acad. Sci. USA* 97, 430–435.

Wang, L., Junker, D., Hock, L., Ebiary, E., Collisson, E. W. (1994). Evolutionary implications of genetic variations in the S1 gene of infectious bronchitis virus. *Virus Res.* 34, 327-338.

Wang, L., Junker, D., Collisson, E. W. (1993). Evidence of natural recombination within the S1 gene of infectious bronchitis virus. *Virology.* 192, 710-716.

Wang, Q., Tsao, S. W., Ooka, T., Nicholls, J. M., Cheung, H. W., Fu, S., Wong, Y. C., Wang, X. (2006). Anti-apoptotic role of BARF1 in gastric cancer cells. *Cancer Lett.* 238, 90-103.

Wang, X., Kenyon, W. J., Li, Q., Mullberg, J., Hutt-Fletcher, L. M. (1998). Epstein-Barr virus uses different complexes of glycoproteins gH and gL to infect B lymphocytes and epithelial cells. *J. Virol.* 72, 5552-5558.

Wang, X. and Hutt-Fletcher, L. (1998) Epstein-Barr virus lacking glycoprotein gp42 can bind to B cells but is not able to infect. *J. Virol.* 72, 158–163.

Wang, Y., Xue, S. A., Hallden, G., Francis, J., Yuan, M., Griffin, B.E. and Lemoine, N. R. (2005). Virus-associated RNA I-deleted adenovirus, a potential oncolytic agent targeting EBV-associated tumors. *Cancer Res.* 65, 1523–1531.

Wasilenko, S. T., Banadyga, L., Bond, D. and Barry, M. (2005). The vaccinia virus F1L protein interacts with the proapoptotic protein Bak and inhibits Bak activation. *J. Virol.* 79, 14031–14043.

Weber, F., Kochs, G., Haller, O., Staeheli, P. (2003). Viral evasion of the interferon system: old viruses, new tricks. *J. Interferon Cytokine Res.* 23, 209-213.

Wei, M. X., de Turenne-Tessier M, Decaussin, G., Benet, G. and Ooka, T. (1997). Establishment of a monkey kidney epithelial cell line with the BARF1 open reading frame from Epstein-Barr virus. *Oncogene* 14, 3073-3081.

Wei, M. X., Moulin, J. C., Decaussin, G., Berger, F. and Ooka, T. (1994). Expression and tumorigenicity of the Epstein-Barr virus BARF1 gene in human Louckes B-lymphocyte cell line. *Cancer Res.* 54, 1843-1848.

Wei, M.X. and Ooka, T. (1989). A transforming function of the BARF1 gene encoded by Epstein-Barr virus. *EMBO. J.* 8, 2897–2903.

Wei, W. I., Sham, J. S. (2005). Nasopharyngeal carcinoma. *Lancet* 365, 2041-2054.

White, E. (1996). Life, death, and the pursuit of apoptosis. *Genes Dev.* *10*, 1-15.

Williams, R. K., Jiang, G. S., Holmes, K. V. (1991). Receptor for mouse hepatitis virus is a member of the carcinoembryonic antigen family of glycoproteins. *Proc. Natl. Acad. Sci. USA.* *88*, 5533-5536.

Wilson, J. B., Bell, J. L. and Levine, A. J. (1996). Expression of Epstein-Barr virus nuclear antigen-1 induces B cell neoplasia in transgenic mice. *EMBO. J.* *15*, 3117-3126.

Wilson, J. B., Weinberg, W., Johnson, R., Yuspa, S., Levine, A. J. (1990). Expression of the BNLF-1 oncogene of Epstein-Barr virus in the skin of transgenic mice induces hyperplasia and aberrant expression of keratin 6. *Cell.* *61*, 1315-1327.

Winter, C., Schwegmann-Wessels, C., Cavanagh, D., Neumann, U., Herrler, G. (2006). Sialic acid is a receptor determinant for infection of cells by avian Infectious bronchitis virus. *J. Gen. Virol.* *87*, 1209-1216.

Wolf, P. R., Ploegh, H. L. (1995). How MHC class II molecules acquire peptide cargo: biosynthesis and trafficking through the endocytic pathway. *Annu. Rev. Cell. Dev. Biol.* *11*, 267-306.

Worobey, M., Holmes, E. C. (1999). Evolutionary aspects of recombination in RNA viruses. *J. Gen. Virol.* *80*, 2535-2543.

Wu, D., LaRosa, G. J., and Simon, M. I. (1993). G protein-coupled signal transduction pathways for interleukin-8. *Science.* *261*, 101-103.

Wu, D. Y., Kalpana, G. V., Goff, S. P., Schubach, W. H. (1996). Epstein-Barr virus nuclear protein 2 (EBNA2) binds to a component of the human SNF-SWI complex, hSNF5/Ini1. *J. Virol.* *70*, 6020-6028.

Wu, H., D., Ceccarelli, F. J. and Frappier, L. (2000). The DNA segregation mechanism of the Epstein-Barr virus EBNA1 protein. *EMBO. Rep.* *1*, 140-144.

Xiang, Y., Condit, R. C., Vijaysri, S., Jacobs, B., Williams, B. R., Silverman, R. H. (2002). Blockade of interferon induction and action by the E3L double-stranded RNA binding proteins of vaccinia virus. *J. Virol.* *76*, 5251-5259.

Xu, L. G., Wang, Y. Y., Han, K. J., Li, L. Y., Zhai, Z., Shu, H. B. (2005). VISA Is an Adapter Protein Required for Virus-Triggered IFN- β Signaling. *Mol. Cell* *19*, 727-740.

Yajima, M., Kanda, T. and Takada, K. (2005). Critical role of Epstein-Barr Virus (EBV)-encoded RNA in efficient EBV-induced B-lymphocyte growth transformation. *J. Virol.* *79*, 4298-4307.

Yang, T. Y., Chen, S. C., Leach, M. W., Manfra, D., Homey, B., Wiekowski, M., Sullivan, L., Jenh, C. H., Narula, S. K., Chensue, S. W., and Lira, S. A. (2000). Transgenic expression of the chemokine receptor encoded by human herpesvirus 8 induces an angioproliferative disease resembling Kaposi's sarcoma. *J. Exp. Med.* *191*, 445-454.

Yaswen, L. R., Stephens, E. B., Davenport, L. C. and Hutt-Fletcher, L. M. (1993). Epstein-Barr virus glycoprotein gp85 associates with the BKRF2 gene product and is incompletely processed as a recombinant protein. *Virology* *195*, 387-396.

Yates, J. L., Warren, N., Sugden, B. (1985). Stable replication of plasmids derived from Epstein-Barr virus in various mammalian cells. *Nature*. *313*, 812-815.

Yeager, C. L., Ashmun, R. A., Williams, R. K., Cardellicchio, C. B., Shapiro, L. H., Look, A. T., Holmes, K. V. (1992). Human aminopeptidase N is a receptor for human coronavirus 229E. *Nature*. *357*, 420-422.

Yoneyama, M., Kikuchi, M., Natsukawa, T., Shinobu, N., Imaizumi, T., Miyagishi, M., Taira, K., Akira, S., Fujita, T. (2004). *Nat. Immunol.* *5*, 730-737.

Yoshiyama, H., Imai, S., Shimizu, N., Takada, K. (1997). Epstein-Barr virus infection of human gastric carcinoma cells: implication of the existence of a new virus receptor different from CD21. *J Virol* *71*, 5688-5691.

Youn, S., Leibowitz, J. L. and Collisson, E. W. (2005). In vitro assembled, recombinant infectious bronchitis viruses demonstrate that the 5a open reading frame is not essential for replication. *Virology* *332*, 206-215.

Young, L. S., Dawson, C. W., Clark, D., Rupani, H., Busson, P., Tursz, T., Johnson, A. and Rickinson, A. B. (1988). Epstein-Barr virus gene expression in nasopharyngeal carcinoma. *J. Gen. Virol.* *69*, 1051-1065.

Young, L. S., Rickinson, A. B. (2004). Epstein-Barr virus: 40 years on. *Nat. Rev. Cancer.* *4*, 757-768.

Zhang, J., Chen, H., Weinmaster, G., Hayward, S. D. (2001). Epstein-Barr virus BamHI-a rightward transcript-encoded RPMS protein interacts with the CBF1-associated corepressor CIR to negatively regulate the activity of EBNA2 and NotchIC. *J. Virol.* *75*, 2946-2956.

Zhang, C. X., Decaussin, G., Daillie, J. and Ooka, T. (1988). Altered expression of two Epstein-Barr virus early genes localized in *BamHI-A* in nonproducer Raji cells. *J. Virol.* *62*, 1862-1869.

Zhao, B., Marshall, D. R., Sample, C. E. (1996). A conserved domain of the Epstein-Barr virus nuclear antigens 3A and 3C binds to a discrete domain of Jkappa. *J. Virol.* *70*, 4228-4236.

Zhao, B., Maruo, S., Cooper, A. R., Chase, M., Johannsen, E., Kieff, E., Cahir-McFarland, E. (2006). RNAs induced by Epstein-Barr virus nuclear antigen 2 in lymphoblastoid cell lines. *Proc. Natl. Acad. Sci. USA.* *103*, 1900-1905.

Zhao, B., Sample, C. E. (2000). Epstein-barr virus nuclear antigen 3C activates the latent membrane protein 1 promoter in the presence of Epstein-Barr virus nuclear antigen 2 through sequences encompassing an spi-1/Spi-B binding site. *J Virol.* *74*, 5151-5160.

Zhou, A., Paranjape, J. M., Der, S. D., Williams, B. R., Silverman, R. H. (1999). Interferon action in triply deficient mice reveals the existence of alternative antiviral pathways. *Virology.* *258*, 435-440.

Zhou, M., Collisson, E. W. (2000). The amino and carboxyl domains of the infectious bronchitis virus nucleocapsid protein interact with 3' genomic RNA. *Virus Res.* *67*, 31-39.

Ziebuhr, J., Snijder, E. J., Gorbalenya, A. E. (2000). Virus-encoded proteinases and proteolytic processing in the Nidovirales. *J. Gen. Virol.* *81*, 853-879.

Zimmermann, J., Hammerschmidt, W. (1995). Structure and role of the terminal repeats of Epstein-Barr virus in processing and packaging of virion DNA. *J. Virol.* *69*, 3147-3155.

zur Hausen, H., Schulte-Holthausen, H., Klein, G., Henle, W., Henle, G., Clifford, P., Santesson, L. (1970). EBV DNA in biopsies of Burkitt tumours and anaplastic carcinomas of the nasopharynx. *Nature* *228*, 1056-1058.

zur Hausen, A., Brink, A. A., Craanen, M. E., Middeldorp, J. M., Meijer, C. J., van den Brule, A. J. (2000). Unique transcription pattern of Epstein-Barr virus (EBV) in EBV-carrying gastric adenocarcinomas: expression of the transforming BARF1 gene. *Cancer Res.* *60*, 2745-2748.